

**Role of tumor architecture in elicitation of effector  
functions of human cytotoxic T-lymphocytes  
recognizing melanoma associated antigens**

Inauguraldissertation

zur  
Erlangung der Würde eines Doktors der Philosophie  
vorgelegt der  
Philosophisch-Naturwissenschaftlichen Fakultät  
der Universität Basel

von

Sourabh Ghosh

aus Kolkata, India

Basel (Switzerland), 2006

Genehmigt von der Philosophisch-Naturwissenschaftlichen Fakultät

auf Antrag von	Prof. Kurt Ballmer-Hofer	(Chairman)
	Prof. Giulio C. Spagnoli	(Supervisor)
	Prof. Alex N. Eberle	(Referee)
	Prof. Gerhard Christofori	(Co-Referee)
	PD Dr. Ivan Martin	(Additional expert)

Basel, 25 September 2006

Prof. Dr. Hans-Jakob Wirz  
Dekan

*Dedicated to my parents*

*Om sahanaa bhavatu sahanau bhunaktu  
Saha veeryam karavaavahai  
Tejasvi naa vadheetamastu maa vidvishaavahai  
Om shanti shanti shanti*

May the God protect us both (teacher and the student)  
May He cause us both to enjoy the bliss of Mukti (liberation)  
May we both exert to discover the true meaning of the scriptures.  
May our studies be fruitful. May we never quarrel with each other.  
Let there be peace.

*No laws of nature,  
however general, has been established all at once;  
its recognition has always been preceded by  
many presentiments. The establishment of a law,  
moreover, does not take place when the  
first thought of it takes form, or even when its  
significances is recognized, but only when it has been  
confirmed by the results of the experiment. The man of  
science must consider these results as the only proof of  
the correctness of his  
conjectures and opinions.*

*Dmitri Ivanovich Mendeleev  
(1834-1907)*

## *Acknowledgements*

The project underlying this thesis emerged from collaboration between the Surgical Oncology group of Prof. Giulio C. Spagnoli and Tissue Engineering group of Dr. Ivan Martin. I would like to take this opportunity to thank my supervisor Prof Giulio C. Spagnoli, for his kind guidance, patience and very useful thoughts throughout my PhD studies. I consider myself extremely fortunate to have a supervisor like him. I shall remain grateful to Dr. Ivan Martin for his very helpful guidance and inspiration, starting from the very first day when I arrived here for the interview. My sincere thanks to Prof Michael Heberer for giving me an opportunity to pursue my PhD in his group.

I would like to thank my thesis committee members, Prof Alex N. Eberle, who kindly agreed to become Fakultätsverantwortlicher and Prof. Gerhard Christofori for kindly being the co-referee of the committee, Prof Kurt Ballmer-Hofer to be the Chairman. Thank you so much for all the support, helpful discussions concerning the project.

I would like to thank my three project-partners, Ms. Sabine Ploegert, Dr. Anca Reschner, Dr. Chantal Feder-Mengus. I have learned so many things from them. I want to thank all the people who provided me with technical help and support. Thanks a lot to Mrs. Marija Plodinec from Biozentrum for a very nice friendship and for the fantastic immunofluorescence studies. I learnt about bioinformatics techniques from Dr. Philippe Demougin (from Prof. Michael Primig's lab, Biozentrum). Big thanks to Mr. Beat Erne for giving the introduction in fascinating field of Confocal microscopy and to Mr. Marcel Düggelein (Biozentrum) for helping me in Scanning Electron Microscopy studies. I must thank all of my labmates for their friendship, support and all the memorable moments in last three years. I have really enjoyed working with all of you.

Thanks to my parents, my sister Sudeshna and my wife Shampa, for all the love, support and wishes throughout my studies abroad- even from half a world away. All the members of Indian students' community in Basel and Zurich helped me a lot in many ways in last few years, but as a representative of them I must specially thank Mr. Manjunath Joshi and Mr. Murali Ghatkesar for always being with me whenever I needed any support.

I have gained experiences in past few years, which will hopefully allow me to tackle even bigger challenges in future. As this chapter of my life comes to a close, I look forward to start new chapters and adventures, may be in another part of the World. But I shall always look forward to be in touch with you all.

## Abstract

Growth in 3D architectures has been shown to promote the resistance of cancers to treatment with drugs, cytokines, or irradiation, thereby potentially playing an important role in tumor expansion. 3D architectures might also play a role in impairing immunorecognition of cancer cells by cytotoxic T lymphocytes (CTLs) specific for tumor-associated antigens.

Culture of HBL, D10 (both HLA-A\*0201+, TAA+) and NA8 (HLA-A\*0201+, TAA-) melanoma cell lines on poly-Hydroxyethylmethacrylate-coated plates, resulted in generation of 3D multicellular tumor spheroids (MCTS). Kinetics of cell proliferation in MCTS was significantly slower than in monolayer cultures. Following long-term culture (>10-15 days) MCTS showed highly compact and organised cell growth in outer layers, with necrotic cores.

To obtain an insight into the role played by tumor architecture in the elicitation of specific gene expression patterns, we addressed gene expression profiles of NA8 melanoma cells cultured in two-dimensional monolayers (2D) or in 3D (MCTS). Oligonucleotide microarray analysis of the expression of over 20,000 genes was performed on cells cultured in standard 2D, in the presence of collagen as model of extracellular matrix (ECM), or in MCTS. Gene expression profiles of cells cultured in 2D in the presence or absence of ECM were highly similar, with more than threefold differences limited to five genes. In contrast, culture in MCTS resulted in the significant, more than threefold, upregulation of the expression of >100 transcripts, while 73 transcripts were more than threefold downregulated. In particular, genes encoding CXCL1, 2, and 3 (GRO- $\alpha$ , - $\beta$ , and  $\gamma$ ), IL-8, CCL20 (MIP-3 $\alpha$ ), and Angiopoietin-like 4 were significantly upregulated, whereas basic-FGF and CD49d encoding genes were significantly downregulated. Oligonucleotide chip data were validated at the gene and protein level by quantitative real-time PCR, ELISA, and cell surface staining assays. Taken together, our data indicate that structural modifications of the architecture of tumor cell cultures result in a significant upregulation of the expression of a number of genes previously shown to play a role in melanoma progression and metastatic process.

Then we investigated the effects of 3D culture on the recognition of melanoma cells by antigen-specific HLA class I-restricted Cytotoxic T-Lymphocytes (CTL). IFN- $\gamma$  production can be used

as a surrogate marker for tumor cell immunorecognition. Co-culture of melanoma spheroids with HLA-A0201 restricted Melan-A/MART-1<sub>27-35</sub>-specific CTL clones resulted in significantly defective TAA recognition by CTL as compared to 2D, as witnessed by decreased IFN- $\gamma$  production and decreased Fas Ligand, perforin and granzyme B gene expression. Indeed, Melan-A/MART-1 expression, at both gene and protein levels, was significantly decreased in 3D as compared with 2D tumor cell cultures. Concomitantly, a parallel decrease of HLA class I molecule expression was also observed. Differential gene profiling studies on HBL cells showed an increased expression of genes encoding molecules involved in intercellular adhesion, such as junctional adhesion molecule 2 and cadherin-like 1 (>20- and 8-fold up-regulated, respectively) in 3D as compared with 2D cultures.

We further identified a multiplicity of mechanisms potentially involved. In particular :

- 1) MCTS *per se* limit CTL capacity of recognizing HLA class I restricted antigens by reducing exposed cell surfaces.
- 2) Expression of melanoma differentiation antigens is down-regulated in tumor cell spheroids as compared to 2D unrelated to hypoxia or increased Oncostatin M gene expression but rather to decreased MITF gene expression.
- 3) Expression of HLA class I molecules is frequently down-regulated in melanoma MCTS, as compared to 2D, possibly due to decreased IRF-1 gene expression.
- 4) Lactate production by melanoma cells is increased in MCTS, as compared to 2D and lactate significantly inhibits TAA triggered IFN- $\gamma$  production by CTL.

Taken together, our data suggest that mere growth of melanoma cells in 3D architectures, in the absence of immunoselective pressure, may result in defective recognition by tumor-associated antigen-specific CTL and a constellation of mechanisms are involved in causing this impairment of immunorecognition.

# Table of content

Page numbers

## 1. Introduction

1.1. Need for in vitro tumor model system	1
1.2. Importance of simulating 3D tumor architecture	2
1.3. Multicellular tumor spheroid model system	3
1.4. Spheroid culturing techniques	
1.4.1. Introduction	4
1.4.1.1. Stirred cultivation methods	5
1.4.1.2. Hanging-drop method	6
1.4.1.3. Gel encapsulation method	7
1.4.1.4. Static cultivation methods	8
1.4.2. MCTS Characterization	
1.4.2.1. Growth kinetics of MCTS	9
1.4.2.2. Morphological features	9
1.5. Gene expression	
1.5.1. Introduction	11
1.5.2. Regulation of gene expression by 3D tumor architecture	11
1.5.3. Gene expression pattern in melanoma	13
1.6. Immune response	
1.6.1. Introduction	15
1.6.2. Infiltration of MCTS by TAA specific T cells	16
1.6.3. Modulation of immunorecognition	17
1.6.4. CTL mediated immune response	17
1.6.5. Lactic acid accumulation & infiltration by immunocompetent cells	18
1.7. Research plan	19

## 2. Materials & methods

2.1. Cells used	21
2.1.1. Melanoma cells	
2.1.2. CTL clones	
2.2. Establishment of spheroid model	
2.2.1. Stirred cultivation methods	22
2.2.2. Hanging-drop method	22
2.2.3. Alginate gel encapsulation	22
2.2.4. Static cultivation methods- agarose, PolyHEMA	22
2.2.5. Morphological evaluation	22
2.2.6. Proliferation	23
2.3. Modulation in Gene expression	24



2.4. Cellular immunology studies	
2.4.1. IFN- $\gamma$ detection by ELISA	25
2.4.2. Chemotaxis assay	25
2.4.3. Immunofluorescence analysis	25
2.4.4. Flow cytometry analysis	
2.4.5. Quantification of gene expression by quantitative Real-Time PCR	26
2.4.6. Lactic acid measurement from tumor supernatant	27
<b>3. Results</b>	
3.1. Spheroid Cultivation Techniques	
3.1.1. Rotating wall vessel bioreactor	29
3.1.2. Hanging drop method	29
3.1.3. Gel encapsulation method	30
3.1.4. Static cultivation technique on non-adhesive surface	31
3.1.5. Effect of culture media	32
3.2. MCTS Characterization	
3.2.1. Proliferation	33
3.2.2. Morphological characterization	34
3.3. Gene expression	38
3.3.1. Validation of differential gene expression	41
3.4. Cellular immunology studies –focus on immunorecognition	
3.4.1. Description of the model	45
3.4.2. Migration of immunocompetent cells in response to MCTS supernatants	45
3.4.3. Morphology of interaction between TAA specific CTLs & melanoma cells cultured in spheroids	46
3.4.4. Immunorecognition	
3.4.4.1. IFN- $\gamma$ as a surrogate marker of antigen recognition	49
3.4.4.2. Antigen recognition by IFN- $\gamma$ secretion measurement	50
3.4.4.3. Effects of interaction with targets cultured in spheroids on CTL machinery	52
3.4.5. Possible mechanisms causing impaired immunorecognition	54
3.4.5.1. Structural hindrance	55
3.4.5.2. Down-modulation in TAA expression	56
3.4.5.2.1. Effect of spheroid size	58
3.4.5.2.2. Recovery of TAA expression	60
3.4.5.2.3. Comparison with clinical specimens	61
3.4.5.2.4. Role of transcription factors downregulating TAA expression	62
3.4.5.3. Modulation of HLA expression	64
3.4.5.4. Effects of Lactate on immunorecognition	67
3.4.5.5. Close cell-cell interaction in specific cell types may lead to dedifferentiation	69
<b>4. Concluding remarks</b>	74
<b>5. References</b>	77

## List of figures

Figure 1: Traditionally used spinner flasks for preparing multicellular spheroids

Figure 2: Rotating wall vessel bioreactor

Figure 3: Chemical composition of Poly-Hydroxy ethyl methacrylate

Figure 4: Similarity of in vivo tumor with in vitro spheroid model system, in simulating the gradient of pH, oxygen concentration, nutrient availability and different proliferative status

Figure 5: Current model of melanoma outgrowth

Figure 6: Mechanism of fluorescently labelling of cells by CFDA-SE

Figure 7: (A) NA8 spheroid in DMEM 10% FCS, (B) Merging of NA8 spheroids, (C) D10 aggregate in DMEM 10% FCS, (D) D10 aggregate in DMEM 20% FCS

Figure 8: melanoma cell aggregates encapsulated within alginate beads

Figure 9: Irregularly shaped aggregates formed over agarose-coated dish

Figure 10: Multicellular spheroids formed on PolyHEMA coated 96 well plates: (A) NA8, (B) HBL

Figure 11: AlamarBlue proliferation curves of (A) NA8 and (B) HBL cells cultured in monolayer and as spheroid

Figure 12: Hematoxylin and Eosin staining of paraffin embedded sections of spheroids, showing NA8 and HBL spheroids formed a necrotic core after 10-12 days of culture on a PolyHEMA coated 96 well plate

Figure 13: Difference of morphology of cells from periphery and central part of the paraffin embedded H&E stained NA8 spheroids

Figure 14: BrdU staining of NA8 spheroid showed that peripheral cells are mainly in proliferating stage, whereas inner cells are mostly in quiescent stage

Figure 15: Gene expression profile for NA8 cells cultured as monolayer (with or without ECM) and as spheroid

Figure 16: AlamarBlue proliferation curves of HBL cells cultured in standard monolayer, monolayer over fibronectin coating and in MCTS

Figure 17: Gene expression profile for HBL cells cultured as monolayer (with or without ECM) and as spheroid

Figure 18: expression of CREB in NA8 cells cultured in monolayer without or with collagen, and as spheroids

Figure 19: expression of MCAM in NA8 cells cultured in monolayer without or with collagen, and as spheroids

Figure 20: Expression of IL-8 transcript in NA8 cells cultured in 2D, 2D with ECM and as MCTS

Figure 21: Expression of Tumor protein p53 transcript in NA8 cells cultured in 2D, 2D with ECM and as MCTS

Figure 22: Chemokine CXCL1 gene expression and protein secretion in NA8 cells cultured in monolayers and MCTS at two different time points

Figure 23: Chemokine IL8 gene expression and protein secretion in NA8 cells cultured in monolayers and MCTS at two different time point

Figure 24: Immunohistochemical detection of IL-8 in MCTS

Figure 25: Chemokine CCL20 (MIP3 $\alpha$ ) gene expression and protein secretion in NA8 cells cultured in monolayers and MCTS at two different time points

Figure 26: Differential chemotactic responses of (A) immature Dendritic cells, (B) total CD8<sup>+</sup> T cells to supernatant of NA8 melanoma cells cultured in 2D or as MCTS

Figure 27: Morphological view of T-lymphocytes attached over HBL spheroid by Scanning Electron Microscopy

Figure 28: Scanning Electron Microscopic view of tumor spheroid, showing integrated 3D structure of HBL spheroid, after 24 hours of co-culture with MART-1-specific CTL clones

Figure 29: Non-brisk infiltration of melanoma MCTS immunocompetent cells

Figure 30: Schematic view of antigen recognition and IFN- $\gamma$  production by T-lymphocytes

Figure 31: Functional activities of HLA-A0201 restricted Melan-A/MART-1<sub>27-35</sub> specific CTL clones (homogeneously tetramer specific, representative example in upper panel), using HBL melanoma cells cultured in 2D and 3D conditions (30000 cells per well) as targets. Panel A, B are representative of two different CTL clones.

Figure 32: Functional activities of a HLA-A0201 restricted gp100 specific CTL clone, showing homogeneous tetramer staining (upper panel), using HBL melanoma cells cultured in 2D and 3D conditions as targets.

Figure 33: Functional activities of HLA-A0201 restricted gp100-specific CTL clones using, D10 melanoma cells as targets cultured in 2D and 3D conditions

Figure 34: functionality of TAA specific CTLs is impaired within the 3D tumor spheroid microenvironment

Figure 35: CFDA-SE labeled proliferation of CTLs stimulated by melanoma cell lines, as detected by flow cytometry

Figure 36: IFN- $\gamma$  secretion by CTLs cultured with HBL from intact or disrupted MCTS

Figure 37: Melan-A/MART-1<sub>27-35</sub> immunostaining on cells from (A) disrupted spheroids and (B) monolayer cultured cells, 40X

Figure 38: MART-1 antigen expression in HBL melanoma cells in 2D or in MCTS: (A) by RT-PCR, (B) by flow cytometric analysis

Figure 39: Expression of gp100 in HBL and D10 cells by quantitative RT-PCR

Figure 40: Seeding of different cell number in single wells can result in the formation of spheroids of different volume

Figure 41: IFN- $\gamma$  production by two different CTL clones upon stimulation with HBL cells cultured in different cell densities (A: CTL clone name 2.6.1; B: CTL clone name 2.7.1)

Figure 42: Melan-A/MART-1 gene expression as related to different cell numbers in 2D and 3D cultures of HBL melanoma cells

Figure 43: Recovery of Melan-A/MART-1 antigen by gene expression by re-culturing in monolayer

Figure 44: Melan-A/MART-1 gene expression in tumor biopsies and comparison with HBL cells cultured in 2D and as 3D spheroid

Figure 45: (A) Modulation of gene expression of three tumor associated antigens with respect to different spheroid size and monolayer, (B) MITF gene expression in melanoma cells cultured in monolayer and as spheroids of different cell densities

Figure 46: HLA expression in HBL cells cultured in monolayer or in spheroid

Figure 47: Modulation of HLA expression in D10 cells cultured in monolayer or spheroid

Figure 48: HLA class I expression in melanoma cells cultured in 2D or in MCTS at different cell numbers

Figure 49: Expression of IRF-1 genes in melanoma cells cultured in 2D or in MCTS at different cell numbers

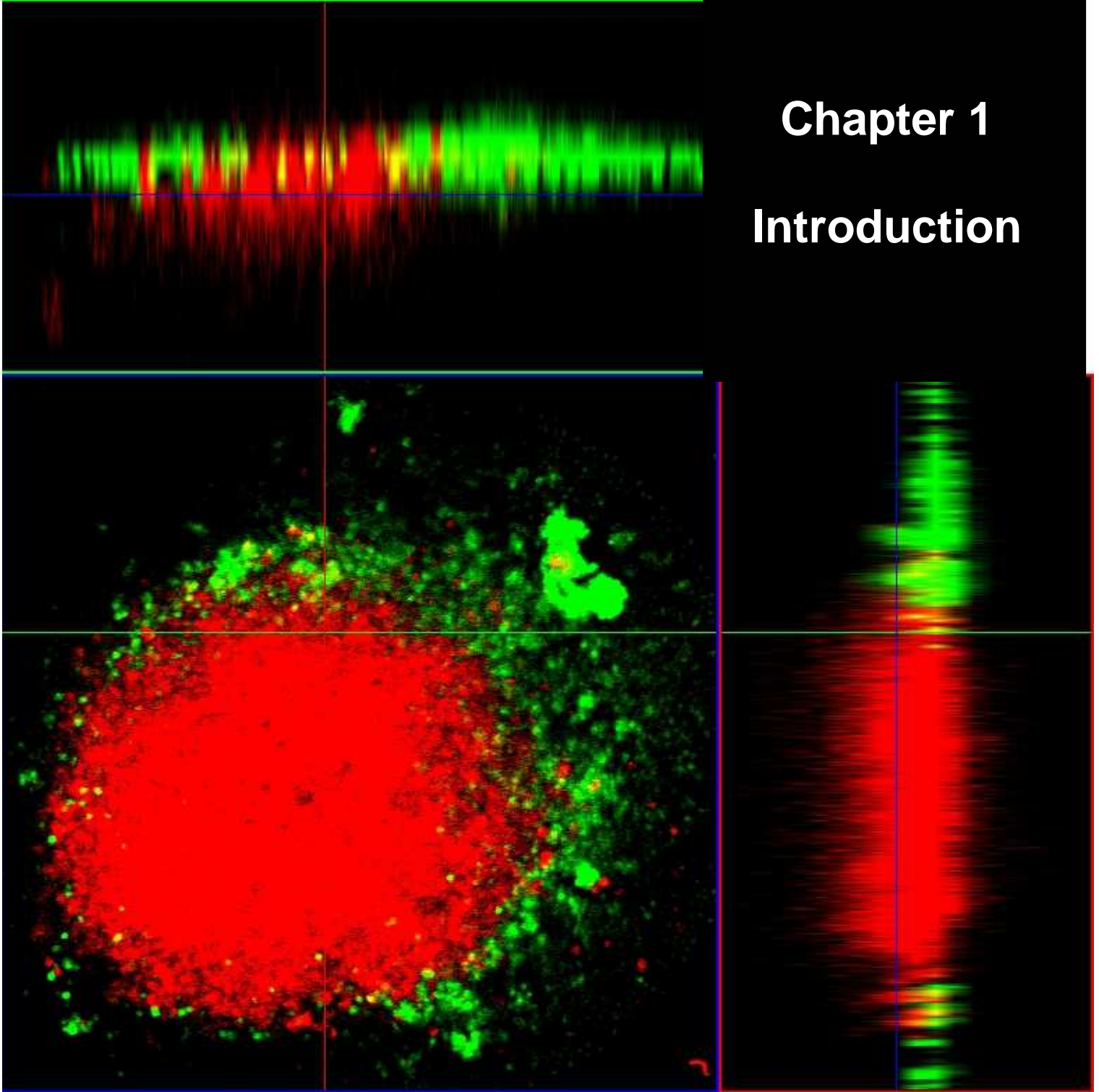
Figure 50: Effects of addition of exogenous lactate to HBL cells cultured in monolayers at different O<sub>2</sub> saturation levels on immunorecognition by antigen specific CTL

Figure 51: Immunofluorescence stainings of NA8 cells : (A) upper panel showing Vimentin (red), actin (green), co-expression in monolayer, (B) lower panel showing Vimentin (red), actin (green), co-expression in spheroid

Figure 52: Immunofluorescence stainings for Vimentin (red), actin (green) expression in HBL cells, (A) upper panel showing monolayer, (B) middle panel showing peripheral part of spheroid, (C) lower panel showing inner part of spheroid

# Chapter 1

## Introduction



*“Wat ik will is dat alles rond is en er als 't ware begin noch eind ergens aan de vorm is, doch die een harmonisch levend geheel uitmaakt”.*

*(What I want is for everything to be round without, so to speak, a beginning or end of the figure anywhere, so that it makes one, lifelike harmonious whole)*

**Vincent Van Gogh**  
(1853-1890)

Melan-A/MART-1<sub>27-35</sub> epitope-specific HLA-A\*0201 restricted CD8+ T lymphocytes could infiltrate only superficially in HBL spheroids, as analyzed by confocal microscopy.

## **1. Introduction**

Skin cancer has increasingly been brought into focus during recent decades in the international epidemiological community, due to steep upwards slope of trends for malignant melanoma. It is expected that more than 60,000 persons will be diagnosed and there will be death of around 8,000 melanoma patients in 2006 only in USA. (American Cancer Society: Cancer Facts and Figures 2006).

Increase in the incidence of malignant melanoma is strongly related to frequency of recreational exposure to the sun and to history of sunburn. United Nations Environment Programme (UNEP) has estimated that more than 2 million non-melanoma skin cancers and 200,000 malignant melanomas occur globally each year. In the event of a 10% decrease in stratospheric ozone, an additional 300,000 non-melanoma and 4,500 melanoma skin cancers could be expected worldwide. Caucasians have a higher risk of skin cancer because of the relative lack of skin pigmentation. Melanoma arises in melanocytes found along the basement membrane of the epithelium which synthesize, store and transfer melanin pigments to surrounding epithelial cells in skin. Radial growth of melanoma (e.g. few layers of neoplastic cells) has traditionally been associated with good prognosis.

### **1.1. Need for simple *in vitro* tumor model system:**

Rapidly developing anticancer research requires better understanding of tumor architectures and better model systems for cheap and rapid testing of therapeutic approaches *in vitro*. Growing evidence is supporting the idea that tumor microenvironment and tumor tissue architectures may be the ultimate regulators of the cellular phenotype and functions. These factors determine how the cancer cells interpret biochemical cues from their immediate surroundings. Currently, there is no “*in vitro*” model, utilizing human cells, allowing to adequately address these issues in controlled conditions. Simple and reproducible *in vitro* model systems using human cells are urgently needed to simulate the *in vivo* microenvironment of small avascular tumour.

Active antigen specific immunotherapy is currently being investigated in a number of clinical centers as treatment option for advanced stage melanoma. Although a variety of different vaccination procedures are capable of inducing Tumor associated antigen (TAA) specific

cytotoxic T-lymphocyte (CTL) “*in vivo*” in large percentages of immunized patients, but clinical responses are only detectable in a minority of them. Cytotoxicity assays or the functional monitoring of clinical immunotherapy trials are usually performed by utilizing, as targets, cell lines, frequently of lympho/myeloid origin, expressing appropriate HLA alleles upon pulsing with specific peptides. At present, in the human setting, typical experimental protocols imply the admixture of effector and target cells pelleted together in culture wells. The lack of correlation between data obtained “*in vitro*” with these technologies and clinical data of immunotherapy trials suggests that this model system might not adequately account for critical aspects of the interaction between immunocompetent cells and cancers.

## **1.2. Importance of simulating 3D tumor architecture**

Experimental murine models indicate that tumor cells in suspension, regardless of their numbers, are frequently unable to produce life threatening cancer outgrowth, as opposed to solid tumor fragments (Ochsenbein AF et al 2001), while inducing specific immune responses. Thus, proliferation in structured architectures appears to represent a pre-requisite for cancer development. Immunocompetent cells infiltrating *in vivo* 3D tumor architectures are often found to be functionally impaired. In particular, tumor infiltrating CD8+ cells staining positive for TAA specific multimers, have been reported to be in a quiescent state and unable to respond with IFN- $\gamma$  production to antigenic challenges.

Human tumours are complex three-dimensional tissues in which extensive cell-cell and cell-extracellular matrix (ECM) interactions take place, gradients of diffusible molecules develop and cells assume particular geometries. In contrast, simple *in vitro* two-dimensional conventional monolayer cultures limit the extent to which cell-cell and cell-ECM interactions can occur, diffusion gradients are absent, and cells are organized (and constrained) in a 2D plane. To a large extent it is these features that dictate the response to treatment, either directly or indirectly. Direct modulation arises for such reasons as drug transport limitations (diffusion) and altered physiochemical environment (e.g., the efficacy of radiotherapy is reduced in low oxygen environments). Indirectly, the microenvironmental features of a tissue direct cellular phenotype and function. Changes in protein expression, cell physiology, and cell-cycle status attenuate the response to anti-tumor treatment. A classic example is that many chemotherapeutic agents target proliferating cell population, yet a significant proportion of tumour cells enter a quiescent state

due to reduced availability of nutrients and oxygen (diffusion limitation). In contrast monolayer cultures are generally in a replicative state, making them more susceptible to treatments.

Hence it is critically important to understand 3D tumor microenvironment for designing a successful treatment protocol. Many microenvironment changes occur within an *in vivo* tumor as a result of its 3D architecture and insufficient vascular function. Small avascular tumor nodules as well as microregions of large tumors can develop a typical tumor microenvironment niche in which there may be major gradients of oxygen, glucose, lactate, H<sup>+</sup> ions, other nutrients, growth factors, toxic waste products. This heterogeneous environment along with instability of malignant genome can generate diverse phenotypes responsible for altered responses to therapeutic agents.

One approach of investigating the biology of this heterogeneous tumor microenvironment is by culturing cancer cells in the form of three-dimensional tumor spheroids. This model system have been developed in the past decade, aiming at exploring radio or chemoresistance of tumor cells in “in vitro” assays more closely related to “*in vivo*” conditions than standard monolayers. In the late 1950s, multicellular aggregates of cells were first proposed by Holtfreter (Holtfreter J 1944) and Moscona (Moscona A 1957). Around early 1970s Sutherland and coworkers systematically investigated the response of tumor cell aggregates to anti-neoplastic therapy. Because the cell lines formed nearly perfect sphere-shaped cell aggregates, they were called "spheroids." (Sutherland RM et al 1971; Sutherland RM 1988).

### **1.3. Multicellular tumor spheroid model system**

Multicellular tumor spheroids (MCTS) have been reported to accurately represent early events of avascular tumor growth especially with respect to growth kinetics, cellular heterogeneity (e.g. the induction of proliferation gradients and quiescence), as well as differentiation characteristics, such as the development of specific histological structures or the expression of antigens, morphological features of poorly vascularised tumour regions and micrometastases (reviewed by Mueller-Klieser W 1987; Sutherland RM 1988; Desoize et al. 2000). MCTS remind *in vivo* cancers in their capacity to develop necrotic areas far from nutrient and oxygen supplies. Furthermore, cells cultured in MCTS are also similar to solid tumors in their proliferation dynamics (Gorlach A et al. 1994). Unlike the conventional monolayer cultures, proliferation curve of MCTS typically fit the Gompertz equation, which is classically used to



quantitatively evaluate neoplastic growth (Bajzer et al. 1997; Chignola et al. 2000). Most importantly, it has been shown that MCTS display different metabolic characteristics (Santini MT et al. 1999) and a decreased sensitivity to apoptosis due to radio-chemo treatments or to death receptors ligation (Santini MT et al. 2000) as compared to their 2D cultured counterparts. As already reported by several groups, 3D architecture of MCTS can regulate gene expression pattern and cellular differentiation (Grover A et al. 1983; Sutherland RM et al. 1986; Dangles V et al 2002). But the genetic and molecular bases of the biological peculiarities found in malignant cells grown as three-dimensional aggregates still need to be systematically investigated.

Due to such close similarities with *in vivo* tumor, MCTS model system have been widely used in biomedical research (Mueller-Klieser W 1997) - mostly as an *in vitro* model for systematic studies of tumor cell response to radiotherapy and chemotherapy. Evidence is accumulating in support of the thought that the tight intercellular contact, rather than attachment to artificial substrate, could represent the key factor for enhanced resistance to cytotoxic agents like, radiation, heat, ultrasound, drugs (Durand RE et al. 1975; Sacks PG et al. 1981). Adjacent cells in MCTS are held together by surface membrane microprojections, extracellular matrix and a variety of cell-cell junctions (desmosomes, tight junctions, junctional complexes, gap junctions). The frequency of these junctions varies widely among spheroids of different cell lines. Cell surface proteins, allowing  $Ca^{2+}$ -dependent or independent adhesion, from the selectin (binding to carbohydrate groups), cadherin and integrin (cell surface protein binding) families facilitate recognition and adherence between cells. In addition to the obvious role of cell-cell adhesion, binding of these proteins to the appropriate ligands results in conformational changes, transmitting a signal across the cell membrane to the cytosol (Bates RC et al. 2000).

However there is a curious paucity of research regarding immune responsiveness to tumor cells cultured in 3D architectures. We envisage that further exploration of the interaction of tumor microenvironment with immune cells may help gathering improved understanding about immune recognition process and in turn this may lead to better therapeutic strategies.

## **1. 4. Spheroid culturing techniques**

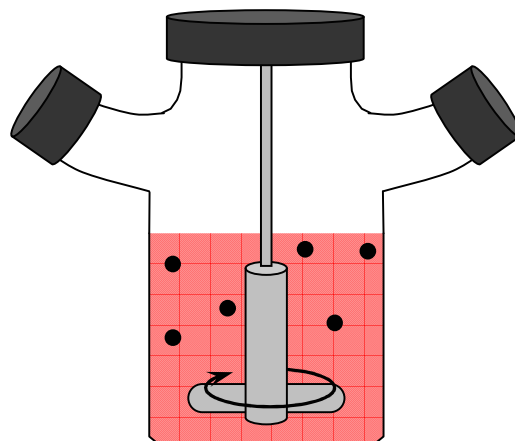
### **1.4.1. Introduction**

The development of appropriate *in vitro* models that may reflect the *in vivo* tumor environment may represent a key factor for the study of malignancies. Although lacking of

stroma and the vasculature of in vivo solid tumors, MCTS model systems have many similarities to in vivo cancers. Several different methods to cultivate MCTS are available, their suitability depending on the particular application. All these methods have in common the cultivation of cells in a non- or poorly adherent environment. With no accessible substratum to which they might adhere, naturally anchorage dependent cells self-aggregate and develop into spheroids.

#### 1.4.1.1. Stirred cultivation methods

To avoid the complication of a nonhomogenous environment, Moscona introduced the spinner flask method in the early 1960's for the cultivation of embryonic cells (Moscona A 1957; Moscona MH et al 1963; Moscona A 1968). This method was later adopted by several groups (Sutherland RM et al. 1976; Wiens AW et al. 1972) for the cultivation of MCTS. In this approach cells are stirred at 150-200 rpm to inhibit adhesion to the flask and to maintain them in



Spinner flask

Figure 1: Traditionally used spinner flasks for preparing multicellular spheroids

suspension (Figure-1). Co-incidental collision and adherence of cells with each other result in the formation of aggregates. Today this is achieved using spinner flasks, shake flasks, or roller bottles, and large numbers of spheroids can be generated with minimal handling. Unfortunately shear sensitive or weakly adherent cells often fail to aggregate and develop into spheroids in these systems, although a pre-formation step in static culture may be used. Additionally, the random nature of aggregate formation typically results in MCTS populations of widely

distributed size, and for analytical purposes a selection step is required (Santini MT et al 1999). Possible effects of the mechanical forces on cellular phenotypes must also be considered.

Another popular approach to MCTS cultivation is the rotating wall vessel bioreactor (RWVB), or microgravity bioreactor (Figure 2). The rotating bioreactor was invented by NASA as a model of microgravity effects on cells to generate a three-dimensional tissue construct (Hammond TG et al 2001). Freed et al (Freed LE et al 1997) grew specimens of bovine cartilage tissue under both normal (Earth) and microgravity conditions (Mir), and reported that initially disk-like specimens became spherical in space, whereas constructs grown on Earth maintained their initial disk shape.

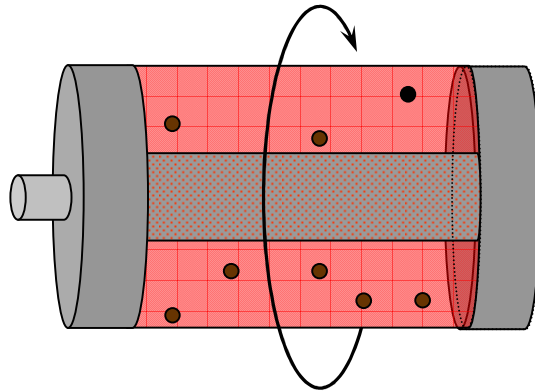


Figure 2: Rotating wall vessel bioreactor

In RWVB cells are maintained in suspension by randomizing the gravity vector, leaving them in a state of perpetual freefall to facilitate aggregation and formation of spheroidal tissue (reviewed in Hammond TG et al 2001). This approach combines the advantages deriving from stirred flasks (e.g., large numbers/volumes) with a gentle environment that facilitates cell-cell adhesion, while providing excellent bulk mixing of the cultivation medium (Licato LL et al 2001; Song H et al 2004; Simons DM et al 2006).

#### 1.4.1.2. Hanging-drop method

The use of hanging drops in the production of cellular aggregates has been first reported for non-neoplastic cells (Kennedy TE et al. 1994). Recently Kelm et al. (Kelm JE et al 2003) adopted this method for the generation of MCTS. In this method a small volume (20–30  $\mu\text{L}$ ) of

cell suspension is dispensed into the wells of a 60-well micro-titer Terasaki plate. The plate is then inverted, resulting in a hanging-drop by surface tension of the culture medium. Under the influence of gravity, cells settle at the medium-air interface, where they subsequently aggregate and develop into multicellular Spheroid. This approach avoids contact with any artificial substratum and provides a very gentle environment, and it has been reported to result in spheroid population of narrowly distributed size. A major drawback is the limited volume of culture medium that can be employed due to the design of the plates, limiting cultivation periods and producing very small spheroids.

Hanging-drop method has also been employed by cancer researchers to generate confrontation cultures for studies of tumour invasion and angiogenesis (Timmins NE et al 2004). As demonstrated by Del Duca et al. (Del Duca D et al 2004), the hanging-drop method can also be combined with that of liquid overlay, aggregating cells in hanging drops and subsequently cultivating in overlay culture.

#### **1.4.1.3. Gel encapsulation**

Gel encapsulation approaches have also been employed for the generation of MCTS (Kupchik HZ 1983; O'Keane JC et al 1990; Kupchik HZ et al 1990; Hoffmann J et al 1997). A cell suspension is mixed with a gelling agent (e.g. alginate or agarose) which is dispensed dropwise into a setting agent (e.g.,  $\text{Ca}^{2+}$  solution for alginate, or reduced temperature for agarose). One advantage of this method is that in some respects it recreates the physically constrained environment encountered *in vivo*, where tumor tissue is surrounded by other tissue. It has been shown that growth induced stress in agarose encapsulated cultures can induce ECM synthesis and growth inhibition, and decrease the rate of apoptosis (Helmlinger G et al. 1997). Solid stress can also facilitate MCTS formation especially for highly metastatic cancer cell lines that do not easily form spheroids. Growth-inhibiting stress in the range of 45-120 mmHg can increase ECM (hyaluronan) synthesis by tumor cells (Koike C et al 2002). Stress release, however, may cause loss of MCTS integrity. Cells have also been cultivated first as spheroids in spinner flasks and then entrapped in alginate-polyLysine beads. But the entrapped spheroids did not increased in size or number whereas free spheroids in suspension increased in size (Papas KK et al. 1993).

#### 1.4.1.4. Static cultivation methods

A most common and simple approach to the cultivation of MCTS is that of liquid overlay. Cell culture dishes are coated with a non-adherent medium (e.g., agarose, agar, poly-Hydroxyethyl methacrylate), or fabricated from non-adherent materials (e.g., polystyrene Petri dishes), and a cell suspension layered over top (Yuhas JM et al 1977). Cells settle onto the non-adherent surface, but are unable to find anchorage site and subsequently assemble into aggregates. This method is well suited for use with cells that are particularly sensitive to shear or are only weakly adherent.

Poly(2-Hydroxyethyl methacrylate) (PolyHEMA) was first described by Woodhouse (Woodhouse JC. US Patent 2 129 722) and later widely used as a hydrogel for making contact lens, as proteins do not easily adhere to it. Application of PolyHEMA hydrogels as biomaterials gained quick popularity as some of its physical properties are similar to living tissue (high water content, soft and rubbery consistency, hydrophilicity, water permeability, low interfacial tension). PolyHEMA is well known to prevent cellular adhesion and spreading (Folkman J et al. 1978).

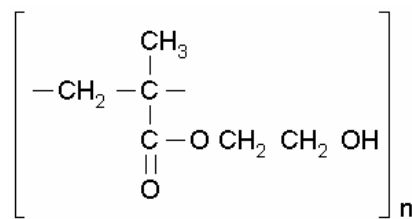


Figure 3: Chemical composition of Poly-Hydroxy ethyl methacrylate

Although widely employed, these static methods of MCTS cultivation have several undesirable features. Under such conditions the rate of aggregate formation is variable, essentially being a random process, and the resulting MCTS vary in size. As the MCTS lie on top of a solid substratum, diffusion may not be homogeneous and this complicates theoretical analysis, while the lack of stirring can lead to heterogeneity in the cultivation medium. Furthermore, possible interactions with the substrate cannot be easily discounted (Santini MT et al 1999). Simple modifications of the general approach can be employed to address some of these issues. Controlled aggregation of individual MCTS can be achieved by cultivation in 96-well plates coated with PolyHEMA (all cells contributing to one MCTS in each well), and shakers can be used to facilitate mixing of the medium.

## 1.4.2. MCTS Characterization

### 1.4.2.1. Growth kinetics of MCTS

Kinetics of cell growth can be measured by incorporation of tritium-thymidine (Carlsson J 1977; Nederman T et al. 1988) or by reduction of Alamar Blue (Ghosh S et al. 2005a). Alamar Blue is a non-toxic chemical, stable at culture medium, which can be used to monitor the reducing environment of the proliferating cell.

Multicellular tumor spheroids closely resemble *in vivo* solid tumors in their growth dynamics. The Gompertz equation is traditionally used to describe the size-limiting growth of tumours and tumour spheroids and is given by:

$$D(t) = D_{\max} \exp\left\{-\exp(-at)\ln\left(\frac{D_{\max}}{D_0}\right)\right\}$$

in which  $D_0$  and  $D(t)$  are measures of spheroid size (either diameter or volume) at initial time and time  $t$  respectively,  $D_{\max}$  is the limiting size, and  $a$  is the specific growth rate (Winsor 1932; Ward JP et al 1997). The resulting growth curve has a sigmoidal shape and reflects a continuously increasing doubling time that causes an asymptotic approach to size  $D_{\max}$ . The Gompertz equation was used to fit the spheroid growth curves of diameter vs time (Marusic M et al 1994).

### 1.4.2.2. Morphological characterization

The value of three-dimensional MCTS in tumour research stems from their similarity to *in vivo* tumours, and this is readily apparent from a comparison of physiochemical environment, cell status and growth kinetics. “*In vivo*” the distance from the nearest capillary limits diffusion resulting in a decrease in the availability of nutrients and oxygen with build-up of gradient of metabolic products. A corresponding gradient in cellular status is observed, with proliferating cells near the capillary and quiescent cells in the underlying regions, followed by areas of necrosis.

Thomlinson et al (Thomlinson RH et al. 1955) and Tannock (Tannock IF 1968) showed that within solid tumor *in vivo* only the cells near capillaries were proliferating and the cells at a distance of about 100–200  $\mu\text{m}$  from the vasculature were degenerating. However, both of these studies were carried out in tumors with a pronounced nodular appearance; penetrating vessels and capillaries were surrounded by rather thin layers of viable cells. In general, regions of massive necrosis are often seen in fast growing *in vivo* malignant tumors (Rubin P et al 1968; Folkman J 1975). The fraction of viable and proliferative cells and the degree of nodular appearance seem to

vary widely between different tumor types (Ackerman LW et al 1974). Vascularisation-deficient areas of tumor have retarded growth rate, due to inadequate nutrition, accumulation of catabolic products- which may produce low pH, high osmolality, or other toxic effects. A continuously decreasing fraction of proliferating cells, a continuously increasing frequency of cell death and

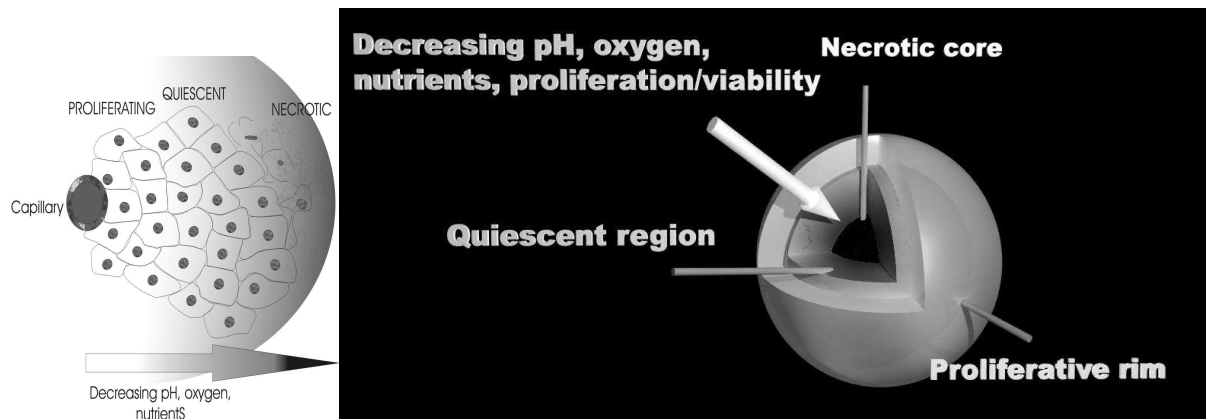


Figure 4: Similarity of in vivo tumor with in vitro spheroid model system, in simulating the gradient of pH, oxygen concentration, nutrient availability and different proliferative status

accumulation of debris from dying cells are some of the histological changes associated with tumor progression (Steel GG, 1977). Poorly vascularized regions may also be difficult to reach with cytotoxic drugs, immunological agents (e.g., immunoglobulins, macrophages, cytotoxic T lymphocytes). Very similar to the morphology of *in vivo* tumor, the same gradient of physiochemical environment and cell status is observed while progressing from the outer edge of MCTS towards the center (Figure 4).

Multicellular tumor spheroid morphology has the potential to closely resemble *in vivo* tumors by their capacity to develop necrotic cells in areas far from nutrient and oxygen supplies. Unlike conventional monolayer cell culture of exponential or plateau phase, there is always significant metabolic diversity in spheroids, somewhat similar to the *in vivo* tumors. Position of a particular cell in the spheroidal aggregate may have critical influence on the fate of governing cellular function (Folkman J et al 1973). Rosenstrauss et al showed that in a spheroid near peripheral position is essential to differentiate embryocarcinoma cells into functional visceral endoderm cells (Rosenstrauss MJ et al 1983).

Within the spheroid, cells deposit their own extra cellular matrix in extensive amount as compared to the monolayer cell culture, which had been reported by many groups (Glimelius B et

al. 1988). Nederman et al showed that spheroids of a human glioma cell line and a human thyroid cancer cell line can generate ECM composed of fibronectin, laminin, collagen (demonstrated by microscopy and indirect immunofluorescence) and glycosaminoglycans in a similar organization to that of tumors *in vivo* (Nederman T et al. 1984).

Beyond a critical size of 500 $\mu$ m, most spheroids from permanent cell lines develop a necrotic core surrounded by a viable rim of cells (100-300  $\mu$ m) consisting of proliferating cells in the spheroid periphery and quiescent, yet intact and viable cells close to the necrotic center. The size at which necrosis starts and the thickness of the viable rim of cells differ from cell types, culture medium, duration of culture etc. Larger dimensions would result in a greater difficulty for oxygen and nutrients to reach the cells located in the center of the spheroid thus leading to the formation of a necrotic central area (Walenta S et al 1990). Consequently, the cell number and culture time after spheroid formation should be critically evaluated before beginning a study, and spheroid size should be established to suit particular experimental needs.

## **1.5. Gene expression**

### **1.5.1. Introduction:**

Hallmark of carcinogenesis is a combination of mainly three factors- (a) decreased genomic stability together with (b) specific genetic changes in oncogenes and tumor suppressor genes and (c) faulty DNA-repair mechanisms. Compared to the cells cultured *in vitro* in monolayer on a Petri dish, the cells in a tumor are in close contact with the extracellular matrix. Growing evidence is indicating that there is a functional continuity between the extracellular matrix, the cytoskeleton, hypoxia, nuclear matrix with both direct and indirect effects on gene expression (Boudreau N et al 1995). Comparison of gene expression pattern in cells cultured in monolayer and 3D spheroid can give some insight about the effect of 3D tumor microenvironment on gene expression profile.

### **1.5.2. Regulation of gene expression by 3D tumor architecture**

Characteristics of cancer cells are traditionally assessed in a monolayer environment in plastic culture dishes in the presence or absence of coating of ECM macromolecules (such as collagen, fibronectin, hyaluronic acid etc). Cell shape can play critical role in gene expression and controlling growth and cellular differentiated functions, via cytoskeleton modulation (Folkman J et al 1975). In conventional monolayer culture the cell shape is mainly governed by



the affinity of the cells for the substratum, surface morphology. So a perfect selection/choice of substratum is needed in monolayer culture, to maintain differentiated cellular functions for each cell type. But in spheroid culture, no particular cell shape is dictated/imposed on the cell. One might postulate that cell shape in spheroid is mainly governed by the intrinsic homotypic cell-cell adhesive interactions, specific microenvironmental conditions and by the nature of extracellular matrix produced by the cell type. This 3D architecture of tumor cells, with a critical influence of hypoxia, may dictate specific gene expression patterns of potentially high functional relevance.

ECM produced by cancer cells in MCTS can regulate gene expression pattern and cellular differentiation. In monolayer culture, differentiation is not markedly observed, but in spheroids often differentiation is induced. This differentiation is reported to be intermediate between monolayer and in vivo xenografts in nude mice (Knuechel R et al. 1990; Sutherland RM et al. 1986). Grover et al (Grover A et al. 1983) showed that when exogenous Laminin was deposited on the outer side of the F9 spheroids in addition to the normal position of endogenous Laminin below the first cell layers a lack of expression of differentiated functions was observed, possibly due to asymmetric arrangement of cells. Endogenous Laminin plays a key role in organizing the epithelial layer of endoderm cells and hence indirectly affects gene expression. It has also been (Grover A et al. 1985) showed that in aggregated F9 embryonal carcinoma cells fibronectin has a role in aggregation whereas laminin is important in the differentiation process.

The expression of specific sets of genes might also be modulated by hypoxia and cell cluster architecture (Poland J. et al. 2002). Systemic studies of modulation of gene expression within the tumour microenvironment could help identifying potential new targets for rational drug design. Knowles et al (Knowles H J et al. 2001) studied the gene expression pattern in spheroids by differential display and validated it by Northern blot or semiquantitative RT-PCR.

Oloumi et al (Oloumi A. et al. 2002) studied gene expression modulation in Chinese hamster V79 cells by differential display technique. Genes upregulated in the outer cell layer of spheroids relative to monolayers included: (1) mts1 (S100A4), a calcium binding protein implicated in proliferation, metastasis, cell adhesion, and angiogenesis, (2) cytochrome c oxidase II, (3) B-ind1, a mediator of Rac-1 signaling, (4) TRAM, an endoplasmic reticulum protein. Genes downregulated in spheroids were: (1) phosphoglycerate kinase, (2) ARL-3, a ras-related GTP binding protein, (3) MHC class III complement 4A and (4) 2,4-dienoyl-CoA.

Dangles et al (Dangles V et al. 2002) studied influence of culture condition over gene expression profiles which enabled them to shortlist 28 key genes using three bladder cancer tissue

specimens and their derived cell lines in single-cell suspensions, 2D monolayers and 3D multicellular spheroids (having 10,000 cancer cells per spheroid) and showed how the *in vitro* spheroid model may closely mimick *in vivo* phenotypes of tumours.

Timmins et al (Timmins NE et al. 2004) used microarrays comprising 18,664 human gene-specific oligonucleotides (Compugen) to shortlist 42 genes which were differentially expressed by more than 2-fold using monolayer and spheroids (8 days old) of HCT116 colon carcinoma cell line. Three of them might contribute to the multicellular drug resistance phenotype (S100A4, SKIP3, and p48). S100A4 was 2.3 fold upregulated in MCTS compared to monolayer. SKIP3 (down-regulated 2.4-fold in MCTS) is an NF- $\kappa$ B inducible gene, and a negative feedback inhibitor of NF- $\kappa$ B dependent gene expression. NF- $\kappa$ B is known to confer resistance to cytotoxic therapies via suppression of apoptosis, and its transcriptional activity is regulated by phosphorylation of the p65 subunit. p48 was up-regulated 4.4-fold in spheroid than monolayer. Out of 42 shortlisted transcripts 13 are involved in interferon response, 10 are differentiation related, and 14 are differentially regulated in tumours as compared to healthy tissue.

### **1.5.3. Gene expression pattern in melanoma**

Most melanomas arise within the epidermis (melanoma in situ) and then invade the basement membrane. These melanoma cells escape from control by keratinocytes through five major mechanisms:

(1) downregulation of receptors important for communication with keratinocytes such as E-cadherin, P-cadherin, and desmoglein, which is achieved through growth factors such as hepatocyte growth factor, platelet-derived growth factor, and endothelin-1 produced by fibroblasts or keratinocytes.

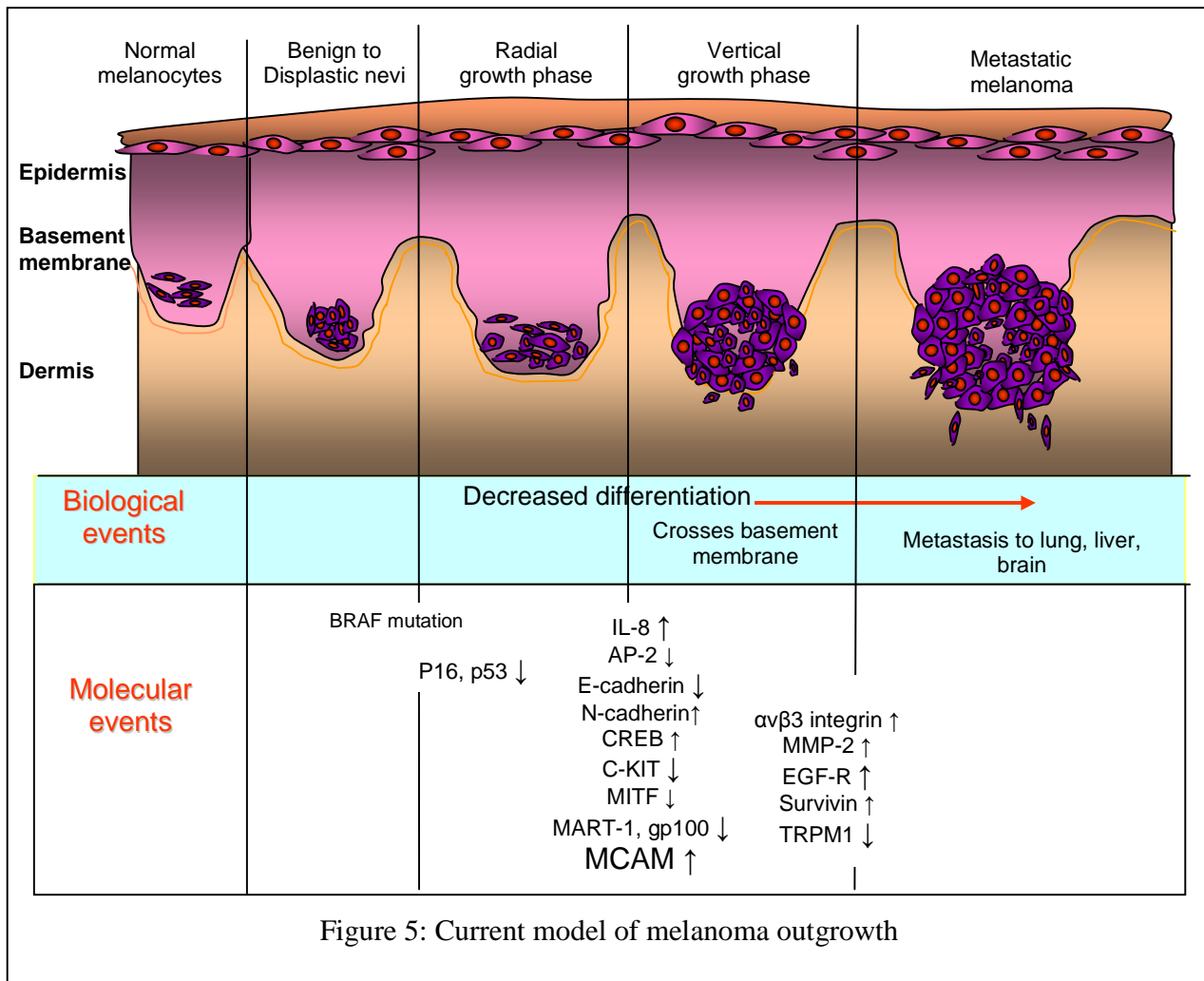
(2) upregulation of receptors and signaling molecules important for melanoma cell-cell and melanoma cell-fibroblast interactions such as N-cadherin, Mel-CAM (MCAM), and zonula occludens protein-1 (ZO-1).

(3) deregulation of morphogens such as Notch receptors and their ligands.

(4) loss of anchorage to the basement membrane due to an altered expression of cell-matrix adhesion molecules.

(5) increased expression of metalloproteinases.

The most frequent genetic aberrations in malignant melanoma are rearrangements in chromosome 1, in tumor suppressor genes. Chromosomal abnormalities such as duplication, deletion, mutation of genes on chromosomes 6, 7, 9, 10, 11, 22 and Y have also been reported. Several groups addressed gene expression profiles of melanoma cells in different clinical and physiological form (Carr KM et al. 2003; Bittner M et al. 2000; Clark EA et al. 2000; Hayward NK 2003).



Normal melanocytes are generally arranged individually at the epidermal-dermal junction or in small organized clusters of benign nevus. Primary melanoma progresses by the steps showed in Figure 5, including:

- (i) **Radial growth phase** which is characterized by horizontal spreading of transformed melanocytic cells within the epidermis and small nests of invasive cells limited to the upper part of dermis.

(ii) **Vertical growth phase** characterized by invasion of melanoma cells into the deeper dermis and underlying subcutaneous tissue. Then melanoma cells from this phase metastasise to regional lymph nodes or to distant organs.

Activating mutations in BRAF are very frequent in melanomas (detected in 59% of melanoma cell lines and 6/9 melanoma specimens) (Davies H et al 2002), indicating that BRAF would be a legitimate target of experimental therapy of melanoma.

Another report shows that overexpression of RhoC, a member of Rho family of GTP-hydrolyzing proteins, is important for tumorigenesis in melanoma and its metastases. (Clark EA et al 2000)

Progression from radial growth phase to vertical growth phase is associated with loss of E-cadherin and expression of N-cadherin. Expression of  $\alpha_v\beta_3$  induces expression of matrix metalloproteinase-2, an enzyme that degrades the collagen in basement membrane. In addition  $\alpha_v\beta_3$  also stimulates the motility of melanoma cells through reorganization of cytoskeleton and increased expression of anti-apoptotic bcl-2 (Petitclerc E et al. 1999). There is no systematic comparative study on melanoma using monolayer cell culture and spheroid culture system, which may simulate progression from radial growth phase to vertical growth phase.

## **1.6. Immune recognition**

### **1.6.1. Introduction**

The identification of a large series of tumor associated antigens (TAA) (Renkvist N et al 2001) has generated high hopes regarding the possibility to take advantage of the enormous increase of knowledge stemming from basic immunology research to favorably steer the prognosis of neoplastic diseases by active antigen specific immunotherapy, i.e. by vaccination. Promising clinical data have been reported in many trials based on diverse immunization procedures (Rosenberg SA 1998; Rosenberg SA et al 1998; Nestle FO et al 1998; Thurner B et al 1999; Slingluff CL et al 2003; Bedrosian I et al 2003). A common finding in these clinical trials irrespective of immunization procedures is that, although cytotoxic T lymphocyte (CTL) responses specific for TAA can be relatively easily induced, clinical responses are only rarely observed. Within that context MCTS model system could be useful tool to simulate the effect of tumor microenvironment /architecture on activation of defense cells and to understand mechanisms of immune escape (Ganss R et al 1998; Parmiani G et al 1990).

The molecular mechanisms underlying the discrepancy between immunological and clinical responsiveness to active antigen specific immunotherapy have been investigated by several groups, but still there is poor understanding about the effect of 3D tumor architecture to the immune responsiveness. Experimental models indicate that tumor cells in suspension, regardless of their numbers, are frequently unable to produce life threatening cancer outgrowth, as opposed to solid tumor fragments (Ochsenbein AF et al 2001), while being able to induce specific immune responses. Radial growth of melanoma (e.g. few layers of neoplastic cells) has traditionally been associated with good prognosis. Thus, proliferation in structured three dimensional architectures appears to represent a pre-requisite for cancer development.

### **1.6.2. Infiltration of MCTS by TAA specific T cells.**

Tumor infiltration by T-lymphocytes, macrophages, monocytes was long thought to be a hallmark of the immune response to the tumor (Virchow R 1863, Brocker EB et al. 1988). T cell infiltration in primary melanoma was reported to correlate with a better eight year survival rate (Halpern AC et al 1997). Previous work on clinical materials suggests that detection of tumor infiltrating lymphocytes is indeed associated with improved prognosis in melanoma, but only in cases where a “brisk” (Clemente CG et al. 1996; Anichini A et al. 1999) and not a merely superficial infiltration can be observed. Interestingly even *in vitro* experiments, tumor infiltrating lymphocytes of undefined antigenic specificity, capable of killing autologous bladder tumor cells cultured in 2D or in suspension, have been shown to be unable of recognizing targets cultured in 3D (Dangles V et al. 2002). Similarly a CTL clone specific for a mutated  $\alpha$ -actinin-4 peptide expressed by autologous lung cancer cells poorly recognized targets growing in MCTS, possibly due to a down-regulation of HSP70 expression (Dangles-Marie V et al. 2003). Furthermore Fas ligand (FasL) gene was found to be expressed in HRT-18 and CX-2 colorectal cancer cell lines cultured as MCTS but not in 2D (Hauptmann et al. 1998). Clearly these data suggest that antigen recognition capacities and resulting functional activities of CTL might be significantly altered in the presence of tumor cells growing in three dimensional architectures.

In melanoma patients, T-lymphocytes specific for TAA do appear to be immunologically silent or anergic not only at the tumor site even when patients display a high frequency of circulating, memory melanoma specific CTL (Anichini A et al 1999), but also in systemic circulation (Lee PP et al 1999). This is consistent with the discrepancies observed between detectable tumor specific immune responses and lack of clinical effectiveness represented by

frequently observed in active specific immunotherapy of melanoma (Anichini A et al 2004). Taken together, these data suggest that antigen recognition capacity and the resulting functional activities of cytotoxic T-Lymphocytes might be significantly altered in the presence of tumor cells growing in multilayered architectures. Although significant amount of work has been done to characterize spatial distribution and infiltration of tumor infiltrating lymphocytes using spheroid models, our understanding of the cancer cell-lymphocyte interaction is still rather limited.

### **1.6.3. Modulation of immunorecognition**

Tumor antigens expressed *in situ* may be capable of inducing antitumor T cell immune responses (Mortarini R et al. 2003). However, past work from our group has underlined the lack of expression of genes typically transcribed upon TCR triggering of T cells in metastatic melanoma biopsies infiltrated by CD8<sup>+</sup> lymphocytes expressing activation markers, and capable, following “*ex vivo*” culture, of recognizing TAA on autologous tumor cells (Luscher U et al. 1994). Tumor escape from CTL recognition has been attributed to down-regulation of TAA or HLA class I molecules expression resulting from the selection of resistant variants in neoplastic cell populations exposed to immunological pressure. However, this mechanism, whose “*in vivo*” relevance is hotly debated, might indirectly support the concept of a clinical efficacy of CTL induction, whose evidence is mostly missing (Marincola FM et al. 2003a; 2003b). On the other hand, more recently, the discrepancy between induction of TAA specific immune responses and clinical responsiveness has also been attributed to CTL defects.

### **1.6.4. CTL mediated immune response**

When the complex of tumor antigen epitope bound to MHC-1 is engaged by antigen-specific T cell receptor, the cytotoxic T cell induces death of the target cells primarily by two pathways, involving granule-mediated apoptosis and/or Fas/Fas-ligand interaction.

When CTLs are activated by recognition of specific antigen on a cell, they release perforin and other lytic enzymes into the intercellular space between lymphocyte and target cells. Perforin undergoes a Ca<sup>2+</sup> induced conformational change, integrates into the membrane of the target cell and forms a membrane pore. This allows the protease granzyme to enter into the cancer cell and activate the apoptotic caspase proteolytic cascade, and also allows other molecules to cross the cell membrane and trigger osmotic lysis of the membrane.

The interaction of T-cell Fas ligand with the Fas receptor in the target cell can also activate the caspase cascade and other pathways involved in apoptosis. The interaction of a CTL with antigen-MHC I complex may induce them to proliferate, thereby amplifying the immune response against that specific antigen.

Lytic functions of CD8<sup>+</sup> TILs have been found to be defective in vivo (Whiteside TL 1998). Typically freshly isolated TILs do not lyse cognate tumor cells or MHC matched tumor cells but this deficient lytic function is transient. Following separation from tumor cells and culture in vitro in presence of exogenous IL-2, tumor specific killing can be detected (Rajoda S et al 2001).

#### **1.6.5. Accumulation of Lactic acid causing poor tumor infiltration by immunocompetent cells**

In previous studies it has been demonstrated that low oxygen level and poor glucose concentration may influence the metabolism and proliferative characteristics of cells (Marx E et al. 1988) and promote the development of necrotic cores (Sutherland RM et al. 1986; Mueller-Klieser W et al. 1986). Furthermore it has been reported (Marx E et al. 1988, Bourrat-Floeck B et al. 1991) that production of lactic acid is substantially enhanced in spheroids as compared to monolayer culture, similarly to in vivo tumor samples. In clinical tumor biopsies lactate has been shown to accumulate up to a concentration of > 20 mM (Rauen et al 1969). Hypoxia in a tumor can induce production of glycolytic enzymes and glucose transporter (LDH), which can lead to enhanced glycolytic flux for energy production, causing accumulation of lactic acid. High lactate level can correlate with metastasis and clinical outcome (Walenta S et al 2000). So accumulation of lactic acid can cause high extracellular acidity in a tumor, preventing immune cells to infiltrate inside the tumor (Walenta S et al 2004; Lardner A 2001). Gottfried et al (Gottfried E et al 2006b) showed that infiltration of monocytes in the melanoma spheroids can be controlled by using oxamic acid (as an inhibitor of LDH) to suppress endogenous production of lactic acid. Thus tumor-derived lactic acid may be considered an important factor modulating the tumor environment, critically contributing to tumor escape mechanisms.

### **1.7. Research plan:**

This thesis work has the following specific aims:

**Specific aim 1:** Development of a simple in vitro three dimensional tumor model

**Specific aim 2:** Characterization and validation of gene expression profiles differentially detectable in melanoma cell lines cultured in standard monolayer conditions and as MCTS.

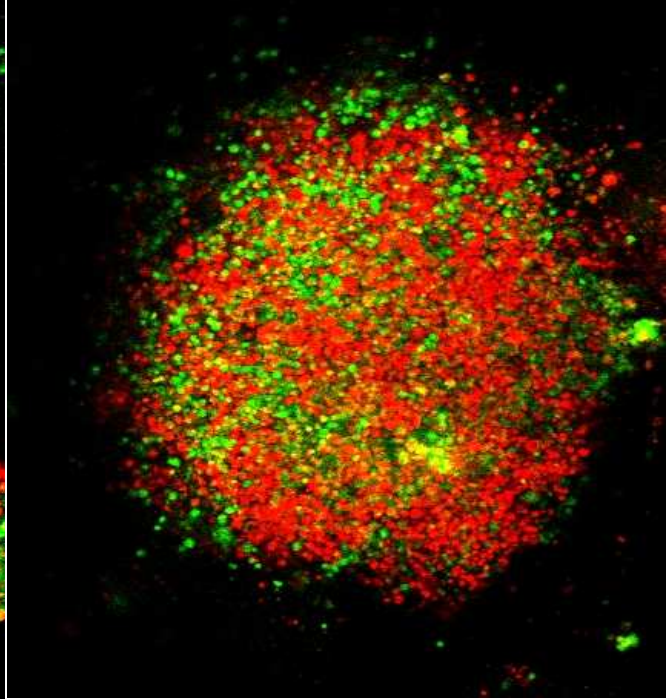
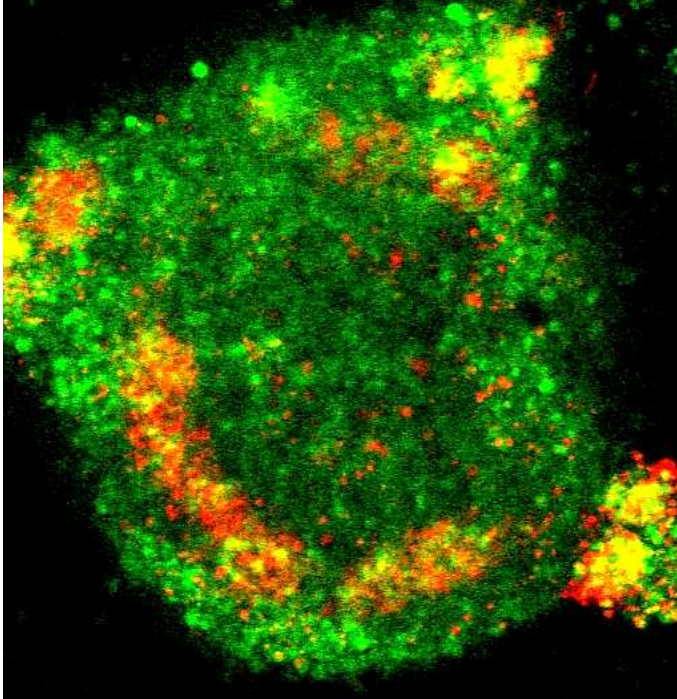
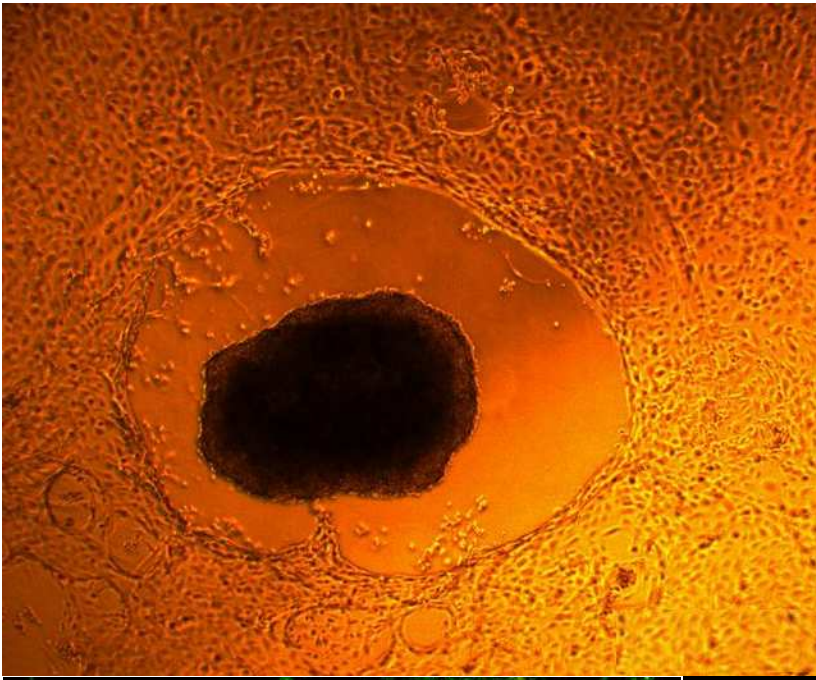
**Specific aim 3:** Evaluation of the TAA recognition ability by HLA class I restricted TAA specific CTL.

**Specific aim 4:** Evaluation of factors affecting immunorecognition when melanoma cells are growing in MCTS.



## Chapter 2

### Materials & methods



*Making the simple complicated is commonplace;  
making the complicated simple, awesomely simple, that's creativity*  
Charles Mingus (1922-1979)

*Creativity is inventing, experimenting, growing, taking risks,  
breaking rules, making mistakes and having fun.*  
Mary Lou Cook (1918- )

HBL spheroid repelled Human microvascular endothelial cells, whereas NA8 spheroids attracted HMECs. T-cadherin was over-expressed 400 times by adenovirus-mediated gene transfer in HMECs. To determine effects of T-cad upregulation per se on behavior of endothelial cells, either HMECs with overexpressed T-cad or control (LacZ-infected) was cocultured with NA8 spheroids. T-cad overexpressed HMECs massively infiltrated within the spheroids and proliferated.

## **2. Materials & methods:**

### **2.1. Cells used**

#### **2.1.1. Melanoma cells**

NA8 (courtesy of Dr. Jotereau, Nantes, France), HBL and D10 cell lines (courtesy of Dr. A. Eberle, Basel, Switzerland) derive from metastatic melanoma and have widely been used in tumor immunology studies in the recent past (Oertli D et al 2002; Zazac P et al 2003). They are all HLA-A\*0201+. However, while HBL and D10 express typical melanoma differentiation TAA, NA8 does not.

Cell lines were routinely passaged in conventional 2D cultures in RPMI 1640 supplemented with 10mM HEPES buffer, 1mM sodium pyruvate, 2mM non-essential amino-acids, 2mM glutamine, 100 µg/ml Kanamycin (Invitrogen, Carlsbad, California) and 10% heat-inactivated FCS, thereafter referred to as complete medium.

#### **2.1.2. CTL clones**

T lymphocyte clones of defined specificity, mostly recognizing HLA-A0201 restricted epitopes from melanoma differentiation antigens gp100<sub>280-288</sub>, Melan-A/MART-1<sub>27-35</sub> were generated from PBMC of patients undergoing specific vaccination procedures and are thus endowed with high functional avidity and capacity to kill target cells endogenously producing the relevant TAA (Ghosh S et al, 2005b). Briefly, cells from bulk cultures showing evidence of antigen specific cytotoxic activity, as detectable by <sup>51</sup>Cr release assays, were cloned in 60 well Terasaki plates (Nunc, Glostrup, Denmark) at 0.3 cells per well in 20 µl volumes in the presence of 10,000 irradiated allogenic PBMC/well, in RPMI 1640 supplemented with 10mM HEPES buffer, 1mM sodium pyruvate, 2mM non-essential amino-acids, 2mM glutamine, 100 µg/ml Kanamycin (Invitrogen, Carlsbad, California) and 5% pooled human serum (RPMI-HS), to which rIL-2 (200 units/ml) and purified phytohemagglutinin (PHA, 0.5 µg/ml, Remel, Dartford, UK) were added. After 14 days, wells where cell growth was microscopically detectable were expanded in RPMI-HS supplemented with 100 units/ml rIL-2 and screened for antigen specific cytotoxic activity by <sup>51</sup>Cr release assay. CTL clones were maintained in RPMI-HS supplemented with 100 units/ml rIL-2 and restimulated periodically with PHA in the presence of irradiated allogenic PBMC. All assays reported here were performed at least one week after re-stimulation.

## **2.2. Preparation of spheroids**

**2.2.1. Stirred culture:** Rotary cell culture bioreactor system (RCCS, Synthecon, USA) spins a fluid medium filled with cells to neutralize most of gravity's effects and encourage cells to aggregate in suspension without being touched by any artificial surface. The RWV bioreactor consisted of a 40 ml culture vessel, a medium recycling system, provided with a bubble trap, an external oxygenator, and a peristaltic pump. The medium was re-circulated at 0.6 ml/min. The angular velocity range of the vessel was 30-50 rpm.

**2.2.2. Hanging drop method:** 20–30  $\mu\text{L}$  of cell suspension was dispensed into the wells of a 60-well micro-titer Terasaki plate. 150-500 melanoma cells (NA8, HBL, D10) per well were cultured in Terasaki plates for 7-10 days.

**2.2.3. Alginate gel encapsulation:** Melanoma cell suspension was mixed at room temperature with a sterile sodium alginate solution (1.5-2%). The mixture was extruded dropwise through a microsyringe needle into a Calcium Chloride solution (200 mM). This resulted in formation of gel beads of 1.5-2.5 mm in diameter, which was hardened for 15 minutes in a sterile  $\text{CaCl}_2$  solution.

### **2.2.4. Agarose or PolyHEMA coated dish:**

96 well plates were coated with 200  $\mu\text{l}$  of 2% agarose gel and after few minutes they were sucked out to leave a thin layer of agarose coating at the bottom. Plates were dried for 3-4 hours before cell seeding.

PolyHEMA crystals (600 mg) were dissolved in 5 ml 95% EtOH by rotating over night at 37°C. This stock solution was diluted by adding 7 ml of 95% EtOH. Plates were coated with 50  $\mu\text{l}$ / well /96 well plate (0.1 ml / $\text{cm}^2$ ) and then dried overnight at room temp in a sterile environment. Plates could be stored indefinitely prior to use.

### **2.2.5. Histological procedures and Morphological evaluation.**

**H&E staining:** Spheroid samples were fixed in 4% formalin, embedded in paraffin, and dissected (5  $\mu\text{m}$  thick). Sections were stained with Hematoxylin and Eosin (H&E) according to standard protocol.

**BrdU staining:** Samples were incubated with BrdU (10 mM) for 12 h followed by histological procedure. The paraffin-embedded tissue sections were completely dewaxed and rehydrated with PBS followed by microwave antigen retrieval. Thereafter they were incubated in 0.3%  $\text{H}_2\text{O}_2$  in methanol for 10 min to inhibit endogenous peroxidase activity and rinsed in PBS. After blocking

with serum at room temperature, the sections were incubated with primary anti-BrdU antibody (Sigma, St. Louis, MO) overnight at 4°C in a humidified chamber followed by washing in PBS. The negative control sample was incubated with PBS. After being incubated with secondary antibody biotin-conjugated rabbit anti-mouse IgG, Sigma, St. Louis, MO) for 1 hr at room temperature and washed in PBS, the sections were incubated with HRP-linked streptavidin at room temperature for 1 hr and washed with PBS. The sections were developed with DAB and examined under a light microscope.

### 2.2.6. Proliferation

Cell proliferation was measured by the AlamarBlue™ reduction assay (Serotec, Oxford, UK) spectrophotometrically. The internal environment of the proliferating cell is more reduced than that of non-proliferating cells. Specifically, the ratios of NADPH/NADP, FADH/FAD, FMNH/FMN, and NADH/NAD, increase during proliferation. AlamarBlue can be reduced by these metabolic intermediates. Hence cell proliferation can be monitored as reduction is accompanied by a measurable shift in color (blue to pink).

Proliferation capacity of CTLs was investigated by using lymphocyte tracking dye carboxyfluorescein diacetate succinimidyl ester (CFDA-SE) (Lyons AB et al 1994; Parish CR 1999). CFDA diffuse into a living cell and de-acetylate and then concentrate. The two acetate side chains make the molecule highly membrane permeant. However, once inside cells, the acetate groups are removed by intracellular esterases and the resultant carboxyfluorescein exits from cells at a much slower rate. The slow exit rate also provides ample time for the CFDA-SE to covalently couple to intracellular molecules. Coupling is via the succinimidyl moiety, which

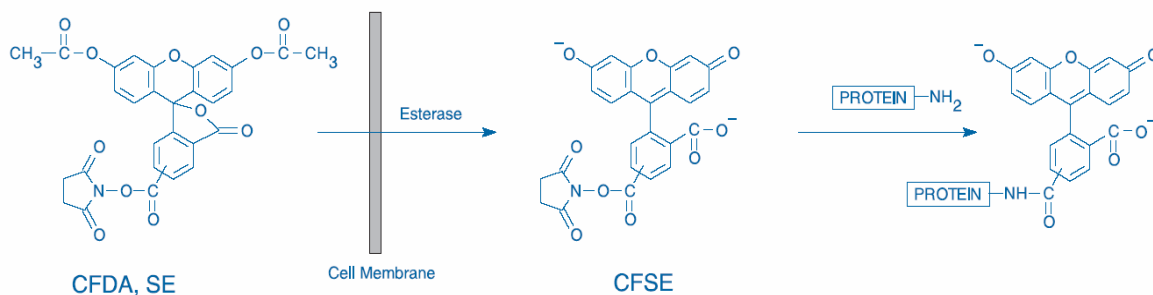


Figure 6: Mechanism of fluorescently labelling of cells by CFDA-SE

reacts with intracellular amine groups, forming a highly stable amide bond. Proliferation rate of the cells was calculated by the progressive halving of the fluorescence intensity of the dye in cells after each cell division.

### **2.3. Modulation of Gene profiling**

Cells were harvested by trypsinization and total RNA extracted using Qiagen RNeasy® Mini Kit (Qiagen, Basel, Switzerland) following suppliers instruction. Its integrity was monitored by using Agilent 2100 Bioanalyzer (Ambion, Austin TX). Ten µg RNA from each sample was reverse transcribed and labeled by utilizing commercial kits according to the suppliers` instructions (MEGAscript T7, Ambion, Austin TX; Bio-11-CTP and Bio-16-UTP, Enzo Biochem, NY). Biotinylated cRNA was then be fragmented by treatment at 94°C for 35 minutes in 40 mM TRIS-acetate, pH 8.1, 100 mM potassium acetate, and 30 mM magnesium acetate and hybridized to oligonucleotide arrays.

Two hybridizations were performed for each sample under investigation. Raw data collected using a confocal laser scanner were analysed using commercial software (Gene Spring Version 7.2, Silicon Genetics, Redwood City, CA) with two separate data readings for each hybridization, as previously described (Padovan E et al. 2002; Ghosh S et al. 2005a; Ghosh S et al., 2005b).

One way ANOVA tests were performed for gene lists filtered on fold change in the log-of-ratio mode of experimental interpretation (Gene Spring 7.2 software, Silicon Genetics, Redwood City, CA). Duplicates of each experimental group were compared and the parametric Welch t test was used with a cut-off p value of 0.05. The false positive rate of finding a gene is associated with the standard p value. A significant p-value in 1-way ANOVA test would indicate that a gene is differentially expressed in at least one of the groups analysed. Genes displaying  $\geq 3$  fold up or down-regulations between 2D and 3D culture conditions were specifically considered.

### **2.4. Cellular immunology studies**

#### **2.4.1. IFN- $\gamma$ detection by ELISA**

IFN- $\gamma$  production was used as antigen recognition assays. As target/stimulator cells, we used melanoma cells cultured in 2D or as MCTS. CTLs, specific for Melan-A/MART-1 or gp100, used as effectors, were co-cultured with target cells at different E:T ratio for 24 hours. Supernatants were collected and IFN- $\gamma$  secretion was measured by using human IFN- $\gamma$  BD

OptEIA™ ELISA Set (BD Biosciences, Franklin Lakes, NJ). All samples were measured in triplicates.

#### **2.4.2. Chemotaxis assay**

Migration assays were performed by using Costar® 24-transwell chemotaxis chambers (Corning Costar Corporation, Cambridge, MA) with 5-µm and 3-µm pore size polycarbonate filters, for immature DC (iDC) and CD8+ T cells, respectively. In brief, 600 µl of supernatant of NA8 cells cultured in 2D or 3D, or as a negative control, complete medium, were placed in the lower wells. CD8+ peripheral blood T cells were purified by using magnetic beads (Miltenyi Biotech, Bergish Gladbach, Germany), whereas iDC were prepared by culturing peripheral blood monocytes in the presence of IL-4 and GM-CSF, as previously detailed (Rommel E et al. 2001). Upper wells of chemotactic chambers were loaded with 100 µl cell suspension of iDC or CD8+ T cells at a concentration of  $1 \times 10^6$ /ml. Each condition was set up in duplicate. Plates were kept at 37°C for 20 hours. Cells suspensions from the upper wells and cells migrated to the lower wells through the filters were then collected, stained with specific mAbs and counted by flow cytometry for a fixed defined time. Chemotactic index was determined by dividing the number of cells migrated in the experimental condition by the number of cells migrated in the negative control cultures (medium only).

#### **2.4.3. Immunofluorescence analysis**

NA8 or HBL cells were stained with PKH26 red fluorescent cell linker (Sigma, Sigma-aldrich Co., St. Louis, MO) following suppliers instructions, and cultured on polyHEMA coated plate for 3 days to form 30,000 cells MCTS. Total CD8+ T cells from a healthy donor and CTL clone specific for HLA-A0201 restricted Melan-A/MART-1<sub>27-35</sub> epitope were stained with CFSE (molecular Probes, Eugene, OR). Cytotoxic cells (E:T ratio = 5:1) were added on each MCTS and co-cultured for 1 day. Confocal images for the evaluation of total CD8+ T cells or CTL infiltration in NA8 and HBL MCTS respectively, were obtained using a laser-scanning confocal microscope Zeiss LSM510 (Carl Zeiss MicroImaging Inc. NY).

Immunofluorescence labeling of permeabilized and fixed cells was done by incubating them for 30 minutes at room temperature and minimal exposure to light. Actin filaments were directly labelled with 488-Alexa phalloidin (Invitrogen, diluted 1: 400 in MHB). Vimentin intermediate filaments were also directly labelled with a monoclonal antibody (Mab) anti-vim

Cy3 (Sigma, diluted 1:900 in MHB). Labelled samples on slides were then washed with MHB and embedded in Mowiol 4–88 (Hoechst) containing 0.75 % of n-propyl-gallate as an anti-bleaching agent. Mounted slides were left dry for 24 hrs at room temperature in dark until viewed.

#### **2.4.4. Flow cytometry analysis**

NA8 cells cultured in 2D were collected by trypsinization after day 3. Accordingly, MCTS obtained after 3 days of culture on polyHEMA treated plasticware were centrifuged and pellets were disrupted by Trypsin-EDTA (Gibco, Paisley, Great Britain) treatment for 10 min at 37°C. Cellular phenotypes were evaluated by surface staining using fluorochrome conjugated mouse monoclonal antibodies recognizing the indicated determinants. Samples were analyzed on a FACS Calibur (Becton Dickinson, San Jose, CA) using propidium iodide (PI) to exclude dead cells.

In particular HLA expression was verified using anti-HLA-A0201 or anti-HLA-A, B, C FITC-conjugated mAb (PharMingen, San Diego, CA). HBL, D10 or NA8 cells cultured in 2D were collected using Trypsin-EDTA (Invitrogen, Carlsbad, CA) after 3 days culture. Accordingly, MCTS obtained after 3 days culture, were disrupted by 5 min trypsinisation at 37°C. Phenotypes were evaluated by staining with specific or control mAbs, incubated 45 min at 4°C in the dark, washed twice in cold PBS, fixed 1 min in Paraformaldehyde 1%, re-suspended in 200 µl PBS, and analyzed on a FACSCalibur® cytometer (Becton Dickinson, NJ).

Melan-A/MART-1 expression was evaluated by intracellular staining after permeabilization using BD Cytotfix/Cytoperm™ kit (BD Biosciences, San Jose, CA), following supplier's protocol. Staining was performed using as primary antibody a specific Melan-A/MART-1 mAbs (Novocastra, Newcastle upon Tyne, UK) and as secondary antibody a FITC-conjugated goat anti-mouse Ig (Southern Biotech, Birmingham, AL).

#### **2.4.5. Quantification of gene expression by quantitative Real-Time PCR**

Cells were collected at the indicated time points and washed in PBS. Surgical samples from metastatic melanoma patients were disrupted and homogenized by sonication. Total RNA were extracted using the RNeasy® Mini Kit protocol (Qiagen, Basel, Switzerland), treated by Deoxyribonuclease I (DNase I) (Invitrogen, Carlsbad, California), and reverse transcribed by

using the Moloney Murine Leukemia Virus Reverse Transcriptase (M-MLV RT, Invitrogen, Carlsbad, California). Quantitative real-time PCR were performed in the ABI prism™ 7700 sequence detection system, using the TaqMan® Universal PCR Master Mix, No AmpErase® UNG (both from Applied Biosystems, Foster City, CA). Quantification of gene expression was calculated by using the  $2^{-\Delta\Delta CT}$  method (Livak KJ et al 2001; Winer J et al 1999). Normalization of gene expression was performed using GAPDH as reference gene and data were expressed as ratio to reference samples.

### ***Primers and probes***

Oncostatin M (OSM), IRF-1 and MITF primers and probes are from pre-developed assays (Assays-on-Demand, Gene Expression Products (Applied Biosystems, Foster City, CA)). Oligonucleotide primers and probes for c-myc, Melan-A/MART-1, gp100 and tyrosinase were generated using appropriate software (Primer Express™, Applied Biosystems, Foster City, CA) from sequences obtained from the NCBI gene bank.

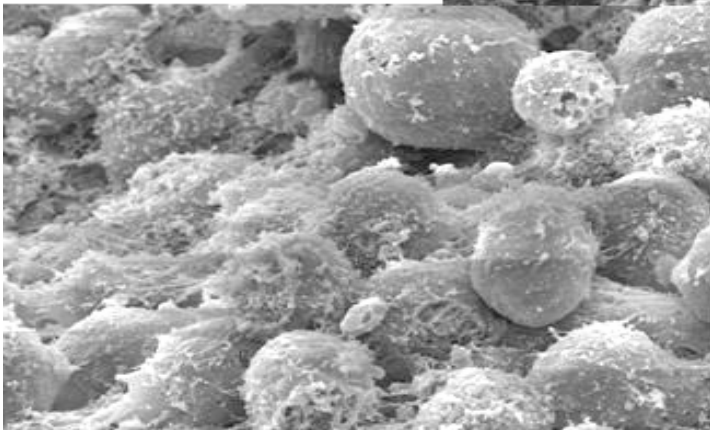
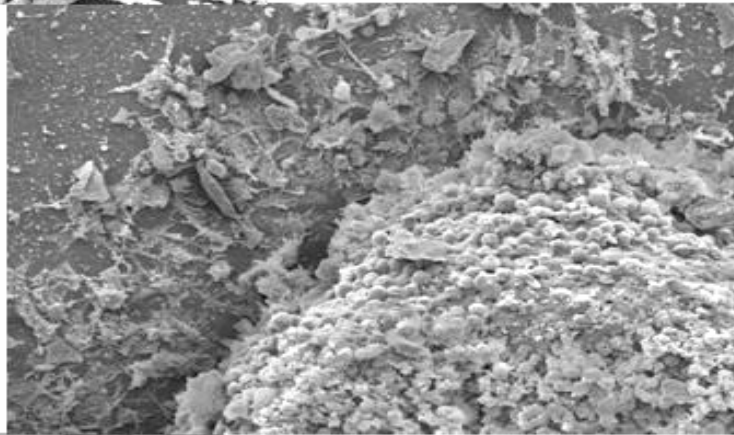
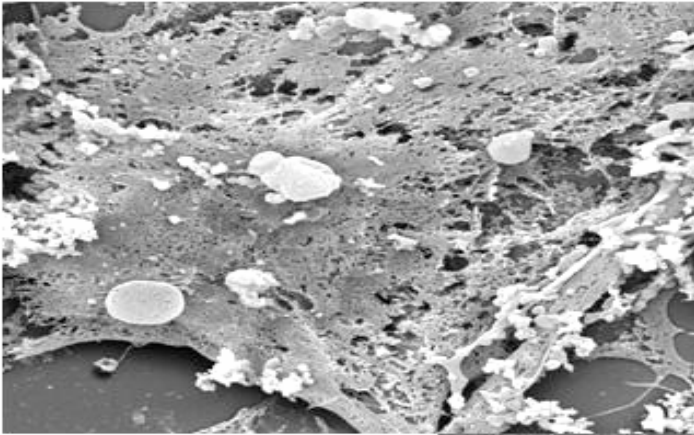
### **2.4.6. Lactic acid measurement from tumor supernatant**

Glucose and lactate concentrations were assessed by an immobilized enzyme biosensor (YSI 2300 STAT Glucose analyzer, Kreienbaum, Germany). Melanoma cells were cultured in spheroids or monolayers in different oxygen environment for 3 days. Then lactate and glucose content were measured from the supernatant.



## Chapter 3

# Results & Discussion



*I am among those who think that science has great beauty.  
A scientist in his laboratory is not only a technician;  
he is also a child placed before natural phenomena  
which impress him like a fairy tale.*

Marie Curie (1867 - 1934)

Scanning Electron microscopic view of HBL cells either as monolayer or spheroid, after 24 hours of coculture with TAA-specific CTL clones. Monolayer cells seemed to have perforated and disrupted surface morphology, whereas spheroids maintained their three dimensional structure.

### 3. Results and discussion

#### 3.1. Spheroid Cultivation Techniques

##### 3.1.1. Rotating wall vessel bioreactor:

NA8 Melanoma cell suspension was cultured in RWV Bioreactor (Synthecon) for 7-10 days with 60-80 rpm of cylinder speed. Aggregation was random and the resulting spheroids were of various sizes. There was absolutely no control over size of the spheroids. Single cells, small aggregates or debris were highly present in the vessel.

##### 3.1.2. Hanging drop method

150-500 melanoma cells (NA8, HBL, D10) per well were cultured in Terasaki plates for 7-10 days. In some cases initially several multicellular spheroids formed in each well and after 1 or 2 days they were merged to form a single spheroid/aggregate per well. Out of the three cell

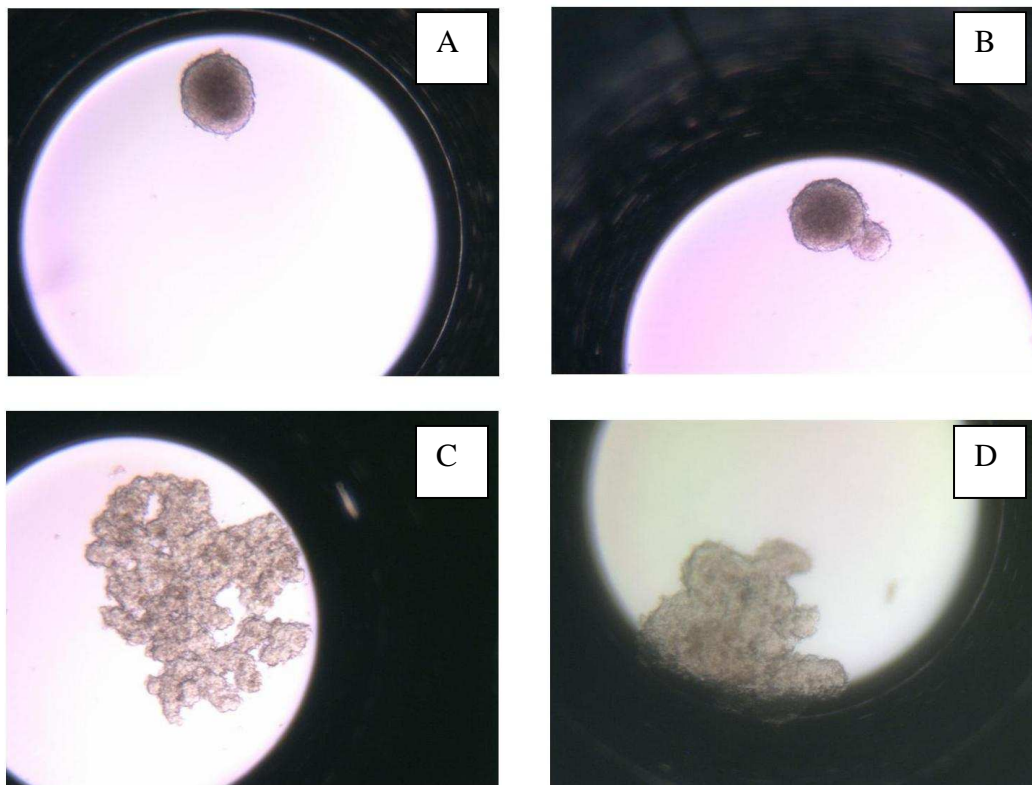


Figure 7: (A) NA8 spheroid in DMEM 10% FCS, (B) Merging of NA8 spheroids, (C) D10 aggregate in DMEM 10% FCS, (D) D10 aggregate in DMEM 20% FCS

lines tested NA8 formed only round spheroids, whereas HBL and D10 formed irregularly shaped aggregates in media containing 10% FCS. However when they were cultured in 20% FCS containing media, aggregates were much firmer (Figure 7 C, D).

Notably as the volume of the media is very low ((20–30  $\mu$ L) only spheroids having 100-500 cells can be generated by this technique. Therefore they might not create typical hypoxic environment needed to produce a typical tumor microenvironment modulating gene expression or impairing immunorecognition. The micro-spheroids were so delicate that it was difficult to transfer them in 96 well plate from Terasaki plates.

### 3.1.3. Gel encapsulation method:

Melanoma cell suspension was mixed at room temperature with a sterile sodium alginate solution. The mixture was extruded dropwise through a microsyringe needle into a Calcium Chloride solution (200 mM). This resulted in formation of gel beads, which were hardened for 15 minutes in a sterile  $\text{CaCl}_2$  solution. With careful optimization of  $\text{CaCl}_2$  solution stirring speed large numbers of spheroids were formed by alginate encapsulation.

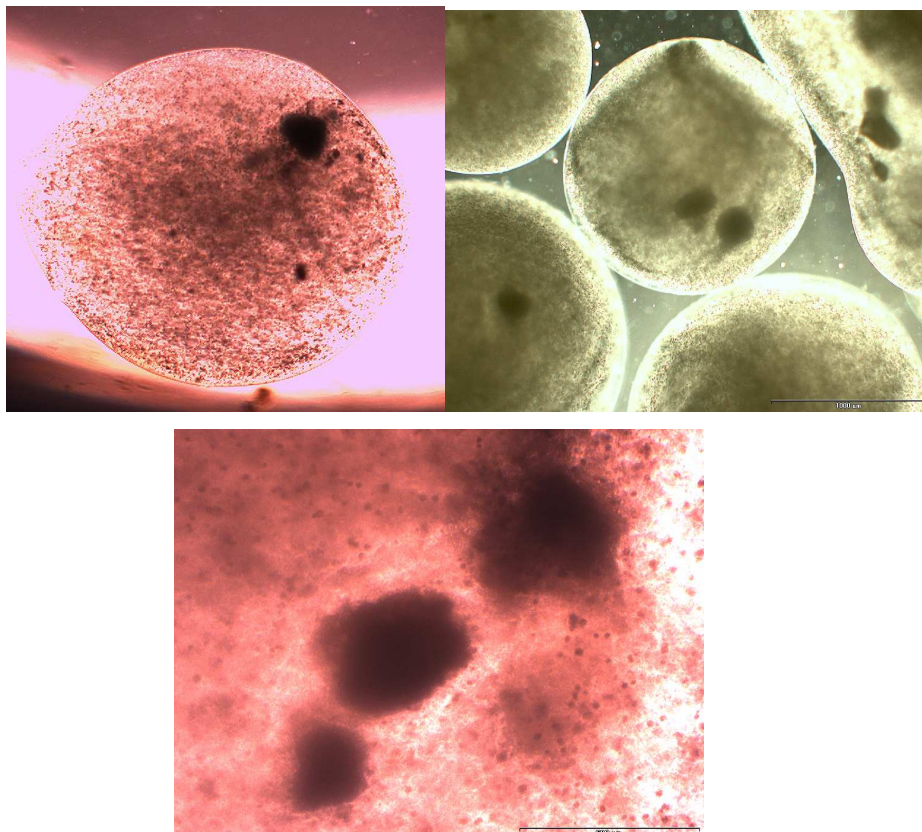


Figure 8: melanoma cell aggregates encapsulated within alginate beads

On the other hand, several aggregates were formed within one alginate bead, without the possibility of controlling the size or cell number (Figure 8). Furthermore some cell aggregates started to come out of the alginate bead. EDTA treatment and pipetting could disrupt spheroids and alginate capsule formed might have acted as a permeability barrier.



Importantly, although no specific interactions between mammalian cells and alginate are known, they cannot be completely discounted.

#### **3.1.4. Static cultivation technique on non-adhesive surface :**

Melanoma cells were cultured on agarose coated 96 well plate. Morphology of the aggregates and cell viability were checked at regular interval. All the cell lines in culture formed only irregularly shaped aggregates, with poor adhesive strength.

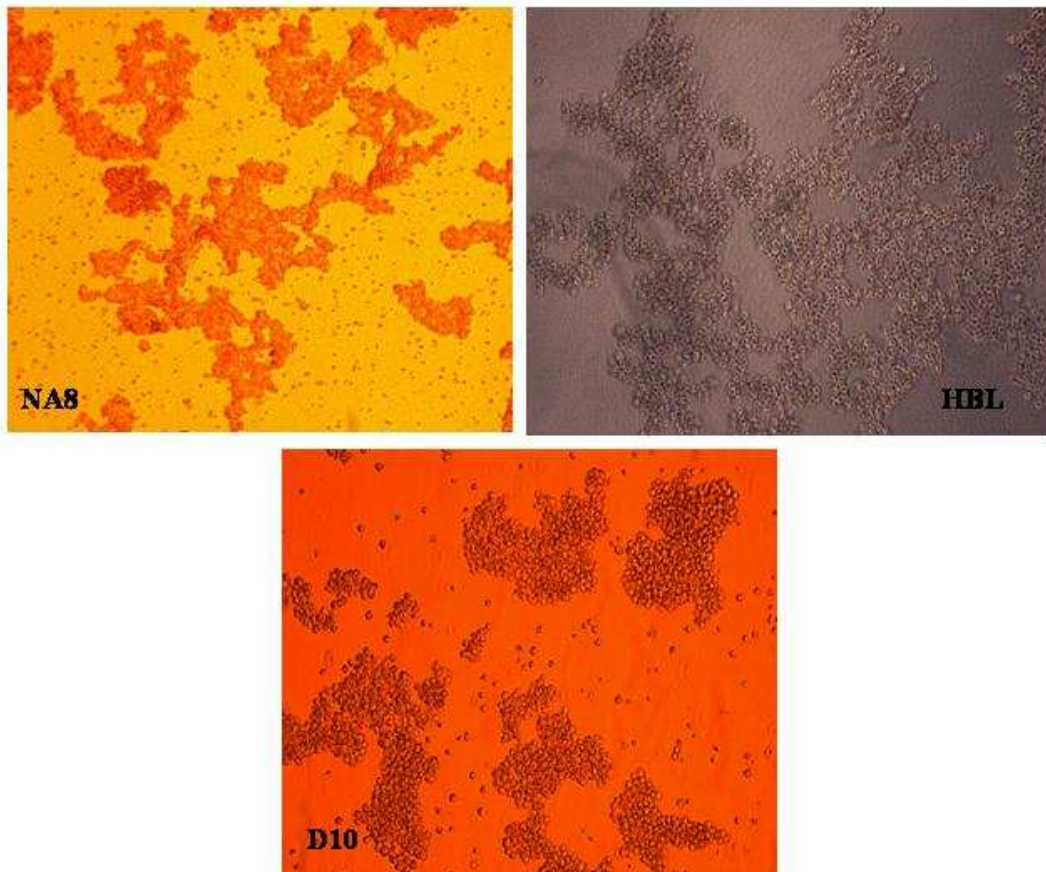


Figure 9: Irregularly shaped aggregates formed over agarose-coated dish

A dramatic improvement of cell-cell adhesion was observed when cells were cultured on PolyHEMA coated dish. NA8 cells formed perfectly round shaped spheroids (Figure 10). Although HBL and D10 cells also formed round shaped spheroids, their level of adhesion was slightly inferior to that of NA8 cells. Cell viability (assessed by trypan blue dye exclusion assay) decreased from 94% in 3<sup>rd</sup> day of culture on PolyHEMA coated dish, to 70% in 21 day old spheroid, which was supported by flowcytometry studies.

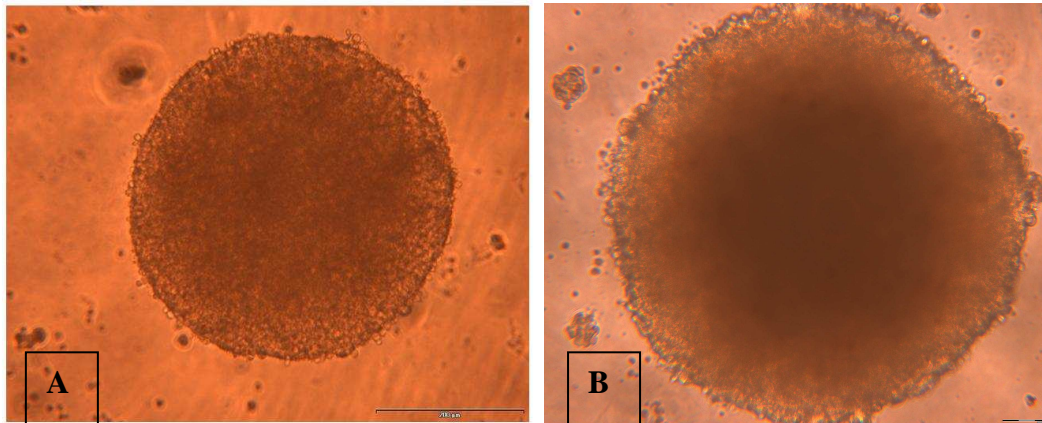


Figure 10: Multicellular spheroids formed on PolyHEMA coated 96 well plates:  
(A) NA8, (B) HBL

### 3.1.5. Effect of culture media

Consideration must be given to the growth medium used; in particular, the influence of serum should not be overlooked. Chun (Chun MH 2000) found that expired/aged human serum, deficient in plasminogen activator inhibitor, resulted in the formation of anchorage independent MCTS from monolayer cultures of BT20 human breast cancer cells, and that addition of fresh serum reverted the culture back to monolayer growth. Furthermore, it is known that various human breast and colon cancer cells form multicellular spheroids in response to the serum signaling factors, plasmin, CEA, interferon- $\gamma$  ( Kanai T. et al. 1993), IGF-II and heregulin $\beta$ 1 (Tan M et al. 1999). But the exact signalling mechanisms by which these factors can induce formation of multicellular spheroids is not yet fully understood. Kelm et al. (Kelm et al. 2003) found that increasing serum concentration improved aggregation and MCTS forming capacity in hanging drop cultures of several melanoma derived cells lines. In accordance with their findings, we have also observed that the use of higher % of FCS resulted in firmer aggregates and culture in DMEM based medium, rather than RPMI-1640 medium, resulted in enhanced aggregation, possibly due to increased calcium levels.

After reviewing all these techniques of spheroid formation, we finally decided to continue our work with MCTS formed over PolyHEMA coated dish, because by using this technique we could prepare round and compact spheroids having highly homogeneous size distribution within a very short time period, having highest viability of cells, as compared to other methods of spheroid formation. By this method, we could generate large numbers of spheroids having uniform characteristics with minimal handling, as compared to other techniques.

### 3.2. MCTS Characterization

#### 3.2.1. Proliferation of melanoma cells

AlamarBlue proliferation curves revealed that proliferation in 2D cultures of NA8 and HBL cells typically reached a plateau within 7-8 days, whereas no apparent increase in cell proliferation was detectable in MCTS for the first two weeks of culture, but could only be observed at later time points (Figure 11), a pattern frequently observed previously in 3D culture models.

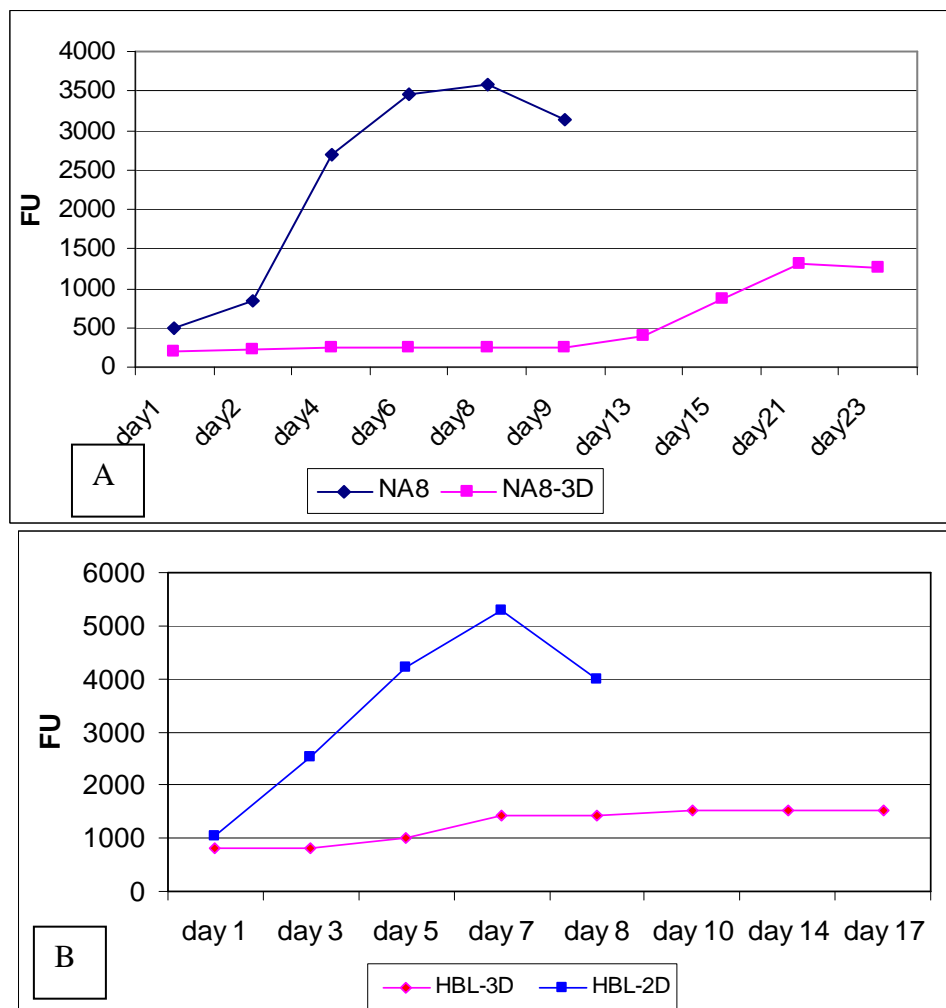


Figure 11: AlamarBlue proliferation curves of (A) NA8 and (B) HBL cells cultured in monolayer and as spheroid

Cells in conventional monolayer cultures grow exponentially. Spheroids display the typical biphasic growth pattern of solid tumors in vivo (an early exponential phase followed by a period of retarded growth) (McCredie JA et al. 1965). In general, three distinct growth phases have been described in tumor spheroids. The first phase is the exponential growth of the cells with little modification in cell cycle distribution as compared to monolayer culture,

until the spheroids reach a diameter of 20-400  $\mu\text{m}$  depending on cell lines. Then the average cell cycle distribution within the spheroids begins to change, resulting in an accumulation of  $G_1$ -like cell at the centre and a sequestration of the proliferating cells at the periphery until a plateau is reached (Freyer JP et al. 1980; Carlsson J 1977). The first phase is independent of external factors while the second depends on the size of the tumor spheroid and the nutritional restrictions imposed to cells located in the spheroid interior. This leads to progressive reduction of growth fraction (Durand RE 1976; Durand RE 1990) and then another growth phase by linear expansion of diameter with time. The observation that final spheroid volume increases slightly with inoculation density suggests that growth after 10-15 days may be hampered by a decay in conditions, such as spontaneous degradation of glutamine, photodegradation of some vitamins and amino acids, accumulation of waste products.

In order to demonstrate the strong similarity that exists between *in vivo* solid tumor growth and growth of multicellular spheroids, various mathematical models have been applied which can account for the three successive phases (geometric, linear and plateau). The exponential-Gompertzian tumor growth model has been applied to several tumor cell lines grown in monolayer and to multicellular spheroids as well as to *in vivo* tumors. Monolayer cultures do not adequately fit this mathematical model while both *in vivo* tumors and spheroids fit the model quite well and strongly resemble each other in their growth characteristics. The geometric phase corresponds to early aggregation and proliferation of small spheroids, while the linear and plateau phases represent the development of a nonproliferative inner region and the formation of a necrotic core in spheroids, respectively. Importantly cells within the same tumor mass can be influenced by different microenvironments. Khaitan et al (Khaitan D et al 2006) compared cell cycle distribution of exponentially growing monolayer and spheroids at different time point (7-28 days). They observed that in spheroids grown on agarose-coated dish, proportion of  $G_1$ -phase cells was higher (approximately 60%) in spheroids as compared to exponentially growing monolayer cells (approximately 48%).

### **3.2.2. Morphological characterisations of MCTS**

We observed that there was no major change in diameter of spheroids during 10-15 days of culture, but Hematoxylin & eosin staining showed that NA8 spheroids of 30000 cells formed necrotic cores within MCTS upon prolonged culture (>10 days), soon resulting in hollow center, with large, compact cells typically detectable in the periphery. HBL and D10 spheroids having 30000 cells also formed necrotic cores, but less prominent as compared with

NA8 cells (Figure 12). Small spheroids of NA8 (500-1000 cells) could not form necrotic core even after 15 days of culture. This suggests that, this small spheroid model system might not be able to simulate typical hypoxic tumor microenvironment.

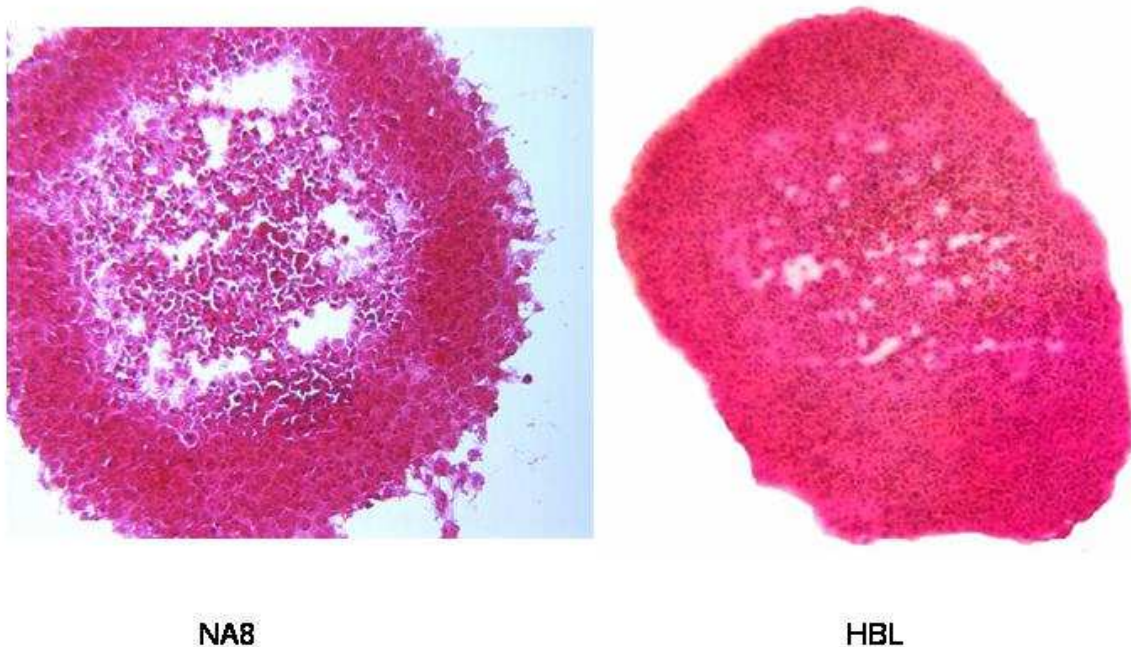


Figure 12: Hematoxylin and Eosin staining of paraffin embedded sections of spheroids, showing NA8 and HBL spheroids formed a necrotic core after 10-12 days of culture on a PolyHEMA coated 96 well plate

Necrosis and slow proliferation rate in the spheroid system might be due to lack of sufficient nutrients and metabolites. For some spheroid types such as WiDr human colon adenocarcinoma and tumorigenic Rat1-T1 rat embryo fibroblasts emergence of necrosis and hypoxia during growth has been documented with the thickness of viable cell rim reflecting oxygen availability (Monz B et al 1996). Role of oxygen gradient has also been studied (Franko AJ et al 1979a; 1979b). Oxygen diffusion within spheroids has been first theoretically calculated (Burton AC 1966). Spherical symmetry of the spheroid is very critical for such calculation. Several research groups have measured  $O_2$  tension ( $pO_2$ ) distributions in spheroids with oxygen-sensitive microelectrodes (Carlsson J et al 1979; Mueller-Klieser W 1984; Mueller-Klieser WF et al 1984). Those measurements showed that  $pO_2$  values may vary considerably depending on different cell lines, culture methods and detection techniques used (Walenta S et al 2001). Mathematical modellings by Groebe et al (Groebe K et al 1996) indicated that no single limiting factor (such as, oxygen deficiency) can account for the development of necrosis.



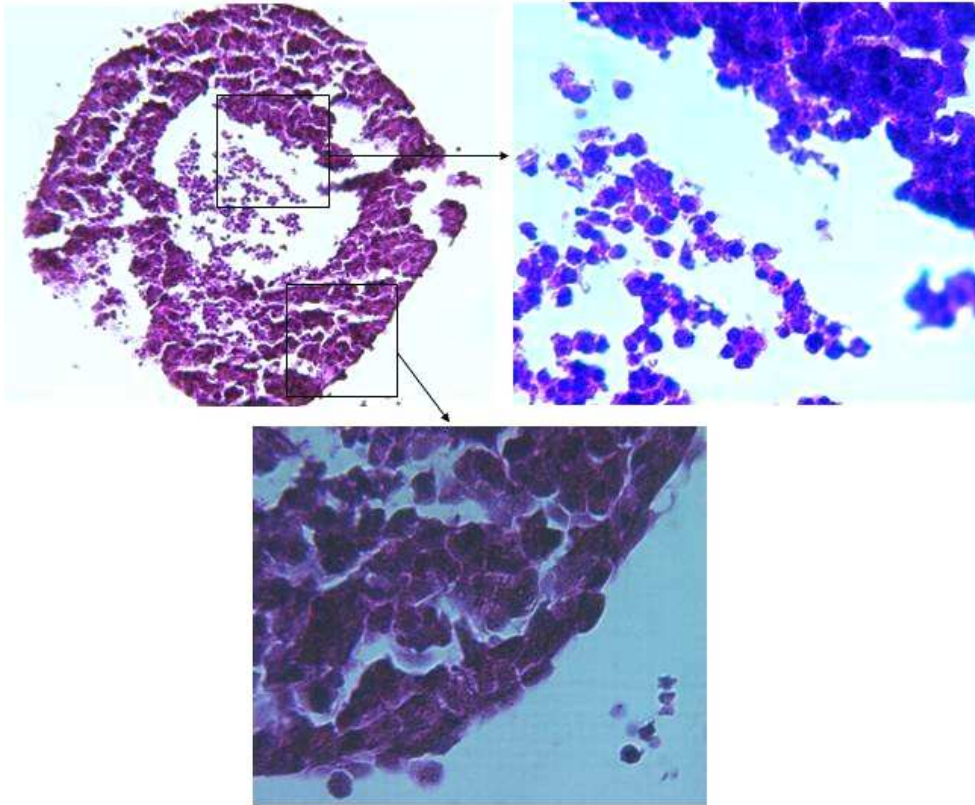


Figure 13: Difference of morphology of cells from periphery and central part of the paraffin embedded H&E stained NA8 spheroids

To verify if all cells in a spheroid have equal proliferative capacity, staining with 5-bromo-2-deoxy-uridine (BrdU) incorporation in DNA using a peroxidase-based immunohistochemical assay was performed. BrdU staining (Figure 14) (Ghosh S et al 2005a)

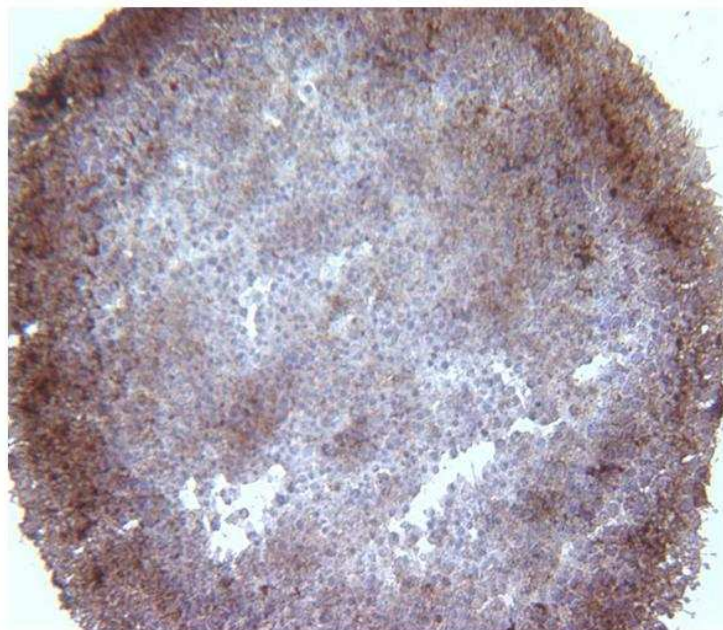


Figure 14: BrdU staining of NA8 spheroid showed that peripheral cells are mainly in proliferating stage, whereas inner cells are mostly in quiescent stage

indicated that the cells located in the center of MCTS are alive but mostly in quiescent state, whereas cells in outer layers are actively cycling, which strongly reminded the historical reports of Thomlinson et al (Thomlinson RH et al 1955) who showed that in tumor biopsies only the cells in periphery were in proliferating stage. Later Sutherland (Sutherland RM 1988) reported that most of the proliferating cells in spheroids are located within outer 3-5 cell layers (75  $\mu\text{m}$ ). Quiescent cells represent the major population of cells in a spheroid and they are reproducibly viable when removed from this environment (Luk [CK et al 1985](#); Luk [CK et al. 1986](#)). Some investigators used autoradiography after pulse labeling with  $^3\text{H}$ -thymidine to confirm this by showing a large fraction of S-phase cells in the outer few cell layers compared to the cells located in central part of the spheroids. Inner cells remain unlabeled in a period of several cell cycles, indicating that they are not cycling through S-phase (Yuhua JM et al 1978).

Typical morphology of MCTS (i.e. presence of proliferating cells at periphery, viable but quiescent cells at intermediate and necrotic core) is a multifactorial event resulting by lack of oxygen and/or nutrients, accumulation of waste products, and low pH as proposed by Acker and coworkers (Acker H et al. 1987; Carlsson J et al. 1988). Mueller-Klieser and his coworkers showed (Bredel-Geissler A et al 1992; Teutsch HF et al 1995; Walenta S et al 1990; Freyer JP et al 1991) in EMT-6 mouse mammary carcinoma spheroids, on steady-state levels of glucose, lactate and energy-rich phosphates, that cells in the inner spheroid regions may adapt their metabolism to environmental stress by reducing their metabolic turnover rates to maintain intracellular homeostasis until shortly before cell death; thus, critical reduction in ATP and intracellular pH can be excluded as a mechanism for cell quiescence and cell destruction by necrosis (Walenta S et al 1990). At later stages of disease progression some of these quiescent cells may act as stem cells to cause regrowth of tumor (Sutherland RM 1988).

### 3.3. Gene expression

Prompted by previous small scale gene expression profile studies on MCTS, we (Ghosh S et al, 2005a) addressed large scale gene profiling in melanoma cells cultured in standard 2D conditions, with or without extracellular matrix and as 3D MCTS, by taking advantage of high density oligonucleotide arrays. For NA8 cells we used Affymetrics genechip Human Genome-U133A allowing the analysis of over 20,000 expressed genes. For HBL cells we used Affymetrics gene chip Human Genome-U133 Plus 2.0 (which includes all of the probe sets of HG-U133A and HG-U133B arrays and more than 10,000 additional probe sets), allowing analysis of more than 54,000 transcripts.

As the model extracellular matrix we chose collagen for NA8 since NA8 cells express both  $\alpha_1\beta_1$  and  $\alpha_2\beta_1$  integrin receptors for collagen and fibronectin for HBL since HBL cells express  $\alpha_4\beta_1$  and  $\alpha_5\beta_1$  integrin receptors for fibronectin. We studied gene expression profile using 3 days old spheroids, which had not formed necrotic cores yet.

Our data provide a first large scale database focused on structure-related gene expression pattern in tumor cells. Most importantly, they show that the architecture of melanoma cells, possibly due to the inherent homotypic cell-cell interaction or specific tumor microenvironmental conditions, may determine specific gene expression patterns of potentially high functional relevance.

In the case of NA8 cells, over 11000 genes were found to be expressed in all three conditions (monolayer, monolayer over collagen coating, spheroid). Cells cultured in monolayers, irrespective of the presence of collagen extracellular matrix, showed remarkably similar gene expression patterns, with statistically significant differences being limited to five genes. In particular, a downregulation (5 fold) of Hsp 40 encoding gene was observed in cells cultured in the presence of collagen. In contrast, cells cultured in MCTS displayed significant modulation in the expression of a number of genes as compared to their monolayer counterparts. 106 genes showed evidence of upregulation and 73 of downregulation. Importantly, significant upregulation of the expression of genes whose products are known to play a critical role in melanoma progression and metastatic process was observed. In particular, a significant upregulation of the expression of genes encoding chemokines, including CXCL1, CXCL2, and CXCL3, (GRO- $\alpha$ , - $\beta$  and - $\gamma$ , 10 fold, 15 fold and 6 fold, respectively), IL-8 (67 fold), CCL20 (75 fold), IL-1A (3 fold), IL-1B (4 fold) were detectable in MCTS, as compared to cells cultured in 2D. The expression of genes encoding pro-angiogenic factors or adhesion molecules, such as angiopoietin-like 4 (34 fold) or hypoxia

inducible protein 2 (HIG2, 7 fold) and CD54 (ICAM1, 3.5 fold) was also found to be significantly upregulated in MCTS in comparison with cells growing in monolayers. Expression of the gene encoding fibroblast growth factor-2 (FGF2) was found to be significantly downregulated (6.8 fold).

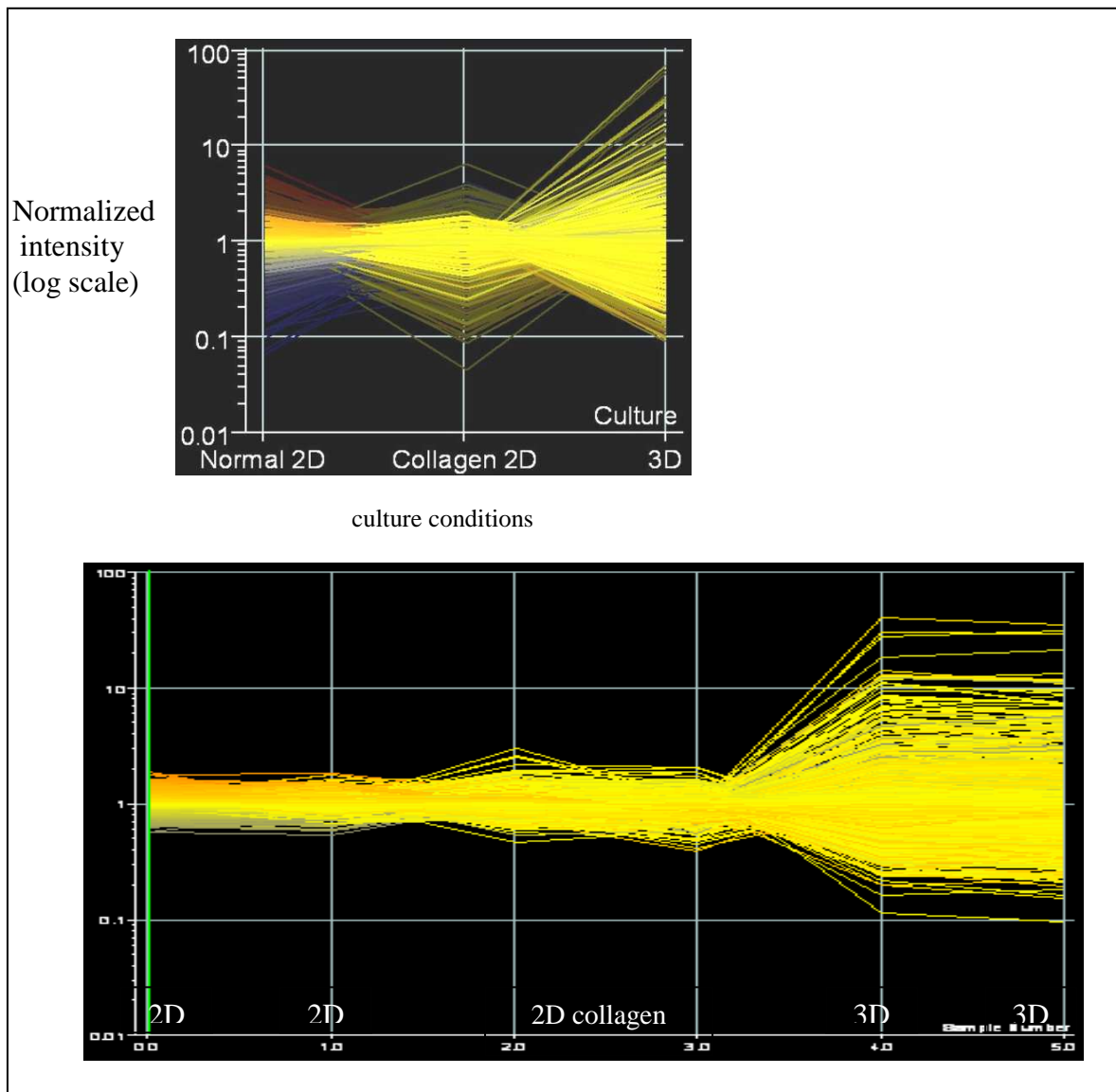


Figure 15: Gene expression profile for NA8 cells cultured as monolayer (with or without ECM) and as spheroid

Strikingly, culture in MCTS appears to result in the upregulation of a constellation of genes whose expression has previously been shown to correlate with high malignancy. CXCL1 (melanoma growth stimulatory activity) is a potent growth factor for melanoma cells, with only limited proliferative activity towards normal melanocytes. IL-8 plays an important role in melanoma progression. Leslie et al (Leslie MC et al 2005) studied gene expression

associated with transition from Radial growth phase (RGP) to Vertical growth phase (VGP). In their study the mostly overexpressed gene was the pro-angiogenic factor IL-8.

In case of HBL cells, our study revealed that culture in 3D spheroid architecture had a relatively modest overall impact on gene expression in HBL cells, whereas a wider range of gene expression pattern was observed when cells were cultured over fibronectin coated dish (Figure 17). However we observed only a slightly higher rate of proliferation in monolayer cells cultured over fibronectin coating, as compared to standard monolayers (Figure 16).

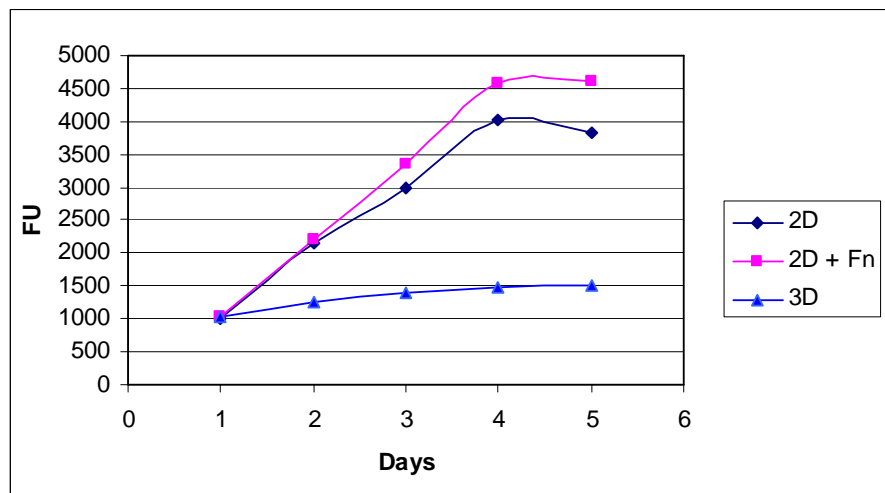


Figure 16: AlamarBlue proliferation curves of HBL cells cultured in standard monolayer, monolayer over fibronectin coating and in MCTS.

Beside a number of expressed sequences encoding undescribed gene products, 47 genes only were significantly modulated more than 3 fold, with down-regulation of 18 and up-regulation of 29 in 3D as compared with 2D cultures.

176 transcripts were upregulated more than 2 fold and 79 transcripts were downregulated more than 2 fold in spheroids compared to monolayer cultures. The gene list for upregulation in spheroids included genes encoding molecules involved in intercellular adhesion such as junctional adhesion molecule 2 (JAM2, >22-fold up-regulated), tight junction protein 4 (peripheral) (5.4 fold up-regulated) and cadherin-like 1 (>8-fold up-regulated). Transcript encoding Podoplanin was 2.5 fold upregulated (Wicki A et al 2006), while interferon gamma receptor-1 was downregulated 4.9 fold in MCTS compared to monolayer cells.



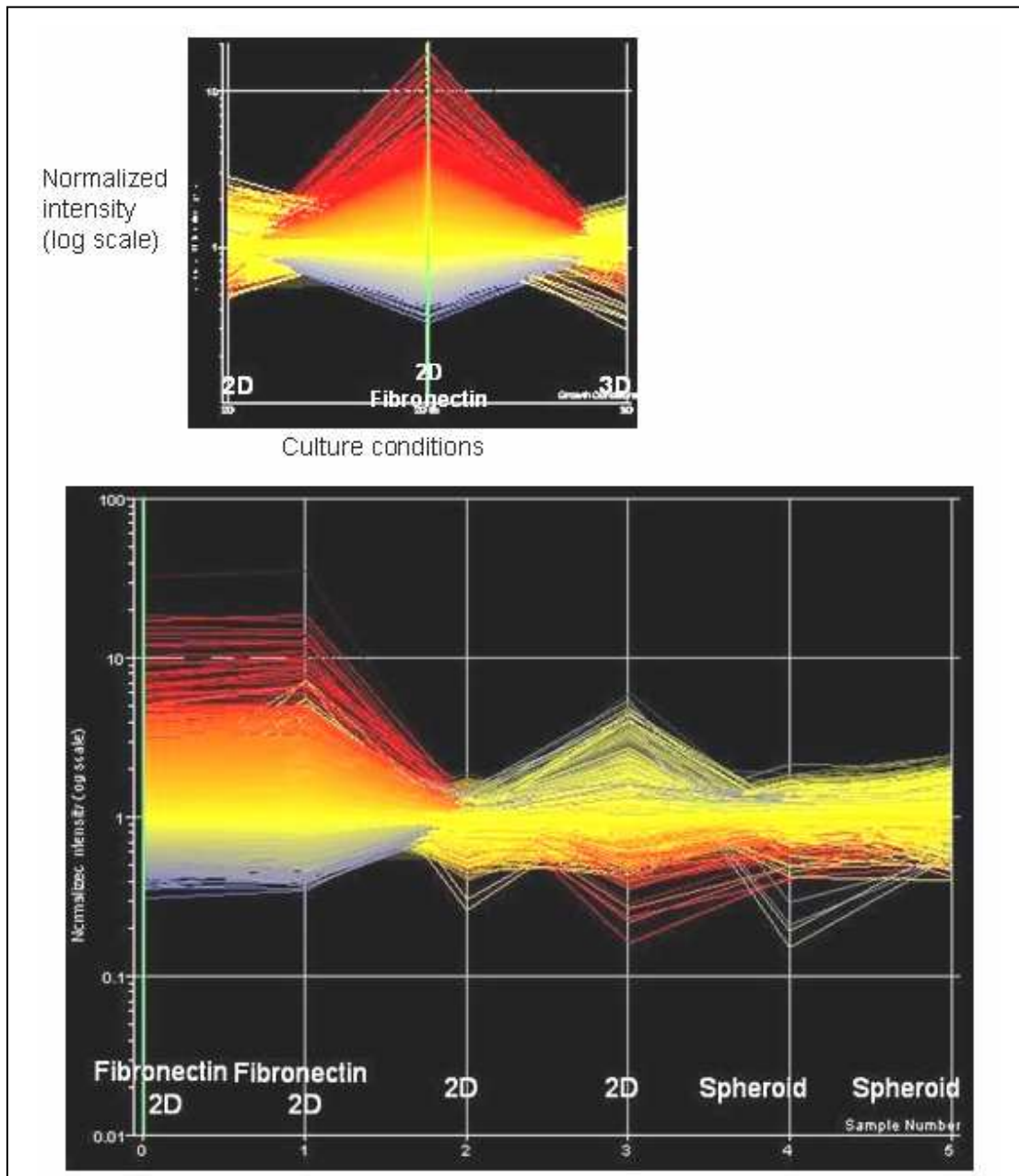


Figure 17: Gene expression profile for HBL cells cultured as monolayer (with or without ECM) and as spheroid

### 3.3.1. Validation of differential gene expression

Large scale gene expression databases require validation at the gene and protein level. We have validated expression pattern of some interesting genes or gene products by Real-time, quantitative RT-PCR or ELISA (Ghosh S et al 2005b). These data strongly support the integrity of the gene profiling methods adopted in these studies.

Two genes whose products, CXCL1 (GRO- $\alpha$ ) and IL-8, have been shown to play a relevant role in melanoma progression and metastatic process were found to be significantly

upregulated in cells cultured in NA8 MCTS as opposed to monolayers NA8. Real-time, quantitative RT-PCR confirmed the upregulation of CXCL1 (GRO- $\alpha$ ) gene expression in cells sampled after 3-day culture in MCTS, as compared with cells growing in monolayers. We were then interested in investigating whether the upregulation of CXCL1 gene reflected transient events, merely related to MCTS formation or more durable modifications of NA8 gene expression profile. Indeed, CXCL1 gene upregulation, although declining, was still observed at 10 days after the initiation of cultures. Accordingly, secretion of this chemokine was significantly increased in cells cultured in MCTS as compared to their monolayer cultured counterparts at both 3 and 10 days of culture (Figure 22).

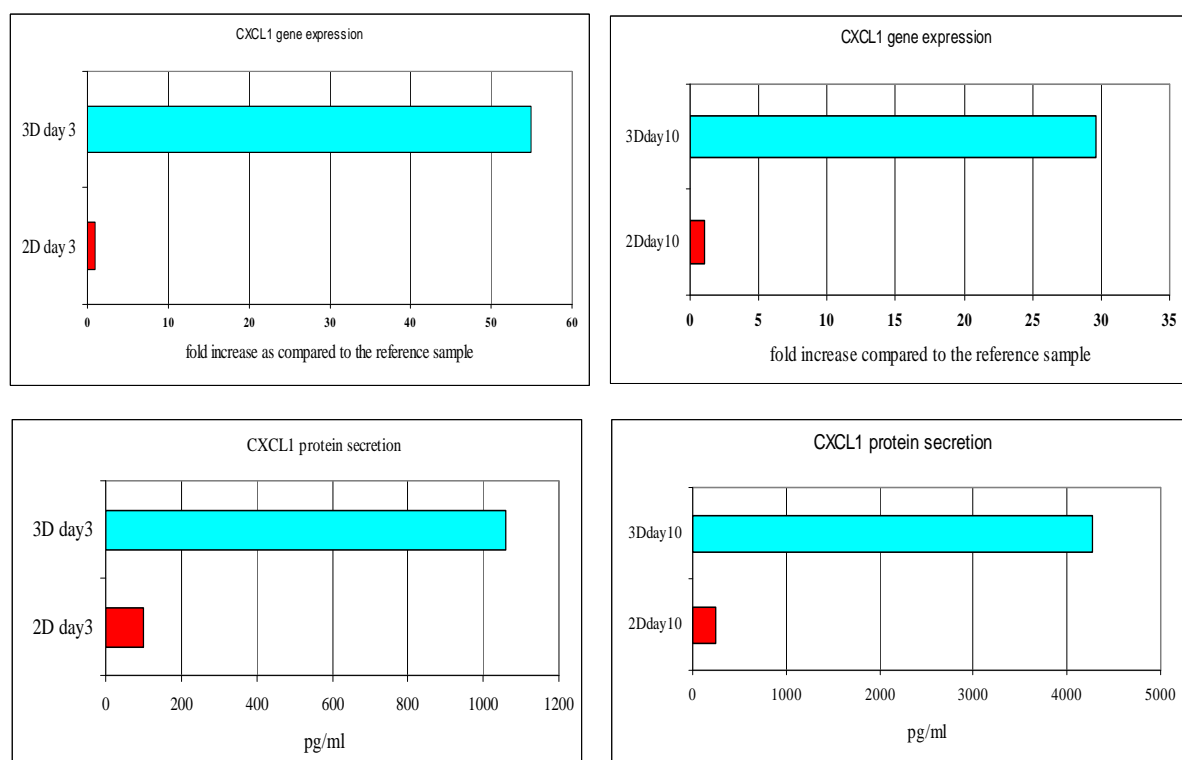


Figure 22: Chemokine CXCL1 gene expression and protein secretion in NA8 cells cultured in monolayers and MCTS at two different time points

Similarly, increased IL-8 gene expression, as detected by oligonucleotide array hybridization of cRNA from 3 days MCTS in comparison to 2D cultures, could be confirmed by real-time RT-PCR at day 3 and, to a lower extent, at 10 days. Accordingly, significant increases in protein secretion were also observed (Figure 23). Most conspicuously, massive IL-8 secretion, exceeding 80 ng/ml, was detected in supernatants of NA8 cells cultured for 10 days in MCTS.

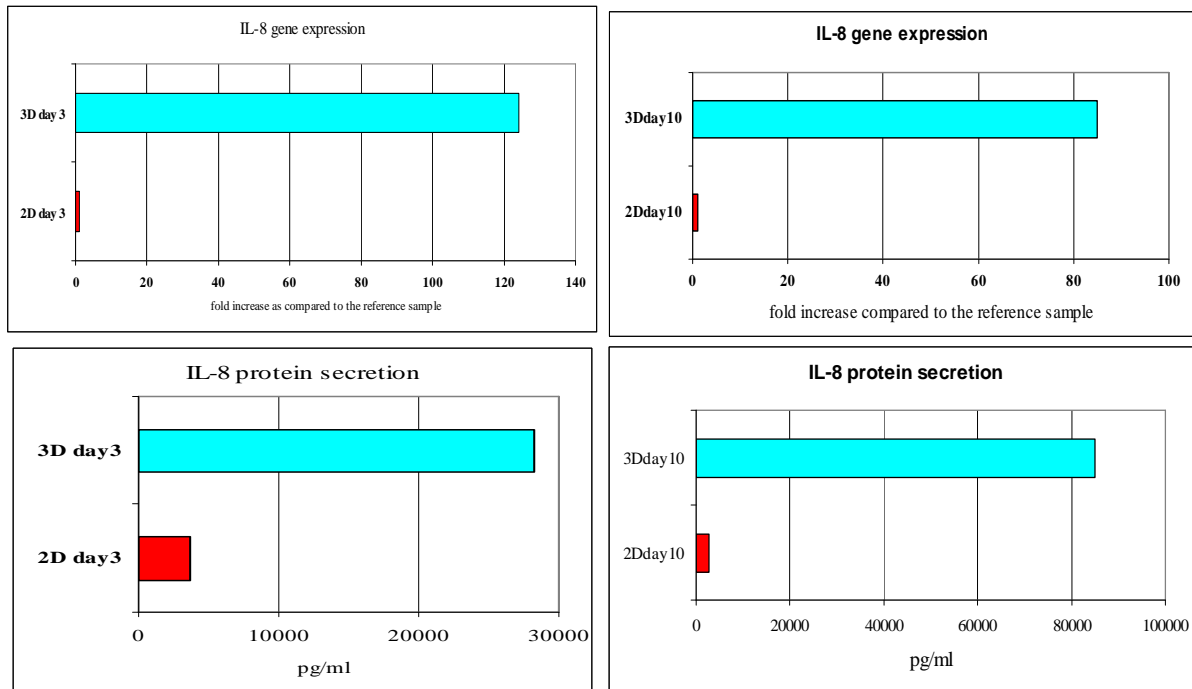


Figure 23: Chemokine IL8 gene expression and protein secretion in NA8 cells cultured in monolayers and MCTS at two different time point

Interestingly, immunohistochemical studies (Figure 24) revealed that IL-8 specific staining was detectable in MCTS, with a preferential localization mostly in inner cell layers. Na8 cells were cultured for 10 days in MCTS. Spheroids were then fixed, processed as detailed in Ghosh S et al 2005a, and incubated in the presence of a monoclonal antibody recognizing IL-8. Specific staining is preferentially detectable in the inner layers of MCTS.

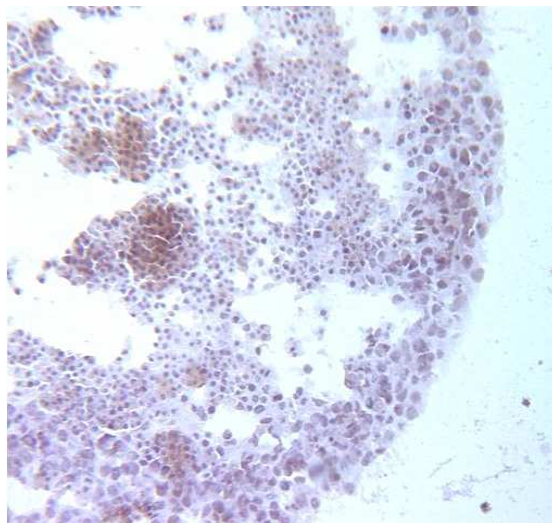


Figure 24: Immunohistochemical detection of IL-8 in MCTS.



The marked increase in the expression of CCL20 (Macrophage inflammatory protein MIP-3 $\alpha$ ) gene in cells cultured in MCTS, as compared to monolayers, detected upon oligonucleotide chip hybridization, was also confirmed by real-time RT-PCR. ELISA assays showed a significant increase in CCL20 protein secretion from MCTS at 3 days and 10 days as compared to cells cultured in 2D for the same time, whereas specific gene expression declined in 10 days MCTS.

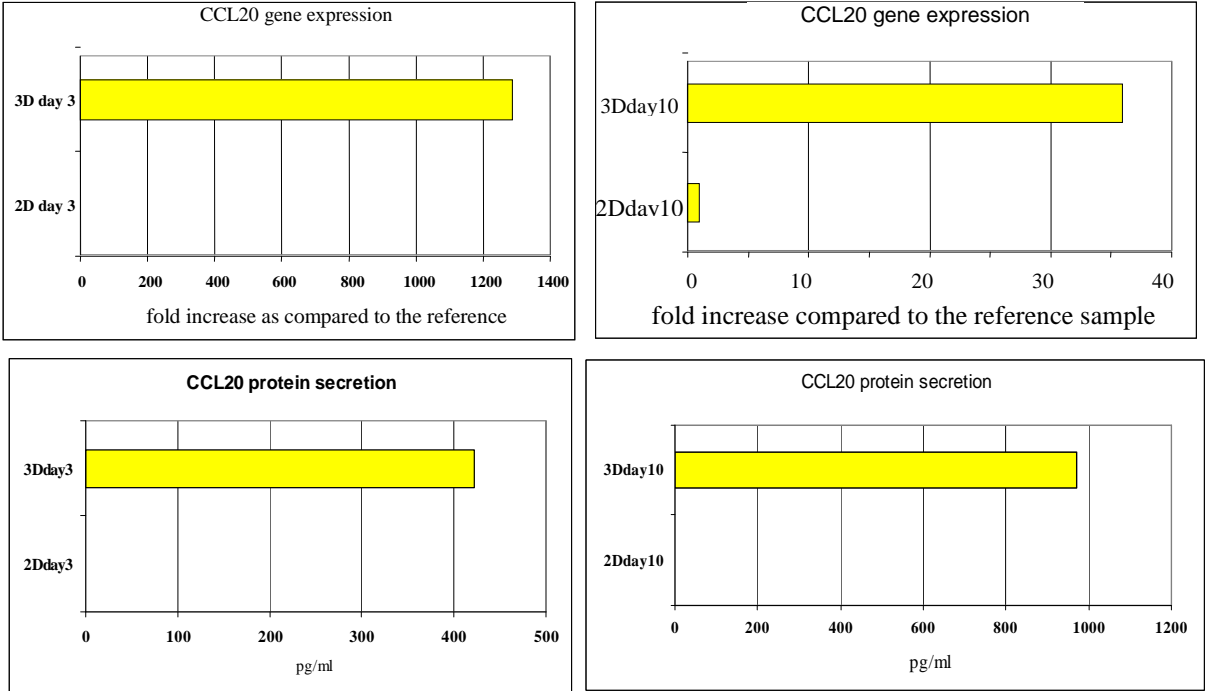


Figure 25: Chemokine CCL20 (MIP3 $\alpha$ ) gene expression and protein secretion in NA8 cells cultured in monolayers and MCTS at two different time points

### **3.4. Cellular immunology studies- focus on immunorecognition**

Growing evidence is accumulating to indicate that functional activities of tumor associated antigen specific cytotoxic T-Lymphocytes might be significantly altered in the presence of tumor cells growing in multilayered architectures, as compared to the monolayer cultures. Clinical data of immunotherapy trials underline that even in the presence of specific immune responses, 3D tumors *in vivo* may be relatively insensitive to their effects. But the molecular mechanisms underlying the discrepancy are still unclear.

#### **3.4.1. Description of the model system**

We selected as model melanoma cell lines HBL and D10 cells, which are HLA-A0201+ve and are characterized by high expression of melanoma differentiation antigens. Percentages of TAA specific T cells “*ex vivo*” are extremely low, and usually do not exceed 0.5% of total CD8+ T cells. To perform our studies in controlled conditions, we resorted to the use of antigen specific cloned T cells as effectors. Importantly, CTL clones are far more efficient in this respect than T cells freshly obtained from peripheral blood.

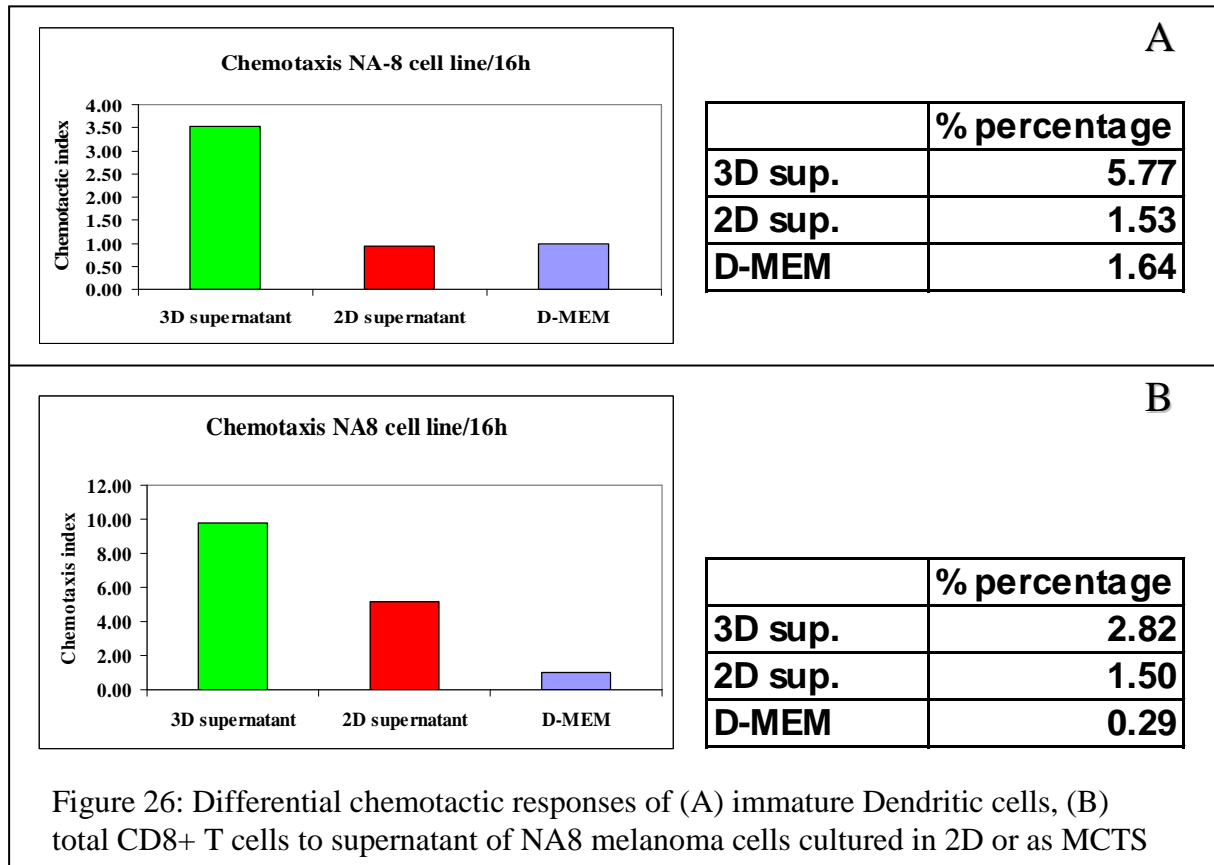
CTL clones, recognizing Melan-A/MART-1<sub>27-35</sub> epitope and/or gp100<sub>280-288</sub> were generated from peripheral blood of patients undergoing active, antigen specific immunotherapy in the context of specific clinical trials. They were able to kill in standard <sup>51</sup>Cr release assays HBL melanoma cells in monolayer expressing both antigen and HLA-A0201 restriction determinant (Ghosh S et al 2005b).

#### **3.4.2. Migration of immunocompetent cells in response to MCTS supernatants**

Melanoma cell lines may produce proinflammatory chemokines. We previously showed that when NA8 cells are cultured as 3D MCTS, there is significant enhancement of the expression of CCL20, CXCL1 and IL-8 genes (Ghosh S et al. 2005a). Receptors for these chemokines are largely expressed on iDC and CD8+ T cells (Greaves DR et al. 1997; Lippert U et al. 2004; Takata H et al. 2004). Thus, chemoattraction by MCTS might reflect the potential chemoattractive capacity of neoplastic tissues.

Then we assessed differential chemotactic responsiveness of iDC and CD8+ T cells to chemokines present in culture supernatants, using, as melanoma model, NA8 cells cultured in 2D or in MCTS. Addition of supernatants of cells growing in monolayers to the lower part of a transwell system induced migration of both iDC and total CD8+ T cells, suggesting that NA8 cells constitutively produce chemotactic factors *in vitro*. Most importantly, supernatants

derived from the same number of NA8 cells growing in MCTS induced a significant increase in the migration of iDC and CD8+ T cells as compared to supernatants of their 2D counterparts. Chemotactic index is defined by the number of migrated cells in the experimental conditions divided by number of migrated cells in negative control (culture medium).



The above data suggest that when melanoma cells are cultured in the form of 3D MCTS, they are capable of attracting APC and CD8+ T cells. But this ability curiously contrasts with the relatively low effectiveness of tumor specific immune responses “*in vivo*”. Puzzled by this discrepancy, we sought to investigate the morphology of the interaction between melanoma cells, iDC and, most importantly, CD8+ T cells, which are largely responsible for tumor specific cytotoxic activities.

### 3.4.3. Morphology of interaction between TAA specific CTLs and melanoma cells cultured in spheroids

To explore CTL-tumor cell interaction, first morphological aspects were addressed ([Ludford-Menting MJ et al 2005](#)). By Scanning electron microscopy one can easily inspect the morphological features of the cells. Antigen-specific T cells get activated after interaction of T cell antigen receptor (TCR) with MHC-peptide complexes expressed on tumor cell

surfaces. This interaction takes place in a 30-40 nanometer scale gap between the two cells, known as an “immunological synapse” (Grakoui A et al 1999; Bromley SK et al 2001).

HBL tumor spheroids were placed on a glass slide and allowed 4-5 hours to attach. Some cells started to proliferate out of the spheroids and started to grow on the slide in monolayer surrounding the spheroid. Then MART-specific CD8+ CTLs (clone E2MA4) were added on top and after 24 hours the whole structure was fixed with 4% glutaraldehyde. No T cells were found to express uropod (Friedl P et al 1998), which forms during migration or cell-cell interaction, but some of them appeared to form stable contacts with cancer cells.

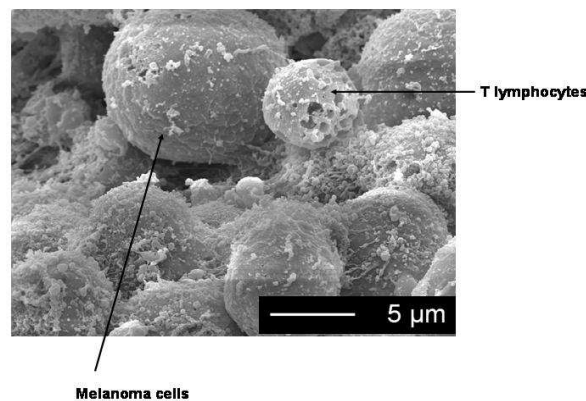


Figure 27: Morphological view of T-lymphocytes attached over HBL spheroid by Scanning Electron Microscopy

It has been suggested that while cells in monolayer are killed by CTL attack, spheroids may be able to maintain their structural integrity. This might lead to the assumption that although some T cells can form immunological synapse, the peripheral cancer cells of the spheroid may not get detached, forming a layer of protection, possibly causing lack of interaction of T cells with the tumor cells embedded within the 3D architecture.

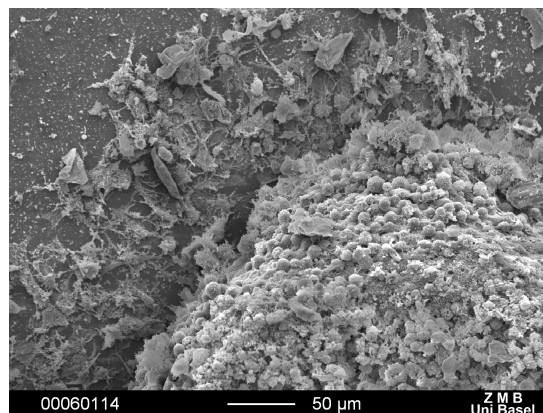
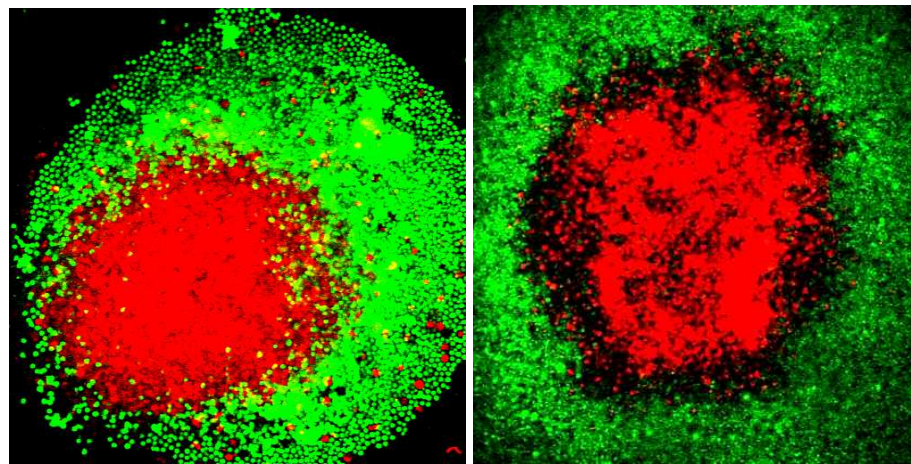


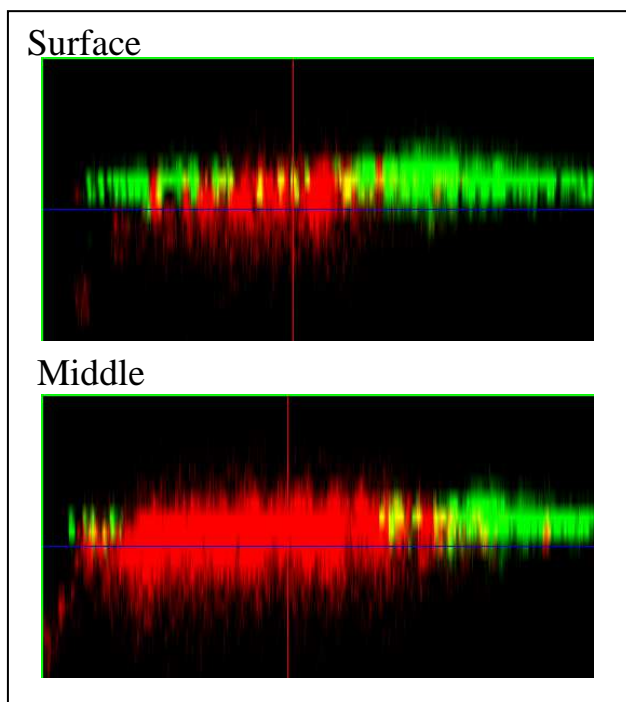
Figure 28: Scanning Electron Microscopic view of tumor spheroid, showing integrated 3D structure of HBL spheroid, after 24 hours of co-culture with MART-1-specific CTL clones

Hence as the next step, by using our spheroid model we investigated whether infiltration of TAA-specific T lymphocytes into tumor spheroid has a “brisk” (deep and/or diffuse) or a “non brisk” (focal and superficial) character and its timing by confocal microscope.



A

B



C

Figure 29: Non-brisk infiltration of melanoma MCTS immunocompetent cells  
**Figure A:** 3D HBL 30,000 & Melan-A /MART-1<sub>27-35</sub> specific CTL clone  
**Figure B:** 3D NA8 30,000 & Total CD8+ T cells  
**Figure C:** 3D projection of HBL spheroid, challenged with CTL clones to show only superficial infiltration

HLA-A0201 restricted MART-1<sub>27-35</sub>-specific T lymphocytes were labelled with CFSE and cocultured overnight with 3 days old HBL spheroids (labelled with PKH 26 Red fluorescent dye). By confocal microscopy we observed that Melan-A/MART-1-specific CTLs could infiltrate only the peripheral part of the HBL spheroid (Figure 29A), although HBL cells express MART-1 antigen and HLA-A0201.

Similarly, total CD8<sup>+</sup> T lymphocytes were freshly isolated from a buffycoat. Melan-A/MART-1 negative and HLA-A0201<sup>+</sup>ve NA8 cells were cocultured with total CD8<sup>+</sup> T cells (undefined antigenic specificity) and they were also unable to penetrate in deep into the 3D architecture of MCTS but rather tended to remain on the spheroid surfaces (Figure 29B). These pictures closely reminded the “non brisk” infiltration of melanoma by T cells observed in the past in clinical tumor specimens (Anichini A et al 1999; Bernsen MR et al 2004).

These data indicate that irrespective of antigenic specificity, three dimensional tumor spheroids are poorly infiltrated by CD8<sup>+</sup> T cells.

### 3.4.4. Immunorecognition:

Lack of MCTS infiltration by TAA specific CTLs hinted at a possible defective killing of tumor cells cultured in 3D spheroids.

#### 3.4.4.1. IFN $\gamma$ as a surrogate marker of antigen recognition:

Cell death is traditionally measured by the quantification of chromium (<sup>51</sup>Cr) release from labeled target cells. In this assay, living cells nonspecifically incorporate and retain the radionuclide. As the cells are killed, <sup>51</sup>Cr is released into the culture medium and is quantified by scintillation counting. This assay is a standard way to measure the cell killing ability of cytotoxic T cells. However tumor cells cultured as 3D spheroids are unfit to serve as target for <sup>51</sup>Cr release

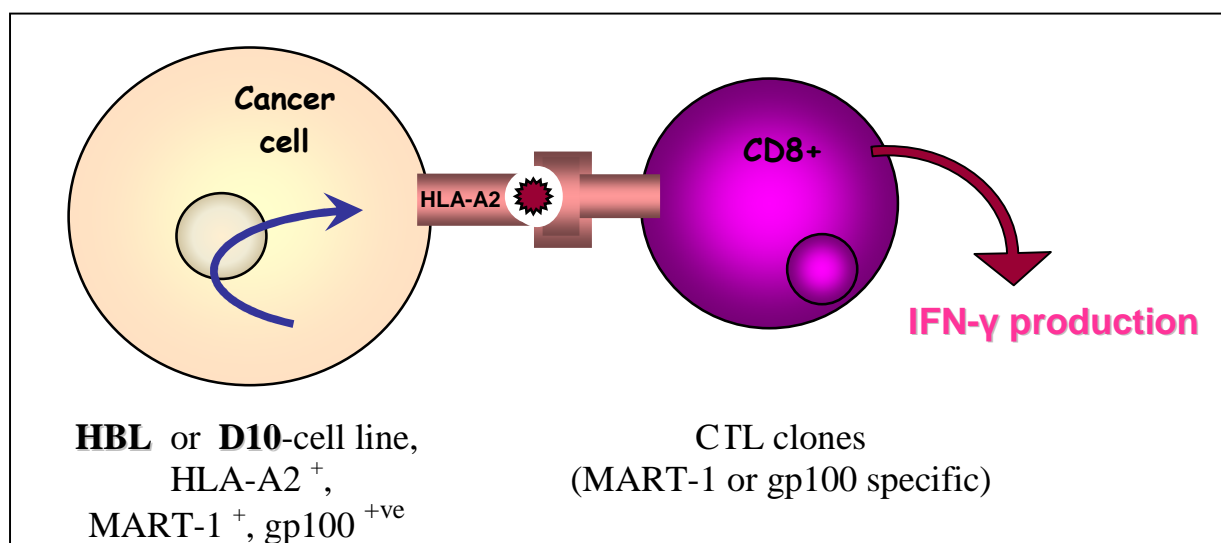


Figure 30: Schematic view of antigen recognition and IFN- $\gamma$  production by T-lymphocytes

assays, because washing steps required after labeling may disrupt cells aggregates. Hence, we decided to measure IFN- $\gamma$  production by antigen specific T cells following interaction with targets expressing appropriate TAA and restriction determinants, as a classical alternative marker of antigen recognition.

### 3.4.4.2. Antigen recognition by IFN- $\gamma$ secretion measurement

HBL spheroids were prepared in so that each spheroid contained 30000 cells. When co-cultured together with HBL melanoma cells cultured in monolayer CTL clones produced high amounts of IFN- $\gamma$ , in the order of magnitude of nanograms. IFN- $\gamma$  production by CTL clones was detectable within 4 hour incubation, with a peak level usually observed at 24 hours (Ghosh S et al 2005b). Instead, significantly lower amounts of cytokine were produced when CTLs were challenged with the same numbers of HBL target cells cultured for 2-3 days in 3D architectures (Figure 31).

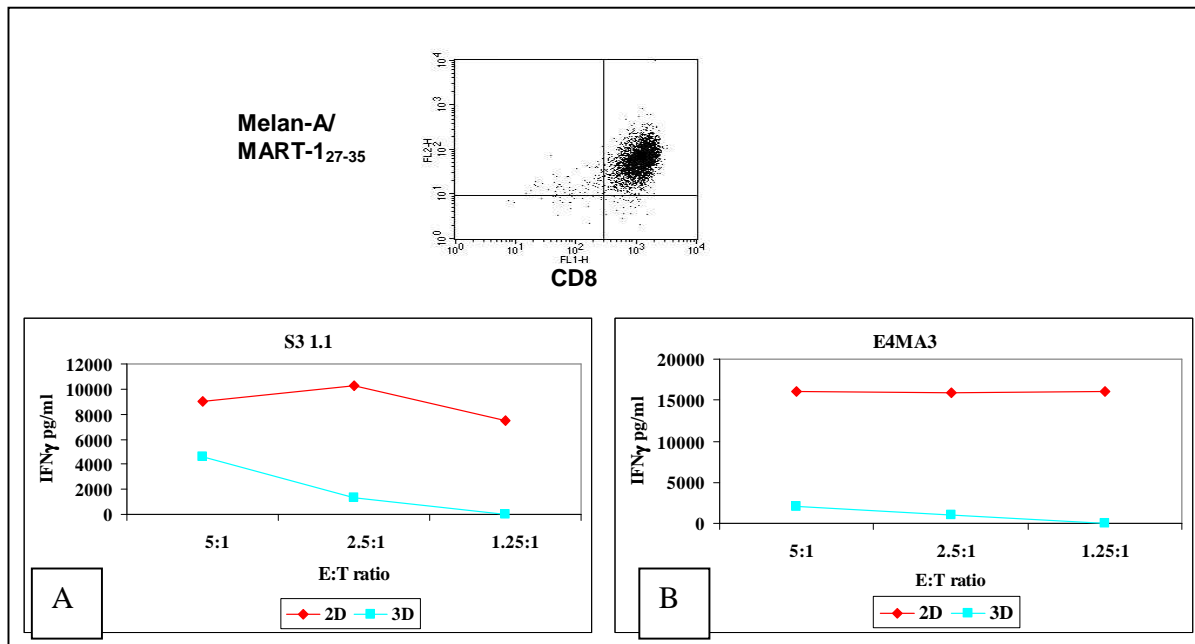


Figure 31: Functional activities of HLA-A0201 restricted Melan-A/MART-1<sub>27-35</sub> specific CTL clones, homogeneously tetramer specific (representative example in upper panel), using HBL melanoma cells cultured in 2D and 3D conditions (30000 cells per well) as targets. Panel A, B are representative of two different CTL clones

Then HBL cells in monolayer and as 3D spheroids were challenged with gp100<sub>280-288</sub> specific CTL clones at different effector: target ratios. In this case too CTL clones produced more IFN- $\gamma$  when they were challenged with HBL cells in monolayer than spheroids.

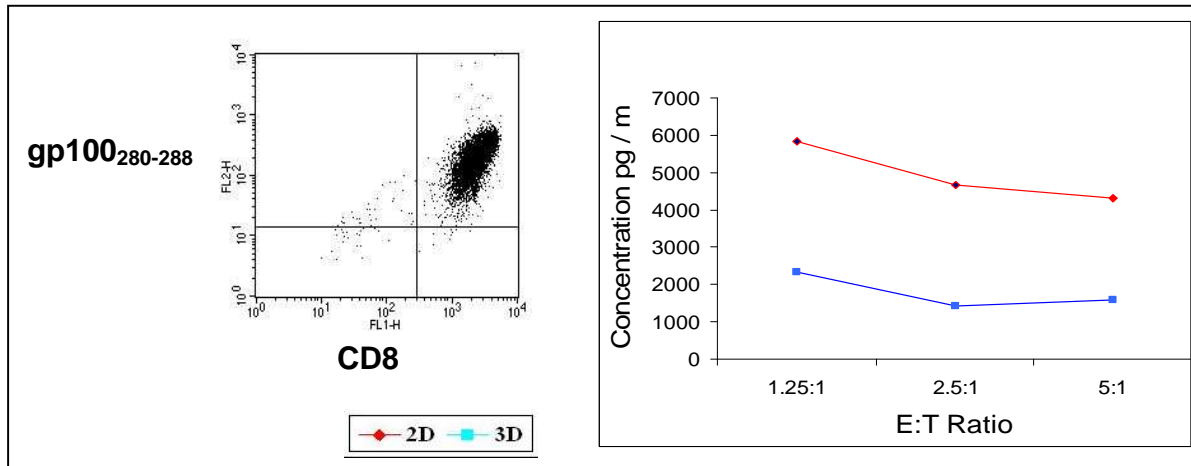


Figure 32: Functional activities of a HLA-A0201 restricted gp100 specific CTL clone, showing homogeneous tetramer staining (left panel), using HBL melanoma cells cultured in 2D and 3D conditions as targets.

These experiments indicated that there is indeed impaired immunorecognition when cancer cells are in the form of 3D spheroid for HBL melanoma cells.

We asked if this phenomenon was only valid for HBL cells or it is more general. Hence we have studied immunorecognition using D10 cells and gp100-specific HLA-A0201 restricted CTL clones at different E:T ratios.

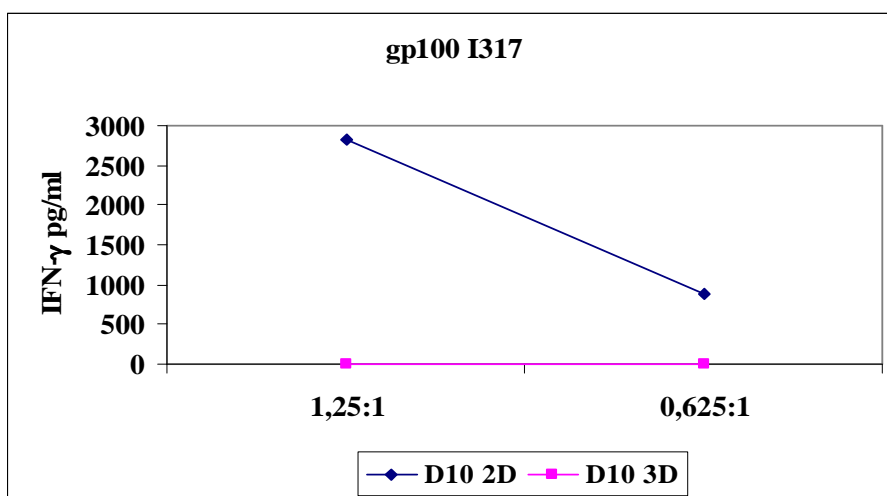


Figure 33: Functional activities of HLA-A0201 restricted gp100-specific CTL clones using, D10 melanoma cells as targets cultured in 2D and 3D conditions.



Thus, growth in 3D architectures indeed appears to impair recognition of TAA by specific effector T cells.

#### **3.4.4.3. Effects of interaction with targets cultured in spheroids on CTL machinery**

Elicitation of CTL functions relies on the expression of an array of components of their lytic machinery. For instance, CTL may kill through Fas pathway and granzymes entering target cells may rapidly induce their DNA fragmentation based apoptosis. Furthermore, perforin in the CTL granules plays a pivotal role in granule-mediated killing. We also assessed CTL functions by evaluating FasL, granzyme B and perforin gene expression in CTLs co-cultured with melanoma target cells growing in 2D or in MCTS (Figure 34). As expected, interaction with targets Melan-A/MART-1<sub>27-35</sub>+HLA-A\*0201+ cultured in monolayer induced the expression of FasL, granzyme B and perforin genes in antigen specific CTL. However, the expression of these genes was significantly lower when effector cells were stimulated by MCTS.

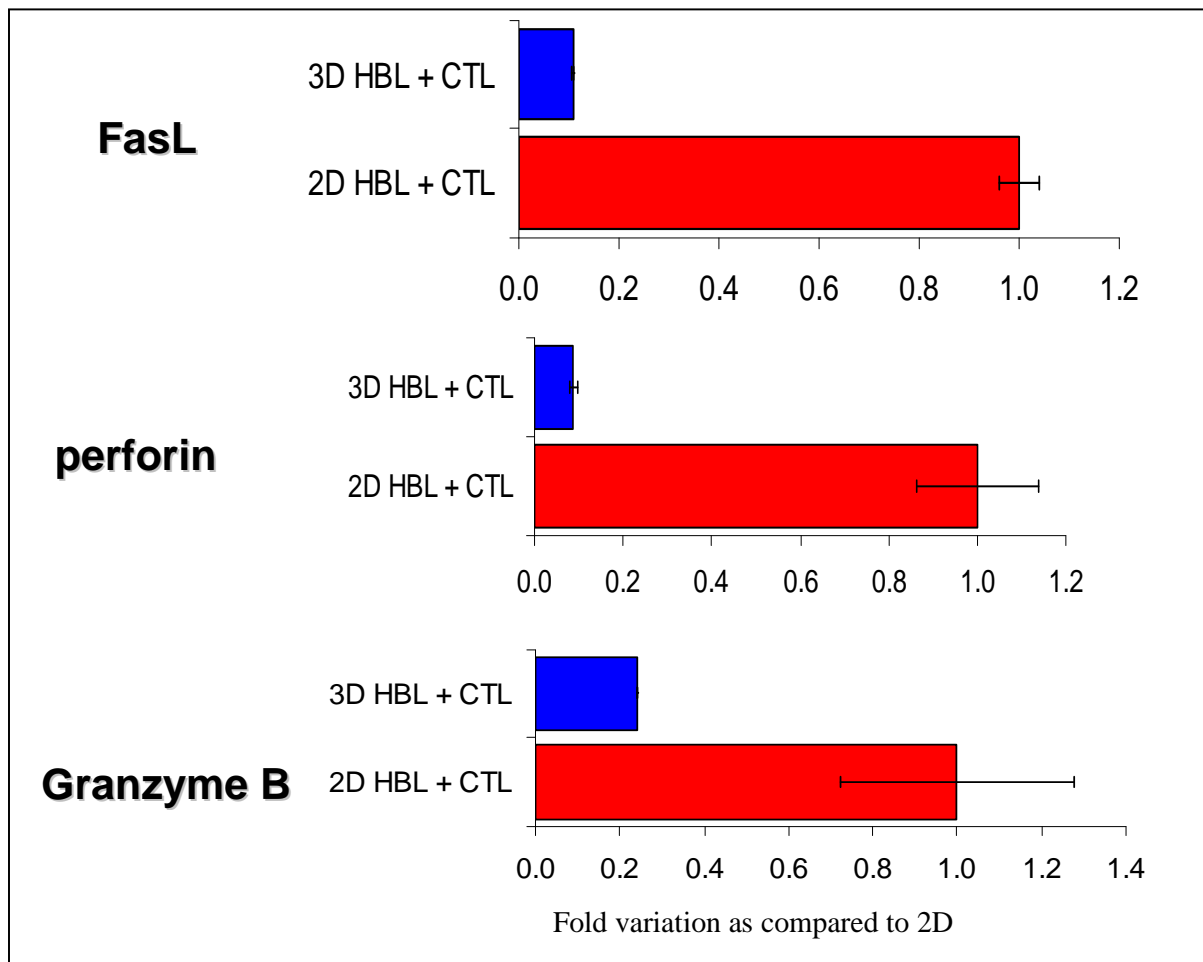


Figure 34: functionality of TAA specific CTLs is impaired within the 3D tumor spheroid microenvironment

Taken together, these data indicate that CTLs exposed to a 3D “in vitro” tumor microenvironment show an impaired functionality of their lytic machinery, reminding situations frequently observed in vivo (Zippelius A et al 2004; Mortarini R et al 2003).

#### **Proliferative capacity of tumor cell stimulated CTL:**

We have also investigated proliferation capacity of CTLs by using lymphocyte tracking dye carboxyfluorescein diacetate succinimidyl ester (CFDA-SE) (Lyons AB et al 1994; Parish CR 1999). CFDA-SE labelled MART-1 specific CTL clones were co-cultured with HBL cells in monolayer and as spheroids at two different cell densities (15000 and 30000 cells per well) and proliferation was measured by fluorocytometry after 4 days of culture. While minimal proliferation was observed in CTL stimulated by 2D cultured melanoma cells, it was totally absent in CTL stimulated by MCTS.

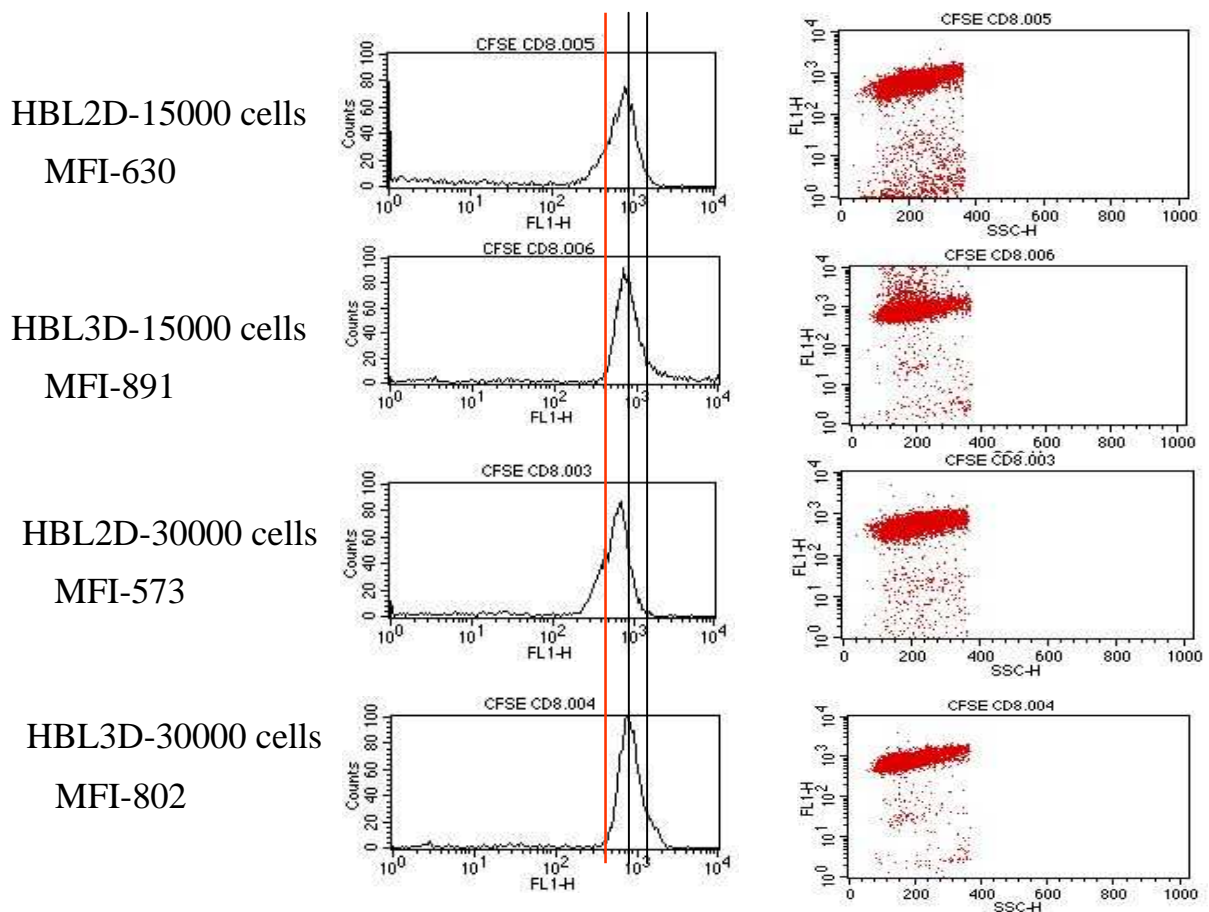


Figure 35: CFDA-SE labeled proliferation of CTLs stimulated by melanoma cell lines, as detected by flow cytometry

### 3.4.5. Possible mechanisms causing impaired immunorecognition

Data from different groups (Dangles V et al 2002, Dangles-Marie V et al 2003), including ours (Ghosh S et al 2005b), indicate that culture of tumor cells in three-dimensional structures modulates their gene expression profiles and decreases their susceptibility to the immunomediated CTL attack although still unclear are the underlying molecular mechanisms. We would like to use our MCTS model system to get some insight about the probable mechanisms. We envisage that this impaired immune recognition might result from many reasons including:

- (a) complex 3D tumor spheroid architecture which prevents penetration of T cells
- (b) downregulation of tumor antigen expression
- (c) downregulation of MHC class-I molecules expression
- (d) accumulation of acidic metabolic products, such as lactate

### 3.4.5.1. Structural hindrance of spheroid:

Poor infiltration of CTLs inside the spheroid might be attributed to the structural constraints of 3D architecture. Culture in spheroids may provide an overall smaller cell surface accessible to CTL attack, as compared to monolayers, resulting in decreased activation of effector cells. To address this issue, HBL cells were cultured as MCTS and after 3 days, spheroids were disrupted by vigorous pipetting and seeded again as monolayer with 30000 cells/well cell density. On the same day, HBL melanoma cells who had never experienced 3D tumor microenvironment were also cultured in monolayer at the same cell density. After 6-8 hours CTL clones were added and IFN- $\gamma$  secretion by the CTL clones was measured after 24 hours.

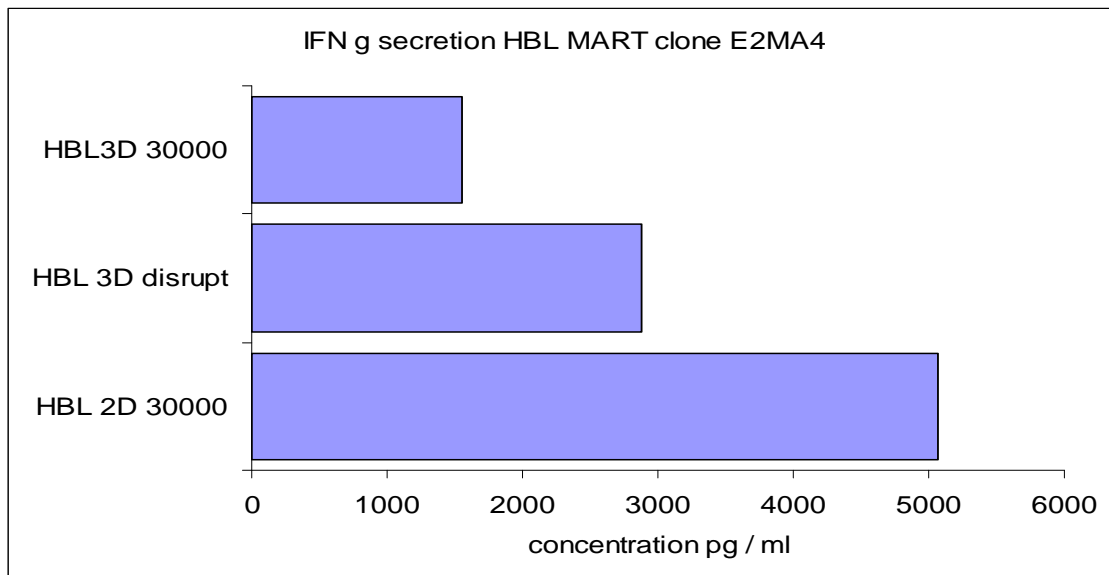


Figure 36: IFN- $\gamma$  secretion by CTLs cultured with HBL cells from intact or disrupted MCTS

Upon stimulation by cells deriving from disrupted spheroids, Melan-A/MART-1<sub>27-35</sub> specific CTLs secreted IFN- $\gamma$  at intermediate levels between 3D spheroids and 2D cultures. These results indicate that the observed impairment of antigen recognition by CTL is at least in part due the smaller cell surface accessible to effectors, but cannot be exclusively ascribed to structural hindrances.

### 3.4.5.2. Downregulation of expression of melanoma differentiation antigens:

We then studied TAA expression, at both gene and protein level, in monolayer cultured cells and spheroids.

Indeed the extent of TAAs expression has major implications for immunorecognition by the antigen-specific CTLs. First HBL cells were stained for MART-1 expression using specific antibody. Spheroids were disrupted by vigorous pipetting and scattered single cells were fixed on a coverslip. Intensity of MART-1 specific staining in cells

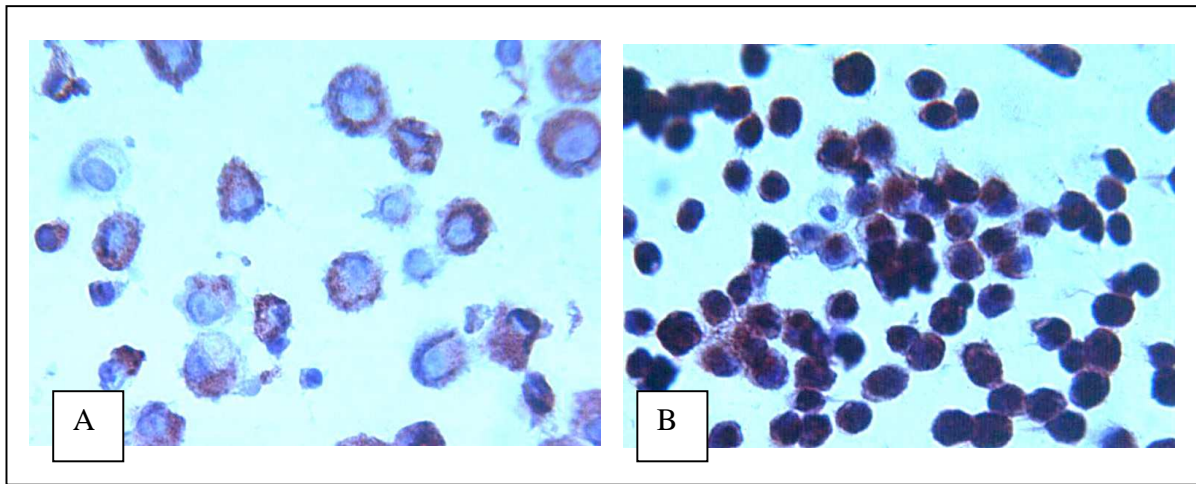


Figure 37: Melan-A/MART-1<sub>27-35</sub> immunostaining on cells from (A) disrupted spheroids and (B) monolayer cultured cells, 40X

from MCTS was compared with monolayer cultured cells. A marked difference in intensity of staining was visible (Figure 37). Some cells from disrupted spheroids were almost clear of MART-1 specific staining, as compared to the HBL cells cultured as monolayer.

To get deeper insights about the event of downregulation of TAA, we performed qRT-PCR analysis of antigen expression in HBL cells in monolayer and spheroids. NA8 was the negative control as it does not express MART-1 antigen. Our experiments indicated that in cells cultured in 3D spheroid six fold lower expression of Melan-A/MART-1 was indeed detectable as compared to 2D conditions (Figure 38A). By FACS analysis, following intracellular staining Melan-A/MART-1<sub>27-35</sub> expression was also found to be at least 4-5 fold downregulated in HBL cells from spheroid cultures (Figure 38B).

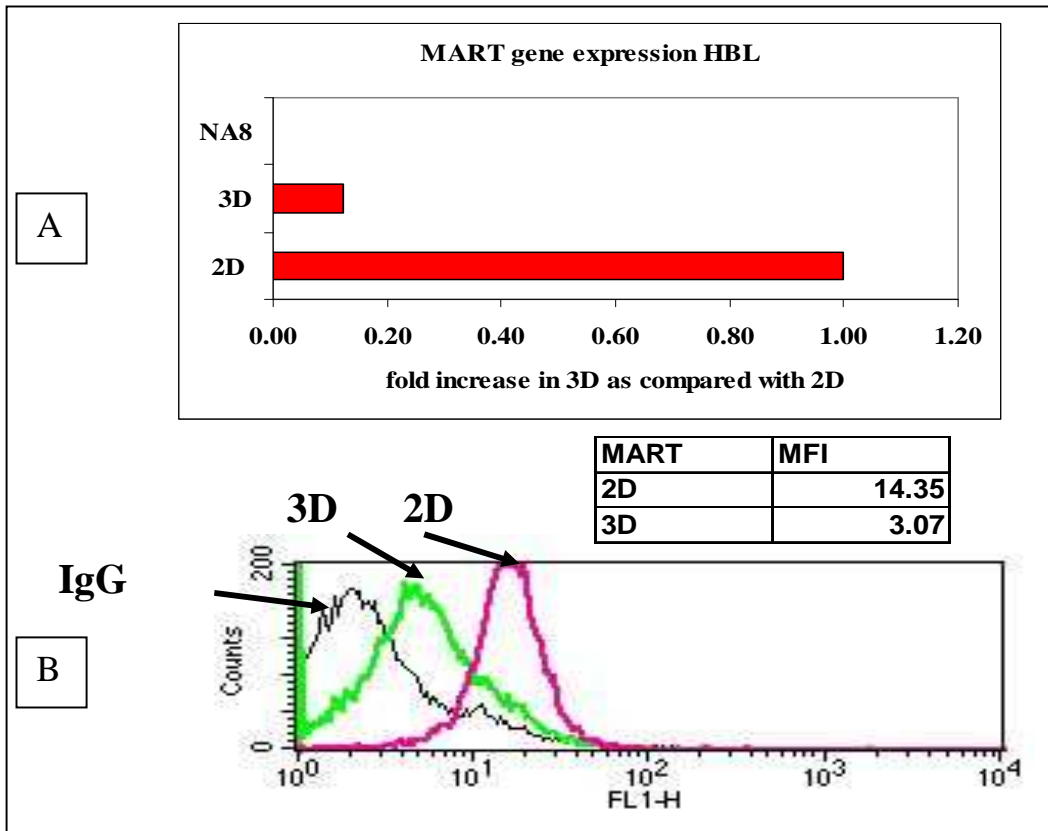


Figure 38: MART-1 antigen expression in HBL melanoma cells in 2D or in MCTS: (A) by RT-PCR, (B) by flow cytometric analysis

Then we tested expression of another TAA, gp100, by quantitative RT-PCR in both HBL and D10 cells cultured in conventional monolayer fashion or as 3D spheroids. Expression of the gene encoding gp100 antigen also was significantly downregulated in 3D spheroids as compared to the cells cultured in monolayers (Figure 39).

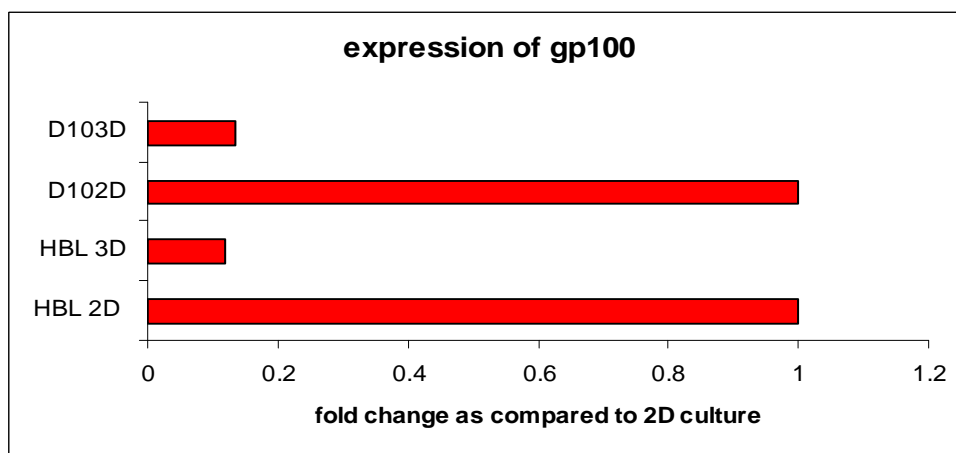


Figure 39: Expression of gp100 in HBL and D10 cells by quantitative RT-PCR

### 3.4.5.2.1. Effect of spheroid size:

Depending upon different cell numbers (e.g. size of the spheroid), there could be different level of hypoxic microenvironment, gradient of nutrients and accumulation of toxic metabolic products. These factors may play important role in governing immunorecognition process. By varying the cell numbers in the spheroid, one can prepare spheroids having wide range of exposed surface (approximately 150-800  $\mu\text{m}$ ).

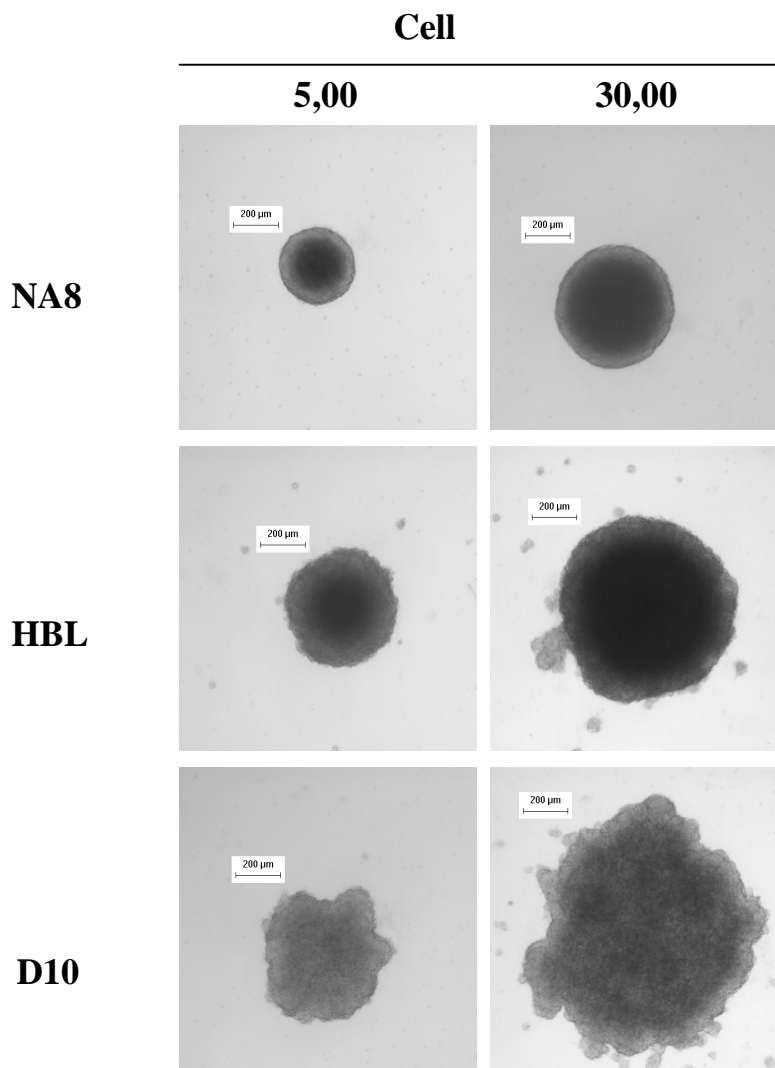


Figure 40: Seeding of different cell number in single wells can result in the formation of spheroids of different volume

Two different CTL clones were cocultured with spheroids of 5 different cell number, starting from 500 cells per spheroid, to a maximum of 50000 cells per spheroid. CTL clones were co-cultured with these spheroids or equal numbers of HBL cells in monolayer for 24 hours at two different effector:target ratios and then IFN- $\gamma$  secretion was measured by ELISA. Interestingly, CTLs produced more IFN- $\gamma$  if stimulated by spheroids than monolayer cultures, when the spheroids contain less than 10000 cells.

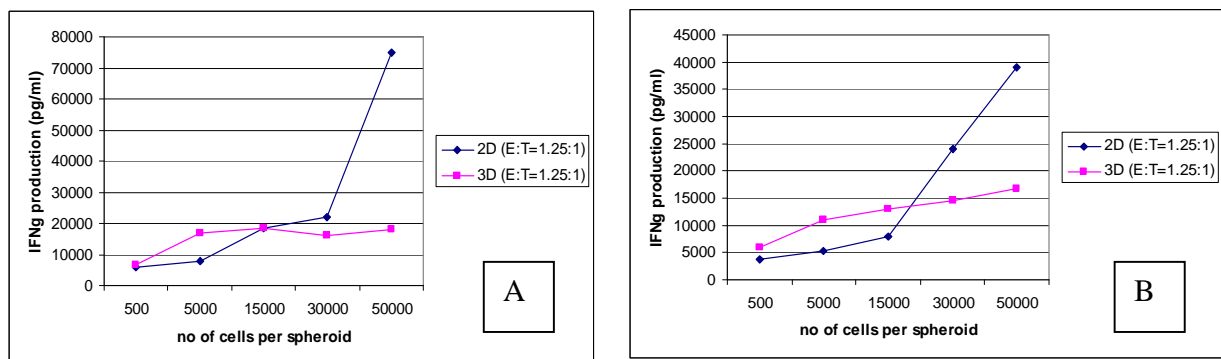


Figure 41: IFN- $\gamma$  production by two different CTL clones upon stimulation with HBL cells cultured in different cell densities (A: CTL clone 2.6.1; B: CTL clone 2.7.1)

Hence the number of cells in a tumor spheroid could play a critical role in T cell activation, as observed by other groups (Dangles V et al 2002) showing that TNF release decreased in an inverse ratio to the spheroid volume; spheroids containing 2,000 cells were still able to stimulate T cells, whereas spheroids containing 5,000 cells had lost this capacity.

We also measured Melan-A/MART-1 gene expression in HBL cells cultured at three different cell densities (5000, 15000, 30000 per well) either as spheroids or as monolayer, and measured Melan-A/MART-1 gene expression by quantitative Real time PCR after 2 days of culture (Figure 43). Indeed the highest down-regulation of the expression of genes encoding



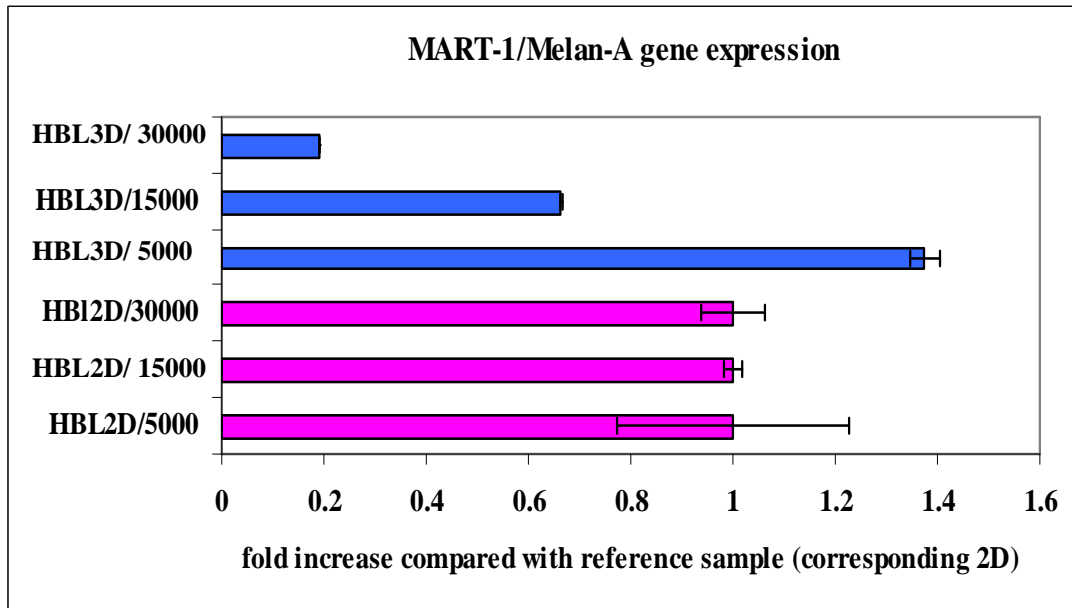


Figure 42: Melan-A/MART-1 gene expression as related to different cell numbers in 2D and 3D cultures of HBL melanoma cells

differentiation TAA was detectable in spheroids containing 30,000 melanoma cells, whereas milder effects were recorded in 3D structures including 15,000 tumor cells. So Melan-A/MART-1 gene expression was strongly correlated with increase in cell number in spheroids, but no major modulation was noticed in monolayer culture (not fully confluent).

#### 3.4.5.2.2. Recovery of TAA after disruption of 3D tumor microenvironment:

Cells from spheroids were disrupted by trypsin treatment or mechanically by vigorous pipetting and subsequently re-cultured again in monolayers for the indicated times. In all cases total cellular RNA was extracted and reverse transcribed. Melan-A/MART-1 gene expression was comparatively evaluated in cells cultured in 2D or in 3D by quantitative real time RT-PCR. Data were expressed as ratio of Melan-A/MART-1 gene expression using as reference value expression in 2D HBL cultures.

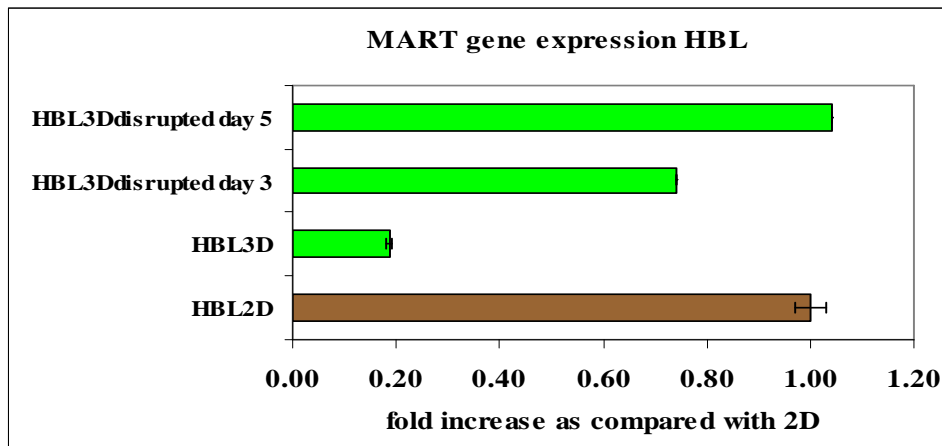


Figure 43: Recovery of Melan-A/MART-1 antigen by gene expression by Re-culturing in monolayer

In our hand, TAA expression was recovered not earlier than after 4-5 days of culture in monolayer.

### 3.4.5.2.3. Comparison of TAA expression with melanoma clinical specimens:

To assess the potential in vivo relevance of our findings, we have also compared expression levels of melanoma associated antigens in tumor spheroids (30000 cells, cultured for 4 days) with those detectable in several tumor biopsies. Although a wide range of antigen expression levels can be observed in biopsies, levels of expression of MART-1 in MCTS frequently matched expression levels in clinical specimens.

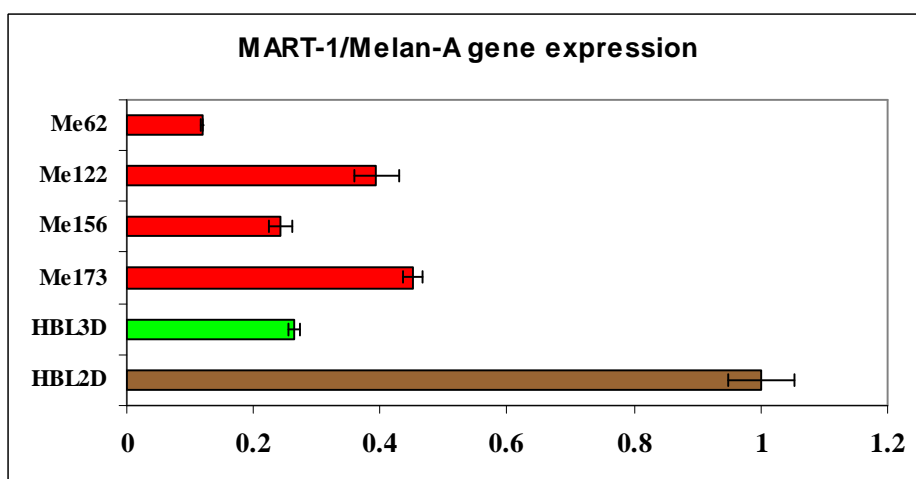


Figure 44: Melan-A/MART-1 gene expression in tumor biopsies and comparison with HBL cells cultured in 2D and as 3D spheroid

#### **3.4.5.2.4. Role of transcription factors downregulating TAA expression:**

We comparatively explored the expression of the genes encoding factors potentially involved in the modulation of antigen expression, in HBL, D10 and NA8 melanoma cells cultured in either MCTS or conventional 2D conditions.

OncostatinM is an interleukin-6 type cytokine originally described by its capacity to inhibit melanoma proliferation in vitro (Zarling JM et al 1986). It has been recently reported that Oncostatin M, produced by melanoma cells cultured in confluent monolayer fashion, can actively down regulate Melan-A/MART-1 mRNA transcription inducing antigen silencing in tumor cells (Durda PJ et al 2003). In our studies, however we could not detect gene expression of Oncostatin M gene in our cells.

On the other hand, Microphthalmia-associated transcription factor is the “master regulator” of melanocytic differentiation (Tachibana M et al 1996). Previously Melan-A/MART-1 and gp100 gene expression have been shown to be transcriptionally regulated by MITF (Du J et al 2003). Indeed, we observed downregulation of Microphthalmia-associated transcription factor (MITF) paralleling with TAA gene expression in our system. These effects also appeared to be cell density dependent (Figure 45).

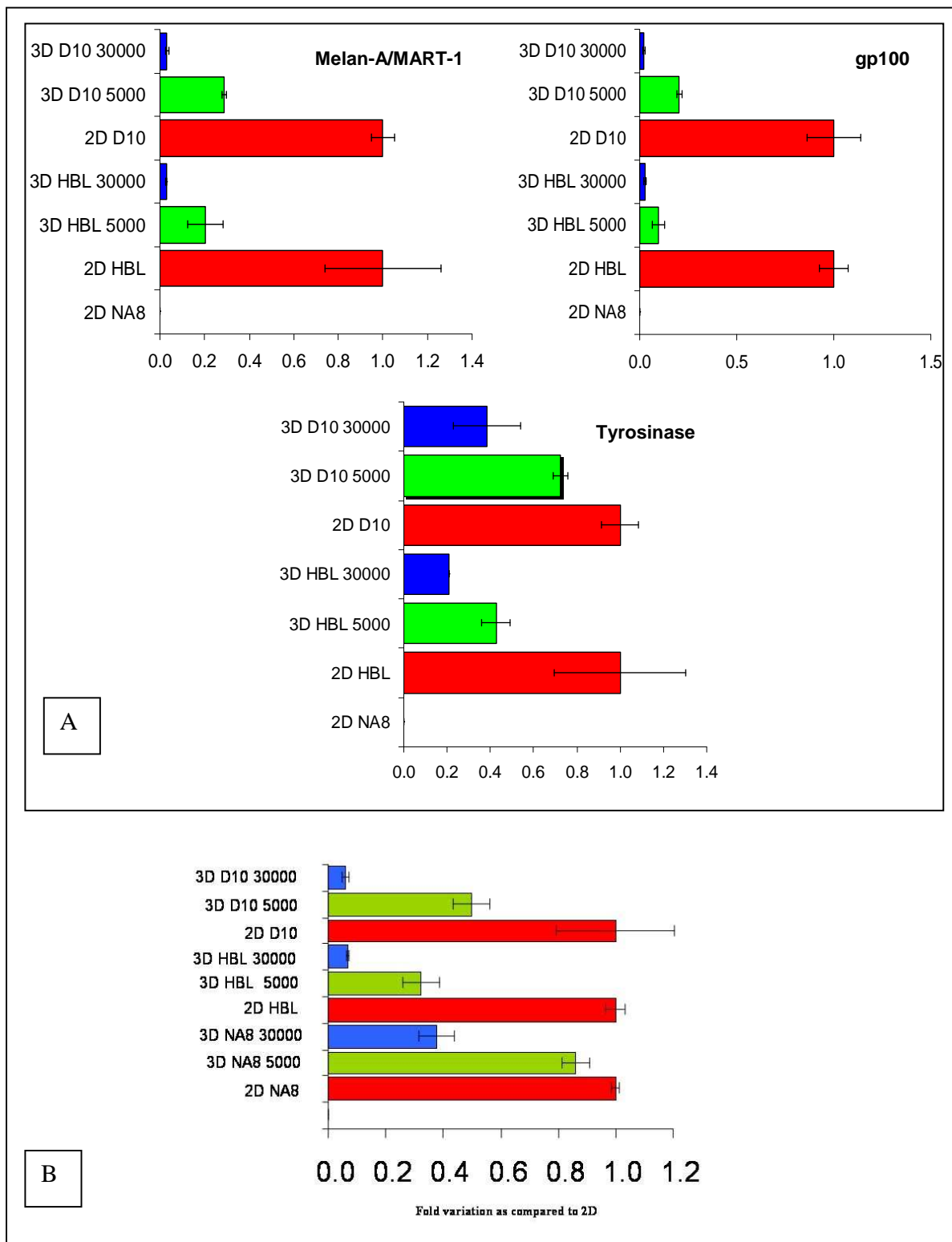


Figure 45: (A) Modulation of gene expression of three tumor associated antigens as related to different spheroid size and culture architectures, (B) MITF gene expression in melanoma cells cultured in monolayer and as spheroids at different cell densities

### 3.4.5.3. Modulation of HLA expression:

Antigen recognition by T cells is restricted by HLA-A2. Loss of HLA-expression may represent an important mechanism by which melanoma evade immune recognition (Garcia-Lora A et al, 2003). HLA class I molecules present peptides from endogenously processed proteins, whereas HLA class II molecules present peptides from exogenous proteins. The level of expression of HLA molecules by cancer cells is decisive to determine the outcome of an immune response. Absence or decreased expression of HLA Class I allele(s) would enable tumor cells to escape from immune response. Downregulation or loss of HLA class I molecules may be due to mutation or loss of  $\beta$ -2 microglobulin gene or of a single HLA allele.

It is of interest that in MCTS a decrease of the surface expression of HLA class I molecules expression can also be observed. HBL cells were cultured in 2D or in 3D for three days. Cells were then trypsinized and stained with monoclonal antibodies specific for HLA-A0201 or a monomorphic epitope of HLA class I heavy chains, or control reagents. Mean fluorescence intensities (MFI) of the specific stainings were also calculated. Data reported in the figure refer to one representative experiment out of three performed (Figure 46).

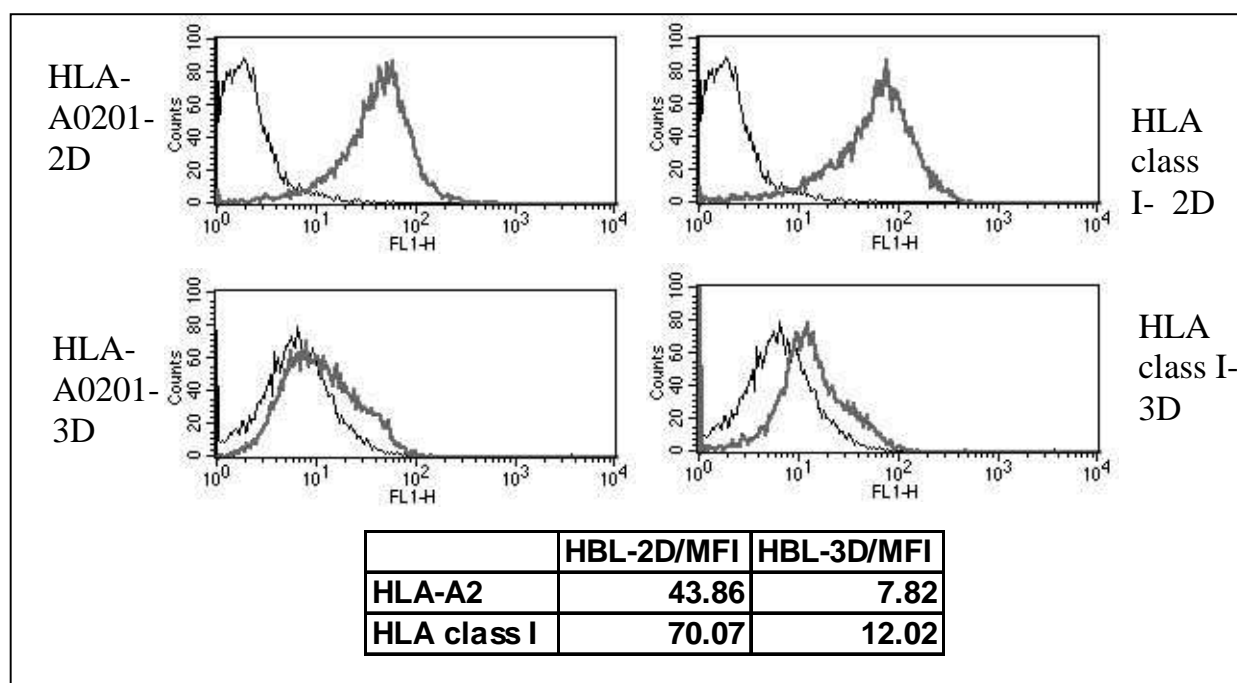


Figure 46: HLA expression in HBL cells cultured in monolayer or in spheroid

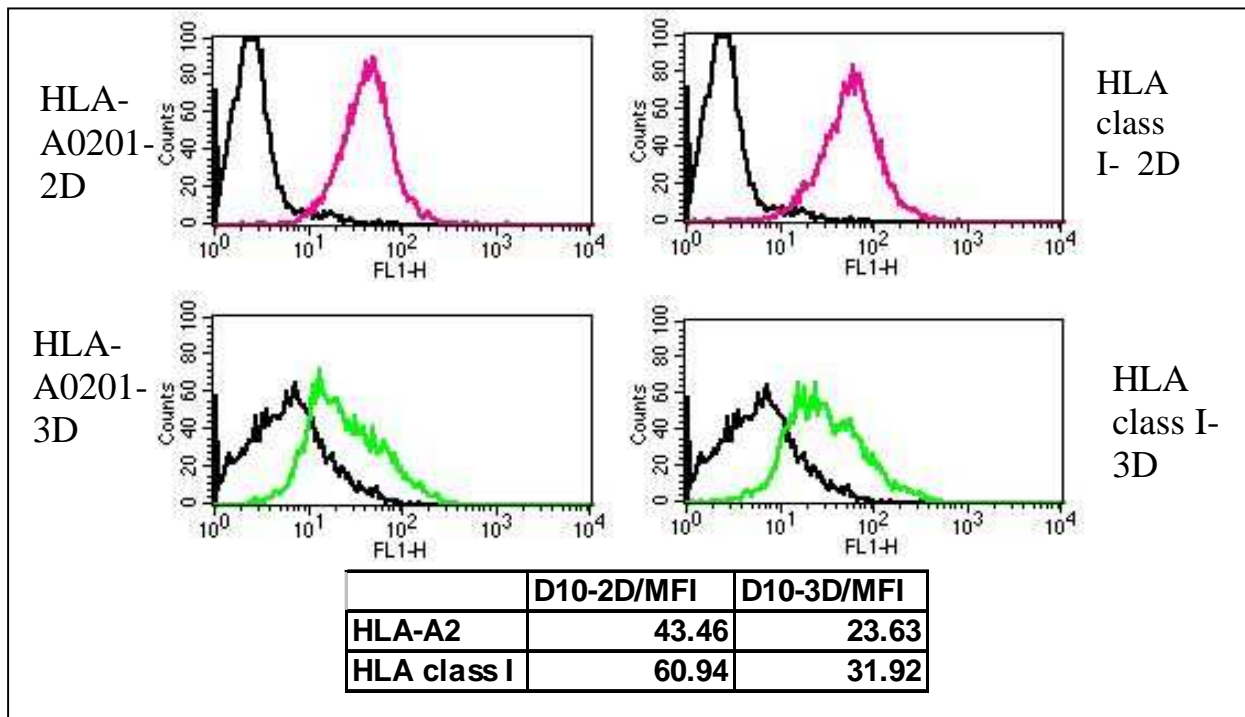


Figure 47: Modulation of HLA expression in D10 cells cultured in monolayer or spheroid

HBL cultured in 3 days old MCTS (30,000 cells per spheroids) displayed a significant (>5 fold) decrease in HLA-A0201 expression at the protein level, as compared to 2D cultures. Importantly, this effect was not allele specific, but concerned all HLA class I gene products, as indicated by staining with a mAb specific for a monomorphic determinant on HLA class I heavy chains (Figure 46). Similar results were observed with D10 MCTS with a significant ( $\geq 2$  fold) decrease in HLA molecules expression as compared to 2D cultures (Figure 47).

This reduction in HLA appeared to be cell density dependent. On the other hand, NA8 melanoma cells (HLA-A\*0201+, TAA-) displayed a divergent HLA modulation pattern as compared to HBL and D10. Indeed, when cultured in MCTS, NA8 showed significant ( $\geq 2$  fold) increases in HLA-A\*0201 and overall HLA class I expression, especially for a cell density of 5,000 cells per spheroid.

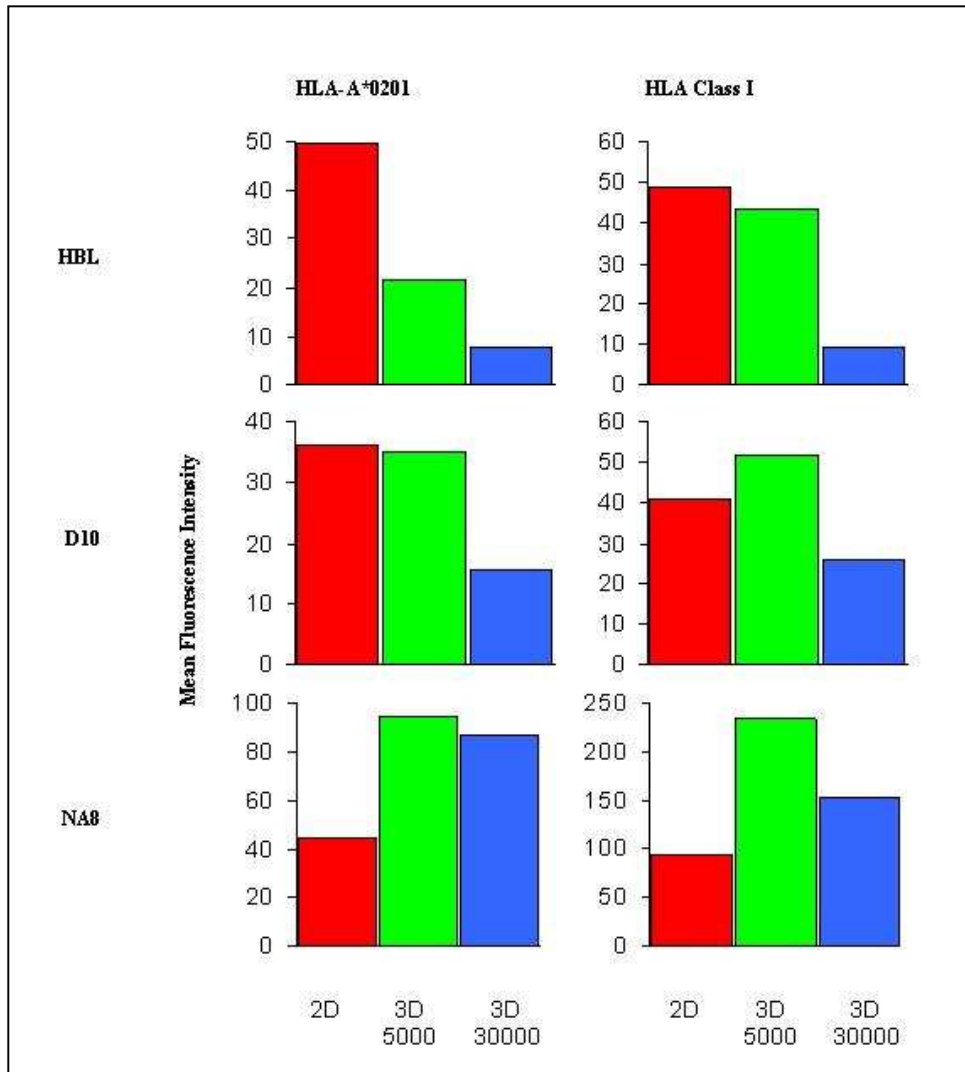


Figure 48: HLA class I expression in melanoma cells cultured in 2D or in MCTS at different cell numbers

HLA class I gene expression is regulated by transcription factors of the Interferon Regulating Factor (IRF) family (Girdlestone J et al 1993). Consistent with the HLA expression data observed at the protein level, IRF-1 gene expression was also cell density dependently down-regulated in HBL and D10 cultured in MCTS as compared to 2D. Accordingly, IRF-1 gene expression was up-regulated in NA8 MCTS in comparison with cells cultured in monolayers.

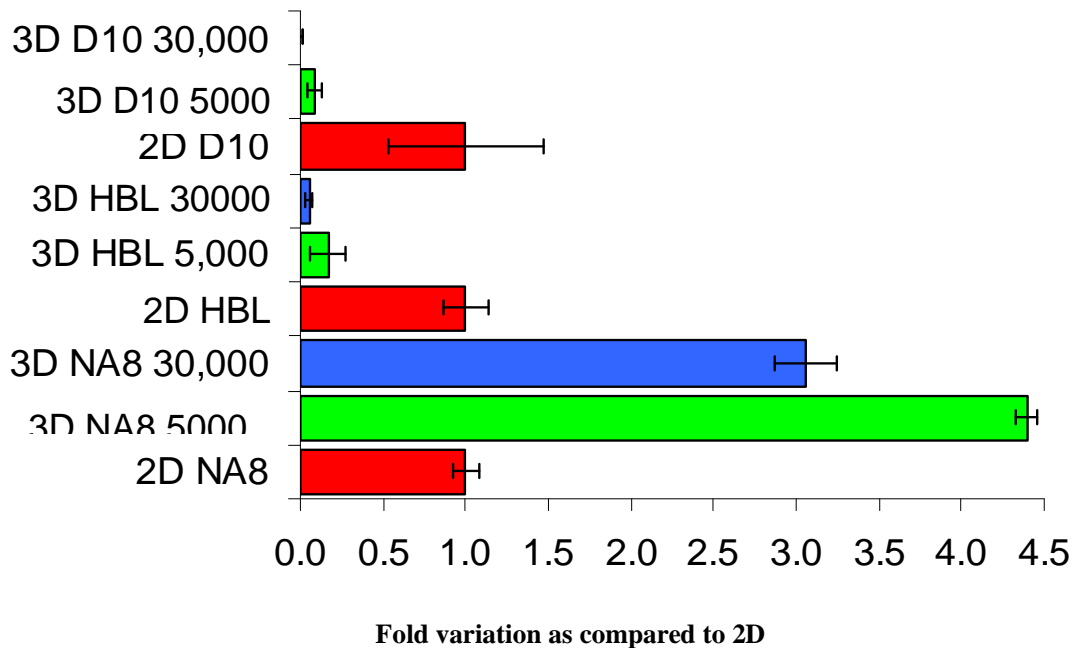


Figure 49: Expression of IRF-1 genes in melanoma cells cultured in 2D or in MCTS at different cell numbers

#### 3.4.5.4. Effects of Lactate on immunorecognition

In previous studies it has been demonstrated that low oxygen level and poor glucose concentration may influence the metabolism and proliferative characteristics of cells (Marx E et al 1988) and promote the development of necrotic cores (Sutherland RM et al 1986; Mueller-Klieser W et al 1986). So far, no study has investigated the effects of lactic acid on immunorecognition. Hypoxia in a tumor can induce production of glycolytic enzymes and glucose transporters (such as, Lactic dehydrogenase LDH), which can lead to enhanced glycolytic flux for energy production, causing high accumulation of lactic acid. Gottfried et al reported that infiltration of monocytes in the melanoma spheroids can be markedly enhanced by using oxamic acid (as an inhibitor of LDH), suppressing endogenous production of lactic acid (Gottfried et al 2006b).

Lactic acid content in the supernatants of tumor spheroids made of 30000 cells was measured after 3 days of culture. In monolayer cultures, cells were cultured for 3 days in 5% and 20% oxygen incubators.

A higher amount (>60% increase) of lactate was produced by HBL spheroids, as compared to 2D cultures. D10 spheroids showed a nominal increase ( $\leq 15\%$ ) of lactate



production as compared to 2D cultures. HBL Cells in 2D produced more lactate in 5% oxygen environment, but still far below production in 3D. Although Glucose consumption was lower when cells were cultured in 5% oxygen environment we did not observe major differences in cell number or cell morphology as compared to cells cultured in 20% oxygen incubator.

Table : Concentration of lactic acid and glucose in supernatants of melanoma cell culture

Samples	Lactate conc (mmol/Lt)	Glucose conc (mMol/Lt)
Fresh DMEM	1.32	24.3
HBL 3D 30000 cells	18.2	18.4
HBL-2D- 5% oxygen	13.8	21.4
HBL-2D- 20% oxygen	11.0	19.5
D10 3D 30000 cells	14.3	19.3
D10-2D- 5% oxygen	12.0	22.5
D10-2D- 20% oxygen	12.5	18.5

We then performed our antigen recognition assays by using HBL melanoma cells cultured in 2D or 3D as targets in the presence or not of exogenously added lactate. 10mM and 20mM L-lactic acid (Sigma) was exogenously added and cancer cells were cultured for 8 hours in 5% and 20% oxygen. Then MART-1-specific CTL clones were cocultured with them (MART-specific CTL E2MA4: HBL = 2:1). After 24 hours IFN- $\gamma$  production was measured.

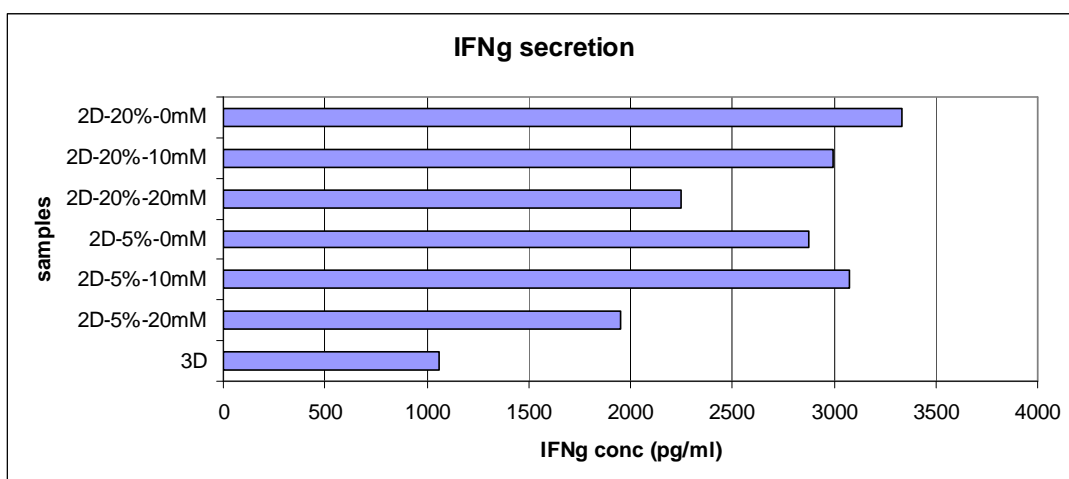


Figure 50: Effects of addition of exogenous lactate to HBL cells cultured in monolayers at different O<sub>2</sub> saturation levels on immunorecognition by antigen specific CTL

Pre-exposure of target cells cultured in 2D to exogenous lactate dose-dependently inhibited antigen stimulated IFN- $\gamma$  production by MART-1 specific HLA-A0201 restricted CTL clones. Importantly, however the addition of exogenous lactate to melanoma cells cultured in monolayer could not induce down-regulation of expression of melanoma differentiation antigens. These data suggest that lactic acid may cause a functional inhibition of effector cells, as also suggested by other groups (Gottfried E et al, 2006a).

#### **3.4.5.5. Close cell-cell interaction in specific cell types may lead to dedifferentiation:**

The process of melanocyte differentiation requires exit from the cell cycle and the expression of genes that encode proteins necessary for the production of pigment — two processes that are often deregulated in melanoma in vivo. Our above data witnessing a decreased expression of HLA and tumor associated antigens of the differentiation antigen family may suggest an ongoing dedifferentiation process in cells cultured in spheroids. Importantly Hypoxic microenvironment in 3D tumor spheroids may also promote dedifferentiation of tumor cells (reviewed by Axelson H et al 2005).

Bodey et al (Bodey B et al 1996) observed in clinical samples that during melanoma progression cells undergo dedifferentiation with increased expression of vimentin, cytokeratin, but reduced expression of actin. Several other groups have reported similar over-expression of vimentin (Hendrix et al 1992). Hence strong co-expression of vimentin and keratin intermediate filaments can be considered as marker of dedifferentiated or interconverted (between epithelial and mesenchymal) phenotype. Upregulation in vimentin expression was interpreted by some researchers as a sign of Epithelial to Mesenchymal Transition, reflecting a major step in tumor dedifferentiation and development of a chemotherapy resistant-phenotype (Thiery JP 2002; Sommers CL et al, 1992).

By immunofluorescence, we have detected a clear change in morphology of actin stress fibre networks in 7-10 days old spheroids as compared to monolayer cells. Actin fibres were more fragmented, whereas vimentin expression pattern is dramatically enhanced, especially in NA8 cells.

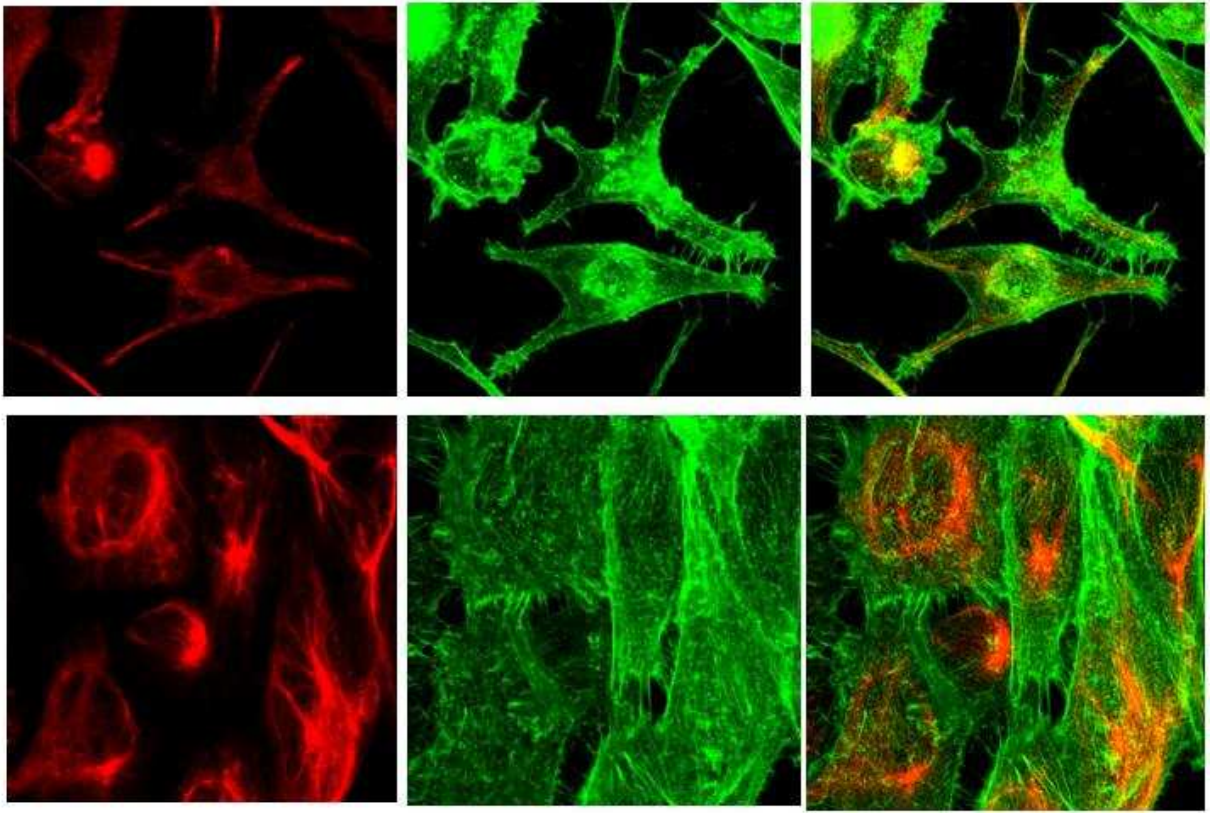


Figure 51: Immunofluorescence stainings of NA8 cells:

(A) upper panel showing Vimentin (red), actin (green), co-expression in monolayer

(B) lower panel showing Vimentin (red), actin (green), co-expression in spheroid

On the other hand, for HBL cells in MCTS, vimentin expression is strongly upregulated in the peripheral part of spheroids.

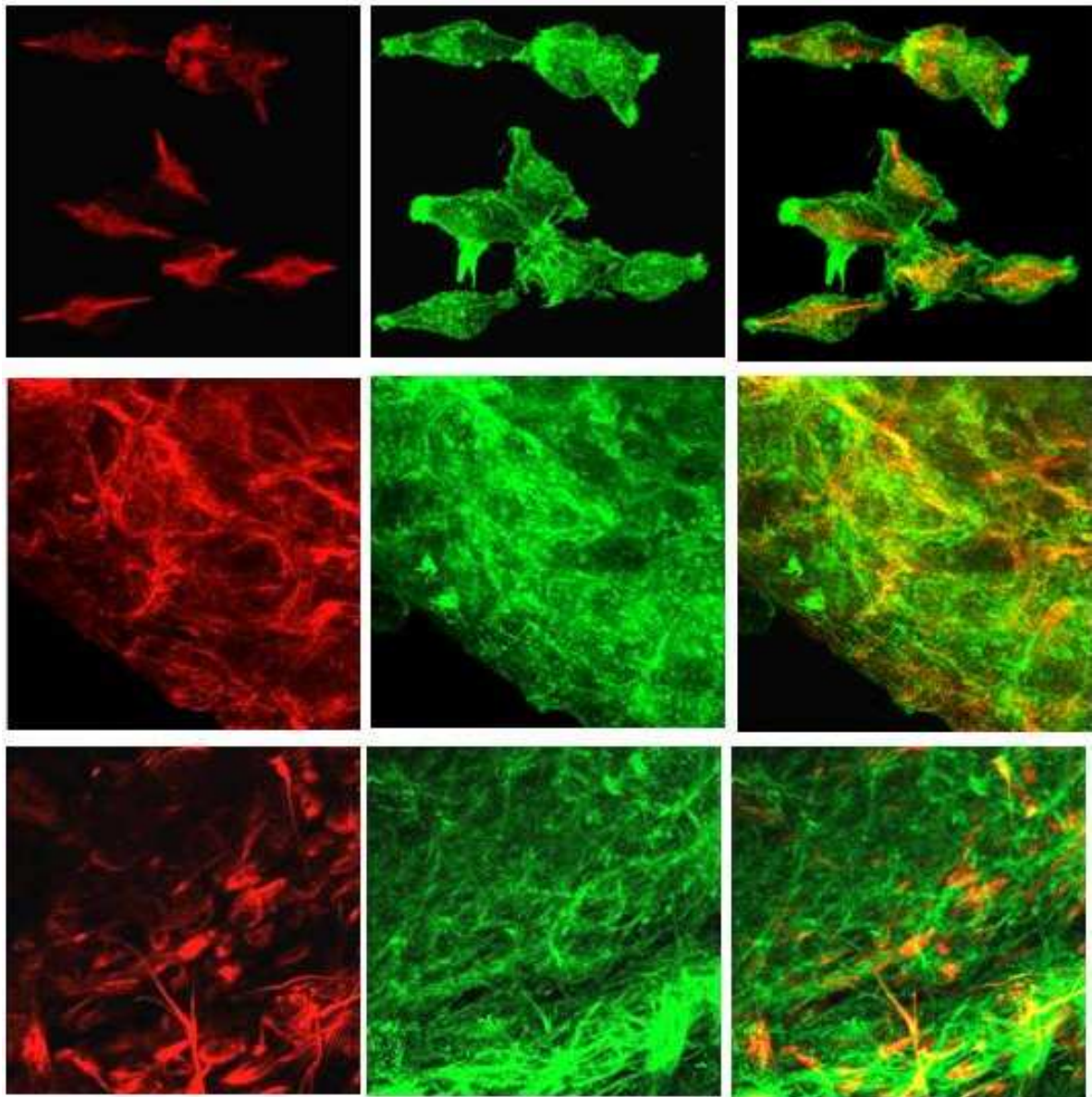


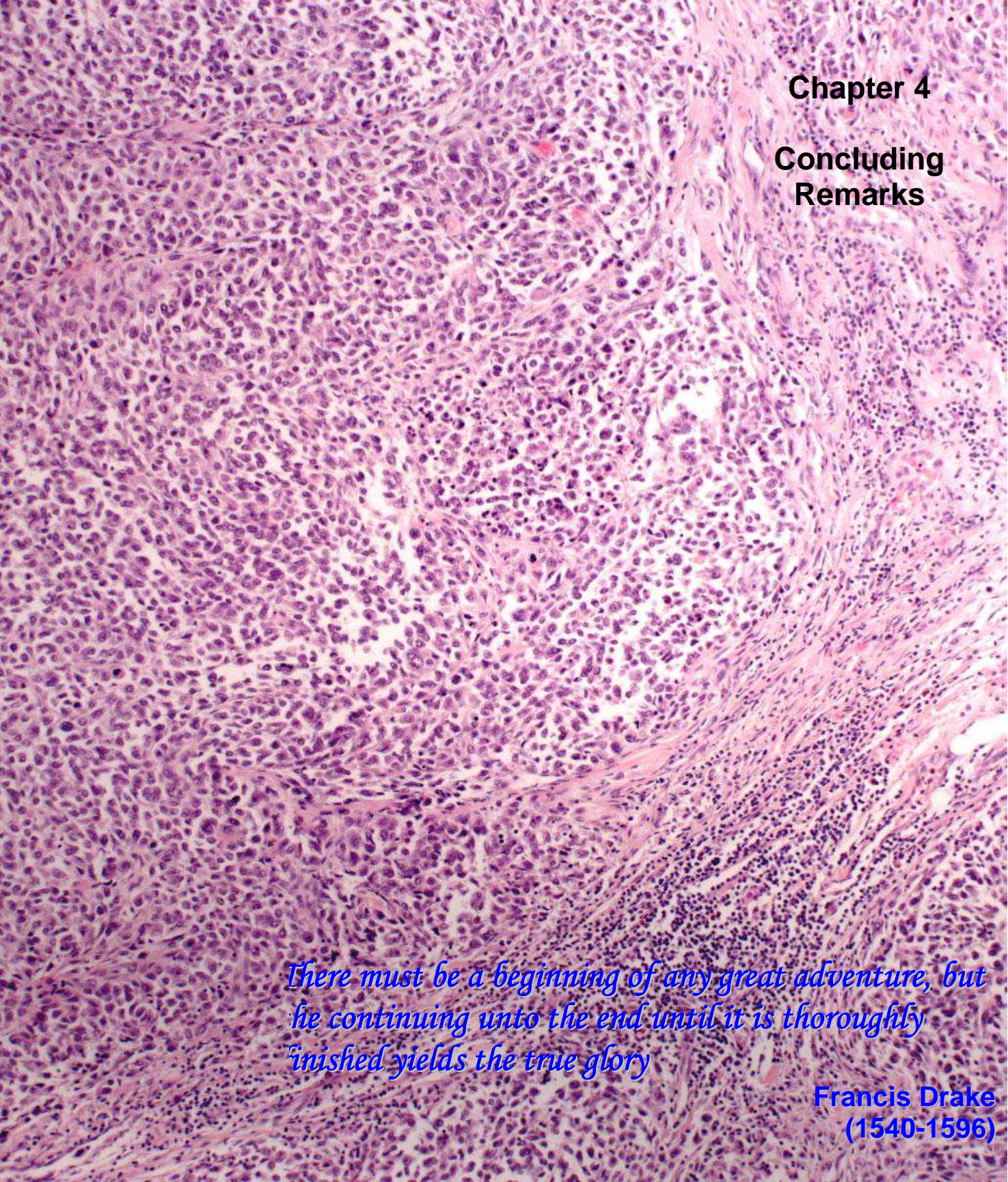
Figure 52: Immunofluorescence stainings for Vimentin (red), actin (green) expression in HBL cells, (A) upper panel showing monolayer, (B) middle panel showing peripheral part of spheroid, (C) lower panel showing inner part of spheroid

These preliminary results indicate that for the investigation is warranted to explore expression of vimentin, and actin in different architectures of melanoma cell cultures.

MITF, whose expression is downmodulated in spheroids (see above), can regulate a number of melanocyte specific genes, including those involved in melanin biosynthesis (such as Melan-A, tyrosinase, TRP-1 etc) by binding to M-box sequences in the promoter regions

(Bentley NJ et al 1994; Bertolotto C et al 1996). Previously, Iwakiri et al showed that transfection of MITF siRNA could reduce MITF synthesis and induced dedifferentiation in retinal pigment cells (Iwakiri R et al 2005). Hence strong expression of vimentin especially in the peripheral part of spheroid, along with severe downregulation of MITF gene expression may suggest ongoing overall dedifferentiation of melanoma cells upon culture in spheroids.





**Chapter 4**  
**Concluding**  
**Remarks**

*There must be a beginning of any great adventure, but  
he continuing unto the end until it is thoroughly  
finished yields the true glory*

**Francis Drake**  
**(1540-1596)**

H&E staining of a representative metastatic melanoma specimen showing evidence of “non brisk” infiltration by lymphocytes, limited to peripheral areas of the neoplastic outgrowth.



#### 4. Concluding remarks

Development of a simple *in vitro* three dimensional tumor model to study human malignancy is crucial to understand the biology of the disease, and the interactions of human tumour cells with their microenvironment, including immunorecognition, so that improved therapies can be designed. In this thesis we addressed the development of novel *in vitro* models utilizing human cells and permitting controlled investigations of the interaction between tumor cells and the immune system.

Culture of melanoma cells over PolyHEMA coated dish resulted in a simple, highly reproducible, *in vitro* multicellular tumor spheroid model system (MCTS) having a highly homogeneous size distribution, as compared with several other spheroid formation techniques. Flow cytometry studies showed minimal cell death within the spheroid in the initial days of culture in PolyHEMA based system in comparison to other techniques. PolyHEMA based MCTS model resemble “*in vivo*” tumors in their slow growth kinetics, capacity to develop necrotic areas far from nutrient and oxygen supplies after 10-12 days of culture, and preferential proliferation of cells located in the peripheral part of spheroid.

Data from different groups, including ours, indicated that culture of tumor cells in tri-dimensional structures modulates their gene expression profiles. The data presented in this thesis provide a large-scale gene profile analysis of tumor cells cultured in different architectures and this indicated that architecture of melanoma cells, possibly due to the inherent homotypic cell-cell interaction or specific microenvironmental conditions, with a putative role of hypoxia, may determine specific gene expression patterns of potentially high functional relevance. Interestingly, the expression pattern of several genes found to be modulated, which are known to play a relevant role in melanoma progression and metastatic process.

We have also showed that culture of tumor cells in tri-dimensional structures decreases their susceptibility to the immune-mediated CTL attack. Functional activity of TAA specific CTLs is impaired when they are challenged with melanoma cells in MCTS, compared to monolayer cells, as evident by lower expression of FasLigand, perforin, Granzyme B genes. Our data indicate that a constellation of mechanisms are probably acting together in decreasing the

susceptibility of melanoma cells cultured as MCTS to the attack of antigen specific CTL, as compared to the melanoma cells cultured in conventional monolayer fashion:

- (1) Three-dimensional structures *per se*, limit the capacity of effector cells of recognizing HLA class I restricted antigens possibly by merely reducing the cell surface exposed to CTL. This mechanism, however, is only partially responsible for the impaired antigen recognition since CTL cultured with melanoma cells from disrupted MCTS secreted IFN- $\gamma$  at a level intermediate in between 2D and MCTS.
- (2) The expression of melanoma differentiation antigens is down-regulated in tumor cells cultured in 3D as compared to monolayers. In our hands, this is neither related to hypoxia nor to increased Oncostatin M gene expression but rather to a decreased MITF gene expression and to the high cell concentrations elicited by culture in MCTS.
- (3) The surface expression of HLA class I molecules can be down-regulated in melanoma cells cultured in 3D, as compared to their counterparts in 2D.
- (4) Lactic acid production by melanoma cells is increased if they are cultured in MCTS, as compared to monolayer cultures, and lactate significantly inhibits infiltration and TAA triggered IFN- $\gamma$  production by antigen-specific CTL.

Most importantly, none of these mechanisms alone is able to entirely account for the inhibition of antigen recognition by specific CTL, detectable upon culture in the presence of melanoma cells cultured in 3D, as opposed to 2D. Their combination, however, elicits powerful inhibitory effects.

These features have been detected relatively frequently in clinical melanoma specimen. Their occurrence has been attributed to the outgrowth of cancer cells characterized by low expression of TAA and/or restricting HLA class I determinants following exposure of tumors to immunoselective pressures. However, our data suggest that a low expression of HLA class I molecules and at least of melanoma differentiation antigens in tumors, could be inherent in their three-dimensional growth, even in the absence of an exogenous immune pressure. We are fully aware of the fact that culture of melanoma cell lines in 3D might only partially reflect the complexity of solid tumors developing *in vivo*. However, the clear discrepancy between data obtained by applying techniques of current use for the *in vitro* detection of antitumor responses and clinical evidence urges the development of alternative experimental models.

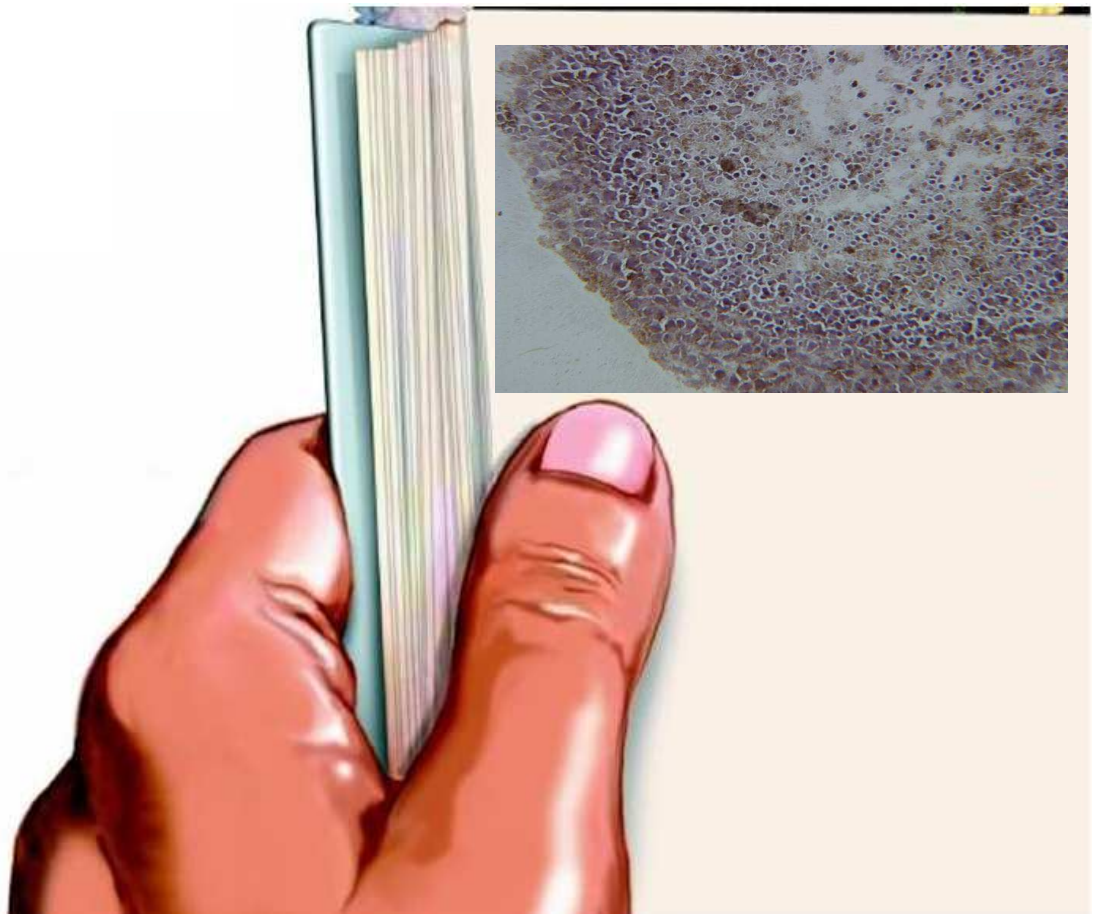


## Chapter 5

### References

*Nothing is a waste of time if you use the experience wisely.*

Auguste Rodin  
(1840-1917)



## Reference List

Ackerman LW, Rosai J, 1974, Surgical Pathology, Mosby, St Louis

Acker H, Carlsson J, Holtermann G, Nederman T, Nylen T. "Influence of glucose and buffer capacity in the culture medium on growth and pH in spheroids of human thyroid carcinoma and human glioma origin." *Cancer Res.* 1987; 47.13: 3504-08

Algarra I, Collado A, Garrido F. Altered MHC class I antigens in tumors. *Int J Clin Lab Res* 1997; 27(2):95-102

American Cancer Society: Cancer Facts and Figures 2006. Atlanta, Ga: American Cancer Society, 2006

Anichini A, Molla A, Mortarini R, Tragni G, Bersani I, Di Nicola M, Gianni AM, Pilotti S, Dunbar R, Cerundolo V, Parmiani G. An expanded peripheral T cell population to a cytotoxic T lymphocyte (CTL)-defined, melanocyte-specific antigen in metastatic melanoma patients impacts on generation of peptide-specific CTLs but does not overcome tumor escape from immune surveillance in metastatic lesions. *J Exp Med.* 1999; 190: 651-667

Anichini A, Vegetti C, Mortarini R. The paradox of T-cell-mediated antitumor immunity in spite of poor clinical outcome in human melanoma. *Cancer Immunol Immunother.* 2004; 53(10): 855-64

Axelson H, Fredlung E, Ovenberger M, Landberg G, Pahlman S, Hypoxia-induced dedifferentiation of tumor cells- a mechanism behind heterogeneity and aggressiveness of solid tumors , *Semin Cell Dev Biol.* 2005; 16(4-5): 554-63

Bates RC, Edwards NS, Yates JD, Spheroids and cell survival. *Crit Rev Oncol Hematol.* 2000; 36(2-3):61-74.

Bajzer Z, Vuk-Pavlovic S, Huzak M. Mathematical modelling of tumor growth kinetics. In: Adam JA, Bellomo N editors. A survey of models for tumor-immune system dynamics. Boston: Birkhauser 1997; 89-133

Bedrosian I, Mick R, Xu S, Nisenbaum H, Faries M, Zhang P, Cohen PA, Koski G, Czerniecki BJ. Intranodal administration of peptide –pulsed nature dendritic cell vaccines results in superior CD8+ T-cell function in melanoma patients. *J Clin Oncol.* 2003; 21:3826-3835.

Bentley NJ, Eisen T, Goding CR, Melanocyte-specific expression of the human tyrosinase promoter: activation by the microphthalmia gene product and role of the initiator, *Moll Cell Biol.* 1994; 14(12): 7996-8006

Bernsen MR, Diepstra JH, van MP, Punt CJ, Figdor, C.G., van Muijen, GN, Adema GJ, and Ruiters, D.J., Presence and localization of T-cell subsets in relation to melanocyte differentiation antigen expression and tumour regression as assessed by immunohistochemistry and molecular analysis of microdissected T cells. *J. Pathol.* 2004; 202: 70-79

Bertolotto C, Bille K, Ortonne JP, Ballotti R, Regulation of tyrosinase gene expression by cAMP in B16 melanoma cells involves two CATGTG motifs surrounding the TATA box: implication of the microphthalmia gene product, *J Cell Biol.* 1996; 134(3):747-55

Bittner M, Meltzer P, Chen Y, Jiang Y, Seftor E, Hendrix M, Radmacher M, Simon R, Yakhinik Z, Ben-Dork A, Sampask N, Dougherty E, Wang F, Marincola F, Gooden C, Lueders J, Glatfelter A, Pollock P, Carpten J, Gillanders E, Leja D, Dietrich E, Beaudry C, Berens M, Alberts D, Sondak V, Hayward N, Trent J, Molecular classification of cutaneous malignant melanoma by gene expression profiling, *Nature* 2000; 406, 536-540

Bonnotte B, et al, MIP-3alpha transfection into a rodent tumor cell line increases intratumoral dendritic cell infiltration but enhances tumor growth and decreases immunogenicity. " *J Immunol.* 2004; 15; 173(8):4929-35

Bodey B, Kaiser HE, Goldfarb RH, Immunophenotypically varied cell subpopulations in primary and metastatic human melanomas. Monoclonal antibodies for diagnosis, detection of neoplastic progression and receptor directed immunotherapy. *Anti Cancer Res.* 1996;16(1):517-31

Bourrat-Floeck B, Groebe K, Mueller-Klieser W, Biological response of multicellular EMT6 spheroids to exogenous lactate, *Int J cancer*, 1991; 47: 792-799

Bredel-Geissler, A. et al. "Proliferation-associated oxygen consumption and morphology of tumor cells in monolayer and spheroid culture." *J.Cell Physiol.* 1992; 153.1: 44-52

Bromley SK et al, The immunological Synapse, *Annu Rev Immunol*, 2001; 19, 375-396

Brocker EB, Zwadlo G, Holzmann B, Macher E, Sorg C. Inflammatory cell infiltrates in human melanoma at different stages of tumor progression. *Int J Cancer* 1988;15;41(4):562-7

Burton AC. "Rate of growth of solid tumours as a problem of diffusion." *Growth.* 1996; 30.2: 157-76

Boudreau N, Myers C, Bissel M, From Laminin to Lamin: regulation of tissue specific gene expression by the ECM, *Trends Cell Biol*, 1995; 5, 1

Carr KM, Bittner M, Trent JM, Gene-expression profiling in human cutaneous melanoma, *Oncogene* 2003; 22, 3076-3080

Carlsson J and Acker H. "Relations between pH, oxygen partial pressure and growth in cultured cell spheroids." *Int.J.Cancer* 1988; 42.5: 715-20

Carlsson, J. et al. "The influence of oxygen on viability and proliferation in cellular spheroids." *Int.J.Radiat.Oncol.Biol.Phys.* 1979; 5.11-12: 2011-20

Carlsson, J. "A proliferation gradient in three-dimensional colonies of cultured human glioma cells." *Int.J.Cancer* 1977; 20.1: 129-36

Chignola R, Schenetti A, Andrighetto G, Chiesa E, Foroni R, Sartoris S, Tridente G, Liberati D. Forecasting the growth of multicell tumour spheroids: implications for the dynamic growth of solid tumours. *Cell Prolif* 2000; 33:219-229

Chun MH. "Serum signaling factors and spheroids." *Crit Rev Oncol Hematol.* 2000; 36.2-3: 89-98

Clark EA, Golub TR, Lander ES, Hynes RO, Genomic analysis of metastasis reveals an essential role for RhoC, Nature. 2000; 406, 532-535

Hayward NK, genetics of melanoma predisposition, Oncogene, 2003; 22,3053-3062

Clemente CG, Mihm MC, Cascinelli N. Tumor infiltrating lymphocytes in lymph node melanoma metastases: a histopathologic prognostic indicator and an expression of local immune response. Lab Invest 1996; 74:43-47

Dangles, V. et al. Gene expression profiles of bladder cancers: evidence for a striking effect of in vitro cell models on gene patterns. Br J Cancer. 2002; 86.8: 1283-89

Dangles V, Validire P, Wertheimer M, Richon S, Bovin C, Zeliszewski D, Vallancien G, Bellet D. Impact of human bladder cancer cell architecture on autologous T-lymphocyte activation. Int J Cancer 2002; 98:51-56

Dangles-Marie V, Richon S, El Behi M, Echchakir H, Dorothee G, Thiery J, Validire P, Vergnon I, Menez J, Ladjimi M, Chouaib S, Bellet D, Mami-Chouaib F. A three-dimensional tumor cell defect in activating autologous CTLs is associated with inefficient antigen presentation correlated with heat shock protein-70 down-regulation. Cancer Res 2003, 63:3682-3687

Davies H, Bignell GR, Cox C, Stephens P, Edkins S, Clegg S, Teague J, Woffendin H, Garnett MJ, Bottomley W et al, Mutations of the BRAF gene in human cancer, Nature, 2002; 417, 949-954

Desoize and Jardillier, Multicellular resistance: a paradigm for clinical resistance? Crit Rev Oncol Hematol. 2000;36(2-3):193-207

Del Duca D, Werbowetski T, Del Maestro RF, Spheroid preparation from hanging drops: characterization of a model of brain tumor invasion. J Neuro-oncol 2004;67(3):295-303

Dertinger H, Hulser D., Increased radioresistance of cells in cultured multicell spheroids. I. Dependence on cellular interaction, Radiat Environ Biophys. 1981;19(2):101-7

De Vries TJ, Fourkour A, Wobbles T, Verkroost G, Ruiter DJ, van Muijen GN. Heterogeneous expression of immunotherapy candidate proteins gp100, MART-1, and tyrosinase in human melanoma cell lines and in human melanocytic lesions. Cancer Res 1997 ;57(15):3223-9

Dong H et al, Tumor-associated B7-H1 promotes T-cell apoptosis: a potential mechanism of immune evasion. Nat Med. 2002 ; 8(8):793-800

Du J, Miller AJ, Widlund HR, Horstmann MA, Ramaswamy S, Fisher DE. MLANA/MART1 and SILV/PMEL17/GP100 are transcriptionally regulated by MITF in melanocytes and melanoma. Am J Pathol 2003;163:333-343

Durand RE, Sutherland RM, Intercellular contact: its influence on the Dq of mammalian cells survival curves, In, Alper T (ed) Cell survival after low doses of radiation, sixth L. H. Gray conference, Bedford Collegege, London, Wiley, NY, 1975, p237-247

Durand RE, Cell cycle kinetics in an in vitro tumor model. Cell Tissue Kinet. 1976;9(5):403-12

Durand RE, Multicell spheroids as a model for cell kinetic studies, *Cell Tissue Kinet.* 1990; 23(3):141-59

Durand, RE. "Isolation of cell subpopulations from in vitro tumor models according to sedimentation velocity." *Cancer Res.* 1975; 35.5:1295-300

Durda PJ, Dunn IS, Boyle Rose L, et al. Induction of 'antigen silencing' in melanomas by Oncostatin M: down-modulation of melanocyte antigen expression. *Mol Cancer Res.* 2003;1:411– 419

Emfietzoglou D, Kostarelos K, Papakostas A, et al. Liposome-mediated radiotherapeutics within avascular tumor spheroids: comparative dosimetry study for various radionuclides, liposome systems, and a targeting antibody. *J Nucl Med* 2005;46(1):89-97

Erllichman C, Vidgen D. Cytotoxicity of adriamycin in MGH-U1 cells grown as monolayer cultures, spheroids, and xenografts in immune-deprived mice. *Cancer Res.* 1984; 44: 5369–5375

Evans R, Kamdar SJ, Duffy TM, Krupke DM, Fuller JA, Dudley ME. The therapeutic efficacy of murine anti-tumor T cells: freshly isolated T cells are more therapeutic than T cells expanded in vitro. *Anticancer Res* 1995 ;15(2):441-7.

Finke J, Ferrone S, Frey A, Mufson A, Ochoa A. Where have all the T cells gone? Mechanisms of immune evasion by tumors. *Immunol Today* 1999 ;20(4):158-60

Folkman J., Moscona A, Role of cell shape in growth control. *Nature* 1978; 273: 345

Folkman J and Hochberg M. "Self-regulation of growth in three dimensions." *J.Exp.Med.* 1973;138.4: 745-53

Folkman, J. and H. P. Greenspan. "Influence of geometry on control of cell growth." *Biochim Biophys Acta.* 1975; 417.3-4: 211-36

Folkman J, Tumor angiogenesis, 1975, In Becker F (ed) *Cellular Biology and growth, Cancer vol 3, NY, pp 355-388 ,*

Franko AJ, RM Sutherland. "Oxygen diffusion distance and development of necrosis in multicell spheroids." *Radiat.Res.* 1979a; 79.3: 439-53.

Franko AJ, RM Sutherland. "Radiation survival of cells from spheroids grown in different oxygen concentrations." *Radiat.Res.* 79.3 (1979b): 454-67

Friedl P, Zanker KS, Bocker EB, Cell migration strategies in 3-D extracellular matrix: differences in morphology, cell matrix interactions, and integrin function. *Microsc Res Tech,* 1998;1;43(5):369-78

Friedl P, den Boer AT, Gunzer M, Tuning immune responses: diversity and adaptation of the immunological synapse. 2005 Jul;5(7):532-45

Freed LE, Langer R, Martin I, Pellis NR, Vunjak-Novakovic G. Tissue engineering of cartilage in space. *Proc Natl Acad Sci USA* 94: 1997. 13885– 13890

Freyer JP, Role of necrosis in regulating the growth saturation of multicellular spheroids, *Cancer Res*, 1988;48, 2432-2439

Freyer, J. P. and R. M. Sutherland. "Selective dissociation and characterization of cells from different regions of multicell tumor spheroids." *Cancer Res*. 1980; 40.11: 3956-65.

Freyer, J. P. et al. "Cellular energetics measured by phosphorous nuclear magnetic resonance spectroscopy are not correlated with chronic nutrient deficiency in multicellular tumor spheroids." *Cancer Res*. 1991;51.15: 3831-37

Ganss R, Hanahan D. Tumor microenvironment can restrict the effectiveness of activated antitumor lymphocytes. *Cancer Res*. 1998;58(20):4673-81.

Garcia-Lora A et al, MHC class I antigens, immune surveillance, and tumor immune escape, *J Cell Physiol*. 2003; 195(3):346-55

Ghosh S, Spagnoli GC, Martin I, Ploegert S, Heberer M, Reschner A. "Three-dimensional culture of melanoma cells profoundly affects gene expression profile: A high density oligonucleotide array study." *J.Cell Physiol*. 2005a; 204: 522-31

Ghosh S, Rosenthal R, Zajac P, Weber WP, Oertli D, Heberer M, Martin I, Spagnoli GC, Reschner A. Culture of melanoma cells in 3-dimensional architectures results in impaired immunorecognition by cytotoxic T lymphocytes specific for Melan-A/MART-1 tumor-associated antigen. *Ann Surg*. 2005b ;242(6):851-7

Girdlestone J, Isamat M, Gewert D, Milstein C. Transcriptional regulation of HLA-A and -B: differential binding of members of the Rel and IRF families of transcription factors. *Proc Natl Acad Sci U S A* 1993;90:11568-11572

Glimelius B et al. "Extracellular matrices in multicellular spheroids of human glioma origin: increased incorporation of proteoglycans and fibronectin as compared to monolayer cultures." *APMIS*. 1988; 96.5: 433-44

Global action against cancer- updated version, World Health Organization Report 2005, ISBN 92 4 159314 8 (WHO) (LC/NLM classification: QZ 200) (ISBN 2-9700492-1-X (UICC)

Gorlach A, Herter P, Hentschel H, Frosch PJ, Acker H. Effects of nIFN beta and rIFN gamma on growth and morphology of two human melanoma cell lines: comparison between two- and three-dimensional culture, *Int J Cancer*. 1994;56(2):249-54

Gorelik L, Flavell RA, Immune-mediated eradication of tumors through the blockade of transforming growth factor-beta signaling in T cells. *Nat Med*. 2001;7(10):1118-22.

Gottfried E, Kunz-Schughart LA, Ebner S, Mueller-Klieser W, Hoves S, Andreesen R, Mackensen A, Kreutz M. Tumor-derived lactic acid modulates dendritic cell activation and antigen expression. *Blood*. 2006a ;110(5):2013-21

Gottfried et al, Brave little world: spheroids as an in vitro model to study tumor-immune-cell interactions, *Cell Cycle*, 2006b, 5(7) 691-695

Grover A, Andrews G, Adamson ED, Role of laminin in epithelium formation by F9 aggregates, *J Cell Biol.* 1983 ;97(1):137-44

Grakoui A, Bromley SK, Sumen C, Davis MM, Shaw AS, Allen PM, Dustin ML, The Immunological Synapse: A Molecular Machine Controlling T Cell Activation, *Science* 1999: 285, 221 – 227

Greaves DR, Wang W, Dairaghi DJ, et al. CCR6, a CC chemokine receptor that interacts with macrophage inflammatory protein 3alpha and is highly expressed in human dendritic cells. *J Exp Med* 1997;186:837-844

Grover A, Adamson ED, Roles of extracellular matrix components in differentiating teratocarcinoma cells, *J Biol Chem.* 1985;260(22):12252-8

Groebe K and W. Mueller-Klieser. "On the relation between size of necrosis and diameter of tumor spheroids." *Int.J.Radiat.Oncol.Biol.Phys.* 1996; 34.2: 395-401

Gullino, P. M., Grantham, F. H., Smith, S. M. & Haggerty, A. C. Modifications of the acid-base status of the internal milieu of tumors.1965; *J. Natl. Cancer Inst.* 34, 857-869

Halaban R, Pomerantz SH, Marshall S et al, Tyrosinase activity and abundance in cloudman melanoma cells, *Arch Biochem Biophys* 1984, 230, 383-7

Halpern AC, Schuchter LM, Prognostic models in melanoma, *Semin Oncol*, 1997, 24, S2-7

Hammond TG, Hammond JM; Optimized suspension culture: the rotating-wall vessel, *Am J Physiol Renal Physiol* 281: F12–F25, 2001

Hayward NK, genetics of melanoma predisposition, *Oncogene*, 22, 2003, 3053-3062

G. Helmlinger, P.A. Netti, H.C. Lichtenbeld, R.J. Melder and R.K. Jain, "Solid Stress Inhibits the Growth of Multicellular Tumor Spheroids," *Nature Biotechnology*, 1997;15:778-783

Holtfreter J, A study of the mechanism of gastrulation, *J Exp Zool*, 95, 1944, 171-212

Muller-Klieser W, Three-dimensional cell cultures: from molecular mechanisms to clinical applications, *Am Physiol soc*, 1997; C1109-1123

Hendrix et al, Coexpression of vimentin and keratin by human melanoma tumor cells: correlation with invasive and metastatic potential, *J Natl Cancer Inst*, 1992; 84, 165-174

Hicklin DJ, Marincola FM, Ferrone S. HLA class I antigen downregulation in human cancers: T-cell immunotherapy revives an old story. *Mol Med Today.* 1999;5(4):178-86

Hofbauer GF, Kamarashev J, Geertsens R, Boni R, Dummer R. Melan A/MART-1 immunoreactivity in formalin-fixed paraffin-embedded primary and metastatic melanoma: frequency and distribution. *Melanoma Res* 1998;8(4):337-43.

Hoffmann J, Schirmer M, Menrad A, Schneider MR, A highly sensitive model for quantification of in vivo tumour angiogenesis induced by alginate-encapsulated tumor cells, *Cancer Res*, 1997, 57 (17): 3847-3851

Houghton AN, Polsky D, Focus on melanoma. *Cancer Cell* 2002; 2(4):275-8

Iwakiri R, Kobayashi K, Okinami S, Kobayashi H, Suppression of MITF by small interfering RNA induces dedifferentiation of chick embryonic retinal pigment epithelium. *Exp Eye Res.* 2005; 81(1):15-21

Jaaskelainen J, Maenpaa A, Patarroyo M, et al. Migration of recombinant IL-2-activated T and natural killer cells in the intercellular space of human H-2 glioma spheroids in vitro. A study on adhesion molecules involved. *J Immunol* 1992 ;149(1):260-8.

Kaaijk P, Troost D, Dast PK, van den BF, Leenstra S, Bosch DA. Cytolytic effects of autologous lymphokine-activated killer cells on organotypic multicellular spheroids of gliomas in vitro. *Neuropathol Appl Neurobiol* 1995;21(5):392-8

Kaaijk P, Troost D, Das PK, Leenstra S, Bosch DA. Long-term culture of organotypic multicellular glioma spheroids: a good culture model for studying gliomas. *Neuropathol Appl Neurobiol* 1995;21(5):386-91

Kanai T. et al. "Carcinoembryonic antigen mediates in vitro cell aggregation induced by interferon-gamma in a human colon cancer cell line: requirement for active metabolism and intact cytoskeleton." *Cancer Lett.* 1993; 71.1-3: 109-17

Kelm JE, Timmins NE, Brown CJ, Fussenegger M, Nielsen LK, Method for generation of homogeneous multicellular tumor spheroids applicable to a wide variety of cell types, *Biotechnol Bioeng* 2003; 20;83(2):173-80

Kennedy TE, Serafini T, de la Torre JR, Tessier-Lavigne M: Netrins are diffusible chemotropic factors for commissural axons in the embryonic spinal cord. *Cell* 1994; 78: 425–435

Khaitan D, Chandna S, Arya MB; Dwarakanath BS, Establishment and characterization of multicellular spheroids from a human glioma cell line; Implications for tumor therapy. *J Transl Med*, 2006;4: 12-25

Koike C, McKee TD, Pluen A, Ramanujan S, Burton K, Munn LL, Boucher Y, Jain RK, Solid stress facilitates spheroid formation: potential involvement of hyaluronan, *Br J Cancer.* 2002;86(6):947-53

Kupchik HZ, Langer RS, Haberern C, El Deriny S, O'Brien M, A new method for the three-dimensional in vitro growth of human cancer cells, *Exp Cell Res* , 1983, 147 (2): 454-460

Kupchik HZ , Collins E, O'Brien MJ, McCaffrey RP, Chemotherapy screening assay using 3-dimensional cell culture, *Cancer Lett*, 1990, 51(1), 11-16

Knowles, H. J. and R. M. Phillips. "Identification of differentially expressed genes in experimental models of the tumor microenvironment using differential display." *Anticancer Res.* 21.4A (2001): 2305-11



Knuechel, R. et al. "Differentiation patterns in two- and three-dimensional culture systems of human squamous carcinoma cell lines." *Am.J.Pathol.* 137.3 (1990): 725-36

Laderoute K. R. et al. "Enhancement of transforming growth factor-alpha synthesis in multicellular tumour spheroids of A431 squamous carcinoma cells." *Br.J.Cancer* 65.2 (1992): 157-62

LaRue KEA, Khalil M, Freyer JP, Microenvironmental regulation of proliferation in multicellular spheroids is mediated through differential expression of cyclin-dependent kinase inhibitors, *Cancer Res*, 64, 2004, 1621-1631

Lardner A, The effects of extracellular pH on immune function, *J Leukoc Biol*, 2001, 69, 522-530

Lee PP, Yee C, Savage PA, et al. Characterization of circulating T cells specific for tumor-associated antigens in melanoma patients. *Nat Med* 1999 ;5(6):677-85

Leslie MC, Bar-Eli M, Regulation of gene expression in melanoma: new approaches for treatment. *J Cell Biochem*, 2005 ;94(1):25-38

Licato LL, Prieto VG, and Grimm EA: A Novel Preclinical Model of Human Malignant Melanoma Utilizing Bioreactor Rotating-Wall Vessels. *In Vitro Cell Dev Biol Anim* 37: 121-126, 2001

Lippert U, Zachmann K, Henz BM, Neumann C. Human T lymphocytes and mast cells differentially express and regulate extra- and intracellular CXCR1 and CXCR2. *Exp Dermatol* 2004;13:520-525

Livak KJ, Schmittgen TD. Analysis of relative gene expression data using real-time quantitative PCR and the 2(-Delta Delta C(T)) Method. *Methods* 2001 Dec;25(4):402-8

Lord EM, Penney DP, Sutherland RM, Cooper RA, Jr. Morphological and functional characteristics of cells infiltrating and destroying tumor multicellular spheroids in vivo. *Virchows Arch B Cell Pathol Incl Mol Pathol* 1979;31(2):103-16

Lord EM, Burkhardt G. Assessment of in situ host immunity to syngeneic tumors utilizing the multicellular spheroid model. *Cell Immunol* 1984;85(2):340-50

Ludford-Menting MJ, Oliaro J, Sacirbegovic F, Cheah ET, Pedersen N, Thomas SJ, Pasam A, Iazzolino R, Dow LE, Waterhouse NJ, Murphy A, Ellis S, Smyth MJ, Kershaw MH, Darcy PK, Humbert PO, Russell SM. A network of PDZ-containing proteins regulates T cell polarity and morphology during migration and immunological synapse formation. *Immunity*. 2005;22(6):737-48.

Luk CK, Keng PC, Sutherland RM, Regrowth and radiation sensitivity of quiescent cells isolated from EMT6/Ro-fed plateau monolayers. *Cancer Res*. 1985;45(3):1020-5.

Luk CK, Keng PC, Sutherland RM. Radiation response of proliferating and quiescent subpopulations isolated from multicellular spheroids. *Br J Cancer*. 1986 ;54(1):25-32

Luscher U, Filgueira L, Juretic A, Zuber M, Luscher NJ, Heberer M, Spagnoli GC. The pattern of cytokine gene expression in freshly excised human metastatic biopsies suggests a state of reversible anergy of tumor-infiltrating lymphocytes. *Int J Cancer* 1994; 57:612-619

Lyons AB, Parish CR, Determination of lymphocyte division by flow cytometry, *J Immunol Methods*, 1994;171;131-7

Marincola FM, Ferrone S. Immunotherapy of melanoma: the good news, the bad ones and what to do next. *Semin Cancer Biol*. 2003a;13:387-389

Marincola FM, Wang E, Herlyn M, Seliger B, Ferrone S. Tumors as elusive targets of T cell-directed immunotherapy. *Trends Immunol* 2003b; 24:334-341

Marusic, M. et al. "Tumor growth in vivo and as multicellular spheroids compared by mathematical models." *Bull.Math.Biol*. 1994;56.4: 617-31

Marx E, Mueller-Klieser W, Vaupel P, Lactate-induced inhibition of tumor cell proliferation, *Int J Oncol Biol Phys* 14, 1988, 947-955

McCredie JA, Inch WR, Krav J: The rate of tumor growth in animals. *Growth* 1965;29: 331–347

Monz B, Karbach U, Groebe K, Mueller-Klieser W, Proliferation and oxygenation status of WiDr spheroids in different lactate and oxygen environments. *Oncol. Rep.* 1996;1, 1177-1183

Monsurro V, Wang E, Panelli MC, Nagorsen D, Jin P, Zavaglia K, Smith K, Ngalame Y, Even J, Marincola FM. Active-specific immunization against melanoma: is the problem at the receiving end? *Semin Cancer Biol* 2003; 13: 473-480.

Monsurro V, Wang E, Yamano Y, Migueles SA, Panelli MC, Smith K, Nagorsen D, Connors M, Jacobson S, Marincola FM . Quiescent phenotype of tumor specific CD8+ T cells following immunization. *Blood* 2004; 104:1970-1978

Mortarini R et al, Lack of terminally differentiated tumor-specific CD8+ T cells at tumor site in spite of antitumor immunity to self-antigens in human metastatic melanoma. *Cancer Res.* 2003 ; 63(10):2535-45

Moscona A, Formation of lentoids by dissociated retinal cells of the chick embryo, *Science*, 1957 Mar 29;125(3248):598-9

Moscona A: The development *in vitro* of chimeric aggregates of dissociated embryonic chick and mouse cells. *Proc Natl Acad Sci* 1957;43:184-194

Moscona MH, Moscona A, Inhibition of adhesiveness and aggregation of dissociated cells by inhibitors of protein and RNA synthesis, *Science*. 1963;142:1070-1

Moscona A, Cell aggregation: properties of specific cell-ligands and their role in the formation of multicellular systems. *Dev Biol* 1968;18(3):250-77.

Mueller-Klieser W. "Method for the determination of oxygen consumption rates and diffusion coefficients in multicellular spheroids." *Biophys.J.* 1984; 46.3: 343-48

Mueller-Klieser WF and R. M. Sutherland. "Oxygen consumption and oxygen diffusion properties of multicellular spheroids from two different cell lines." *Adv.Exp.Med.Biol.* 1984;180: 311-21

Mueller-Klieser W, Freyer JP, Sutherland RM Influence of glucose and oxygen supply conditions on the oxygenation of multicellular spheroids. *Brit J Cancer*, 1986, 53, 345-353

Mueller-Klieser W, Multicellular spheroids. A review on cellular aggregates in cancer research. *J cancer Res Clin Oncol*, 1987;113(2):101-22

Mueller-Klieser W, Three-dimensional cell cultures:from molecular mechanisms to clinical applications, *Am J Physiol.* 1997;273(4 Pt 1):C1109-23.

Nederman, T. et al. "Demonstration of an extracellular matrix in multicellular tumor spheroids." *Cancer Res.* 1984;44.7: 3090-97

Nederman, T., J. Carlsson, and K. Kuoppa. "Penetration of substances into tumour tissue. Model studies using saccharides, thymidine and thymidine-5'-triphosphate in cellular spheroids." *Cancer Chemother.Pharmacol.* 1988;22.1: 21-2

Nestle FO, Alijagic S, Gilliet M, Sun Y, Grabbe S, Dummer R, Burg G, Schadendorf D. Vaccination of melanoma patients with peptide or tumor lysate -pulsed dendritic cells. *Nat Med* 1998; 4:328-332.

Newell K et al, Studies with glycolysis-deficient cells suggest that production of lactic acid is not the only cause of tumor acidity, *PNAS*, 1993, 90(3) 1127-31

Nishiyama, T. et al. "Growth rate of human fibroblasts is repressed by the culture within reconstituted collagen matrix but not by the culture on the matrix." *Matrix* 1989;9.3: 193-99

Ochsenbein AF, Sierro S, Odermatt B et al. Roles of tumour localization, second signals and cross priming in cytotoxic T-cell induction. *Nature* 2001; 411:1058-1064

Ochalek T, von Kleist S. Study of the resistance of tumor-cell spheroids to penetration and lysis by activated effector cells. *Int J Cancer* 1994;57(3):399-405.

Oertli D, Marti WR, Zajac P, et al. Rapid induction of specific cytotoxic T lymphocytes against melanoma-associated antigens by a recombinant vaccinia virus vector expressing multiple immunodominant epitopes and costimulatory molecules in vivo. *Hum Gene Ther* 2002;13:569-575

O'Keane JC, Kupchik HZ, Schroy PC, Andry CD, Collins E, O'Brien MJ, A three-dimensional system for long term culture of human colorectal adenomas, *Am J Pathol*, 1990, 137 (6): 1539-1547

Oloumi, A. et al. "Identification of genes differentially expressed in V79 cells grown as multicell spheroids." *Int.J.Radiat.Biol.* 78.6 (2002): 483-92

Padovan E, Terracciano L, Certa U, Jacobs B, Reschner A, Bolli M, Spagnoli GC, Borden EC, Heberer M. Interferon stimulated gene 15 constitutively produced by melanoma cells induces e-cadherin expression on human dendritic cells. *Cancer Res* 2002; 62:3453-3458

Papas KK, Constantinidis I, Sambanis A. Cultivation of recombinant, insulin-secreting AtT-20 cells as free and entrapped spheroids, *Cytotechnology*. 1993;13(1):1-12

Parish CR, Fluorescent dyes for lymphocyte migration and proliferation studies *Immunol Cell Biol*. 1999; 77: 499-508

Parmiani G, Anichini A, Fossati G. Cellular immune response against autologous human malignant melanoma: are in vitro studies providing a framework for a more effective immunotherapy? *J Natl Cancer Inst* 1990;82(5):361-70

Paulus W et al., C. Huettner, and J. C. Tonn. "Collagens, integrins and the mesenchymal drift in glioblastomas: a comparison of biopsy specimens, spheroid and early monolayer cultures." *Int.J.Cancer* 58.6 (1994): 841-46

Petitclerc E; Stromblad S, von Schalscha TL, et al, Integrin alpha(v)beta3 promotes M21 melanoma growth in human skin by regulating tumor cell survival. *Cancer Res* 1999 59, 2724-30

Poland, J. et al. "Comparison of protein expression profiles between monolayer and spheroid cell culture of HT-29 cells revealed fragmentation of CK18 in three-dimensional cell culture." *Electrophoresis* 2002; 23.7-8 :1174-84

Powis G, Bonjouklian R, Berggren MM, Gallegos A, Abraham R, Ashendel C, Zalkow L, Matter WF, Dodge J, Grindey G *et al* Wortmannin, a potent and selective inhibitor of phosphatidylinositol-3-kinase. *Cancer Research* 1994; 54. 2419-2423

Rajoda S, Saio M, Frey AB, CD8+ Tumor infiltrating lymphocytes are primed for Fas-mediated activation-induced cell death but are not apoptotic in situ, *J immunol*. 2001,166, 6074

Ramirez-Montagut T, Andrews DM, Ihara A, Pervaiz S, Pandolfi F, Van Den PJ, waitkus R, Boyle LA, et al, Melanoma antigen recognition by tumour-infiltrating T lymphocytes (TIL): effect of differential expression of melan-A/MART-1. *Clin Exp immunol* 2000;119(1):11-8

Rauen HM, Norpoth K, Wenderl P, Boehm E, van Husen N, Metabolitanalysen bei schnell wachsenden DS-carcinosarkomen der Huehner-Chorioallantois , *Z. Krebsforsch.*, 1969,; 72, 88-101

Rommel E, Terracciano L, Noppen C, et al. Modulation of dendritic cell phenotype and mobility by tumor cells in vitro. *Hum Immunol* 2001;62(1):39-49

Renkvist N, Castelli C, Robbins PF, Parmiani G. A listing of human tumor antigens recognized by T cells. *Cancer Immunol Immunother* 2001;50(1):3-15.

Rosenstraus, MJ, Spadaro JP, and Nilsson J. "Cell position regulates endodermal differentiation in embryonal carcinoma cell aggregates." *Dev. Biol*. 1983; 98.1: 110-16

Rosenberg SA, Yang JC, Schwatrzentruber DJ, Hwu P, Marincola FM, Topalian SL, Restifo NP, Dudley ME, Schwarz SL, Spiess PJ, Wunderlich JR, Parkhurst MR, Kawakami Y, Seipp CA, Einhorn, JH, White DE. Immunologic and therapeutic evaluation of a synthetic peptide vaccine for the treatment of patients with metastatic melanoma. *Nat Med* 1998; 4:321-327.

Rosenberg SA. New opportunities for the development of cancer immunotherapies. *Cancer J Sci Am* 1998;4 Suppl 1:S1-S4.

Rubin, P. and G. W. Casarett. "Clinical radiation pathology as applied to curative radiotherapy." *Cancer* 22.4 (1968): 767-78

Rubinstein N et al, Targeted inhibition of galectin-1 gene expression in tumor cells results in heightened T cell-mediated rejection; A potential mechanism of tumor-immune privilege. *Cancer Cell*. 2004 ;5(3):241-51

Sacks PG, Miller MW, Sutherland RM., Influences of growth conditions and cell-cell contact on responses of tumor cells to ultrasound, *Radiat Res*. 1981 ;87(1):175-86

Santini MT, Rainaldi G. Three-dimensional spheroid model in tumor biology. *Pathobiology* 1999;67:148-157

Santini MT, Rainaldi G , Indovina PL, Apoptosis, cell adhesion and the extracellular matrix in the three-dimensional growth of multicellular tumor spheroids. *Crit Rev Oncol Hematol*. 2000; 36(2-3):75-87

Shih IM. The role of CD146 (Mel-CAM) in biology and pathology. *J Pathol* 1999; 189 (1):4-11

Singh RK, Gutman M, Radinsky R, Bucana CD, Fidler IJ: Expression of interleukin 8 correlates with the metastatic potential of human melanoma cells in nude mice. *Cancer Res* 1994, 54:3242-3247

Slingluff CL, Petroni GR, Yamshchikov GV, Barnd DL, Eastham S, Galavotti H, Patterson JW, Deacon DH, Hibbitts S, Teates D, Neese PY, Grosh WW, Chianese-Bullock KA, Woodson EM, Wiernasz CJ, Merrill P, Gibson J, Ross M, Engelhard VH. Clinical and immunological results of a randomized phase II trial of vaccination using four melanoma peptides either administered in granulocyte-macrophage colony-stimulating factor in adjuvant or pulsed on dendritic cells. *J Clin Oncol* 2003; 21:4016-4026

Sordat B, MacDonald HR, Lees RK. The multicellular spheroid as a model tumor allograft. III. Morphological and kinetic analysis of spheroid infiltration and destruction. *Transplantation* 1980 Feb;29(2):103-12.

Steel GG, *Growth kinetics of tumours*, 1977, Clarendon, Oxford

Sutherland RM, McCredie JA, Inch WR: Growth of multicellular spheroids in tissue culture as a model of nodular carcinomas. *J Nat Canc Inst* 1971; 46:113-120

Sutherland RM, Durand RE, Radiation response of multicell spheroids- an in vitro tumour model. *Curr Top Radiat Res Q*. 1976 Jan;11(1):87-139

Sutherland, R. M. et al. "Oxygenation and differentiation in multicellular spheroids of human colon carcinoma." *Cancer Res.* 46.10 (1986): 5320-29

Sutherland RM. Cell and environment interactions in tumor microregions: the multicell spheroid model. *Science* 1988; 240:177-184

Sutherland RM, Ausserer WA, Murphy BJ, Laderoute KR, Tumor hypoxia and heterogeneity: challenges and opportunities for the future , *Semin Radiatio Oncol*, 6, 1996, 59-70

Sutherland RM; Importance of critical metabolites and cellular interactions in the biology of microregions of tumors, *cancer* 58, 1986, 1668-1680

Simons DM, Gardner EM, Lelkes PI, Dynamic culture in a rotating-wall vessel bioreactor differentially inhibits murine T-lymphocyte activation by mitogenic stimuli upon return to static conditions in a time-dependent manner. *J Appl Physiol* 100: 2006,1287–1292

Sommers CL et al, Loss of epithelial markers and acquisition of vimentin expression in adriamycin- and vinblastine-resistant human breast cancer cell lines. *Cancer Res.* 1992; 1;52(19):5190-7

Song H, David O, Clejan S, Giordano CL, Pappas-Lebeau H, Xu, L, O'Connor KC: Spatial Composition of Prostate Cancer Spheroids in Mixed and Static Cultures. *Tissue Eng.* 2004; 10: 7/8, 1266-1276

Tachibana M et al, Ectopic expression of MITF, a gene for Waardenburg syndrome type 2, converts fibroblasts to cells with melanocyte characteristics, *Nature Genetics.* 1996;14, 50 - 54

Takata H, Tomiyama H, Fujiwara M, Kobayashi N, Takiguchi M. Cutting edge: expression of chemokine receptor CXCR1 on human effector CD8+ T cells. *J Immunol* 2004;173:2231-2235

Tannock, I. F. "The relation between cell proliferation and the vascular system in a transplanted mouse mammary tumour." *Br.J.Cancer* 1968; 22.2: 258-73

Tan, M., R. Grijalva, and D. Yu. "Heregulin beta1-activated phosphatidylinositol 3-kinase enhances aggregation of MCF-7 breast cancer cells independent of extracellular signal-regulated kinase." *Cancer Res.* 1999; 59.7: 1620-25

Theodorescu, D., C. Sheehan, and R. S. Kerbel. "TGF-beta gene expression depends on tissue architecture." *In Vitro Cell Dev.Biol.* 1993; 29A.2: 105-08

Thiery JP, Epithelial-Mesenchymal transitions in tumour progression, *Nat Rev Cancer*, 2002, 2, 442-454

Thurner B, Haendle I, Roder C, Dieckmann D, Keikavoussi P, Jonuleit H, Bender A, Maczek C, Schreiner D, von den Driesch P, Brocker EB, Steinman RM, Enk A, Kampgen E, Schuler G. Vaccination with mage-3A1 peptide pulsed mature monocyte-derived dendritic cells expands specific cytotoxic T cells and induces regression of some metastases in advanced stage IV melanoma. *J Exp Med* 1999; 190:1669-1678.

Timmins NE, Maguire TL, Grimmond SM, Nielsen LK, Identification of three gene candidates for multicellular resistance in colon Carcinoma, *Cytotechnology* (2004) 46:9–18

Timmins NE, Dietmair S, Nielsen SK, Hanging-drop multicellular spheroids as a model of tumour angiogenesis. *Angiogenesis* 2004;7(2):97-103

Teutsch, H. F., A. Goellner, and W. Mueller-Klieser. "Glucose levels and succinate and lactate dehydrogenase activity in EMT6/Ro tumor spheroids." *Eur.J.Cell Biol.* 66.3 (1995): 302-07

Thomlinson RH and L. H. GRAY. "The histological structure of some human lung cancers and the possible implications for radiotherapy." *Br.J.Cancer* 9.4 (1955): 539-49

Tobari, C., van Kersen, I. & Hahn, G. M. Modification of pH of normal and malignant mouse tissue by hydralazine and glucose, with and without breathing of 5% CO<sub>2</sub> and 95% air. *Cancer Res.* 1988; 48, 1543-1547.

Uyttenhove C et al, Evidence for a tumoral immune resistance mechanism based on tryptophan degradation by indoleamine 2,3-dioxygenase, *at Med* 9, 2003, 1269-74

Vaupel, P., Kallinowski, F. & Okunieff, P. Blood flow, oxygen and nutrient supply, and metabolic microenvironment of human tumors: a review (1989) *Cancer Res.* 49, 6449-6465.

Virchow R. 1863. Aetologie der neoplastischen Geschwulste/ Pathogenie der neoplastischen Geschwulste. In *Die Krankhaften Geschwulste*, p. 58. Verlag von August Hirschwald, Berlin, Germany

Ward JP, JR. King. "Mathematical modelling of avascular-tumour growth." *IMA J.Math.Appl.Med.Biol.* 14.1 (1997): 39-69

Walenta, S., J. Dotsch, and W. Mueller-Klieser. "ATP concentrations in multicellular tumor spheroids assessed by single photon imaging and quantitative bioluminescence." *Eur.J.Cell Biol.* 1990; 52.2: 389-93

Walenta S et al. "Size-dependent oxygenation and energy status in multicellular tumor spheroids." *Adv.Exp.Med.Biol.* 277 (1990): 889-93

Walenta S et al. "Interrelationship among morphology, metabolism, and proliferation of tumor cells in monolayer and spheroid culture." *Adv.Exp.Med.Biol.* 1989; 248: 847-53.

Walenta et al, High lactate levels predict likelihood of metastasis, tumor recurrence and restricted patient survival, *Cancer Res*, 2000; 60, 916-21

Walenta S, S. Snyder, Z. A. Haroon, R. D. Braun, K. Amin, D. Brizel, W. Mueller-klieser, B. Chance, M.W. Dewhirst: Tissue gradients of energy metabolites mirror oxygen tension gradients in a rat mammary carcinoma model. *Int. J. Radiat. Oncol. Biol. Phys.* 2001; 51(3), 840-848

Walenta S, Mueller-Klieser WF. Lactate: Mirror and motor of tumor malignancy. *Semin Radiat Oncol* 2004; 14:267-74

Weber WP, et al, Differential effects of the tryptophan metabolite 3-hydroxyanthranilic acid on the proliferation of human CD8+ T cells induced by TCR triggering or homeostatic cytokines. *Eur J Immunol*, 2006 ;36(2):296-304.

Whiteside TL, Sung MW, Nagashima S, Chikamatsu K, Okada K, Vujanovic NL. Human tumor antigen-specific T lymphocytes and interleukin-2-activated natural killer cells: comparisons of antitumor effects in vitro and in vivo. *Clin Cancer Res* 1998 ;4(5):1135-45.

Whiteside TL, et al. Immune cells in the tumor microenvironment. Mechanisms responsible for functional and signaling defects. *Adv Exp Med Biol* 1998;451, 167

Wiens AW., A Moscona, Preferential inhibition by proflavine of the hormonal induction of glutamine synthetase in embryonic neural retina, *Proc Nat Acad Sci USA*, 1972;69(6):1504-7

Wicki A, Lehembre F, Wick N, Hantusch B, Kerjaschki D, Christofori G, Tumor invasion in the absence of epithelial-mesenchymal transition: podoplanin-mediated remodeling of the actin cytoskeleton. *Cancer Cell*. 2006 ;9(4):261-72

Winsor, The Gompertz curve as a growth curve. *PNAS USA*. 1932;18:1– 7

Winer J, Jung CK, Shackel I, Williams PM. Development and validation of real-time quantitative reverse transcriptase-polymerase chain reaction for monitoring gene expression in cardiac myocytes in vitro. *Anal Biochem* 1999 May 15;270(1):41-9

Wike-Hooley, J. L., Haveman, J. & Reinhold, H. S. The relevance of tumour pH to the treatment of malignant disease. *Radiother. Oncol.* 1984; 2, 343-366

Woodhouse JC., Esters of methacrilate acid, 1938; US Patent 2 129 722

Yamagata M, Hasuda K, Stamato T, Tannock IF, The contribution of lactic acid to acidification of tumours: studies of variant cells lacking lactate dehydrogenase, *Br J cancer*, 1998; 77(11) 1726-31

Yuhas JM, Li AP, Martinez AO, Ladman AJ.. A simplified method for production and growth of multicellular tumor spheroids. *Cancer Res* 1977; 37: 3639–3643.

Yuhas, J. M. and A. P. Li. "Growth fraction as the major determinant of multicellular tumor spheroid growth rates." *Cancer Res*. 1978; 38.6: 1528-32

Zarling JM, Shoyab M, Marquardt H, Hanson MB, Lioubin MN, Todaro GJ. Oncostatin M: a growth regulator produced by differentiated histiocytic lymphoma cells. *Proc Natl Acad Sci USA* 1986;83:9739–9743.

Zajac P, Oertli D, Marti W, et al. Phase I/II clinical trial of a nonreplicative vaccinia virus expressing multiple HLA-A0201-restricted tumor-associated epitopes and costimulatory molecules in metastatic melanoma patients. *Hum Gene Ther* 2003;14:1497-1510

Zheng P, Sarma S, Guo Y, Liu Y. Two mechanisms for tumor evasion of preexisting cytotoxic T-cell responses: lessons from recurrent tumors. *Cancer Res* 1999;59(14):3461-7



Zippelius A, Batard P, Rubio-Godoy V, Bioley G, Lienard D, Lejeune F, Rimoldi D, Guillaume P, Meidenbauer N, Mackensen A, Rufer N, Lubenow N, Speiser D, Cerottini JC, Romero P, Pittet MJ. Effector function of human tumor-specific CD8 T cells in melanoma lesions: a state of local functional tolerance. *Cancer Res* 2004; 64:2865-2873

## Publications

# Three-Dimensional Culture of Melanoma Cells Profoundly Affects Gene Expression Profile: A High Density Oligonucleotide Array Study

SOURABH GHOSH,<sup>1</sup> GIULIO C. SPAGNOLI,<sup>1</sup> IVAN MARTIN,<sup>1</sup> SABINE PLOEGERT,<sup>1</sup> PHILIPPE DEMOUGIN,<sup>2</sup> MICHAEL HEBERER,<sup>1</sup> AND ANCA RESCHNER<sup>1\*</sup>

<sup>1</sup>*Institut für Chirurgische Forschung und Spitalmanagement (ICFS) and Departement Forschung, University of Basel, Basel, Switzerland*

<sup>2</sup>*Biocenter/Pharmazentrum, University of Basel, Basel, Switzerland*

Growth in three-dimensional (3D) architectures has been suggested to play an important role in tumor expansion and in the resistance of cancers to treatment with drugs or cytokines or irradiation. To obtain an insight into underlying molecular mechanisms, we addressed gene expression profiles of NA8 melanoma cells cultured in bidimensional monolayers (2D) or in 3D multicellular tumor spheroids (MCTS). MCTS containing 10–30,000 cells were generated upon overnight culture in poly-Hydroxyethylmethacrylate (polyHEMA) coated plates. Kinetics of cell proliferation in MCTS was significantly slower than in monolayer cultures. Following long-term culture (>10 days), however, MCTS showed highly compact and organized cell growth in outer layers, with necrotic cores. Oligonucleotide microarray analysis of the expression of over 20,000 genes was performed on cells cultured in standard 2D, in the presence of collagen as model of extracellular matrix (ECM), or in MCTS. Gene expression profiles of cells cultured in 2D in the presence or absence of ECM were highly similar, with  $\geq$ threefold differences limited to five genes. In contrast, culture in MCTS resulted in the significant,  $\geq$ threefold, upregulation of the expression of >100 transcripts while 73 were  $\geq$ threefold downregulated. In particular, genes encoding CXCL1, 2, and 3 (GRO- $\alpha$ , - $\beta$ , and  $\gamma$ ), IL-8, CCL20 (MIP-3 $\alpha$ ), and Angiopoietin-like 4 were significantly upregulated, whereas basic FGF and CD49d encoding genes were significantly downregulated. Oligonucleotide chip data were validated at the gene and protein level by quantitative real-time PCR, ELISA, and cell surface staining assays. Taken together, our data indicate that structural modifications of the architecture of tumor cell cultures result in a significant upregulation of the expression of a number of genes previously shown to play a role in melanoma progression and metastatic process. *J. Cell. Physiol.* 204: 522–531, 2005. © 2005 Wiley-Liss, Inc.

Experimental models indicate that tumor cells in suspension, regardless of their numbers, are frequently unable to produce life threatening cancer outgrowth, as opposed to solid tumor fragments (Ochsenbein et al., 2001), while being able to induce specific immune responses. Thus, proliferation in structured architectures appears to represent a pre-requisite for cancer development. Therefore, development of three-dimensional (3D) models of neoplastic cell culture may represent a technological approach of potentially high clinical relevance.

Indeed, cells cultured in 3D conditions have been shown to be endowed with specific characteristics, including resistance to apoptosis or to the cytotoxic activity of specific T-cells “in vitro” (Sutherland, 1988; Desoize and Jardillier, 2000; Dangles et al., 2002; Weaver et al., 2002; Dangles-Marie et al., 2003). Notably, multicellular tumor spheroids (MCTS) display drug and radiation resistance features closely matching those frequently detectable “in vivo” (Desoize and Jardillier, 2000).

Taken together, these studies suggest that in tumor cells growing in structured architectures the preferential expression of specific constellations of genes might occur.

In order to obtain insights into similarities and differences between tumor cells growing in physically different microenvironments, here we analyzed gene expression profiles of melanoma cells (Certa et al., 2001) cultured in standard 2D conditions or as MCTS.

## MATERIALS AND METHODS

### Cell cultures

NA8 cell line was derived from a metastatic melanoma and has widely been used in tumor immunology studies in the

recent past (Gervois et al., 1996; Oertli et al., 2002; Zajac et al., 2003). It is HLA-A0201+ but fails to express typical differentiation or cancer/testis (C/T) tumor-associated antigens (TAA) (Renkvist et al., 2001). NA8 cells were routinely passaged in conventional monolayer cultures in DMEM supplemented with Kanamycin, glutamin, non-essential amino acids, sodium pyruvate, HEPES buffer, and 10% heat-inactivated FCS (all from Gibco, Paisley, Scotland), thereafter referred to as complete medium. When indicated, cells were also cultured in dishes previously coated (2 h at 37°C) with a 50  $\mu$ g/ml solution of purified collagen (Vitrogen, Palo Alto CA) in PBS. MCTS were prepared in plastic culture plates following coating with a 50  $\mu$ g/ml poly-(2-hydroxyethyl methacrylate, polyHEMA, Sigma, St. Louis, MO) solution, preventing cell binding, as described (Folkman and Moscona, 1978). Cell proliferation was measured by the Alamar Blue assay (Hamid et al., 2004).

### Gene expression profiling

Na-8 cells were harvested by trypsinization after 3 days cultures according to the different protocols indicated. Total RNA was extracted using Qiagen Rneasy<sup>®</sup> Mini Kit (Qiagen, Basel, Switzerland) and its integrity was monitored using Agilent 2100 Bioanalyzer (Ambion, Austin TX). Ten micrograms of RNA from each sample were reverse transcribed and

Contract grant sponsor: Swiss National Science Foundation; Contract grant sponsor: Swiss Bridge Foundation.

\*Correspondence to: Anca Reschner, ICFS, Lab. 401, ZLF, 20, Hebelstrasse, 4031, Basel, Switzerland.  
E-mail: areschner@uhbs.ch

Received 27 September 2004; Accepted 29 November 2004

DOI: 10.1002/jcp.20320

labeled by using commercial kits according to the suppliers' instructions (MEGAscriptT7, Ambion, Austin TX; Bio-11-UTP and Bio-16-UTP, Enzo Biochem, NY). Biotinylated cRNA was then fragmented by treatment at 94°C for 35 min in 40 mM TRIS-acetate, pH 8.1, 100 mM potassium acetate, and 30 mM magnesium acetate and hybridized to human oligonucleotide array HG-U-133A (Affymetrix, Santa Clara CA). Two separate hybridizations were performed for each sample under investigation. Raw data were collected using a confocal laser scanner, and pixel levels were analyzed using commercial software (Gene Spring Version 1.6, Silicon Genetics, Redwood City, CA). For each hybridization, two separate data readings were performed.

#### Histology and immunohistochemistry

Tumor spheroids were fixed in 4% formaldehyde, washed in PBS, and embedded in paraffin. Sections were stained with hematoxylin and eosin. BrdU staining was performed on fresh frozen MCTS sections, following endogenous peroxidase blocking by incubation with hydrogen peroxide, by taking advantage of a reagent kit (Pharmingen, San Diego, CA), according to the instructions of the supplier. In specific experiments, slides were incubated in the presence of an anti-human IL-8 monoclonal antibody (BD Biosciences Pharmingen, San Diego, CA) for 4 h and specific staining was detected by adding a biotinylated secondary antibody, avidin-HRP, and

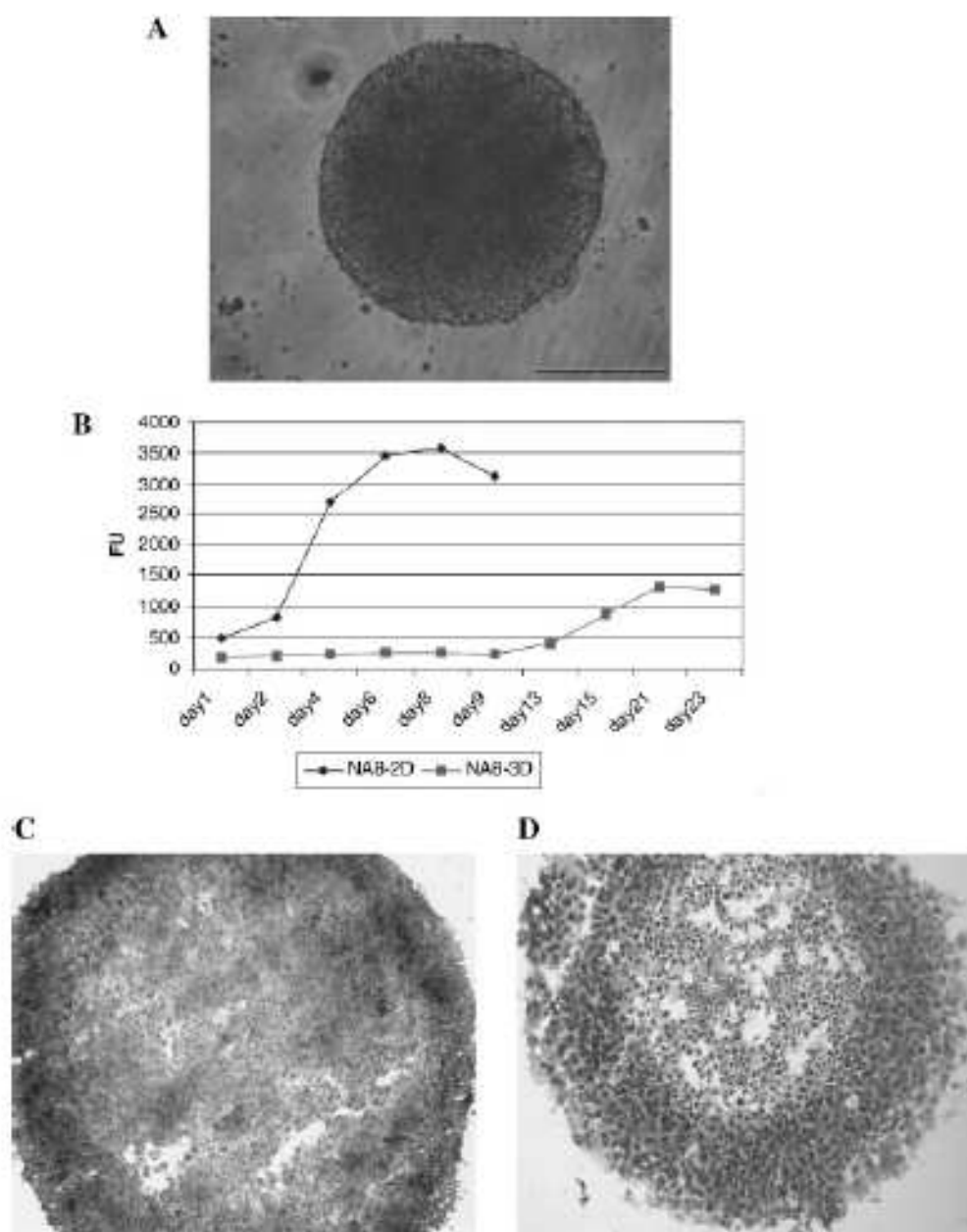


Fig. 1. Generation and characterization of multicellular tumor spheroids of NAS cells. NAS cells cultured on a polyHEMA coated plate give rise to the formation of multicellular tumor spheroids (MCTS, part A). Alamar blue cell proliferation assays (part B) show distinct kinetics for cells cultured in monolayers or MCTS. BrdU

staining (part C) indicates that while cells located in the center of MCTS are prevalently in quiescent state, those in outer layers are actively cycling. Prolonged culture (>10 days) results in apoptosis of cells sitting in the inner MCTS layers, resulting in the formation of hollow centers (part D).

3,3'-diaminobenzidine hydrochloride. In all cases, slides were counterstained with hematoxylin.

#### Real-time RT-PCR

NA-8 cells cultured in 2D or as MCTS were collected at the indicated time points and washed in PBS. Total RNA was extracted using the RNeasy® Mini Kit Protocol (Qiagen, Basel, Switzerland) and treated with deoxyribonuclease I (DNase I) (Invitrogen, Carlsbad, CA). Real-time quantitative RT-PCR assays were conducted on a ABI prism™ 7700 sequence detection system, using TaqMan® One Step PCR Master Mix Reagents Kit (Master Mix without UNG, Multiscribe™ and RNase Inhibitor Mix, Applied Biosystems, Branchburg, NJ).

The oligonucleotide primers and the Taq Man probe for GAPDH were designed using the Primer Express software (Perkin Elmer Applied Biosystems, Inc., Foster City, CA) and sequences from the NCBI gene bank. The primers and probes for CXCL1 (GRO  $\alpha$ ), CXCL8 (IL-8), and CCL20 (MIP-3 $\alpha$ ) were purchased as Assays on Demand, Gene Expression Products (Perkin Elmer Applied Biosystems, Inc., Foster City, CA).

To quantify gene expression in each sample, we used the comparative threshold cycle (Ct) method (Primer Express software, Applied Biosystem, Foster City, CA). Normalization of gene expression was performed by using GAPDH as reference gene, and data were expressed as ratio to a reference sample, namely to cells cultured in standard monolayers.

#### Protein detection by ELISA

CXCL1, CCL20, and IL-8 secretion was tested by quantitative ELISA assays (sensitivity:  $\geq 30$  pg/ml) in supernatants from NA-8 monolayer cultures or MCTS sampled at different time points. Antibody pairs and standards for CXCL1 were from R&D Systems (Abingdon, Great Britain), whereas CCL20 and IL-8 ELISA sets were obtained from Becton Dickinson Bioscience Pharmingen, San Diego, CA. All samples were measured in duplicates.

#### Flow cytometry

NA-8 cells cultured in 2D were collected by trypsinization on day 3. Accordingly, MCTS obtained after 3 days of culture on polyHEMA treated plasticware were centrifuged and pellets were disrupted by Trypsin-EDTA (Gibco, Paisley, Great Britain) treatment for 30 min at 37°C. Phenotypes of NA-8 cells cultured in 2D or 3D were evaluated by surface staining using fluorochrome conjugated mouse monoclonal antibodies recognizing the indicated determinants. Samples were analyzed on a FACSCalibur (Becton Dickinson, San Jose, CA) using propidium iodide (PI) to exclude dead cells.

#### Statistical analysis

One-way ANOVA tests were performed for gene lists filtered on fold change in the log-of-ratio mode of experimental interpretation (Gene Spring 6 software, Silicon Genetics, Redwood City, CA). Duplicates of each experimental group were compared. The parametric Welch *t*-test was used within the study with a cut-off *P*-value of 0.05.

## RESULTS

### Morphological characterization and growth pattern of NA8 melanoma cell spheroids

NA8 cells were routinely maintained in 2D cultures in complete medium. However, treatment of culture trays with polyHEMA (Folkman and Moscona, 1978), preventing cell attachment, gave rise within 24 h to the formation of MCTS structures. Each MCTS, displaying 400–500- $\mu$ m diameter, contained between 10,000 and 30,000 cells (Fig. 1A). NA8 cell proliferation in 2D cultures was reaching a plateau within 7 days, whereas, in contrast, no major increases in cell numbers were detectable in MCTS for the first 2 weeks of culture, but they could only be observed at later time points (Fig. 1B). BrdU staining indicated that while cells in the outer

MCTS layers were entering cell cycle, those of inner layers were mostly quiescent (Fig. 1C). Furthermore, upon prolonged culture (>10 days), HE staining showed necrotic cores within MCTS soon resulting in hollow centers with large, compact cells being typically detectable in the periphery (Fig. 1D).

### Gene expression profiles of NA8 cells cultured in 2D and in spheroids

The expression of specific sets of genes has previously been shown to be modulated by cell culture architecture (Dangles et al., 2002), possibly also in relation to signals effectively transduced upon interaction of adhesion molecules with their counter receptors (Cavallaro and Christofori, 2004). Prompted by these studies, we addressed thorough gene profiling in NA8 cells cultured in standard 2D conditions, in the presence of extracellular matrix (ECM) or in MCTS, by taking advantage of high-density oligonucleotide arrays allowing the analysis of over 20,000 expressed genes. As ECM model, we

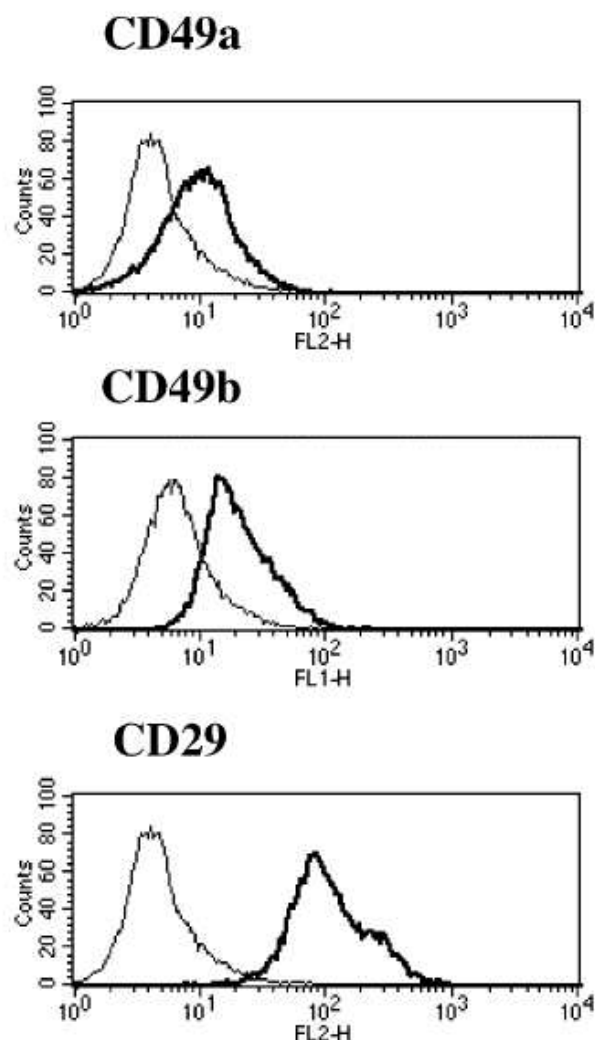


Fig. 2. Expression of receptors for collagen in NA8 cells. NA8 cells cultured in standard monolayers were trypsinized and stained with monoclonal antibodies specific for  $\alpha 1$ ,  $\alpha 2$ , and  $\beta 1$  (CD49a, CD49b, and CD29, respectively), integrin chains.



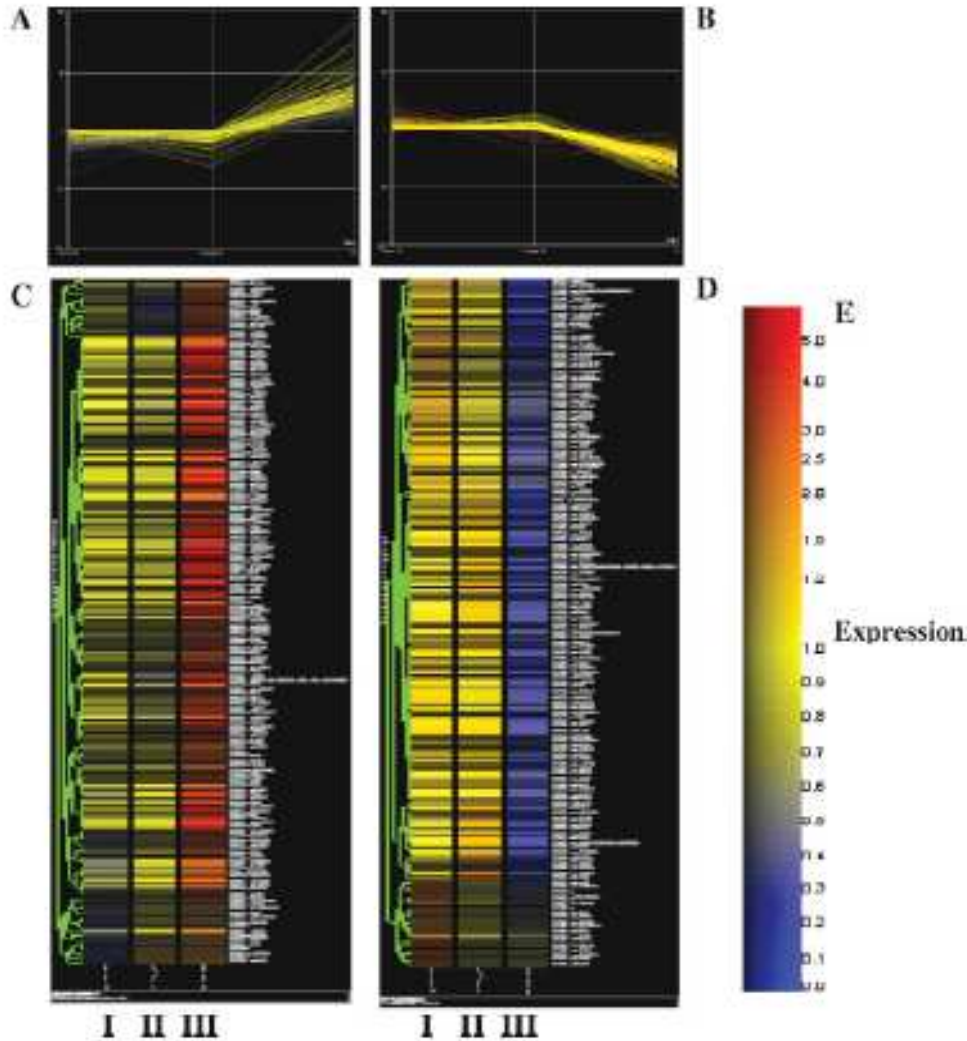


Fig. 3. Modulation of gene expression in NA8 cells cultured in 2D or MCTS. NA8 melanoma cells were cultured in standard monolayers (I), in 2D in the presence of solid phase bound collagen (II) or in MCTS (III). Parts A and B refer to genes significantly up- or downregulated, respectively, in either of these culture conditions. The extent of the up- or downregulation of each gene is presented in parts C and D, respectively, according to the color scale shown in part E.

chase collagen since NA8 cells express both  $\alpha1\beta1$  and  $\alpha2\beta1$  integrin receptors (Fig. 2).

Over 11,000 genes were found to be expressed in NA8 cells. Cells cultured in monolayers, irrespective of the presence of ECM, showed remarkably similar gene expression patterns (Fig. 3), with statistically significant differences (see above) being limited to five genes

(Table 1). In particular, a downregulation (fivefold) of Hsp 40 encoding gene was observed in cells cultured in the presence of collagen.

In contrast, cells cultured in MCTS displayed significant modulation in the expression of a number of genes as compared to their monolayer counterparts. Indeed, 106 genes showed evidence of upregulation and 73

TABLE 1. Modulation of gene expression in NA8 monolayers in the presence or absence of collagen coating

Common name	Genbank	Description	P-value	Fold change
<b>Genes upregulated in 2D NA8 cultures in the presence of collagen (as compared to monolayer NA8 cells)</b>				
INHBA	NM_002192	Inhibin, beta A (activin A, activin AB alpha polypeptide)	0.03785189	3.23
<b>Genes downregulated in 2D NA8 cultures in the presence of collagen (as compared to monolayer NA8 cells)</b>				
LRRC19	NM_022901	Leucine-rich repeat containing 19	0.04999528	3.36
	AB025191	<i>Howe sapiens</i> cDNA: FLJ21538 fis, clone COL06151	0.02274983	4.49
DNAJC6	NM_014787	DnaJ (Hsp40) homolog, subfamily C, member 6	0.02692304	5.05
PF4V1	NM_002620	Platelet factor 4 variant 1	0.04518665	10.36

NA8 cells were cultured in monolayers in the presence or absence of collagen coating for 3 days. Total cellular RNA was then extracted, reverse transcribed, and labeled as described in Materials and Methods prior to hybridization to oligonucleotide chips. Only genes displaying a  $\geq 2$  fold up- or downregulation (fold change) in either culture conditions are reported. Statistical significance ( $P < 0.05$ ) refers to duplicate readings of data obtained from two distinct hybridization experiments.

TABLE 2. Modulation of gene expression in NA5 cells cultured in MCTS, as compared to standard monolayers

Common name	Genbank	Description	P-value	Fold change
Genes upregulated in MCTS as compared to monolayer NA5 cells				
CCl20	NM_004691	Chemokine (C-C motif) ligand 20	0.00260	75.29
IL8	NM_000584	Interleukin 8	0	67.9
IL8	AF043317	Human sapiens interleukin 8 C-terminal variant (IL8) mRNA, complete cds.	0.0006	69.76
ANGPTL4	NM_016109	Angiogenin-like 4	0.00139	34.37
SLC2A3	NM_006931	Solute carrier family 2 (facilitated glucose transporter), member 3	0.00021	33.63
CA9	NM_001216	Carbonic anhydrase IX	0.00119	31.38
MDR11	NM_006046	N-myc downstream regulated gene 1	0.03635	28.71
STC1	NM_003155	Stanniocalcin 1	0.00178	23.63
ITPR3	NM_002232	Inositol 1,4,5-trisphosphate receptor, type 1	0.0033	23.76
ADFP	BC035127	Adipose differentiation-related protein	0.02111	17.27
LOX	L36895	Human lysyl oxidase (LOX) gene, exon 7	0.03528	16.23
CXCL2	M57731	Chemokine (C-X-C motif) ligand 2	0.01739	15.90
LOX	HE63435	Lysyl oxidase	0.00662	14.45
ISG20	NM_002201	Interferon-stimulated gene 20kDa	0.02148	14.11
ADM	NM_001124	Adrenomedullin	0.00801	13.36
C10orf10	A190200	Chromosome 10 open reading frame 10	0.0454	13.04
TBC1D3	AL136880	TBC1 domain family, member 3	0.04100	12.69
SLC2A3	NM_006931	Solute carrier family 2 (facilitated glucose transporter), member 3	0.0037	12.66
CXCL1	NM_001511	Chemokine (C-X-C motif) ligand 1 (melanoma growth stimulating activity, alpha)	0.03033	10.14
TNFAIP3	NM_006290	Tumor necrosis factor, alpha-induced protein 3	0.03666	9.38
DUSP6	BC031143	Dual specificity phosphatase 6	0.00858	9.21
SPAG4	NM_003116	Sperm associated antigen 4	0.01191	9.06
ANXA10	AF196478	Annexin A10	0.03017	8.89
MAFF	AF021977	Human DNA sequence from clone CTA-447C4 on chromosome 22q12.2-13.2, complete sequence.	0.04029	8.83
BHLHB3	BC338045	Basic helix-loop-helix domain containing, class B, 2	0.01762	8.49
SAT	HE971389	Spermin/ spermine N1-acetyltransferase	0.01839	8.35
SCD2	AL050388	Superoxide dismutase 2, mitochondrial	0.04234	8.11
RIS1	BF062629	Ras-induced senescence 1	0.02817	7.7
STC1	A1360820	Stanniocalcin 1	0.02172	7.54
NTSE	NM_002626	N-nucleotidase, ecto (CD33)	0.01339	7.50
Clorf29	NM_006820	Chromosome 1 open reading frame 29	0.04604	7.29
HIG2	NM_013933	Hypoxia-inducible protein 2	0.02166	7.02
RNASE4	A1951738	Ribonuclease, RNase A family, 4	0.01998	6.76
FLJ10134	NM_018004	Hypothetical protein FLJ10134	0.00498	6.63
BNIP3	NM_004093	BCL2/adenovirus E1B 19kDa interacting protein 3	0.01031	6.56
SLC2A14	AL110266	Solute carrier family 2 (facilitated glucose transporter), member 14	0.01999	6.57
IER3	NM_003897	Immediate early response 3	0.02379	6.34
CXCL3	NM_002040	Chemokine (C-X-C motif) ligand 3	0.00576	6.17
TNFAIP3	A1758496	Tumor necrosis factor, alpha-induced protein 3	0.04375	6.04
ENK2	NM_001975	Enkephalin 2 (granule, neuronal)	0.04872	5.99
SCD2	W46388	Superoxide dismutase 2, mitochondrial	0.01667	5.96
STC2	A1495826	Stanniocalcin 2	0.04571	5.69
E2F3	NM_014867	Growth and transformation-dependent protein	0.03707	5.69
HSPA6	NM_002155	Heat shock 70-kDa protein 6 (HSP70H)	0.02325	5.49
PPP1R15A	NM_014330	Protein phosphatase 1, regulatory (inhibitor) subunit 15A	0.01399	5.44
MXI1	NM_003962	MAX interacting protein 1	0.00364	5.36
PPP1R3C	N36305	Protein phosphatase 1, regulatory (inhibitor) subunit 3C	0.001	5.32
SLC04A1	NM_016354	Solute carrier organic anion transporter family, member 4A1	0.02663	5.26
SERPINE1	AF044210	Serpin (or cysteine) proteinase inhibitor, clade E (nexin, plasminogen activator inhibitor type 1), member 1	0.04304	5.22
BNIP3	U15174	Human sapiens BCL2/adenovirus E1B 19kDa-interacting protein 3 (BNIP3) mRNA, complete cds.	0.00914	5.16
BTG1	AL555390	B-cell translocation gene 1, anti-proliferative	0.03111	5.14
SCD2	BF575213	Superoxide dismutase 2, mitochondrial	0.00027	5.11
IGFBP3	NM_000596	Insulin-like growth factor binding protein 3	0.01595	5.05
CDCP1	NM_022842	CUB domain-containing protein 1	0.04963	5.03
SERPINA3	NM_001036	Serpin (or cysteine) proteinase inhibitor, clade A (alpha-1 antitrypsin, antitrypsin), member 3	0.00283	4.72
BHLHB2	NM_003670	Basic helix-loop-helix domain containing, class B, 2	0.03066	4.66
DPYSL4	NM_006426	Dihydropyrimidinase-like 4	0.02427	4.6
MT1H	NM_006951	Metallothionein 1H	0.03048	4.42
SERPINE4	AB046400	Serpin (or cysteine) proteinase inhibitor, clade E (ovalbumin), member 4	0.0285	4.39
TFPI2	L27624	Tissue factor pathway inhibitor 2	0.04993	4.38
KIAA1641	NM_026130	KIAA1641 protein	0.03702	4.35
IL1B	NM_000576	Interleukin 1, beta	0.03032	4.22
KIAA0703	AW291664	KIAA0703 gene product	0.02645	4.21
NFIL3	NM_000584	Nuclear factor, interleukin 3 regulated	0.00834	4.21
DPA	BG251266	Hepatitis delta antigen-interacting protein A	0.00501	4.19
GOLGIN-67	AF204281	Golgin-67	0.03727	4.13
RNU2	BC003629	Synonym: U2; Homo sapiens RNA, U2 small nuclear, mRNA (cDNA clone MGC2284 IMAGE:268705), complete cds.	0.00906	4.13
INSIG2	AL080184	Insulin induced gene 2	0.00932	4.13
PHLJ A1	AA876961	Phlebotin homology-like domain, family A, member 1	0.02627	4.09
LAMB3	L36541	Laminin, beta 3	0.01540	3.99
DUSP1	NM_004417	Dual specificity phosphatase 1	0.00041	3.99

TABLE 2. (Continued)

Common name	Gen bank	Description	P-value	Fold change
KNR2	AA284076	Kinase 2 607kDa	0.0068	4.30
SCD	AB022281	Stearoyl-CoA desaturase (delta-9-desaturase)	0.0163	4.26
CD24	AA761181	nc00903.1 NCI CCLAP GCB1 Homo sapiens cDNA clone IMAGE:22875163 similar to gbM57627 INTERLEUKIN-10 PRECURSOR (HUMAN); mRNA sequence	0.0477	4.12
TPM1	NM_000366	Tropomyosin 1 (alpha)	0.0058	4.09
RHOBTB3	NM_014899	Rho-related BTB domain containing 3	0.0277	3.99
C14orf1	AC007182		0.0491	3.96
SCD	AA678241	Stearoyl-CoA desaturase (delta-9-desaturase)	0.0273	3.97
SEC28B	AI121900		0.0413	3.97
DCN	AF138302	Decorin	0.0146	3.83
IDE	N22903	Insulin-degrading enzyme	0.0079	3.82
MYL9	NM_006097	Myosin, light polypeptide 9, regulatory	0.0235	3.82
NaGLT1; KIAA1919; MGC33953	AK000166	Homo sapiens cDNA FLJ20161 fa, clone COL09282, highly similar to L83980 Homo sapiens CD24 signal transducer mRNA	0.0032	3.76
MEP50	BF975273	MEP50 protein	0.0269	3.76
TAGLN	NM_003186	Transgelin	0.0452	3.75
SFHS1	M22709		0.0164	3.72
BMP2K	AW694018	BMP2 inducible kinase	0.0276	3.71
G6PD	NM_000402	Glucose-6-phosphate dehydrogenase	0.0273	3.65
NRG1	NM_013959	Neuregulin 1	0.0471	3.60
GCLM	NM_002061	Glutamate-cysteine ligase, modifier subunit	0.0180	3.57
TACSTD2; M181; EGF-1; GA733; TROP2; GA733-1	J04752	GA733-1 protein precursor; Human gastrointestinal tumor-associated antigen GA733-1 protein gene, complete cds, clone 05516	0.0069	3.50
NQO1	NM_000303	NAD(P)H dehydrogenase, quinone 1	0.0246	3.44
NOL6	NM_022917	Nuclear protein family 6 (RNA-associated)	0.0403	3.39
FLJ21126	NM_024627	Hypothetical protein FLJ21126	0.0238	3.39
	AI358976		0.0087	3.31
ALDH3A2	L47182	Aldehyde dehydrogenase 3 family, member A2	0.0003	3.30
FZD2	L37882	Frizzled homolog 2 (Drosophila)	0.0256	3.27
LDLR	A1861942	Low-density lipoprotein receptor (familial hypercholesterolemia)	0.0498	3.27
NICE-4	NM_014847	NICE-4 protein	0.0110	3.23
CDC42BPB	NM_008035	CDC42 binding protein kinase beta (DMPK-like)	0.0280	3.23
JAG1	U77914	Jagged 1 (Alagille syndrome)	0.0274	3.21
TPM1	M19287	Tropomyosin; human tropomyosin mRNA, complete cds.	0.0004	3.21
HSPA1A	U86735	Alternatively spliced mRNA corresponding to the rodent testis enriched heat shock protein 70 kDa family member; Human heat shock protein mRNA, complete cds.	0.0455	3.20
CPA4	NM_018352	Carboxypeptidase A4	0.0216	3.20
FLJ20010	NM_019021	Hypothetical protein FLJ20010	0.0259	3.18
CD24	M55864	CD24 antigen (small cell lung carcinoma cluster 4 antigen)	0.0294	3.17
PAPSS2	AW299958	3'-Phosphoadenosine 5'-phosphosulfate synthase 2	0.0051	3.17
GPC1	A135484	Glypican 1	0.0498	3.17
GTF3C1	NM_001520	General transcription factor IIC, polypeptide 1, alpha 220kDa	0.0485	3.14
RRM14	NM_008928	RNA binding motif protein 14	0.0139	3.14
NFATC3	U85430	Nuclear factor of activated T-cells, cytoplasmic, calcineurin-dependent 3	0.0221	3.13
ACTBP9	D50604	Human beta-cytoplasmic actin (ACTBP9 pseudogene)	0.0183	3.09
RBM5	NM_008778	RNA binding motif protein 5	0.0413	3.09
VCP	AF100752	Valosin-containing protein	0.0009	3.09
ACTN4; FSG8; FSG81	U48734	Human non-muscle alpha-actinin mRNA, complete cds.	0.0416	3.08
ITGA4	L12002	Integrin, alpha 4 (antigen CD40D, alpha 4 subunit of VLA-4 receptor)	0.0044	3.06
LSS	AW094510	Lanosterol synthase (2,3-oxidosqualene-lanosterol cyclase)	0.0001	3.06
LAPTM4B	NM_018407	Lysosomal associated protein transmembrane 4 beta	0.0081	3.05

NA8 cells were cultured in MCTS (3D) or in 2D monolayers for 3 days. Total cellular RNA was reverse transcribed, labeled, and hybridized to oligonucleotide chips. Only genes displaying a 2-fold or greater up- or downregulation (fold change) in either culture conditions are reported. Statistical significance ( $P < 0.05$ ) refers to data obtained from duplicate readings of two distinct hybridization assays.

of downregulation (Fig. 3, parts A, C and parts B, D, respectively). Table 2 reports the names of the genes of interest and their change factors depending on the architecture of NA8 cell culture.

In particular, a significant upregulation of the expression of genes encoding a number of chemokines, including CXCL1, CXCL2, and CXCL3, (GRO- $\alpha$ ,  $\beta$ , and  $\gamma$ , 10-, 15-, and 6-fold, respectively), IL-8 (67 fold), and CCL20 (75-6H) was detectable in MCTS, as compared to cells cultured in 2D.

The expression of genes encoding pro-angiogenic factors or adhesion molecules, such as angiopoietin-like 4 (34-fold) or hypoxia inducible protein 2 (HIG2, 7-fold) and CD54 (ICAM1, 3.5-fold), was also found to be significantly upregulated in MCTS in comparison with cells growing in monolayers. Interestingly, however, the

expression of the genes encoding  $\alpha 4$  integrin subunit and fibroblast growth factor 2 (FGF2) was found to be significantly downregulated (3- and 6.8-fold, respectively) in these same conditions.

#### Validation of differential gene expression

Large gene expression databases require validation at the gene and protein level. Real-time, quantitative RT-PCR confirmed the upregulation of CXCL1 (GRO- $\alpha$ ), gene expression in cells sampled after 3-day culture in MCTS, as compared with cells growing in monolayers (Fig. 4, part A). We were then interested in investigating whether the upregulation of CXCL1 gene reflected transient events, merely related to MCTS formation or more durable modifications of NA8 gene expression profile. Indeed, CXCL1 gene upregulation,



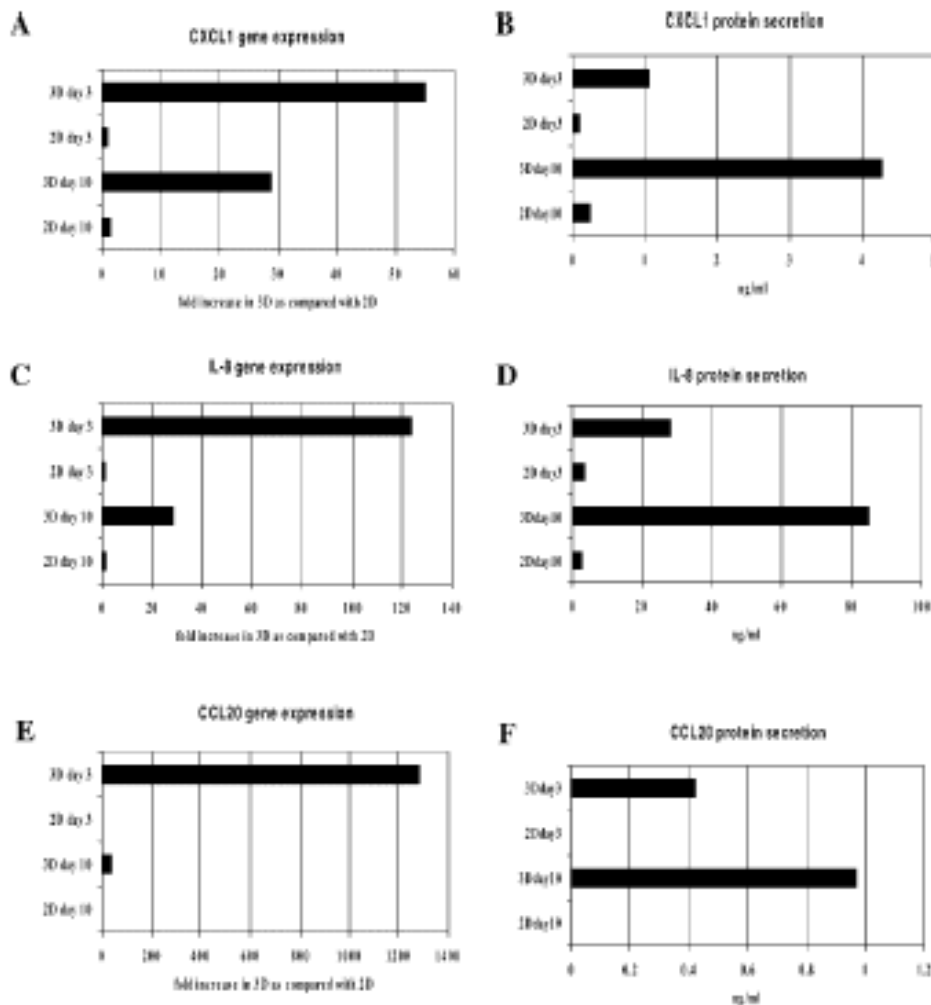


**Fig. 4.** Chemokine gene expression and protein secretion in NA8 cells cultured in monolayers and MCTS. NA8 cells were cultured for 3 or 10 days in standard monolayer cultures (2D) or in MCTS (3D). Total cellular RNA was then extracted and CXCL1 (GRO- $\alpha$ ), IL-8, and CCL20 (MIP-3 $\alpha$ ) gene expression was evaluated comparatively in cells cultured in 2D or in 3D at the indicated time points by quantitative real-time RT-PCR (parts A, C, and E, respectively). Data are

expressed as fold increases of specific gene expression in samples from 3D MCTS cultures as compared to the corresponding samples from 2D cultures at the indicated time points. Secretion of the specific gene products was measured by ELISA in supernatants of cultures containing  $3 \times 10^6$  cells/ml concomitantly collected (parts B, D, and F, respectively). Standard deviations, never exceeding 10% of the values reported, were omitted.

although declining, was still observed at 10 days after the initiation of cultures. Accordingly, secretion of this chemokine was significantly increased in cells cultured in MCTS as compared to their monolayer cultured counterparts at both 3 and 10 days of culture (Fig. 4, part B).

Similarly, increased IL-8 gene expression, as detected by oligonucleotide array hybridization of cRNA from 3 days MCTS in comparison to 2D cultures, could be confirmed by real-time RT-PCR at 3 and, to a lower extent, at 10 days. Accordingly, significant increases in protein secretion were also observed (Fig. 4, parts C and D). Most conspicuously, massive IL-8 secretion, exceeding 80 ng/ml, was detected in supernatants of NA-8 cells cultured for 10 days in MCTS. Interestingly, immunohistochemical studies (Fig. 5) revealed that IL-8 specific staining was detectable in MCTS, with a preferential localization in inner cell layers.

The marked increase in the expression of CCL20 (MIP-3 $\alpha$ ) gene in cells cultured in MCTS, as compared to monolayers, detected upon oligonucleotide chip hybridization, was also confirmed by real-time RT-PCR.

ELISA assays showed a significant increase in CCL20 protein secretion from MCTS at 3 and 10 days as compared to cells cultured in 2D for the same time, whereas specific gene expression declined in 10 days MCTS (Fig. 4, parts E and F).

On the other hand, regarding adhesion molecules, the genes encoding CD49d and CD54 were shown to be significantly down- and upregulated, respectively, in cells cultured in MCTS as compared to monolayers, by oligonucleotide chip analysis. Cells cultured with different architectures were trypsinized and stained with specific mAb. As reported in Figure 6, flow-cytometry surface expression data were found to be consistent with gene expression results.

Taken together, these data strongly support the integrity of the gene profiling methods adopted in the current study.

#### DISCUSSION

Three-dimensional (3D) culture models have been explored in the past decade, aiming at the development

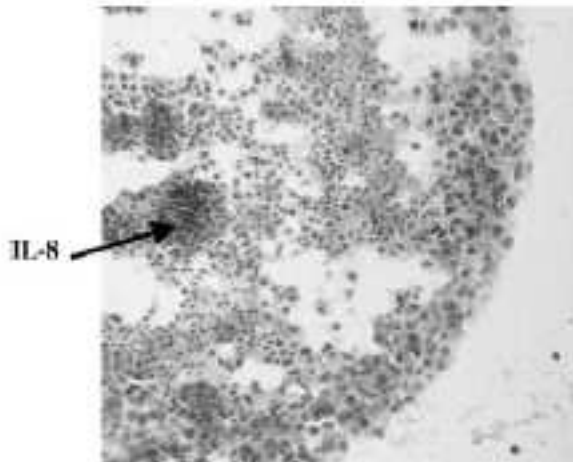


**Fig. 5.** Immunohistochemical detection of IL-8 in MCTS. NA8 cells were cultured for 10 days in MCTS. Spheroids were then fixed, processed as detailed in Materials and Methods, and incubated in the presence of a monoclonal antibody recognizing IL-8. Specific staining is preferentially detectable in the inner layers of MCTS.

of "in vitro" assays of radio or chemoresistance more closely related to "in vivo" conditions than standard monolayer cultures (Sutherland, 1988). In particular, multicellular tumor spheroids (MCTS) have been suggested to closely reflect early events of avascular tumor growth (Hauptmann et al., 1998; Desoize and Jardillier, 2000). Indeed, MCTS resemble "in vivo" tumors in their capacity to develop necrotic areas far from nutrient and oxygen supplies. Furthermore, MCTS are also similar to solid tumors in their growth dynamics, fitting the Gompertz equation, traditionally used to describe the

size limiting growth of tumors (Bajzer et al., 1997; Chignola et al., 2000).

Different methods may be used to obtain MCTS (Kelm et al., 2003). Easy formation in a short time, homogeneous size distribution and reproducibility represent essential requirements. However, extensive manipulation or binding to artificial substrates or beads might result in alterations of the original characteristics of the cells under investigation (Santini et al., 1999). Therefore, in this work, we chose to generate MCTS by merely preventing cell attachment on culture plasticware by polyHEMA (Folkman and Moscona, 1978). In these conditions, spheroid formation was rapidly obtained from NA8 melanoma cells. These MCTS presented features largely overlapping with those of published cell models, regarding slow proliferation (Görlach et al., 1994) and formation of necrotic/hollow cores following long-term culture (Hauptmann et al., 1998). We have comparatively assessed gene expression in identical cells cultured in MCTS or in conventional monolayers. The data presented here provide the first large-scale gene profile analysis of tumor cells cultured in different architectures.

Interestingly, although NA8 cells expressed receptor integrins,  $\alpha\beta1$  and  $\alpha2\beta1$ , culture on collagen-coated plasticware did not appear to result in major alterations of their gene expression profile. In contrast, culture in MCTS determined profound modifications of the gene expression pattern of NA8 cells, as compared with their counterparts cultured in 2D.

Most remarkably, at least two genes whose products, CXCL1 (GRO- $\alpha$ ) and IL-8, have been shown to play a relevant role in melanoma progression and metastatic process (Balentien et al., 1991; Koch et al., 1992; Singh et al., 1994; Luan et al., 1997; Bar-Eli, 1999) were found to be significantly upregulated in cells cultured in MCTS as opposed to monolayers. Massive increases in the

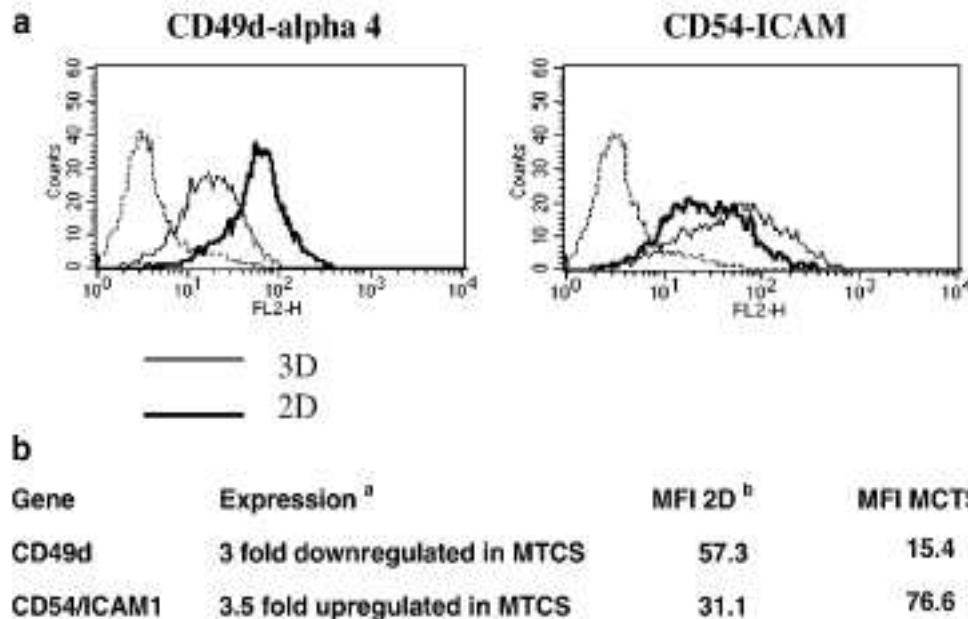


**Fig. 6.** Modulation of adhesion molecule expression in NA8 cells cultured in monolayers or MCTS. NA8 cells were cultured for 3 days in standard monolayer cultures (2D) or in MCTS (3D). They were subsequently trypsinized and stained with CD49d or CD54 specific monoclonal antibodies or isotype matched controls. **a:** Data refer to modulation of gene expression in MCTS as compared to 2D cultures,

as detected upon oligonucleotide array hybridization. **b:** Data are reported as mean fluorescence intensity (MFI) observed in cells from 2D or MCTS cultures upon staining with fluorescein-labeled monoclonal antibodies (mAbs) recognizing the indicated markers. MFI observed upon staining with isotype control mAbs were subtracted.

secretion of the corresponding proteins were also observed in these conditions. Indeed, IL-8 production was also detectable by immunohistochemistry in MCTS, mostly in inner cell layers.

There are no specific studies exploring the association between CCL20 gene expression and tumor progression in melanoma. However, in pancreatic cancers, tumorigenesis has been suggested to be associated with CCL20 gene expression (Kleeff et al., 1999). Furthermore, this chemokine has been suggested to favor the infiltration of melanoma by antigen presenting cells producing the immunosuppressive enzyme indoleamine 2,3-dioxygenase (IDO) (Lee et al., 2003).

In addition, notably, CXCL1, IL-8, and CCL20 are known to promote angiogenesis *in vivo*. Other genes whose products enhance angiogenesis, such as those encoding angiopoietin-like 4 and hypoxia-induced protein 2, were also overexpressed in MCTS. In striking contrast, however, basic FGF gene was downregulated in NAS cells cultured in spheroids.

Genes encoding or regulating the production of ECM components, such as laminin or hyaluronic acid, were also upregulated together with the gene encoding CD54 (ICAM-1) in MCTS, as compared to monolayer cultures.

Taken together our data provide a first database focused on structure-related gene expression in tumor cells. Most importantly, they underline that the architecture of melanoma cells, possibly due to the inherent homotypic cell-cell interaction or specific microenvironmental conditions, with a putative role of hypoxia, may determine specific gene expression patterns of potentially high functional relevance. Strikingly, culture in MCTS appears to result in the upregulation of a constellation of genes whose expression has previously been shown to correlate with high malignancy.

The evaluation of the role of the third dimension, while adding to the complexity of model culture systems, might prove critical for the investigation of the tumor microenvironment including the interaction between tumor cells and autologous healthy cells with diverse physiological functions.

ACKNOWLEDGMENTS

This work was partially supported by grants from the Swiss National Science Foundation and by the Swiss Bridge Foundation to G.C.S.

LITERATURE CITED

Bajzer Z, Vuk-Pavlovic S, Huzak M. 1997. Mathematical modelling of tumor growth kinetics. In Adam JA, Silliman N editors. *A survey of models for tumor-nutrient system dynamics*. Boston: Birkhauser, pp 89-131.  
 Bolewicz K, Marfen H, Smetacek J, Deynck R, Richardson A. 1991. Effects of M219A/GRO alpha on melanocyte transformation. *Oncogene* 6:1115-1124.  
 Ise-Ni M. 1999. Role of intercellular-6 in tumor growth and metastasis of human melanoma. *Patholol* 67:12-18.  
 Cavalitto U, Cristofari G. 2004. Cell adhesion and signaling by ephrins and Ig-CAM5 in cancer. *Nat Rev Cancer* 4:118-132.

Certa U, Sider M, Padovan R, Spagnoli GC. 2001. High density oligonucleotide array analysis of interferon- $\alpha$  sensitivity and transcriptional response in melanoma cells. *Br J Cancer* 85:107-114.  
 Chignola R, Schinetti A, Andighetto G, Grassi R, Foroni R, Sartorio S, Tindato G, Liberati D. 2000. Forecasting the growth of multifocal tumour spheroids: Implications for the dynamic growth of solid tumours. *Cell Prolif* 33:219-229.  
 Douglas V, Lasse V, Valdeke P, Rihon S, Werthamer M, Lovell V, Jansson JL, Barozzi M, Rovin C, Foyand T, Vallandron G, Sidel D. 2002. Gene expression profiles of bladder cancers: Evidence for a striking effect of *in vitro* cell models on gene patterns. *Br J Cancer* 86:1283-1289.  
 Douglas-Marie V, Rihon S, El Behi M, Kichakir H, Doroshin G, Thiery J, Valdeke P, Vergaud I, Meunier J, Ladjani M, Chouah S, Sidel D, Maucq-Chouah F. 2003. A three-dimensional tumor cell defect in activating autologous CTLs associated with inefficient antigen presentation correlated with heat shock protein-70 down-regulation. *Cancer Res* 63:3632-3637.  
 Doreno B, Jordiller JC. 2000. Multicellular resistance: A paradigm for clinical resistance? *Crit Rev Oncol Hematol* 35:193-207.  
 Follman J, Mesner A. 1978. Role of cell shape in growth control. *Nature* 273:345-349.  
 Gerwin N, Gulloux Y, Dier R, Jossseau F. 1996. Suboptimal activation of melanoma infiltrating lymphocytes (TIL) due to low avidity of TCR/MHC-tumor peptide interactions. *J Exp Med* 183:3403-3407.  
 Gotlach A, Heese P, Hentchel H, Froeh PJ, Arler H. 1994. Effects of nBFGF and nBFGF on growth and morphology of two human melanoma cell lines: Cooperation between two- and three-dimensional cultures. *Int J Cancer* 56:249-254.  
 Harari R, Rotshen Y, Raback I, Pnishi R, Shulock P. 2004. Comparison of alkaline blue and MTT assays for high throughput screening. *Toxicol In Vitro* 18:703-710.  
 Hauptmann S, Gebauer-Hartung P, Lederer A, Denkert C, Frentz S, Lutterbach B, Sidel M. 1998. Induction of apoptosis in the center of multicellular tumor spheroids of colorectal carcinoma—Involvement of CD95 pathway and differentiation. *Apoptosis* 3:267-273.  
 Klein JM, Timmons NE, Brown GJ, Puzosnegger M, Nelson LE. 2003. Method for the generation of homogeneous multicellular tumor spheroids applicable to a wide variety of cell types. *Biochem Biophys Res Commun* 311:73-100.  
 Kirsch J, Kitazawa T, Koki D, Ishiyama T, Matsuyama H, Frossa H, Buchler MW, Zlotnik A, Kore M. 1999. Detection and localization of Mip-1alpha/IL-8/CXCR2, a macrophage proinflammatory chemokine, and its CXCR2 receptor in human pancreatic cancer. *Int J Cancer* 81:650-657.  
 Koch AK, Polverini PJ, Kimble SB, Horlow LA, DiStefano LA, Kiser VM, Kiser SG, Krieger RM. 1992. Interleukin-6 as a macrophage-derived mediator of angiogenesis. *Science* 258:1788-1801.  
 Lee JH, Dalton EB, Meesala JJ, Sharma MH, Smith DM, Burgess EE, Manolis F, Antonia SJ, Miller AL, Munn DH. 2003. Pattern of immunoregulatory antigen presenting cells in malignant melanoma. *Lab Invest* 83:1457-1465.  
 Luan J, Shastrik-Simch R, Haghshaghadar H, Owen JH, Strieter R, Burdick M, Nicosk C, Beutcher D, Johnson KN, Richmond A. 1997. Mechanism and biological significance of constitutive expression of M219A/GRO chemokine in malignant melanoma tumor progression. *J Leukoc Biol* 6:2589-2597.  
 Ohsanben AF, Saero S, Ohtsuki S, Heikin M, Karer U, Hermann J, Herreri S, Hoeglinger H, Zankeragel RM. 2001. Role of tumor localization, second signals and cross priming in cytotoxic T-cell induction. *Nature* 411:1058-1064.  
 Oestli D, Marti WR, Zagar F, Noppen C, Kocher T, Padovan R, Adamina M, Schumacher R, Harder F, Heese M, Spagnoli GC. 2002. Rapid induction of specific cytotoxic T lymphocytes against melanoma-associated antigens by a recombinant vaccinia virus vector expressing multiple immunodominant epitopes and costimulatory molecules *in vivo*. *Hum Gene Ther* 13:659-675.  
 Roncivati N, Caselli C, Riboldi PP, Parmiani G. 2001. A listing of human tumor antigens recognized by T cells. *Cancer Immunol Immunother* 50:3-15.  
 Santini MT, Rainaldi G, Indovina PL. 1989. Multicellular tumor spheroids in radiation biology. *Int J Radiat Biol* 75:787-799.  
 Singh RK, Gurnan M, Radinsky R, Stuzans CJ, Friker M. 1994. Expression of inter-leukin-6 correlates with the metastatic potential of human melanoma cells in nude mice. *Cancer Res* 54:3342-3347.  
 Sutherland RM. 1988. Cell and environment interactions in tumor microsystems: The multicell spheroid model. *Science* 240:177-184.  
 Weaver VM, Lalavre S, Liskin JN, Chromik MA, Jones JCR, Giancomi F, Werb Z, Bissel MJ. 2002. E6 integrin-dependent formation of polarized three-dimensional architecture confers resistance to apoptosis in normal and malignant mammary epithelium. *Cancer Cell* 2:205-216.  
 Zagar F, Certa U, Marti W, Adamina M, Sidel M, Grotzer U, Noppen C, Padovan R, Schinetti-Thaler R, Heese M, Spagnoli G. 2003. Phase I/II clinical trial of a non replicative vaccinia virus expressing multiple HLA-A0201 restricted tumor associated epitopes and costimulatory molecules in metastatic melanoma patients. *Hum Gene Ther* 14:1497-1510.

# Culture of Melanoma Cells in 3-Dimensional Architectures Results in Impaired Immunorecognition by Cytotoxic T Lymphocytes Specific for Melan-A/MART-1 Tumor-Associated Antigen

Sourabh Ghosh, MTech, Rachel Rosenthal, MD, Paul Zajac, PhD, Walter P. Weber, MD, Daniel Oertli, MD, Michael Heberer, MD, Ivan Martin, PhD, Giulio C. Spagnoli, MD, and Anca Reschner, PhD

**Objective:** To assess the effects of the culture of melanoma cells in 3-dimensional (3D) architectures on their immunorecognition by cytotoxic T lymphocytes (CTLs) specific for tumor-associated antigens. **Summary Background Data:** Growth in 3D architectures has been shown to promote the resistance of cancers to treatment with drugs, cytokines, or irradiation, thereby potentially playing an important role in tumor expansion. We investigated the effects of 3D culture on the recognition of melanoma cells by antigen-specific HLA class I-restricted CTLs.

**Methods:** Culture of HBL melanoma cells expressing Melan-A/Mart-1 tumor-associated antigen and HLA-A0201 on poly-2-hydroxyethyl methacrylate (polyHEMA)-coated plates resulted in the generation of aggregates of 400- to 500- $\mu$ m diameters containing on average 30,000 cells and characterized by slower proliferation, as compared with monolayer (2-dimensional) cultures. HLA-A0201 restricted Melan-A/Mart-1<sub>27-35</sub>-specific CTL clones were used to evaluate tumor cell immunorecognition measured as specific IFN- $\gamma$  production. Comparative gene and protein expression in 2D and 3D cultures was studied by real-time PCR and flow cytometry, respectively. Overall differences in gene expression profiles between 2D and 3D cultures were evaluated by high-density oligonucleotide array hybridization.

**Results:** HLA-A0201 restricted Melan-A/Mart-1<sub>27-35</sub> specific CTL clones produced high amounts of IFN- $\gamma$  upon short-term (4–24 hours) coinubation with HBL cells cultured in 2D but not in 3D, thus suggesting altered antigen recognition. Indeed, Melan-A/Mart-1 expression, at both gene and protein levels, was significantly decreased in 3D as compared with 2D cultures. Concomitantly, a parallel decrease of HLA class I molecule expression was also observed. Differential gene profiling studies on HBL cells showed an increased expression of genes encoding molecules involved in

intercellular adhesion, such as junctional adhesion molecule 2 and cadherin-like 1 (>20- and 8-fold up-regulated, respectively) in 3D as compared with 2D cultures.

**Conclusions:** Taken together, our data suggest that mere growth of melanoma cells in 3D architectures, in the absence of immunoselective pressure, may result in defective recognition by tumor-associated antigen-specific CTL.

(*Ann Surg* 2005;242: 851–858)

Experimental models indicate that tumor cells in suspension, regardless of their numbers, are frequently unable to produce life-threatening cancer outgrowth, as opposed to solid tumor fragments,<sup>1</sup> while being able to induce specific immune responses. Thus, proliferation in structured architectures appears to represent a prerequisite for cancer development.

Interestingly, tumor infiltrating lymphocytes (TILs) of undefined antigenic specificity, capable of killing autologous bladder tumor cells cultured in monolayers (2D) or in suspension, have been shown to be unable of recognizing targets cultured in 3-dimensional (3D) structures.<sup>2</sup> Similarly, a cytotoxic T lymphocyte (CTL) clone specific for a mutated  $\alpha$ -actinin-4 peptide expressed by autologous lung cancer cells poorly recognized targets growing in multicellular tumor spheroids (MCTS), possibly due to a down-regulation of HSP70 expression.<sup>3</sup>

Although melanoma is the tumor most frequently targeted in active specific immunotherapy clinical trials,<sup>4</sup> there is a paucity of studies on immune responsiveness to these neoplastic cells when cultured in 3D architectures.

Importantly, radial growth of melanoma (eg, few layers of neoplastic cells) has traditionally been associated with good prognosis. Furthermore, previous work on clinical materials suggests that detection of TILs is indeed associated with improved prognosis in melanoma, but mostly only in cases where a “brisk”<sup>5,6</sup> and not a merely superficial infiltration can be observed. Taken together, these data suggest that antigen recognition capacity and the resulting functional

From the Institut für Chirurgische Forschung und Spitalmanagement and Departement Forschung, University of Basel, Basel, Switzerland.

Supported in part by a research grant from the Regional Cancer League of Basel Stadt and Basel Land (to A.R.).

Reprint: Anca Reschner, PhD, ICFS, c/o ZLF, 20 Hebelstrasse, 4031, Basel, Switzerland. E-mail: arechner@thbs.ch

Copyright © 2005 by Lippincott Williams & Wilkins

ISSN: 0003-4932/05/24206-0851

DOI: 10.1097/SLA.0000189571.84213.00

activities of CTL might be significantly altered in the presence of tumor cells growing in multilayered architecture.

In a previous paper, we have shown that culture of melanoma cells in MCTS profoundly affects their gene expression profile, as compared with conventional 2D cultures.<sup>7</sup>

In this work, we report that culture of melanoma cells in 3D architecture may prevent their recognition by CTLs specific for a tumor-associated antigen (TAA), Melan-A/MART-1, frequently used in clinical active antigen specific immunotherapy.<sup>8</sup>

## MATERIALS AND METHODS

### Cell Cultures

HBL cell line derived from a metastatic melanoma and has widely been used by our group in tumor immunology studies in the past.<sup>9,10</sup> It is HLA-A0201+, and it expresses typical melanoma-associated differentiation antigens.<sup>8</sup> HBL cells were routinely passaged in conventional 2D cultures in RPMI 1640 supplemented with kanamycin, glutamine, non-essential amino acids, sodium pyruvate, HEPES buffer, and 10% heat-inactivated FCS (all from Gibco, Paisley, Scotland), thereafter referred to as complete medium. 3D aggregates were prepared in plastic culture plates following coating with a 50  $\mu$ g/mL poly-2-hydroxyethyl methacrylate (polyHEMA, Sigma, St. Louis, MO) solution, preventing cell binding, as described.<sup>11</sup> Cell proliferation was measured by the Alamar Blue assay.<sup>12</sup>

CTL clones were generated from peripheral blood CD8+ cells of patients undergoing active, antigen specific immunotherapy in the context of specific clinical trials, as previously detailed.<sup>9,10</sup> Briefly, cells from bulk cultures showing evidence of antigen specific cytotoxic activity, as detectable by <sup>51</sup>Cr release assays (see below), were cloned in 60-well Terasaki plates (Nunc, Gloustrup, Denmark) at 0.3 cells per well in 20  $\mu$ L volume, in the presence of 10,000 irradiated allogeneic PBMC/well, in RPMI 1640 medium, supplemented with 1 mmol/L sodium pyruvate, 2 mmol/L non-essential amino acids, 2 mmol/L L-glutamine, 10 mmol/L HEPES buffer, and kanamycin (all from GibcoBRL, Paisley, UK) and 5% pooled human serum (RPMI-HS), to which rIL-2 (200 units/mL) and purified phytohemagglutinin (PHA, 0.5  $\mu$ g/mL, Remel, Dartford, UK) were added. After 10 to 14 days, wells where cell growth was microscopically detectable were expanded in RPMI-HS supplemented with 100 units/mL rIL-2 and screened for antigen specific cytotoxic activity (see below). CTL clones were maintained in RPMI-HS supplemented with 100 units/mL rIL-2 and restimulated periodically with PHA in the presence of irradiated allogeneic PBMC. All assays reported here were performed at least 1 week after restimulations.

### Antigen Recognition Assays

<sup>51</sup>Cr release and IFN- $\gamma$  production were used as antigen recognition assays. As target/stimulator cells, we used either HBL or NAB melanoma cells (courtesy of Dr. Jeteroux, Nantes, France).<sup>10</sup> Both are HLA-A0201+ melanoma cell lines, but HBL expresses Melan-A/MART-1 gene<sup>8,10</sup> whereas NAB does not. In specific assays, NAB cells were

pooled for 2 hours at 37°C with synthetic HLA-A0201 restricted Melan-A/MART-1<sub>27-33</sub> peptide (Orpegen, Heidelberg, Germany) at a 2  $\mu$ g/mL concentration. In all cases, 1000 <sup>51</sup>Cr-labeled cells were added to different numbers of effector cells together with 10<sup>5</sup> unlabeled K562 cells (decoy target for NK-like non-specific lytic activity). After a 4-hour incubation, 50  $\mu$ L of supernatants was transferred onto Luma-plates (Packard Bioscience S.A., Zürich, Switzerland) that were dried and counted into a scintillation counter (TopCount, Packard Bioscience). Percentages of specific lysis were then calculated according to the standard formula.

Alternatively, CTLs were cultured together with target cells at different effector:target ratios for 3 to 24 hours. Culture supernatants were then collected and IFN- $\gamma$  production was measured by ELISA (Pharmingen, San Diego, CA).

### Cell Phenotyping

FITC labeled monoclonal antibodies (mAb) specific for HLA-A0201 or a monomorphic determinant of HLA class I heavy chain were obtained from Pharmingen and were used for surface staining of the cells under investigation. A Melan-A/MART-1 specific mAb (Novocentra, Newcastle, UK), was used for intracellular staining of cells permeabilized byaponis treatment. Specific binding was then revealed by staining with an FITC-labeled goat anti-mouse Ig reagent (Southern Biotech, Birmingham, AL). Samples were analyzed on a FACSCalibur flow-cytometer equipped with Cellquest software (Becton Dickinson, San Jose, CA) using propidium iodide (PI) to exclude dead cells.

### Real-Time RT-PCR

HBL cells cultured in 2D or 3D were collected at different time points and washed in PBS. Total RNA was extracted using the RNeasy Mini Kit Protocol (Qiagen, Basel, Switzerland) and treated with Deoxyribonuclease I (DNase I) (Invitrogen, Carlsbad, CA). Real-time quantitative RT-PCR assays were conducted on a ABI prism 7700 sequence detection system, using TaqMan One Step PCR Master Mix Reagent Kit (Master Mix without UNG, Multiscribe and RNase Inhibitor Mix, Applied Biosystems, Branchburg, NJ). Oligonucleotide primers and the Taq Man probe for Melan-A/MART-1 gene were designed by using the Primer Express software (Perkin Elmer Applied Biosystems Inc, Foster City, CA) and sequences from the NCBI gene bank. To quantify gene expression in each sample, we used the comparative threshold cycle (Ct) method (Primer Express software, Applied Biosystem, Foster City, CA). Normalization was performed by using gene expression in 2D cultured cells as reference sample.

### Gene Expression Profiling

HBL cells were harvested by trypsinization after 3 days culture in 2D or 3D. Five micrograms of total RNA extracted using Qiagen RNeasy Mini Kit (Qiagen) from each sample was reverse-transcribed and labeled by using commercial kits (Superscript H, Invitrogen; Bio-11-CTP and Bio-16-UTP, Enzo Biochem, NY). Biotinylated cRNA, fragmented by treatment at 94°C for 35 minutes in 40 mmol/L Tris-acetate, pH 8.1, 100 mmol/L potassium acetate, and 20

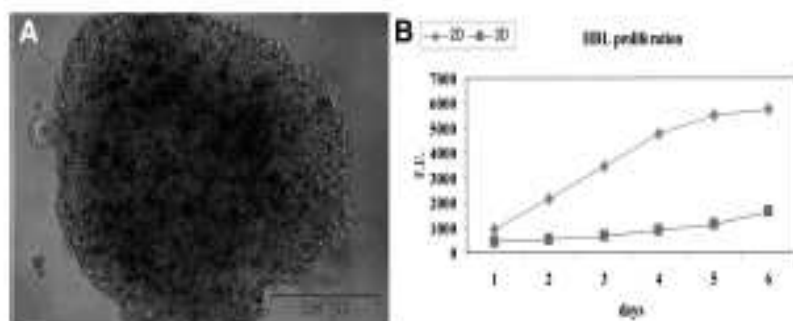


**FIGURE 1.** Generation and characterization of 3D cultures of HBL cells. HBL cells were cultured for 72 hours on polyHEMA-coated plates, thus giving rise to the formation of multicellular aggregates (A) of an average diameter of 400 to 500  $\mu\text{m}$ . Alamar blue cell proliferation assays (B) show distinct kinetics for cells cultured in 2D or in 3D.

mmol/L magnesium acetate, was hybridized to human oligonucleotide array HG-U-133 plus 2.0 allowing the analysis of over 38,000 genes (Affymetrix, Santa Clara, CA). Two separate hybridizations were performed for each sample under investigation. Raw data were collected using a confocal laser scanner and pixel levels were analyzed using commercial software (Gene Spring Version 7, Silicon Genetics, Redwood City, CA). Two separate data readings were performed for each hybridization. One-way ANOVA tests were performed for gene lists filtered on fold change in the log-of-ratio mode of experimental interpretation (Gene Spring 7 software, Silicon Genetics). Duplicates of each experimental group were compared. The parametric Welch *t* test was used within the study with a cutoff *P* value of 0.05.

## RESULTS

### Characterization and Growth Features of HBL Cells Cultured in 2D or in 3D

Upon culture on polyHEMA-coated plastic surfaces, HBL cells formed 3D aggregates of 400- to 500- $\mu\text{m}$  diameter containing on average 30,000 cells (Fig. 1A). Proliferation kinetics of HBL cells cultured in 2D or 3D sharply differed. 2D cultures showed rapid cell proliferation, reaching a plateau within 6 days. In contrast, only minor increases in cell numbers were detectable in 3D cultures during the same time (Fig. 1B).<sup>7</sup> Comparable results were obtained by Alamar blue staining or direct count of trypsinized cells (data not shown).

### Characterization of CTL Clones Specific for Melanoma Cells

CTL clones recognizing Melan-A/MART-1<sub>27-35</sub> epitope in the context of HLA-A0201 restriction were generated following culture of CD8<sup>+</sup> T cells from patients with metastatic melanoma undergoing active antigen specific immunotherapy.<sup>9,10</sup> They were able to kill, in standard <sup>51</sup>Cr release assays, HBL melanoma cells expressing both antigen and HLA-A0201 restriction determinant, but not NA-8 melanoma cells expressing HLA-A0201 and not Melan A/MART-1. However, exogenous pulsing of the latter cells with specific peptide at concentrations  $\geq 10$  ng/mL sufficed to sensitize them to killing by specific CTL (a representative example is shown in Figure 2).

### CTL Clones Fail to Recognize Endogenously Processed TAA From HBL Melanoma Cells in 3D Cultures

Data obtained in bladder and lung cancers<sup>2,3</sup> suggest that growth in 3D architectures may prevent the recognition of TAA by specific effector T cells. We aimed at verifying whether similar events occurred in melanoma, a type of cancer targeted by a number of immunotherapy trials. Cells cultured in 3D are unfit to serve as targets in <sup>51</sup>Cr release assays because the washing steps required after labeling disrupt cell aggregates and MCTS. Alternative antigen recognition assays rely on IFN- $\gamma$  production by selected CTL clones following interaction with appropriate target cells. HBL HLA-A0201<sup>+</sup> melanoma cells expressing Melan-A/MART-1 differentiation antigen cultured in 2D or 3D were used to stimulate IFN- $\gamma$  production by the previously characterized CTL clones.

As expected, HBL cells cultured in 2D induced specific IFN- $\gamma$  production in CTL clones detectable within a 4-hour

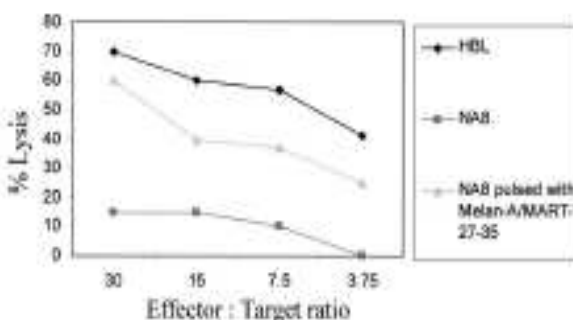
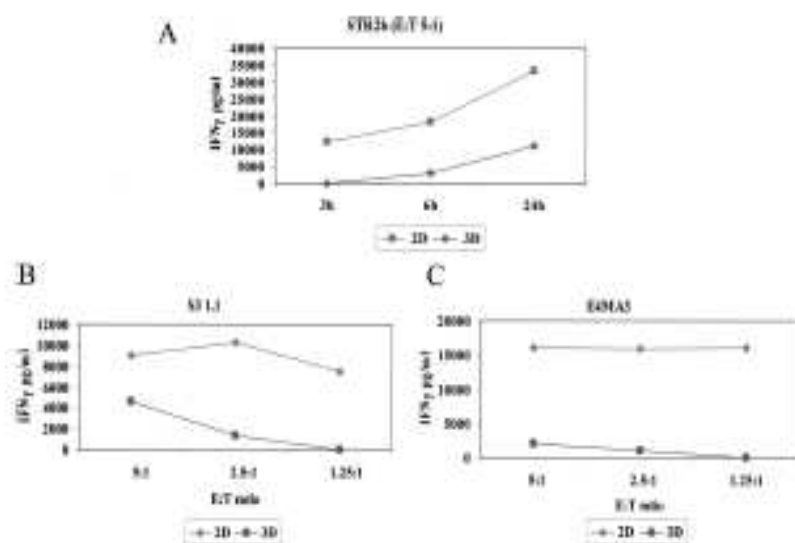


**FIGURE 2.** Cytotoxic activity and antigen specificity of CTL. CTL clones were generated by limiting dilution from cell lines derived from peripheral blood CD8<sup>+</sup> cells of metastatic melanoma patients undergoing active specific immunotherapy. Specific antigen recognition was assessed by standard <sup>51</sup>Cr release assays, using, as target cells, HLA-A0201-positive melanoma cells not expressing Melan-A/MART-1 (NA8) in the presence (triangles) or absence (squares) of pulsing with Melan-A/MART-1<sub>27-35</sub> peptide (2  $\mu\text{g}/\text{mL}$ ). HBL melanoma cells (diamonds), expressing both HLA-A0201 and Melan-A/MART-1, were killed by Melan-A/MART-1<sub>27-35</sub> specific CTL. Data are reported as average of specific lysis from triplicate wells. Standard deviations, always lower than 10% of the values reported, were omitted.



**FIGURE 3.** IFN- $\gamma$  production by Melan-A/MART-1<sub>27-35</sub> specific CTL clones upon stimulation with HBL cells cultured in 2D or in 3D. A CTL clone specific for HLA-A0201 restricted Melan-A/MART-1<sub>27-35</sub> epitope was cocultured for the indicated times at 5:1 E/T ratio in the presence of similar numbers of HBL melanoma cells, expressing both HLA-A0201 and Melan-A/MART-1, cultured in 2D (squares) or in 3D (diamonds) (A). Additional CTL clones were incubated for 24 hours in the presence of target HBL cells cultured in 2D or in 3D at the indicated E/T ratios (B, C). In all cases, supernatants were harvested and IFN- $\gamma$  production was measured by ELISA. Data are reported as average of triplicate measurements (as pg/mL). Standard deviations, never exceeding 10% of the reported values, were omitted.



incubation with a peak usually observed at 24 hours (Fig. 3A), whereas NA8 cells expressing HLA-A0201 but not Melan-A/MART-1 were unable of stimulating IFN- $\gamma$  production (data not shown). Instead, significantly lower, if any, amounts of cytokine were produced if CTLs were challenged with the same numbers of HBL target cells cultured for 2 to 3 days in 3D architectures (Fig. 3A). Similar results were obtained in 4 independent experiments performed by using 5 different CTL clones obtained from 3 patients, at different effector:target ratios. Representative data are reported in Figure 3B, C.

#### Melan-A/MART-1 and HLA-A0201 Expression in HBL Cells Cultured in 2D and 3D

These data suggested that tumor cells fail to be recognized by specific CTL when cultured in 3D structures. To obtain an insight into underlying molecular mechanisms, we comparatively explored Melan-A/MART-1 expression in HBL cells cultured in either 3D or conventional 2D conditions. Quantitative PCR analysis indicated that in cells cultured in 3D a 6-fold lower expression of Melan-A/MART-1 as compared with 2D conditions was indeed detectable (Fig. 4A). Importantly, cells from aggregates disrupted by trypsin treatment and subsequently cultured in monolayers had not recovered baseline (2D) Melan-A/MART-1 expression after 2 days (Fig. 4B). Full recovery required more than 4 days of culture following aggregate disruption (data not shown).

To obtain an insight into the impact of reduced gene expression on the production of the corresponding protein, HBL cells cultured according to either protocol were permeabilized and stained with a Melan-A/Mart-1 specific mAb. Consistent with gene expression data, intracellular staining revealed a 4-fold decrease of antigen expression in HBL cells cultured for 3 days in 3D, as compared with their counterparts in 2D (Fig. 5). A similar reduction was also evident in standard immunocytochemistry preparations (data not shown).

HLA-0201 expression in cells cultured in 3D was also investigated. HBL cells from 2- to 3-day-old aggregates

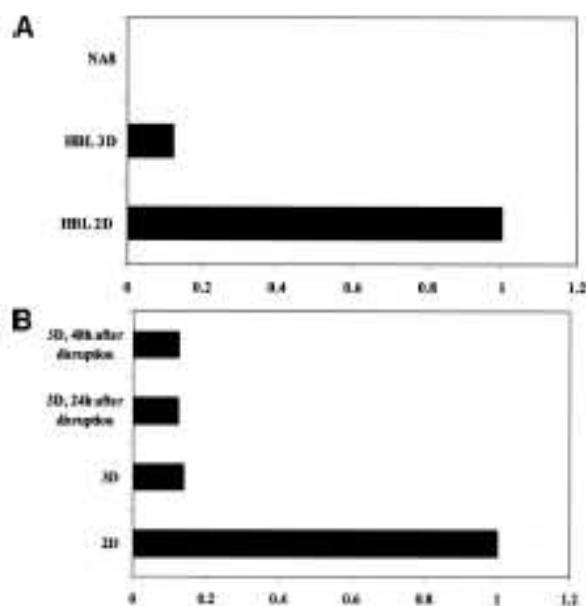


**FIGURE 4.** Melan-A/MART-1 gene expression in HBL cells cultured in 2D or in 3D. HBL cells were cultured in monolayers or in 3D for 3 days (A). Alternatively (B), aggregates were disrupted by trypsinization and cells were recultured in monolayers for the indicated times. In all cases, total cellular RNA was extracted and reverse transcribed. Melan-A/MART-1 gene expression was comparatively evaluated in cells cultured in 2D or in 3D by quantitative real-time RT-PCR. Data are expressed as ratio of Melan-A/MART-1 gene expression using as reference value expression in 2D HBL cultures. Negative control NA8 cells were also studied.

displayed a significant (>3-fold) reduction of HLA-0201 expression, as detectable by specific mAb staining, in comparison with their counterparts cultured in 2D (Fig. 6). Im-





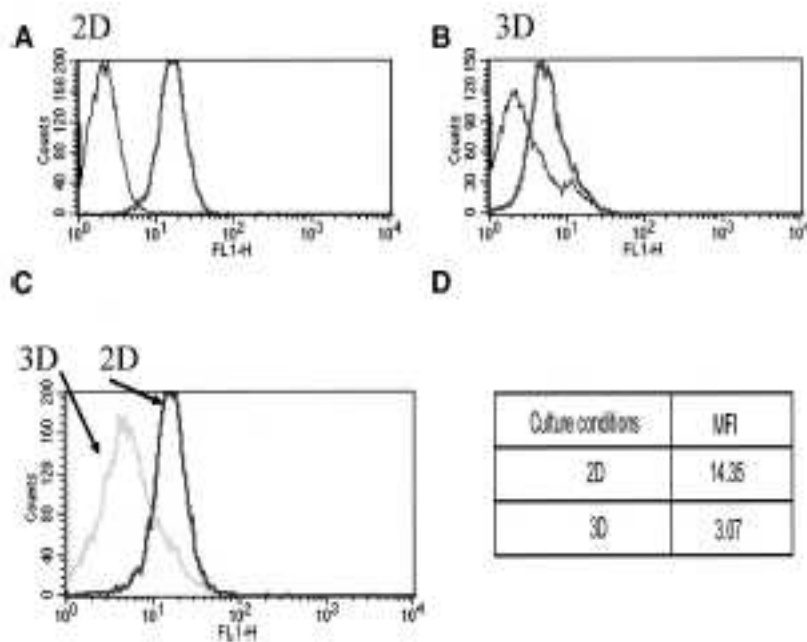


FIGURE 5. Melan-A/MART-1 protein expression in HBL cells cultured in 2D or in 3D. HBL cells were cultured in 2D (A) or in 3D (B) for 3 days. They were then trypsinized, permeabilized, and stained with monoclonal antibodies specific for Melan-A/MART-1 or control reagents. Melan-A/MART-1 histograms from 2D or 3D cultures were overlaid in panel C. D, Corresponding mean fluorescence intensities (MFI) of specific stainings. Data refer to one representative experiment of 3 performed.

portantly, this effect was not allele specific but concerned all HLA class I gene products, as indicated by staining with a mAb specific for a monomorphic determinant on HLA class I heavy chains (Fig. 6).

#### Gene Profiling Studies

In an attempt to thoroughly assess specific gene expression profiles<sup>7,14,15</sup> associated with either 2D or 3D culture conditions, we hybridized cRNA from either cultures on

high-density oligonucleotide chip arrays allowing the analysis of more than 38,000 expressed genes.

Our study revealed that culture in 3D architecture had a relatively modest overall impact on gene expression in HBL cells (Fig. 7A). Beside a number of expressed sequences encoding undescribed gene products, 47 genes only were significantly modulated, with down-regulation of 18 and up-regulation of 29 (Fig. 7B,C) in 3D as compared with 2D cultures. The latter group conspicuously included genes en-

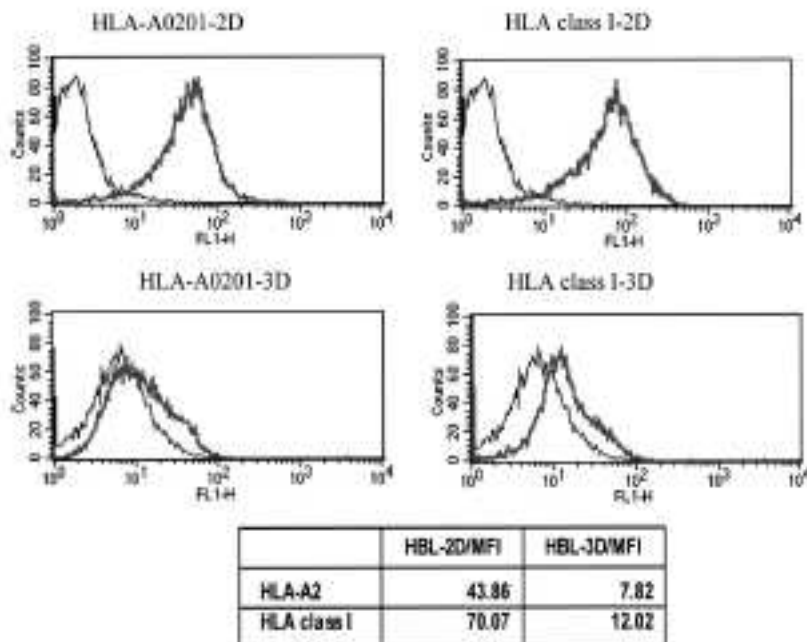


FIGURE 6. HLA class I expression in HBL melanoma cells cultured in 2D or in 3D. HBL cells were cultured in 2D or in 3D for 3 days. Cells were then trypsinized and stained with monoclonal antibodies specific for HLA-A0201 or a monomorphic epitope of HLA class I heavy chains, or control reagents. Mean fluorescence intensities (MFI) of the specific stainings are also reported. Data refer to one representative experiment of 3 performed.

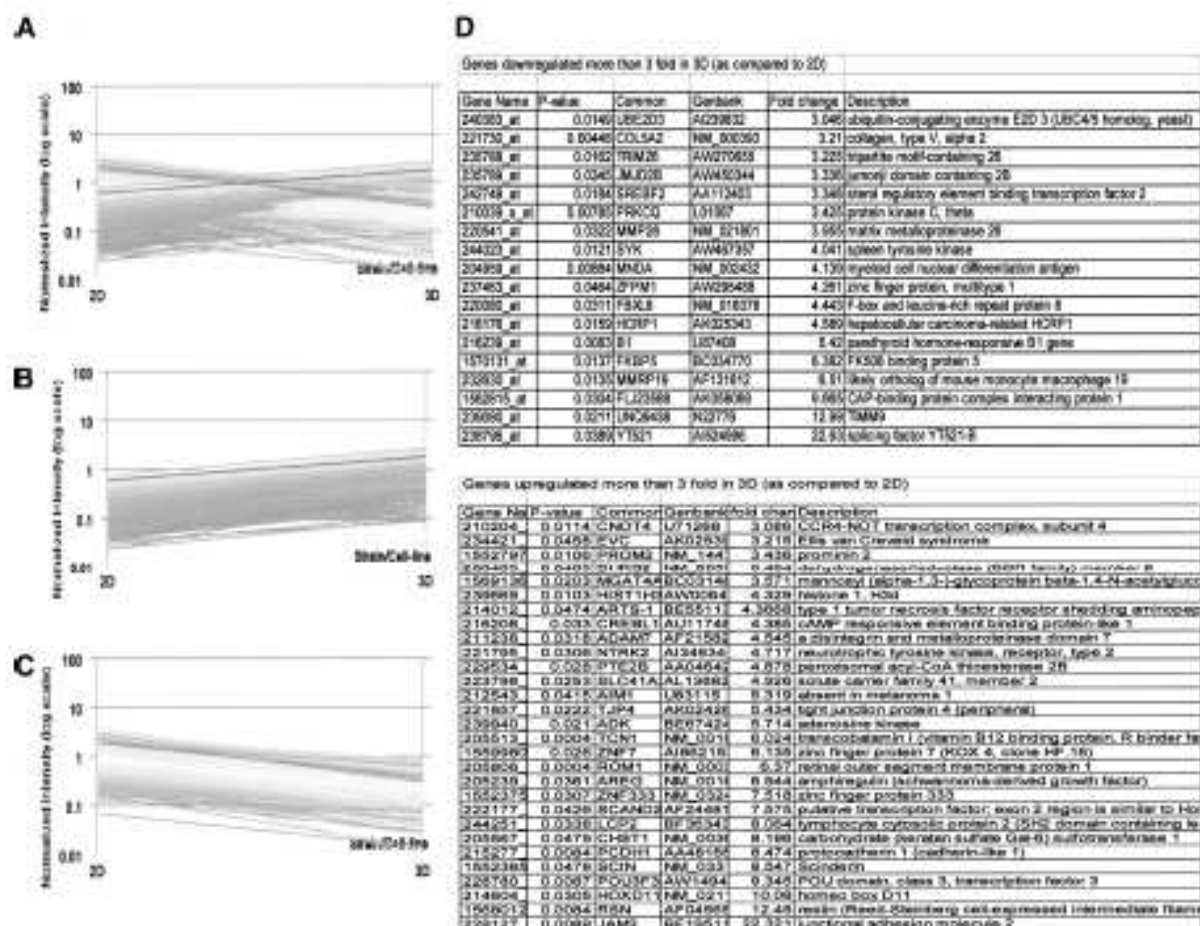


FIGURE 7. Modulation of gene expression in HBL cells cultured in 3D as compared with 2D. HBL cells were cultured in 2D or in 3D for 3 days. Total cellular RNA was then extracted, reverse transcribed, and labeled as described in Materials and Methods prior to hybridization to oligonucleotide chips. Only characterized genes displaying a  $\geq 3$ -fold up- or down-regulation (fold change) in either culture conditions are reported. Statistical significance ( $P < 0.05$ ) refers to duplicate readings of data obtained from 2 distinct hybridization experiments. A, Overall modulation of gene expression. B and C refer to genes up-regulated or down-regulated in 3D as compared with 2D cultures, respectively. Genes whose expression is modulated upon 3D as compared with 2D culture are listed in D.

coding molecules involved in intercellular adhesion such as junctional adhesion molecule 2 (JAM2,  $>22$ -fold up-regulated)<sup>16</sup> and cadherin-like 1 ( $>8$ -fold up-regulated)<sup>17</sup> (Fig. 7D).

## DISCUSSION

A number of studies indicate that CTLs, naturally generated or expanded during the clinical course of melanoma or induced by specific vaccination for immunotherapy purposes, are usually able to recognize target cells, at least in standard "in vitro" assays.<sup>9,10</sup> On the other hand, discrepancies between detectable tumor specific immune responses and lack of clinical effectiveness represent frequent observations in active specific immunotherapy of melanoma.<sup>13</sup>

In previous work, we have explored the effects of culture of melanoma cells in 3D architectures on gene ex-

pression profiles. We showed that culture of NAS cells in MCTS resulted in an increased expression of genes encoding proangiogenic and melanoma growth factors as compared with standard 2D cultures.<sup>7</sup>

Capitalizing on this background, here we have addressed the effects of culture of melanoma cells in 3D on their immunorecognition by CTLs specific for Melan-A/MART-1 melanoma associated antigen. As a model cell line, we chose HBL cells, characterized by a high expression of melanoma differentiation antigens, frequently used as targets in active specific immunotherapy trials.<sup>3</sup>

Culture of HBL cells on polyHEMA-treated plastic surfaces results in the generation of cellular aggregates displaying typical 3D features such as slow cell proliferation.

Most strikingly, however, HBL cells cultured in 3D fail to be recognized by Melan-A/MART-1<sub>27-35</sub> specific, HLA-A0201 restricted, CTL clones. Impaired recognition does not appear to be related to structural constraints deriving from 3D architectures but rather to a decreased expression of both Melan-A/MART-1 and HLA determinants, in 3D cultures as compared with cells cultured in 2D.

Defective immunorecognition of tumor cells cultured in 3D has been reported previously in renal and lung cancer.<sup>2,3</sup> In both cases, however, neither HLA nor specific antigen expression was found to be affected by cell culture model.

Recently, it has been reported that culture of melanoma cells at high concentrations in standard 2D conditions might negatively affect Melan-A/MART-1 expression,<sup>19,20</sup> due to the effects of at least one soluble factor, later identified as oncostatin M.<sup>21</sup> In this case, too, however, HLA expression was not affected.

Importantly, a number of studies have suggested that antigen specific immunotherapy could result in the immunoselection of tumor cell variants failing to express not only specific antigens but, most importantly, restriction determinants.<sup>22</sup> Paradoxically, these studies may support the notion of a high effectiveness of the current immunization protocols.<sup>23</sup> Our data provide the first indication that mere culture in 3D, in the absence of specific immunoselective pressure, may result in a down-regulation not only of HLA expression but also of a melanoma-associated antigen, thereby profoundly affecting tumor cell immunorecognition by specific CTL.

We have attempted to thoroughly explore differential gene profiles in HBL cells cultured in either 2D or 3D by oligonucleotide chip hybridization. Although this technology provides important insights, it proved to be insufficiently sensitive in our conditions, since, for instance, Melan-A/MART-1 expression was not detectable in 2D cultured HBL. This relative insensitivity, as compared with quantitative real-time PCR, is likely related to the fact that standard oligonucleotide chip hybridization is usually performed after a single cDNA amplification step only, as suggested by others<sup>24</sup> also focusing on the expression of TAAs.

Our data might have important clinical implications in that they suggest that growth in 3D architectures significantly affects phenotypic and functional characteristics of tumor cells, thereby modulating their capacity of being targeted by antigen specific immune responses. As a potential consequence, active specific immunotherapy might likely be more effective in the presence of minimal tumor burden rather than in the presence of established solid tumor masses.<sup>25</sup>

## REFERENCES

- Orhsebein AF, Siem S, Odematt B, et al. Roles of tumor localization, second signals and cross priming in cytotoxic T-cell induction. *Nature*. 2001;411:1058-1064.
- Dangles V, Valdire P, Wertheimer M, et al. Impact of human bladder cancer cell architecture on autologous T-lymphocyte activation. *Int J Cancer*. 2002;98:51-56.
- Dangles-Marie V, Rithon S, El Behi M, et al. A three-dimensional tumor cell defect in activating autologous CTLs is associated with inefficient antigen presentation correlated with heat shock protein-70 down-regulation. *Cancer Res*. 2003;63:3682-3687.
- Famiani G, Pilla L, Castelli C, et al. Vaccination of patients with solid tumors. *Ann Oncol*. 2003;14:817-824.
- Milam MC, Clemente CG, Cascinelli N. Tumor infiltrating lymphocytes in lymph node melanoma metastases: a histopathologic prognostic indicator and an expression of local immune response. *Lab Invest*. 1996;74:43-47.
- Aiuchini A, Molla A, Mortarini R, et al. An expanded peripheral T cell population to a cytotoxic T lymphocyte (CTL)-defined, melanocyte-specific antigen in metastatic melanoma patients impacts on generation of peptide-specific CTLs but does not overcome tumor escape from immune surveillance in metastatic lesions. *J Exp Med*. 1999;190:651-667.
- Gilsh S, Spagnoli GC, Martin I, et al. Three dimensional culture of melanoma cells profoundly affects gene expression profile: a high density oligonucleotide array study. *J Cell Physiol*. 2005;204:522-531.
- Renkivi N, Castelli C, Robbins PF, et al. A listing of human tumor antigens recognized by T cells. *Cancer Immunol Immunother*. 2001;50:3-15.
- Oertli D, Marti WR, Zajac P, et al. Rapid induction of specific cytotoxic T lymphocytes against melanoma-associated antigens by a recombinant vaccinia virus vector expressing multiple immunodominant epitopes and costimulatory molecules in vivo. *Hum Gene Ther*. 2002;13:569-575.
- Zajac P, Oertli D, Marti W, et al. Phase I/II clinical trial of a non-replicative vaccinia virus expressing multiple HLA-A0201 restricted tumor associated epitopes and costimulatory molecules in metastatic melanoma patients. *Hum Gene Ther*. 2003;14:1497-1510.
- Folkman J, Moscona A. Role of cell shape in growth control. *Nature*. 1978;273:345-349.
- Hamid R, Roshkiny Y, Rabadi L, et al. Comparison of Alamar blue and MTT assays for high throughput screening. *Toxicol In Vitro*. 2004;18:703-710.
- Gervois N, Guilleux Y, Diez E, et al. Suboptimal activation of melanoma infiltrating lymphocytes due to low avidity of TCR/MHC-tumor peptide interactions. *J Exp Med*. 1996;183:2403-2407.
- Dangles V, Lazar V, Valdire P, et al. Gene expression profiles of bladder cancer: evidence for a striking effect of *in vitro* cell models on gene patterns. *Br J Cancer*. 2002;86:1283-1289.
- Ceria U, Seiler M, Padovan E, et al. High density oligonucleotide array analysis of interferon- $\alpha$ 2a sensitivity and transcriptional response in melanoma cells. *Br J Cancer*. 2001;85:107-114.
- Bazzoni G. The JAM family of junctional adhesion molecules. *Curr Opin Cell Biol*. 2003;15:525-530.
- Seifor EA, Meltzer PS, Schattman GC, et al. Expression of molecular phenotypes by aggressive melanoma tumor cells: role in vasculogenic mimicry. *Crit Rev Oncol Hematol*. 2002;44:17-27.
- Aiuchini A, Vegetti C, Mortarini R. The paradox of T cell-mediated antitumor immunity in spite of poor clinical outcome in human melanoma. *Cancer Immunol Immunother*. 2004;53:855-864.
- Ramirez-Montagut T, Andrews DM, Ihara A, et al. Melanoma antigen recognition by tumour-infiltrating T lymphocytes (TIL): effect of differential expression of Melan-A/MART-1. *Clin Exp Immunol*. 2000;119:11-18.
- Kamick JT, Ramirez-Montagut T, Boyle LA, et al. A novel autocrine pathway of tumor escape from immune recognition: melanoma cell lines produce a soluble protein that diminishes expression of the gene encoding the melanocyte lineage Melan-A/MART-1 antigen through down-modulation of its promoter. *J Immunol*. 2001;167:1204-1211.
- Darda PJ, Duna IS, Boyle Rose L, et al. Induction of 'antigen silencing' in melanomas by Oncostatin M: down-modulation of melanocyte antigen expression. *Mol Cancer Res*. 2003;1:411-419.
- Seliger B, Cabrera T, Garrido F, et al. HLA class I antigen abnormalities and immune escape by malignant cells. *Semin Cancer Biol*. 2002;12:3-13.
- Nagorn D, Scheibenbogen C, Marincola FM, et al. Natural T cell immunity against cancer. *Clin Cancer Res*. 2003;9:4296-4303.
- Gotter J, Brors B, Hergenhan M, et al. Medullary epithelial cells of the human thymus express a highly diverse selection of tissue-specific genes colocalized in chromosomal clusters. *J Exp Med*. 2004;199:155-166.
- Mocella S, Mandruzzato S, Bronte V, et al. Cancer vaccines: pessimism in check. *Nat Med*. 2004;10:1278-1279.

---

## Discussions

DR. EGGERMONT: Thank you very much for presenting this rather exceptional work. I want to make the following comments.

This is a very interesting study because we all know that *in vivo* the problem in melanoma and in a number of other tumors known to be antigenic is that tumors are characterized by a high heterogeneity in tumor-associated antigen expression, and there is a lot of down-regulation. There are 2 sides of the equation, both the HLA-restricting molecules and the antigen are down-regulated, and there is hampered antigen recognition. This may be one of the reasons why correlations between *in vitro* data and *in vivo* results are highly difficult to interpret, at least because in the *in vitro* monolayer system there is an abundance of antigen presentation.

The remarkable thing is that here you have a close to *in vivo* culture system that induces down-regulation of HLA molecules and tumor-associated antigens at the gene and at the protein level. Therefore, the reduced killing by cytotoxic T-lymphocytes is not the result of steric hindrance or access problems.

At the same time, you show that the one molecule thus far identified that can mediate these types of down regulations, oncostatin M, is not playing a role in your system. You

must have a program running to identify which novel messenger mediates this down-regulation in your system.

My first question is: is there any emerging new direction in that particular part of your research?

Secondly, what I really do not understand is that after 48 hours, the cells that you take out of your spheroid culture system and you bring back to monolayers, still are suppressed in terms of antigen expression. I would predict normally that within a rather short amount of time in the absence of such a suppressive environment, they would restore their expression. My question is: how much time does it take for the cells to recover their original phenotype? Is it 1 week, 2 weeks or, which I would not be able to believe, is this forever? Are there any intracellular messengers involved in this? I would like to hear your comment on that please.

DR. GHOSH: Regarding the first question, we are trying to make gene profiling analysis using oligonucleotide chips to identify gene products playing key roles in these processes.

For example, junctional adhesion molecule-2 might be involved in the formation of 3-dimensional structure. We are planning to use neutralizing antibodies to clarify its role.

Regarding your second question, in our hands, it indeed takes over 96 hours to restore in cells from disrupted spheroids a Melan-A/MART-1 expression comparable to that detectable in cells cultured in monolayers.

# **Multiple mechanisms underlie defective recognition of melanoma cells cultured in three-dimensional architectures by antigen specific cytotoxic T lymphocytes**

Chantal FEDER-MENGUS\*<sup>1</sup>, Sourabh GHOSH\*<sup>1</sup>, Walter P.WEBER<sup>1</sup>, Paul ZAJAC<sup>1</sup>, Luigi TERRACCIANO<sup>2</sup>, Daniel OERTLI<sup>1</sup>, Michael HEBERER<sup>1</sup>, Ivan MARTIN<sup>1</sup>, Giulio C. SPAGNOLI<sup>1</sup> and Anca RESCHNER<sup>1</sup>

\* The first two authors contributed equally to this work.

1. ICFS, Departments of Surgery and Research, Basel University Hospital, Basel, Switzerland
2. Department of Pathology, Basel University Hospital, Basel, Switzerland

Correspondence: Dr. Chantal FEDER-MENGUS, Basel University Hospital Research Center, ICFS, Laboratory 404, Hebelstrasse 20, CH-4031 Basel, Switzerland

E-mail: [cfeder@uhbs.ch](mailto:cfeder@uhbs.ch)

Phone: (0041) 61 265 2376

Fax: (0041) 61 265 3990

This work was partially supported by grants from the Cancer League of Basel Stadt and Basel Land to AR and by the Swiss National Fond for Scientific Research to GCS.

Running title: Immune-recognition of cancer cell spheroids

Key Words: melanoma, immunorecognition, CTL, Spheroids, anti-tumor response

## Abstract

Cancer cells growth in three-dimensional (3D) architectures promotes resistance to drugs, cytokines, or irradiation. We investigated effects of 3D culture as compared to monolayers (2D) on melanoma cells recognition by tumor-associated antigen (TAA)-specific HLA-A\*0201-restricted cytotoxic T-Lymphocytes (CTL).

Culture of HBL, D10 (both HLA-A\*0201+, TAA+) and NA8 (HLA-A\*0201+, TAA-) melanoma cell lines on polyHEMA-coated plates, resulted in generation of 3D multicellular tumor spheroids (MCTS) characterized by slow proliferation. IFN- $\gamma$  production by HLA-A\*0201-restricted Melan-A/MART-1<sub>27-35</sub> or gp100<sub>280-288</sub>-specific CTL clones served as marker for immunorecognition.

Co-culture with melanoma cells MCTS, resulted in significantly defective TAA recognition by CTL as compared to 2D, as witnessed by decreased IFN- $\gamma$  production and decreased Fas Ligand, perforin and granzyme B gene expression. We identified a multiplicity of mechanisms potentially involved. First, MCTS *per se* limit CTL capacity of recognizing HLA class I restricted antigens by reducing exposed cell surfaces. Second, expression of melanoma differentiation antigens is down-regulated in tumor cell spheroids as compared to 2D unrelated to hypoxia or increased Oncostatin M gene expression but rather to decreased MITF gene expression. Third, expression of HLA class I molecules is frequently down-regulated in melanoma MCTS, as compared to 2D, possibly due to decreased IRF-1 gene expression. Fourth, lactate production by melanoma cells is increased in MCTS, as compared to 2D and lactate significantly inhibits TAA triggered IFN- $\gamma$  production by CTL.

Taken together, our data suggest that melanoma cells growing in 3D, even in the absence of immune selection, feature characteristics capable of dramatically inhibiting TAA recognition by specific CTL.

## Introduction

The identification of a large number of tumor associated antigens (TAA) (1) has raised the hope of taking advantage of the enormous increase of knowledge stemming from basic immunology research to ameliorate the prognosis of neoplastic diseases by active antigen specific immunotherapy, i.e. by vaccination. Trials based on diverse immunization procedures have been performed in different types of cancer and promising data have been reported (2-6).

Indeed, immune responses specific for TAA can be generated relatively easily “*in vitro*” and “*in vivo*”, as detectable by phenotypic and functional assays. However, only in a minority of patients showing evidence of successful immunization, clinical responses are also detectable.

Interestingly, experimental murine models indicate that tumor cells in suspension, regardless of their numbers, are frequently unable to produce life threatening cancer outgrowth, as opposed to solid tumor fragments (7), while inducing specific immune responses. Thus, proliferation in structured architectures appears to represent a pre-requisite for cancer development.

In the human experimental setting, cytotoxicity assays or the functional monitoring of clinical immunotherapy trials are usually performed by utilizing, as targets, cell lines, frequently of lympho/myeloid origin, expressing appropriate HLA alleles upon pulsing with specific peptides. TAA recognition may eventually be confirmed by using, as additional targets, tumor cell lines expressing specific HLA determinants and transcribing relevant TAA encoding genes. Current protocols typically imply the admixture of effector and target cells pelleted together in culture wells. The lack of correlation between data obtained “*in vitro*” with these technologies and clinical data suggests that this model might not adequately account for critical aspects of the interaction between immunocompetent cells and cancers.



Three-dimensional (3D) culture models have been developed in the past decade, aiming at exploring radio or chemoresistance of tumor cells in “*in vitro*” assays more closely related to “*in vivo*” conditions than standard monolayers (8). In particular, multicellular tumor spheroids (MCTS) have been suggested to accurately represent early events of avascular tumor growth (9).

MCTS remind *in vivo* cancers in their capacity to develop necrotic areas far from nutrient and oxygen supplies. Furthermore, cells cultured in MCTS are also similar to solid tumors in their proliferation dynamics (10), since, at difference with monolayer cultures, they fit the Gompertz equation, classically used to quantitatively evaluate neoplastic growth (11).

Three-dimensional growth of tumor cell *in vitro* has been shown to affect antigen recognition by specific CTL. For instance, tumor infiltrating lymphocytes capable of killing autologous bladder tumor cells in 2D, failed to recognize targets when cultured in 3D (12). Similarly, a CTL clone specific for a mutated  $\alpha$ -actinin-4 peptide expressed by autologous lung cancer cells poorly recognized targets growing in MCTS, possibly due to a down-regulation of HSP70 expression (13).

Regarding melanoma, a cancer frequently targeted in clinical immunotherapy trials, we recently showed that the architecture of tumor cell growth determines specific gene expression profiles, of potentially high functional significance. Furthermore, we showed that the recognition of a melanoma TAA by a specific CTL clone was impaired when target cells were cultured in MCTS (14, 15).

These data suggest that antigen specific functional activities of CTL might be significantly altered in the presence of tumor cells growing in multilayered architectures. Underlying mechanisms, however, are still poorly investigated.

In this work we explored the molecular bases of impaired recognition by CTL specific for TAA of melanoma cells cultured in tri-dimensional architectures. We report that a multiplicity of mechanisms ranging from structural hindrances to down regulation of antigen and HLA expression to lactic acid overproduction concurrently limit the susceptibility of melanoma cells cultured in MCTS to the attack by TAA specific CTL.

## Materials and Methods

### *Cell culture*

NA8 (courtesy of Dr. Jotereau, Nantes, France), HBL and D10 cell lines (courtesy of Dr. A. Eberle, Basel, Switzerland) derive from metastatic melanoma and have widely been used in tumor immunology studies in the recent past (16-18). They are all HLA-A\*0201+. However, while HBL and D10 express typical melanoma differentiation TAA (1, 19), NA8 does not (1).

Cell lines were routinely passaged in conventional 2D cultures in RPMI 1640 supplemented with 10mM HEPES buffer, 1mM sodium pyruvate, 2mM non-essential amino-acids, 2mM glutamine, 100  $\mu$ g/ml Kanamycin (Invitrogen, Carlsbad, California) and 10% heat-inactivated FCS, hereafter referred to as complete medium.

Multicellular tumor spheroids (MCTS) were prepared in U-bottom 96-wells plates previously coated with 50  $\mu$ g/ml poly-2-hydroxyethylmethacrylate (polyHEMA, Sigma, St. Louis, MO) solution, preventing cell binding, as described (20). Cells proliferation was measured by the alamarBlue™ Assay (Serotec, Oxford, UK) (21).

CTL clones were generated from peripheral blood CD8+ T cells of patients undergoing active antigen specific immunotherapy in the context of specific clinical trials, as previously described (17, 18). Briefly, cells from bulk cultures showing evidence of antigen specific cytotoxic activity, as detectable by <sup>51</sup>Cr release assays, were cloned in 60 well Terasaki plates (Nunc, Glostrup, Denmark) at 0.3 cells per well in 20  $\mu$ l volumes in the presence of 10,000 irradiated allogenic PBMC/well, in RPMI 1640 supplemented with 10mM

HEPES buffer, 1mM sodium pyruvate, 2mM non-essential amino-acids, 2mM glutamine, 100 µg/ml Kanamycin (Invitrogen, Carlsbad, California) and 5% pooled human serum (RPMI-HS), to which rIL-2 (200 units/ml) and purified phytohemagglutinin (PHA, 0.5 µg/ml, Remel, Dartford, UK) were added. After 14 days, wells where cell growth was microscopically detectable were expanded in RPMI-HS supplemented with 100 units/ml rIL-2 and screened for antigen specific cytotoxic activity by <sup>51</sup>Cr release assay. CTL clones were maintained in RPMI-HS supplemented with 100 units/ml rIL-2 and restimulated periodically with PHA in the presence of irradiated allogenic PBMC. All assays reported here were performed at least one week after re-stimulation.

### ***Chemotaxis assays***

Migration assays were performed by using Costar® 24-transwell chemotaxis chambers (Corning Costar Corporation, Cambridge, MA) with 5-µm and 3-µm pore size polycarbonate filters, for immature DC (iDC) and CD8+ T cells, respectively. Briefly, 600 µl of supernatant of NA8 cells cultured in 2D or 3D, or as a negative control, complete medium, were placed in the lower wells. CD8+ peripheral blood T cells were purified by using magnetic beads (Miltenyi Biotech, Bergisch Gladbach, Germany), whereas iDC were prepared by culturing peripheral blood monocytes in the presence of IL-4 and GM-CSF, as previously detailed (22). Upper wells of chemotactic chambers were loaded with 100 µl cell suspension of iDC or CD8+ T cells at a concentration of 1 x 10<sup>6</sup>/ml. Each condition was set up in duplicate. Plates were kept at 37°C for 20 hours. Cells suspensions from the upper wells and cells migrated to the lower wells through the filters were then collected, stained with specific mAbs and counted by flow cytometry for a fixed defined time. Chemotactic index was determined by dividing the number of cells migrated in the experimental condition by the number of cells migrated in the negative control cultures (medium only).

### ***Confocal microscopy***

Cells were stained with PKH26 red fluorescent cell linker (Sigma-Aldrich, St. Louis, MO) following suppliers instructions, and cultured on polyHEMA coated plates for 3 days to form 30,000 cells MCTS. Total CD8+ T cells from healthy donors and CTL clones specific for HLA-A\*0201 restricted Melan-A/MART-1<sub>27-35</sub> epitope were stained with CFSE (molecular Probes, Eugene, OR). Cells (E:T ratio = 2.5:1) were added to each MCTS and co-cultured for 1 day. Confocal images for the evaluation of total CD8+ T cells or CTL infiltration in NA8 and HBL MCTS respectively, were obtained using a laser-scanning confocal microscope Zeiss LSM 510 (Carl Zeiss Microimaging Inc., Thornwood, NY).

### ***IFN-γ detection by ELISA***

IFN-γ production was used as antigen recognition assays. As target/stimulator cells, we used melanoma cells cultured in 2D or in MCTS. CTL specific for Melan-A/MART-1 or gp100, used as effectors, were co-cultured with target cells at 2.5:1 ratio for 24 hours. When indicated, assays were performed by using, as target, HBL cells previously cultured in monolayers in the presence of 0-20mM lactate (Sigma-Aldrich, St. Louis, MO) for three days. In all cases, supernatants were collected and IFN-γ secretion was measured by using human IFN-γ BD OptEIA™ ELISA Set (BD Biosciences, Franklin Lakes, NJ). All samples were measured in duplicates.

### ***Quantification of gene expression by quantitative Real-Time PCR***

Cells were collected at the indicated time points and washed in PBS. Surgical samples from metastatic melanoma patients were disrupted and homogenized by sonication. Total RNA were extracted using the RNeasy® Mini Kit protocol (Qiagen, Basel, Switzerland), treated by Deoxyribonuclease I (DNase I) (Invitrogen, Carlsbad, California), and reverse transcribed by using the Moloney Murine Leukemia Virus Reverse Transcriptase (M-MLV RT, Invitrogen, Carlsbad, California). Quantitative real-time PCR were performed in the ABI



prism™ 7700 sequence detection system, using the TaqMan® Universal PCR Master Mix, No AmpErase® UNG (both from Applied Biosystems, Foster City, CA).

Specific gene expression was quantitated by using the  $2^{-\Delta\Delta C_T}$  method(23-26). Normalization of gene expression was performed using GAPDH as reference gene and data were expressed as ratio to reference samples.

### **Primers and probes**

Oncostatin M (OSM), IRF-1 and MITF primers and probes are from pre-developed assays (Assays-on-Demand, Gene Expression Products (Applied Biosystems, Foster City, CA)). Oligonucleotide primers and probes for c-myc, Melan-A/MART-1, gp100 and tyrosinase were generated using appropriate software (Primer Express™, Applied Biosystems, Foster City, CA) from sequences obtained from the NCBI gene bank.

Furthermore, a number of sequences for primers and probes were derived from existing literature, as indicated below.

#### **GAPDH (27)**

Fwd ATGGGGAAGGTGAAGGTCG

Rev TAAAAGCAGCCCTGGTGACC

Probe FAM-CGCCCAATACGACCAAATCCGTTGAC-TAMRA

#### **FasL (28)**

Fwd CCATTTAACAGGCAAGTCCAAC

Rev TCACTCCAGAAAGCAGGACAATT

Probe FAM-TCACTCCAGAAAGCAGGACAATT-TAMRA

#### **Perforin (29)**

Fwd TTCTACAGTTTCCATGTGGTACACACT

Rev GTGGGTGCCGTAGTTGGAGATA

Probe FAM-ACCCAGCCCGCCTACCTCAGGC-TAMRA

#### **Granzyme B (30)**

Fwd TCCTAAGAACTTCTCCAACGACACT

Rev GCACAGCTCTGGTCCGCT

Probe FAM-TGCTACTGCAGCTGGAGAGAAAGGCC-TAMRA

#### **Melan-A/MART-1**

Fwd TCTATGGTTACCCCAAGAAGGG

Rev GATCACTGTCAGGATGCCGA

Probe FAM-ACGGCTGAAGAGGCCGCTGGGAT-TAMRA

#### **gp100**

Fwd TCCCCCTGGATTGTCTTCTG

Rev CTCAAATGCATCCCCCTCA

Probe FAM-CCCTGGACATTGTCCAGGGTATTGAAAGTGA-TAMRA

#### **Tyrosinase**

Fwd TTTGCCTGAGTTTGACCCAAT

Rev AGAGGCATCCGCTATCCCA

Probe FAM-TAGAAATACACTGGAAGGATTTGCTAGTCCACTTACTA-TAMRA

#### **c-myc**

Fwd GCCACGTCTCCACACATCAG

Rev TCTTGGCAGCAGGATAGTCCTT

Probe FAM-ACGCAGCGCCTCCCTCCACTC-TAMRA

### **Flow cytometry analysis**

HLA class I expression was quantified using FITC-conjugated mAb specific for HLA-A\*0201 or a similar reagent specific for a non polymorphic determinant of HLA

class I heavy chain (PharMingen, San Diego, CA). HBL, D10 or NA8 cells cultured in 2D were collected using Trypsin-EDTA (Invitrogen, Carlsbad, CA) after 3 days culture. Accordingly, MCTS obtained after 3 days culture, were disrupted by 5 min trypsinisation at 37°C. Cells were then incubated with specific or control mAbs, for 45 min at 4°C in the dark, washed twice in cold PBS, fixed 1 min in Paraformaldehyde 1%, re-suspended in 200  $\mu$ l PBS, and analyzed on a FACSCalibur® cytometer (Becton Dickinson, Franklin Lakes, NJ).

### ***Lactate measurement***

Quantification of lactate production by melanoma cells was performed after 3 day cultures in 2D or in 3D (30,000 cell density), using as immobilized enzyme biosensor, YSI 2300 STAT Glucose & Lactate analyzer (YSI, Yellow Springs, Ohio), following suppliers' protocols.

## **Results**

### ***Morphological characterization and growth pattern of melanoma spheroids***

Melanoma cells were routinely maintained in monolayer (2D) cultures in complete medium. Upon culture on 96-wells plates coated with polyHEMA preventing cell attachment (20), they formed three-dimensional aggregates. Multicellular tumor spheroids (MCTS) of a 0.3 to 0.8 mm diameter contained from 5,000 to 30,000 cells, depending on their size (Figure 1A).

Consistent with previous results by our group (14, 15), proliferation kinetics of cells cultured in 2D or 3D were dramatically different. Data reported in figure 1B regarding D10 melanoma cell line as representative example, indicate that proliferation in 2D cultures reached a plateau within 5 days, whereas, in contrast, no major increases in cell numbers were detectable in MCTS within 20 days of culture.

### ***Immature Dendritic Cells and CD8+ T cells migrate in response to MCTS supernatants***

Previous studies by us and others indicate that tumor cells from melanoma and colorectal cancer cell lines produce proinflammatory chemokines (22, 31, 32). For instance, HBL cells express RANTES gene (22). Importantly, we previously showed that culture in 3D of NA8 cells significantly enhances the expression of CCL20, CXCL1 and IL-8 genes (14). Receptors for these chemokines are largely expressed on iDC and CD8+ T cells (33-37).

Thus, chemoattraction by MCTS might reflect the potential chemoattractive capacity of neoplastic tissues. Therefore, we assessed differential chemotactic responsiveness of iDC and CD8+ T cells to chemokines present in culture supernatants, using, as melanoma model, NA8 cells cultured in 2D or in MCTS (Figure 2A).

Addition of supernatants of cells growing in monolayers to the lower part of a transwell system induced migration of both iDC and total CD8+ T cells, suggesting that NA8 cells constitutively produce chemotactic factors *in vitro*. Most importantly, supernatants derived from the same number of NA8 cells growing in MCTS induced a significant increase in the migration of iDC and CD8+ T cells as compared to supernatants of their 2D counterparts.

### ***Morphology of the interaction between TAA specific CTL and melanoma cells cultured in spheroids***

The above data suggested that melanoma cells, particularly if cultured in 3D are characterized by a peculiar capacity of attracting APC and CD8<sup>+</sup> T cells. This ability curiously contrasts with the relatively low effectiveness of tumor specific immune responses “*in vivo*”. Puzzled by this discrepancy, we sought to investigate the morphology of the interaction between melanoma cells, iDC and, most importantly, CD8<sup>+</sup> T cells, largely responsible for tumor specific cytotoxic activities.

NA8 (HLA-A\*0201+, Melan-A/MART-1-) or HBL (HLA-A\*0201+, Melan-A/MART-1+) cells cultured as MCTS, iDC, total CD8<sup>+</sup> T cells and HLA-A\*0201-restricted Melan-A/MART-1<sub>27-35</sub> specific CTL clones were labeled with different fluorochromes. NA8 cells were co-cultured with either iDC or total CD8<sup>+</sup> T cells. Furthermore, HBL cells were co-incubated for 24 hours together with TAA specific CTL clones. Confocal microscopy was then used to verify the consequences of this interaction at morphological level. Typically, iDC, CD8<sup>+</sup> T cells in general and TAA specific CTL in particular were unable to penetrate in deep the 3D architecture of MCTS but rather tended to remain on their surfaces (Figure 2B). These pictures closely reminded the “non brisk” infiltration of melanoma by T cells, as frequently observed in clinical tumor specimens (38, 39) (Figure 2C).

*CTL clones display a differential capacity of recognizing endogenously processed tumor associated antigens in melanoma cells cultured in monolayers or in MCTS of different sizes.*

Lack of MCTS infiltration by TAA specific CTL hinted at a possible defective killing of tumor cells cultured in spheroids. Indeed, growth in 3D architectures was previously suggested to prevent the recognition of TAA by specific effector T cells (12, 13, 15). We intended to verify if similar events occur when melanoma cells are cultured in MCTS and the eventually underlying molecular mechanisms.

Percentages of TAA specific T cells “*ex vivo*” are extremely low, and usually do not exceed 0.5% of total CD8<sup>+</sup> T cells, at best (40). Thus, to perform our studies in controlled conditions, we again resorted to the use of antigen specific cloned T cells as effectors. Importantly, CTL clones are far more efficient in this respect than T cells freshly obtained from peripheral blood (41). Since tumor cells cultured in 3D are unfit to serve as targets for <sup>51</sup>Cr release assays, because washing steps required after labeling disrupt cells aggregates, we turned to IFN- $\gamma$  production by antigen specific T cells following interaction with targets expressing appropriate TAA and restriction determinants, as a classical alternative antigen recognition assay (42, 43).

HBL and D10 HLA-A\*0201+ melanoma cells expressing Melan-A/MART-1 and gp100 differentiation TAA cultured in 2D or 3D were used to stimulate IFN- $\gamma$  production by previously characterized specific CTL clones (18). NA8 cells (HLA-A\*0201+, TAA-) were used as negative controls.

As expected, HBL and D10 cells cultured in 2D induced high IFN- $\gamma$  production in gp100<sub>280-288</sub> or Melan-A/MART-1<sub>27-35</sub> specific CTL clones. In sharp contrast, considerably lower amounts of cytokine were produced if CTL were stimulated with spheroids of 30,000 HBL or D10 target cells following 3 day culture in 3D. Similar results were obtained in independent experiments performed by using different gp100<sub>280-288</sub> or Melan-A/MART-1<sub>27-35</sub> specific, HLA-A\*0201 restricted CTL clones, at different E:T ratios. Representative data are reported in figure 3A.

Elicitation of CTL functions relies on the expression of an array of components of their lytic machinery. For instance, CTL may kill through Fas pathway (44, 45), and granzymes entering target cells (46-49) may rapidly induce their DNA fragmentation based apoptosis (50, 51). Furthermore, perforin in the CTL granules plays a pivotal role in granule-mediated killing (52-55). Thus, we also assessed CTL functions by evaluating FasL, granzyme B and perforin gene expression in CTL co-cultured with melanoma target cells growing in 2D or in MCTS (Figure 3B). As expected, interaction with targets Melan-A/MART-1<sub>27-35</sub>+HLA-A\*0201+ cultured in 2D resulted in the expression of FasL, granzyme

B and perforin genes in antigen specific CTL. However, the expression of these genes was significantly lower when effector cells were stimulated by MCTS.

These data indicated that antigen recognition by CTL can be impaired if target cells are cultured in 3D, rather than in monolayers. A possible explanation for this observation could be offered by merely structural considerations: culture in spheroids may provide an overall smaller cell surface accessible to CTL attack, as compared to monolayers, resulting in decreased activation of effector cells. To address this issue, HBL cells were cultured in MCTS and subsequently disaggregated. The resulting cell suspensions were used to stimulate antigen specific CTL. Melanoma cells from freshly disrupted spheroids indeed induced IFN- $\gamma$  secretion in Melan-A/MART-1<sub>27-35</sub> specific CTL clones, to intermediate levels between those induced by 2D or 3D cultured HBL (Figure 3C). These results indicate that the observed impairment of antigen recognition by CTL is at least in part due the smaller cell surface accessible to effectors, but cannot be exclusively ascribed to structural hindrances.

### ***Melan-A/MART-1, gp100 and tyrosinase expression in HBL and D10 cells cultured in 2D and 3D***

Previous works suggest that high cell density in monolayer cultures could affect TAA expression (56). In an attempt to clarify molecular mechanisms underlying our observations, we addressed antigen expression in target cells. Thus, we comparatively explored the expression not only of Melan-A/MART-1 and gp100 but also of tyrosinase genes, encoding differentiation antigens widely used in active specific immunotherapy (18) in HBL and D10 melanoma cells cultured in either MCTS or conventional 2D conditions. NA8 cells (1) were used as negative control (Figure 4A).

Quantitative real-time PCR analysis revealed that HBL and D10 cells cultured in MCTS display a significantly lower ( $\leq 40\%$ ) expression of Melan-A/MART-1, gp100 and tyrosinase differentiation TAA as compared to similar numbers of cells cultured in 2D conditions. Importantly, this down-modulation was visible in 3 days old spheroids, well before the appearance of inner necrotic cores on days 10-12 (14, 57, 58). Most interestingly, it was clearly related to cell density. Indeed the highest down-regulation of the expression of genes encoding differentiation TAA was detectable in spheroids containing 30,000 melanoma cells, whereas milder effects were recorded in 3D structures including 5,000 tumor cells.

Interestingly, HBL and D10 cells from aggregates disrupted by vigorous pipetting, and subsequently cultured in monolayers could not recover baseline (2D) TAA gene expression before 3-5 days (data not shown).

Since hypoxia may represent an early event in inner MCTS layers, leading, as reviewed previously (59, 60), to typical gene expression profiles, we investigated whether it could play a role in the down-regulation of the expression of melanoma differentiation antigens observed in spheroids. Monolayer cultures of D10 and HBL cell lines were incubated in low (5%) pO<sub>2</sub> for three days and the expression of the genes under investigation was subsequently assessed. In no case we observed a significant down-modulation of melanoma TAA in cells cultured in hypoxic conditions (data not shown).

Taken together these data indicated that the architecture of cultures may regulate the expression of melanoma differentiation antigens. Three-dimensional cultures are frequently assumed to be closer to “*in vivo*” conditions than standard monolayers. To validate this model we addressed the quantification of Melan-A/MART-1 and gp100 gene expression in surgical specimens from metastatic melanoma patients.

Data from 11 clinical samples are displayed in figure 4B. In at least 5/11 cases, levels of Melan-A/MART-1 gene expression were similar to those observed in 3D cultures at 30,000 cells density, namely from 2 to over 5 fold lower than levels detectable in melanoma cells cultured in monolayers. Regarding gp100, with one exception (Me 60), specific gene

expression was either undetectable (6/11) or, anyway, significantly lower than that detectable in 2D cultured HBL cells.

It has been recently reported that Oncostatin M, produced by melanoma cells actively down regulates Melan-A/MART-1 mRNA transcription inducing antigen silencing in tumor cells (61). On the other hand, Melan-A/MART-1 and gp100 gene expression have been shown to be transcriptionally controlled by microphthalmia-associated transcription factor (MITF) (62), the master regulator of melanocytic differentiation.

We comparatively explored the expression of the genes encoding these soluble factors potentially involved in the modulation of antigen expression, in HBL, D10 and NA8 melanoma cells cultured in either MCTS or conventional 2D conditions (Figure 4C). While Oncostatin M gene expression was not detectable (data not shown), MITF gene expression was down-regulated in the three cell lines under investigation, when cultured in MCTS as compared to 2D. These effects appeared to be cell density dependent.

### ***HLA modulation in different size spheroids***

The expression of HLA class I molecules and, in particular, of HLA-A\*0201, the allele restricting the immunodominant CTL response to the gp100 and Melan-A/MART-1 epitopes under investigation, was also evaluated in melanoma cells cultured in MCTS as compared to 2D. Figure 5A reports data from one representative experiment out of 3 performed. HBL MCTS (30,000 cells per spheroids) displayed a significant (>5 fold) decrease in HLA-A\*0201 expression at the protein level, as compared to 2D cultures. Importantly, this modulation did not appear to be allele specific, since similar results were obtained by using a mAb specific for a monomorphic epitope on HLA class I heavy chain. This reduction also appeared to be cell density dependent. Similar results were observed with D10 MCTS with a significant ( $\geq 2$  fold) decrease in HLA molecules expression as compared to 2D cultures.

On the other hand, NA8 melanoma cells (HLA-A\*0201+, TAA-) displayed a divergent HLA modulation pattern as compared to HBL and D10. Indeed, when cultured in MCTS, NA8 showed significant ( $\geq 2$  fold) increases in HLA-A\*0201 and overall HLA class I expression, especially for a cell density of 5,000 cells per spheroids.

HLA class I gene expression is regulated by transcription factors of the Interferon Regulating Factor (IRF) family (63), while c-myc has been shown to down-regulate HLA class I expression in human melanoma (64).

Consistent with the HLA expression data observed at the protein level, IRF-1 gene expression was also cell density dependently down-regulated in HBL and D10 cultured in MCTS as compared to 2D. Accordingly, IRF-1 gene expression was up-regulated in NA8 MCTS in comparison with cells cultured in monolayers.

On the other hand, surprisingly, c-myc expression was significantly down-regulated in D10 and HBL spheroids, as compared to cells cultured in monolayer, but it was unaffected in NA8 spheroids (Figure 5B).

### **Role of lactic acid in the defective recognition by TAA specific CTL of tumor cells cultured in spheroids.**

Recently, it has been shown that production of lactate is enhanced in tumor cells cultured in spheroids, as compared to monolayers (65). Most importantly, lactate, at the concentrations produced by tumor cells in these culture conditions inhibits the proliferation of antigen specific CTL lines co-cultured with autologous dendritic cells in the presence of antigenic peptides (65). Prompted by this report we evaluated the production of lactic acid by the melanoma cell lines under investigation and its eventual role in the defective antigen recognition by specific CTL.

Culture of HBL cells in MCTS induced a >60% increase in their lactate production (Figure 6, panel A). More modest effects were detected in D10 cells ( $\leq 15\%$  increases). We then performed our antigen recognition assays by using as targets HBL melanoma cells cultured in 2D in the absence or in the presence of graded concentrations of exogenous lactate.

Indeed, pre-exposure of target cells cultured in 2D to exogenous lactate dose-dependently inhibited antigen stimulated IFN- $\gamma$  production by a Melan-a/MART-1<sub>27-35</sub> HLA-A\*0201 restricted CTL clone. However, cytokine production was still significantly higher than that induced by stimulating the same clone with HBL cell cultured in spheroids (Figure 6, panel B). Importantly, addition of exogenous lactate to melanoma cells cultured in monolayers did not induce the down regulation of the expression of melanoma differentiation antigens (data not shown).

## Discussion

The past decade has witnessed an unprecedented wave of cancer immunotherapy trials, prompted by the identification of large numbers of TAA and by major advances in basic immunology. Most of these efforts have targeted metastatic melanoma. A large majority of published reports suggest that a variety of different vaccination procedures are capable of inducing TAA specific CTL in high percentages of immunized patients. However, clinical responses are only detectable in a minority of them. These data underline that even in the presence of specific immune responses, tumors may be relatively insensitive to their effects.

Molecular mechanisms underlying the discrepancy between immunological and clinical responsiveness to active antigen specific immunotherapy have been investigated by several groups.

Tumor escape from CTL recognition has been attributed to down-regulation of TAA or HLA class I molecules expression (66) possibly resulting from the selection of resistant variants in neoplastic cell populations exposed to immunological pressure. However, this mechanism, whose *in vivo* relevance is debated, might indirectly support the concept of a clinical efficacy of CTL induction, whose evidence is mostly missing (67).

More recently, the discrepancy between induction of TAA specific immune responses and clinical responsiveness has also been attributed to CTL defects. TAA specific T cells sampled *ex vivo* from tumor metastases have been shown to be quiescent (68-70), and characterized by an impaired capacity to produce IFN- $\gamma$  upon antigenic challenge. Still unclear, however, is the role of the tumor cells, if any, in inducing such state.

These reports urge the development of novel *in vitro* models utilizing human cells and permitting controlled investigations of the interaction between tumor cells and the immune system.

Data from different groups, including ours, indicate that culture of tumor cells in tri-dimensional structures modulates their gene expression profiles and decreases their susceptibility to the immune-mediated CTL attack although still unclear are the underlying molecular mechanisms (14, 15).

Consistent with our previous report, showing a significant up-regulation of genes encoding CCL20, IL-8, CXCL1 chemokines in melanoma cells cultured in MCTS, as compared to 2D (14), here we demonstrated the high chemoattractive capacity of MCTS for iDC and CD8<sup>+</sup> T cells. Interestingly, however, iDC, CD8<sup>+</sup> T cells in general and TAA specific CTL in particular, were unable to penetrate in deep the 3D architecture of MCTS, closely reminding the “non brisk” infiltration of melanoma by T cells observed in clinical cancer tissues (38, 39). This lack of infiltration by TAA specific CTL suggested a possible defective killing of tumor cells cultured in spheroids. Indeed, our study shows that lower

amounts of IFN- $\gamma$  are produced by CTL stimulated by melanoma cells cultured in MCTS as compared to those cultured with tumor cell monolayers. The concept of impaired elicitation of CTL functions was reinforced by decreases in FasL, granzyme B and perforin gene expression in antigen specific CTL when cultured with MCTS as compared with their counterparts cultured in 2D.

Our data indicate that a multiplicity of mechanisms concur in decreasing the susceptibility of melanoma cells cultured in MCTS to the effects of antigen specific CTL, as compared to cell monolayers.

First, tri-dimensional structures *per se*, limit the capacity of effector cells of recognizing HLA class I restricted antigens possibly by merely reducing the cell surface exposed to CTL. This mechanism, however, is only partially responsible for the impaired antigen recognition since CTL cultured with melanoma cells from disrupted MCTS secreted IFN- $\gamma$  at a level intermediate in between 2D and MCTS.

Second, the expression of melanoma differentiation antigens is down-regulated in tumor cells cultured in 3D as compared to monolayers. In our hands, this is neither related to hypoxia nor to increased Oncostatin M gene expression but rather to a decreased MITF gene expression and to the high cell concentrations elicited by culture in MCTS.

Third, the surface expression of HLA class I molecules can be down-regulated in melanoma cells cultured in 3D, as compared to their counterparts in 2D.

These features have been detected relatively frequently in clinical melanoma specimen. Their occurrence has been attributed to the outgrowth of cancer cells characterized by low expression of TAA and/or restricting HLA class I determinants following exposure of tumors to immunoselective pressures (66). However, our data suggest that a low expression of HLA class I molecules and at least of melanoma differentiation antigens in tumors, could be inherent in their tri-dimensional growth, even in the absence of an exogenous immune pressure.

Fourth and finally, lactic acid production by melanoma cells is increased if they are cultured in MCTS, as compared to monolayer cultures, and lactate significantly inhibits TAA triggered IFN- $\gamma$  production by specific CTL. Consistent with previous reports (71), these effects appear to be mediated by functional inhibition of effector cells, since no down-regulation of TAA expression is detectable in melanoma cells cultured in these conditions. Interestingly, lactic acid produced within melanoma and prostate cancer MCTS has also been shown to impair the phenotypic and functional maturation of infiltrating dendritic cells thereby inhibiting their antigen presenting capacity (71).

Most importantly, none of these mechanisms alone is able to entirely account for the inhibition of antigen recognition by specific CTL, detectable upon culture in the presence of melanoma cells cultured in 3D, as opposed to 2D. Their combination, however, elicits powerful inhibitory effects.

We are fully aware of the fact that culture of melanoma cell lines in 3D might only partially reflect the complexity of solid tumors developing *in vivo*. However, the clear discrepancy between data obtained by applying techniques of current use for the *in vitro* detection of antitumor responses and clinical evidence urges the development of alternative experimental models. MCTS may then qualify as technology of choice for the screening not only of novel drugs, but also of immune-mediated therapeutic procedures.

Further research is warranted to explore in this controlled *in vitro* model the consequences on effector cells of their interaction with tumor cells growing in tri-dimensional architectures, as opposed to monolayers or in suspension.

Importantly, providing a molecular background to widespread clinical experience, our data suggest that the effectiveness of anti-tumor immune response may largely depend not only on affinity and functional capacities of effector cells, but also on the structural characteristics of the growth of cancer cells, rather than on their mere numbers and strongly support the use of active antigen specific immunotherapies in minimal residual disease states.

## Reference List

1. Renkvist N, Castelli C, Robbins PF, Parmiani G. A listing of human tumor antigens recognized by T cells. *Cancer Immunol Immunother* 2001;50:3-15.
2. Bedrosian I, Mick R, Xu S, et al. Intranodal administration of peptide-pulsed mature dendritic cell vaccines results in superior CD8+ T-cell function in melanoma patients. *J Clin Oncol* 2003;21:3826-3835.
3. Nestle FO, Alijagic S, Gilliet M, et al. Vaccination of melanoma patients with peptide- or tumor lysate-pulsed dendritic cells. *Nat Med* 1998;4:328-332.
4. Rosenberg SA, Yang JC, Schwartzentruber DJ, et al. Immunologic and therapeutic evaluation of a synthetic peptide vaccine for the treatment of patients with metastatic melanoma. *Nat Med* 1998;4:321-327.
5. Slingluff CL, Jr., Petroni GR, Yamshchikov GV, et al. Clinical and immunologic results of a randomized phase II trial of vaccination using four melanoma peptides either administered in granulocyte-macrophage colony-stimulating factor in adjuvant or pulsed on dendritic cells. *J Clin Oncol* 2003;21:4016-4026.
6. Thurner B, Haendle I, Roder C, et al. Vaccination with mage-3A1 peptide-pulsed mature, monocyte-derived dendritic cells expands specific cytotoxic T cells and induces regression of some metastases in advanced stage IV melanoma. *J Exp Med* 1999;190:1669-1678.
7. Ochsenbein AF, Sierro S, Odermatt B, et al. Roles of tumour localization, second signals and cross priming in cytotoxic T-cell induction. *Nature* 2001;411:1058-1064.
8. Sutherland RM. Cell and environment interactions in tumor microregions: the multicell spheroid model. *Science* 1988;240:177-184.
9. Desoize B, Jardillier J. Multicellular resistance: a paradigm for clinical resistance? *Crit Rev Oncol Hematol* 2000;36:193-207.
10. Gorlach A, Herter P, Hentschel H, Frosch PJ, Acker H. Effects of rIFN beta and rIFN gamma on growth and morphology of two human melanoma cell lines: comparison between two- and three-dimensional culture. *Int J Cancer* 1994;56:249-254.
11. Chignola R, Schenetti A, Andrighetto G, et al. Forecasting the growth of multicell tumour spheroids: implications for the dynamic growth of solid tumours. *Cell Prolif* 2000;33:219-229.
12. Dangles V, Validire P, Wertheimer M, et al. Impact of human bladder cancer cell architecture on autologous T-lymphocyte activation. *Int J Cancer* 2002;98:51-56.
13. Dangles-Marie V, Richon S, El-Behi M, et al. A three-dimensional tumor cell defect in activating autologous CTLs is associated with inefficient antigen presentation correlated with heat shock protein-70 down-regulation. *Cancer Res* 2003;63:3682-3687.
14. Ghosh S, Spagnoli GC, Martin I, et al. Three-dimensional culture of melanoma cells profoundly affects gene expression profile: a high density oligonucleotide array study. *J Cell Physiol* 2005;204:522-531.



15. Ghosh S, Rosenthal R, Zajac P, et al. Culture of melanoma cells in 3-dimensional architectures results in impaired immunorecognition by cytotoxic T lymphocytes specific for Melan-A/MART-1 tumor-associated antigen. *Ann Surg* 2005;242:851-7, discussion.
16. Gervois N, Guilloux Y, Diez E, Jotereau F. Suboptimal activation of melanoma infiltrating lymphocytes (TIL) due to low avidity of TCR/MHC-tumor peptide interactions. *J Exp Med* 1996;183:2403-2407.
17. Oertli D, Marti WR, Zajac P, et al. Rapid induction of specific cytotoxic T lymphocytes against melanoma-associated antigens by a recombinant vaccinia virus vector expressing multiple immunodominant epitopes and costimulatory molecules in vivo. *Hum Gene Ther* 2002;13:569-575.
18. Zajac P, Oertli D, Marti W, et al. Phase I/II clinical trial of a nonreplicative vaccinia virus expressing multiple HLA-A0201-restricted tumor-associated epitopes and costimulatory molecules in metastatic melanoma patients. *Hum Gene Ther* 2003;14:1497-1510.
19. Certa U, Seiler M, Padovan E, Spagnoli GC. High density oligonucleotide array analysis of interferon- alpha2a sensitivity and transcriptional response in melanoma cells. *Br J Cancer* 2001;85:107-114.
20. Folkman J, Moscona A. Role of cell shape in growth control. *Nature* 1978;273:345-349.
21. Hamid R, Rotshteyn Y, Rabadi L, Parikh R, Bullock P. Comparison of alamar blue and MTT assays for high through-put screening. *Toxicol In Vitro* 2004;18:703-710.
22. Remmel E, Terracciano L, Noppen C, et al. Modulation of dendritic cell phenotype and mobility by tumor cells in vitro. *Hum Immunol* 2001;62:39-49.
23. Livak KJ, Schmittgen TD. Analysis of relative gene expression data using real-time quantitative PCR and the  $2^{-\Delta\Delta C(T)}$  Method. *Methods* 2001;25:402-408.
24. Malec M, Soderqvist M, Sirsjo A, et al. Real-time polymerase chain reaction determination of cytokine mRNA expression profiles in Hodgkin s lymphoma. *Haematologica* 2004;89:679-685.
25. Nieman DC, Davis JM, Brown VA, et al. Influence of carbohydrate ingestion on immune changes after 2 h of intensive resistance training. *J Appl Physiol* 2004;96:1292-1298.
26. Winer J, Jung CK, Shackel I, Williams PM. Development and validation of real-time quantitative reverse transcriptase-polymerase chain reaction for monitoring gene expression in cardiac myocytes in vitro. *Anal Biochem* 1999;270:41-49.
27. Martin I, Jakob M, Schafer D, Dick W, Spagnoli G, Heberer M. Quantitative analysis of gene expression in human articular cartilage from normal and osteoarthritic joints. *Osteoarthritis Cartilage* 2001;9:112-118.
28. Stylianou E, Yndestad A, Sikkeland LI, et al. Effects of interferon-alpha on gene expression of chemokines and members of the tumour necrosis factor superfamily in HIV-infected patients. *Clin Exp Immunol* 2002;130:279-285.

29. Miles MP, Mackinnon LT, Grove DS, et al. The relationship of natural killer cell counts, perforin mRNA and CD2 expression to post-exercise natural killer cell activity in humans. *Acta Physiol Scand* 2002;174:317-325.
30. Mocellin S, Provenzano M, Lise M, Nitti D, Rossi CR. Increased TIA-1 gene expression in the tumor microenvironment after locoregional administration of tumor necrosis factor-alpha to patients with soft tissue limb sarcoma. *Int J Cancer* 2003;107:317-322.
31. Mrowietz U, Schwenk U, Maune S, et al. The chemokine RANTES is secreted by human melanoma cells and is associated with enhanced tumour formation in nude mice. *Br J Cancer* 1999;79:1025-1031.
32. Yang SK, Eckmann L, Panja A, Kagnoff MF. Differential and regulated expression of C-X-C, C-C, and C-chemokines by human colon epithelial cells. *Gastroenterology* 1997;113:1214-1223.
33. Greaves DR, Wang W, Dairaghi DJ, et al. CCR6, a CC chemokine receptor that interacts with macrophage inflammatory protein 3alpha and is highly expressed in human dendritic cells. *J Exp Med* 1997;186:837-844.
34. Lippert U, Zachmann K, Henz BM, Neumann C. Human T lymphocytes and mast cells differentially express and regulate extra- and intracellular CXCR1 and CXCR2. *Exp Dermatol* 2004;13:520-525.
35. Sozzani S, Luini W, Borsatti A, et al. Receptor expression and responsiveness of human dendritic cells to a defined set of CC and CXC chemokines. *J Immunol* 1997;159:1993-2000.
36. Takata H, Tomiyama H, Fujiwara M, Kobayashi N, Takiguchi M. Cutting edge: expression of chemokine receptor CXCR1 on human effector CD8+ T cells. *J Immunol* 2004;173:2231-2235.
37. Gasser O, Missiou A, Eken C, Hess C. Human CD8+ T cells store CXCR1 in a distinct intracellular compartment and up-regulate it rapidly to the cell surface upon activation. *Blood* 2005;106:3718-3724.
38. Bernsen MR, Diepstra JH, van MP, et al. Presence and localization of T-cell subsets in relation to melanocyte differentiation antigen expression and tumour regression as assessed by immunohistochemistry and molecular analysis of microdissected T cells. *J Pathol* 2004;202:70-79.
39. Mihm MC, Jr., Clemente CG, Cascinelli N. Tumor infiltrating lymphocytes in lymph node melanoma metastases: a histopathologic prognostic indicator and an expression of local immune response. *Lab Invest* 1996;74:43-47.
40. Seiter S, Monsurro V, Nielsen MB, et al. Frequency of MART-1/MelanA and gp100/PMel17-specific T cells in tumor metastases and cultured tumor-infiltrating lymphocytes. *J Immunother* 2002;25:252-263.
41. Pittet MJ, Rubio-Godoy V, Bioley G, et al. Alpha 3 domain mutants of peptide/MHC class I multimers allow the selective isolation of high avidity tumor-reactive CD8 T cells. *J Immunol* 2003;171:1844-1849.

42. Butterfield LH, Koh A, Meng W, et al. Generation of human T-cell responses to an HLA-A2.1-restricted peptide epitope derived from alpha-fetoprotein. *Cancer Res* 1999;59:3134-3142.
43. Pelfrey CM, Rudick RA, Cotleur AC, Lee JC, Tary-Lehmann M, Lehmann PV. Quantification of self-recognition in multiple sclerosis by single-cell analysis of cytokine production. *J Immunol* 2000;165:1641-1651.
44. Ostergaard HL, Kane KP, Mescher MF, Clark WR. Cytotoxic T lymphocyte mediated lysis without release of serine esterase. *Nature* 1987;330:71-72.
45. Rouvier E, Luciani MF, Golstein P. Fas involvement in Ca(2+)-independent T cell-mediated cytotoxicity. *J Exp Med* 1993;177:195-200.
46. Edwards KM, Kam CM, Powers JC, Trapani JA. The human cytotoxic T cell granule serine protease granzyme H has chymotrypsin-like (chymase) activity and is taken up into cytoplasmic vesicles reminiscent of granzyme B-containing endosomes. *J Biol Chem* 1999;274:30468-30473.
47. Froelich CJ, Orth K, Turbov J, et al. New paradigm for lymphocyte granule-mediated cytotoxicity. Target cells bind and internalize granzyme B, but an endosomolytic agent is necessary for cytosolic delivery and subsequent apoptosis. *J Biol Chem* 1996;271:29073-29079.
48. Jans DA, Briggs LJ, Jans P, et al. Nuclear targeting of the serine protease granzyme A (fragmentin-1). *J Cell Sci* 1998;111 ( Pt 17):2645-2654.
49. Pinkoski MJ, Hobman M, Heibein JA, et al. Entry and trafficking of granzyme B in target cells during granzyme B-perforin-mediated apoptosis. *Blood* 1998;92:1044-1054.
50. Heusel JW, Wesselschmidt RL, Shresta S, Russell JH, Ley TJ. Cytotoxic lymphocytes require granzyme B for the rapid induction of DNA fragmentation and apoptosis in allogeneic target cells. *Cell* 1994;76:977-987.
51. Shresta S, MacIvor DM, Heusel JW, Russell JH, Ley TJ. Natural killer and lymphokine-activated killer cells require granzyme B for the rapid induction of apoptosis in susceptible target cells. *Proc Natl Acad Sci U S A* 1995;92:5679-5683.
52. Helgason CD, Prendergast JA, Berke G, Bleackley RC. Peritoneal exudate lymphocyte and mixed lymphocyte culture hybridomas are cytolytic in the absence of cytotoxic cell proteinases and perforin. *Eur J Immunol* 1992;22:3187-3190.
53. Kagi D, Ledermann B, Burki K, et al. Cytotoxicity mediated by T cells and natural killer cells is greatly impaired in perforin-deficient mice. *Nature* 1994;369:31-37.
54. Kojima H, Shinohara N, Hanaoka S, et al. Two distinct pathways of specific killing revealed by perforin mutant cytotoxic T lymphocytes. *Immunity* 1994;1:357-364.
55. Lowin B, Beermann F, Schmidt A, Tschopp J. A null mutation in the perforin gene impairs cytolytic T lymphocyte- and natural killer cell-mediated cytotoxicity. *Proc Natl Acad Sci U S A* 1994;91:11571-11575.
56. Ramirez-Montagut T, Andrews DM, Ihara A, et al. Melanoma antigen recognition by tumour-infiltrating T lymphocytes (TIL): effect of differential expression of melan-A/MART-1. *Clin Exp Immunol* 2000;119:11-18.

57. Santini MT, Rainaldi G. Three-dimensional spheroid model in tumor biology. *Pathobiology* 1999;67:148-157.
58. Walenta S, Dotsch J, Bourrat-Flock B, Mueller-Klieser W. Size-dependent oxygenation and energy status in multicellular tumor spheroids. *Adv Exp Med Biol* 1990;277:889-893.
59. Douglas RM, Haddad GG. Genetic models in applied physiology: invited review: effect of oxygen deprivation on cell cycle activity: a profile of delay and arrest. *J Appl Physiol* 2003;94:2068-2083.
60. Zhou J, Schmid T, Schnitzer S, Brune B. Tumor hypoxia and cancer progression. *Cancer Lett* 2006;237:10-21.
61. Durda PJ, Dunn IS, Rose LB, et al. Induction of "antigen silencing" in melanomas by oncostatin M: down-modulation of melanocyte antigen expression. *Mol Cancer Res* 2003;1:411-419.
62. Du J, Miller AJ, Widlund HR, Horstmann MA, Ramaswamy S, Fisher DE. MLANA/MART1 and SILV/PMEL17/GP100 are transcriptionally regulated by MITF in melanocytes and melanoma. *Am J Pathol* 2003;163:333-343.
63. Girdlestone J, Isamat M, Gewert D, Milstein C. Transcriptional regulation of HLA-A and -B: differential binding of members of the Rel and IRF families of transcription factors. *Proc Natl Acad Sci U S A* 1993;90:11568-11572.
64. Versteeg R, Noordermeer IA, Kruse-Wolters M, Ruiters DJ, Schrier PI. c-myc down-regulates class I HLA expression in human melanomas. *EMBO J* 1988;7:1023-1029.
65. Gottfried E, Kunz-Schughart LA, Ebner S, et al. Tumor-derived lactic acid modulates dendritic cell activation and antigen expression. *Blood* 2005;
66. Marincola FM, Jaffee EM, Hicklin DJ, Ferrone S. Escape of human solid tumors from T-cell recognition: molecular mechanisms and functional significance. *Adv Immunol* 2000;74:181-273.
67. Marincola FM, Wang E, Herlyn M, Seliger B, Ferrone S. Tumors as elusive targets of T-cell-based active immunotherapy. *Trends Immunol* 2003;24:335-342.
68. Monsurro V, Wang E, Panelli MC, et al. Active-specific immunization against melanoma: is the problem at the receiving end? *Semin Cancer Biol* 2003;13:473-480.
69. Monsurro V, Wang E, Yamano Y, et al. Quiescent phenotype of tumor-specific CD8<sup>+</sup> T cells following immunization. *Blood* 2004;104:1970-1978.
70. Zippelius A, Batard P, Rubio-Godoy V, et al. Effector function of human tumor-specific CD8 T cells in melanoma lesions: a state of local functional tolerance. *Cancer Res* 2004;64:2865-2873.
71. Gottfried E, Kunz-Schughart LA, Ebner S, et al. Tumor-derived lactic acid modulates dendritic cell activation and antigen expression. *Blood* 2006;107:2013-2021.

## Figure legends

Figure 1. Generation and characterization of multicellular tumor spheroids (MCTS) of melanoma cells.

**A.** 5,000 and 30,000 melanoma cells (NA8, HBL, and D10) were cultured on polyHEMA coated plates to prevent cell attachment for 3 days, resulting in the formation of MCTS of an average of 300 to 800  $\mu\text{m}$  diameter.

**B.** D10 cells proliferation was evaluated by alamarBlue™ Assay (Serotec, Oxford, UK). Divergent kinetics were detectable for D10 cells cultured in monolayer (2D) or MCTS (3D). Similar results were observed for NA8 (14) and HBL cells (15).

**Figure 2: Chemotactic responses of immunocompetent cells to melanoma cells cultured in 2D or in MCTS.**

**(A.) Differential chemotactic responses of immature Dendritic Cells and total CD8+ T cells to supernatants of NA8 cells cultured in 2D or in MCTS.** The chemotactic responsiveness of iDC and total CD8+ T cells to supernatants of NA8 cells cultured in 2D or in MCTS was tested by using 24-well chemotaxis chambers. Monocyte-derived iDC or purified total CD8+ T cells ( $10^6$  cells) resuspended in medium were loaded into the upper wells and supernatants of NA8 cells cultured in 2D or in 3D were placed in lower chambers, in duplicates. Cells migrated through the filter to the lower wells were collected after 20 hours incubation and counted by flow cytometry. Data reported refer to one representative experiment out of three independently performed with similar results.

**(B.) Infiltration of melanoma MCTS by iDC, total CD8+ T cells and antigen specific CTL clone.** NA8 and HBL cells were stained with PKH26 red fluorochrome and cultured on polyHEMA coated plates for 3 days to form 30,000 cells MCTS. Immature DC, total CD8+ T cells from a healthy donor and a CTL clone specific for HLA-A\*0201 restricted Melan-A/MART-1<sub>27-35</sub> epitope were labeled with CFSE. Cells were added at a 2.5:1 ratio to each MCTS and co-cultured for 24 hours. Immature DC, total CD8+ T cells and CTL infiltration in NA8 and HBL MCTS, respectively, was analyzed by confocal microscopy.

**(C.) „Non brisk“ infiltration of tumor biopsies by T cells.** HE staining of a representative metastatic melanoma specimen showing evidence of “non brisk” infiltration by lymphocytes, limited to peripheral areas of the neoplastic outgrowth.

**Figure 3: Functionality of TAA specific CTL is impaired if target melanoma cells are cultured in MCTS.**

**(A.) IFN- $\gamma$  secretion by CTL clones upon stimulation with HBL, D10 or NA8 cells cultured in 2D or in MCTS.** CTL clones specific for HLA-A\*0201 restricted gp100<sub>280-288</sub> or Melan-A/MART-1<sub>27-35</sub> epitopes and displaying corresponding tetramer binding profiles (right panels) were co-incubated for 24 hours at 2.5:1 E:T ratio in the presence of similar numbers of HBL or D10 melanoma cells (HLA-A\*0201+,gp100+,Melan-A/MART-1+), cultured in 2D (□) or in 3D (■). IFN- $\gamma$  secretion was measured by ELISA in culture supernatants. Data are reported as average of triplicate measurements.

**(B.) FasL, perforin and granzyme B gene expression in CTL stimulated by 2D or 3D cultured HBL.** Cells from a CTL clone specific for HLA-A\*0201 restricted Melan-A/MART-1<sub>27-35</sub> epitope were co-cultured for 24 hours at 2.5:1 E:T ratio in the presence of HBL melanoma cells cultured in 2D (□) or in 3D (■). Total cellular RNA was extracted and reverse transcribed. FasL, perforin and granzyme B gene expression were analyzed by quantitative real-time PCR. Data were expressed as ratio to 2D sample.

**(C.) IFN- $\gamma$  secretion by CTL cultured with HBL cells from intact or disrupted MCTS.** Cells from a CTL clone specific for HLA-A\*0201 restricted Melan-A/MART-1<sub>27-35</sub> epitope were stimulated for 24 hours at 2.5:1 E:T ratio in the presence of HBL melanoma cells cultured in 2D (□), in 3D (■) or following MCTS disruption (▣). IFN- $\gamma$  secretion was measured by ELISA in culture supernatants. Data are reported as average of triplicate measurements.

**Figure 4. TAA expression in melanoma cells cultured in 2D or in MCTS.**

(A.) Melan-A/MART-1, gp100 and tyrosinase gene expression in melanoma cells cultured in 2D or in MCTS at different cell densities. HBL and D10 cells were cultured for three days in monolayer or in 3D at different cell densities (5,000 and 30,000 cells). Total cellular RNA was extracted, reverse transcribed. Melan-A/MART-1, gp100 and Tyrosinase gene expression were analyzed by quantitative real-time PCR. Data were expressed as ratio to the corresponding 2D sample. NA8 cells, known to be negative for TAA expression, were used as negative control.

(B.) Melan-A/MART-1 and gp100 gene expression in melanoma biopsies. Surgical specimens from metastatic melanoma patients were mechanically disrupted and homogenized by sonication. Total cellular RNA was extracted and reverse transcribed. Melan-A/MART-1 and gp100 gene expression were analyzed by quantitative real-time PCR. Data are expressed as ratio to the expression of the same genes by HBL cells cultured in 2D. NA8 cells were used as negative control.

(C.) MITF gene expression in melanoma cells cultured in 2D or in MCTS at different cell densities. Melanoma cells (HBL, D10 and NA8) were cultured for 3 days in 2D (□) or in 3D (■: 5,000 cells - ■: 30,000 cells). Gene expression was analyzed by quantitative real-time PCR. Data are expressed by using, as reference, specific gene expression observed in the corresponding 2D sample.

***Figure 5. HLA class I expression in melanoma cells cultured in 2D or in MCTS.***

**(A.) Flow cytometric analysis of HLA-A\*0201 and HLA Class I expression in melanoma cells cultured in 2D or in MCTS at different cell densities.** HBL, D10 and NA8 cells were cultured for 7 days in 2D (□) or in 3D (■: 5,000 cells - ■: 30,000 cells). Cells were then harvested, and aggregates were disrupted by vigorous pipetting and trypsinisation. Cells were stained either with control antibodies or with mAbs recognizing HLA-A\*0201 or a monomorphic epitope on HLA class I heavy chains. Relevant mean fluorescence intensities were calculated by subtracting values deriving from isotype control staining from experimental values.

**(B.) Expression of c-myc and IRF-1 genes in melanoma cells cultured in 2D or in MCTS at different cell densities.** HBL, D10 or NA8 cells were cultured for 3 days in 2D (□) or in 3D (■: 5,000 cells - ■: 30,000 cells). Gene expression was analyzed by quantitative real-time PCR and results are expressed as ratio to specific gene expression observed in the corresponding 2D sample, used as reference.

***Figure 6. Lactic acid production by tumor cells cultured in different conditions and its role in antigen recognition by CTL.***

**(A.) Lactic acid production by melanoma cells cultured in 2D or in 3D.** HBL and D10 cells were cultured in standard monolayers or in MCTS (30,000 cells) for 3 days. Supernatants were then harvested and their lactic acid content was measured as described in “materials and methods”.

**(B.) Effects of lactate on antigen recognition by CTL.** CTL from a MelanA/MART-1<sub>27-35</sub> specific HLA-A\*0201 restricted clone were co-incubated with HBL melanoma cells cultured in 2D (□) or 3D (■), as indicated, in the presence of lactate at the indicated concentrations.

**Figure 1. Generation and characterization of multicellular tumor spheroids (MCTS) of melanoma cells.**

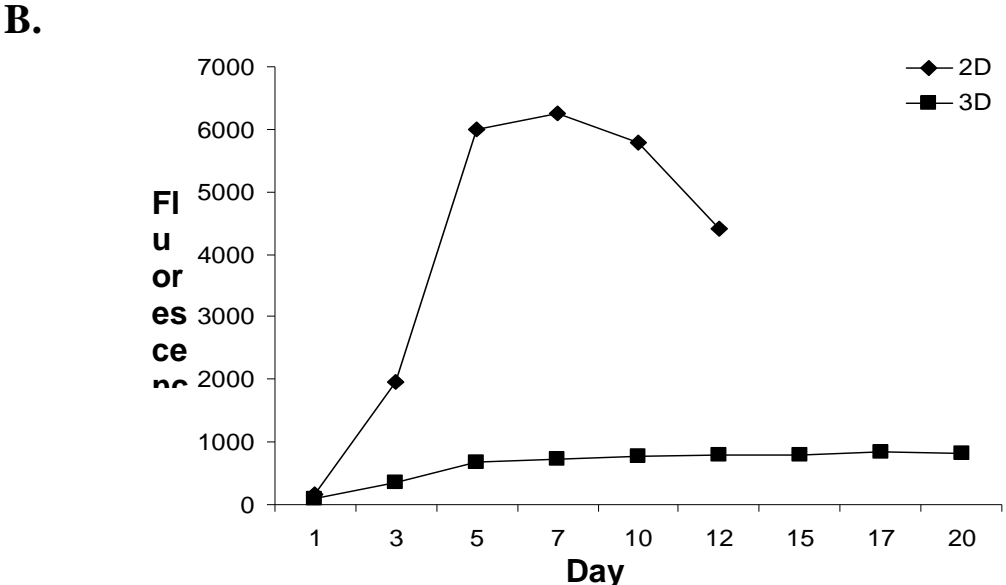
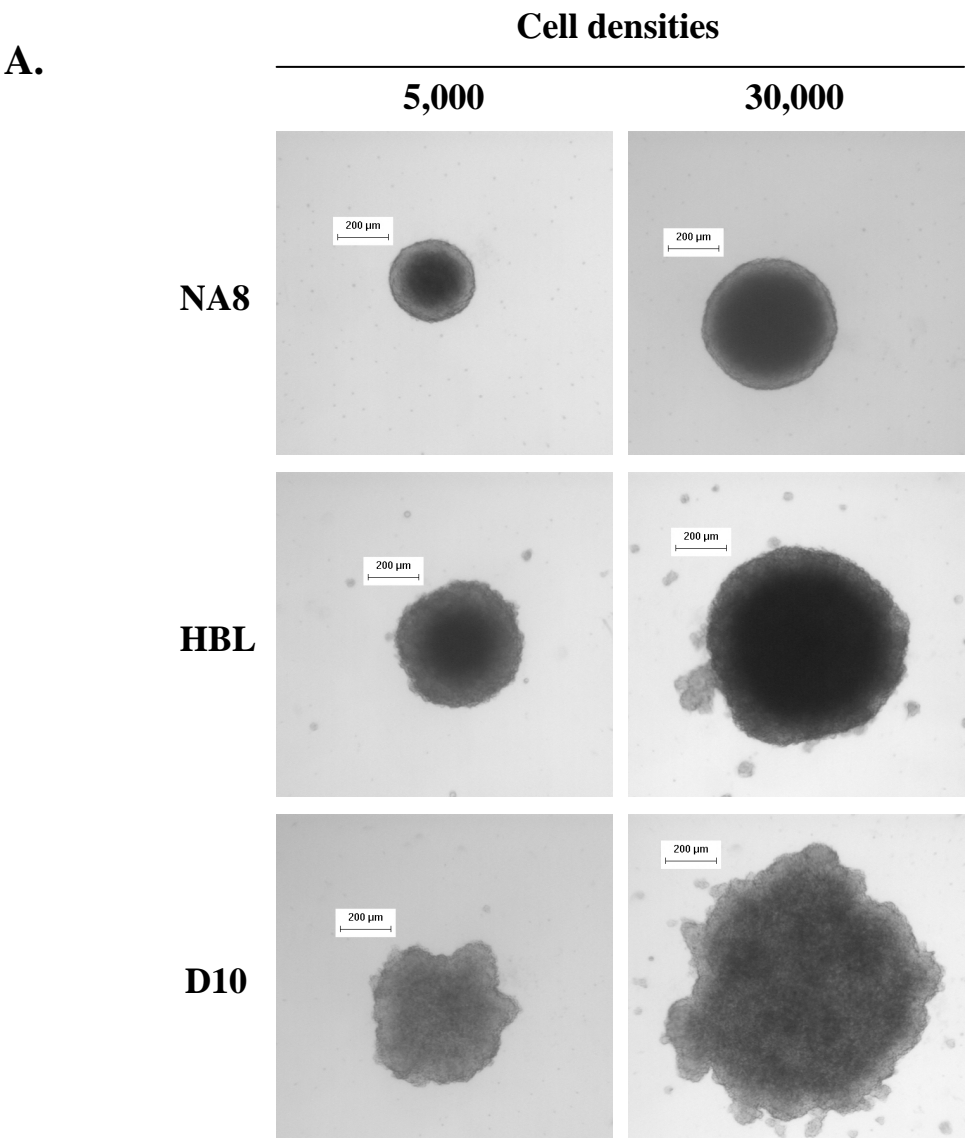
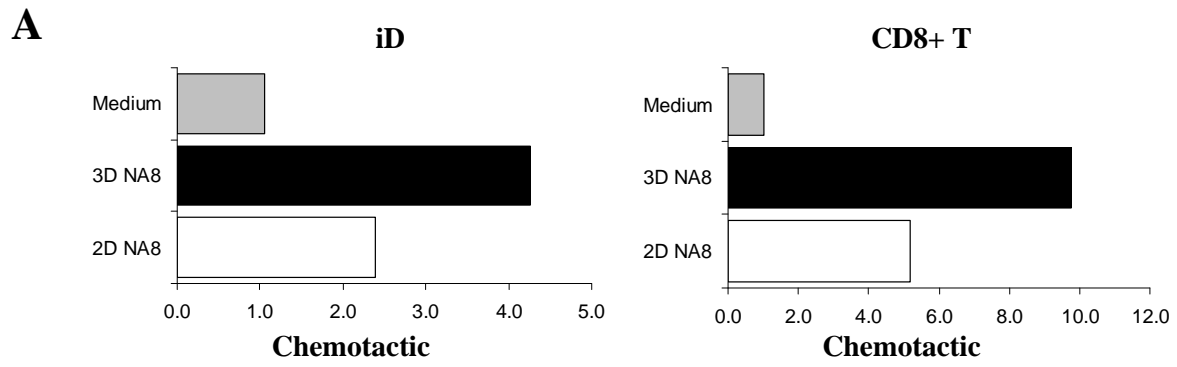


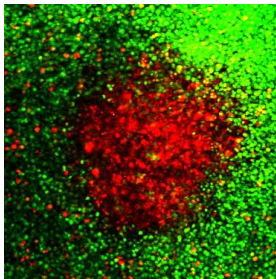


**Figure 2. Chemotactic responses of immunocompetent cells to melanoma cells cultured in 2D or in MCTS.**

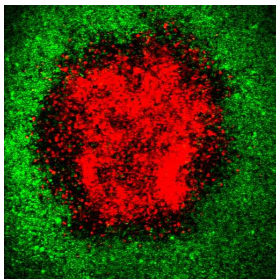


**B**

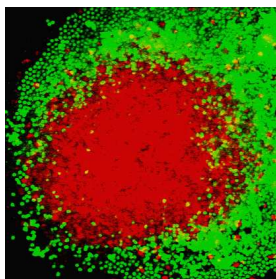
**3D NA8<sub>30,000</sub> + iDC**



**3D NA8<sub>30,000</sub> + Total CD8+ T cells**



**3D HBL<sub>30,000</sub> + Melan-A/MART-1<sub>27-35</sub> specific CTL clone**



**C.**

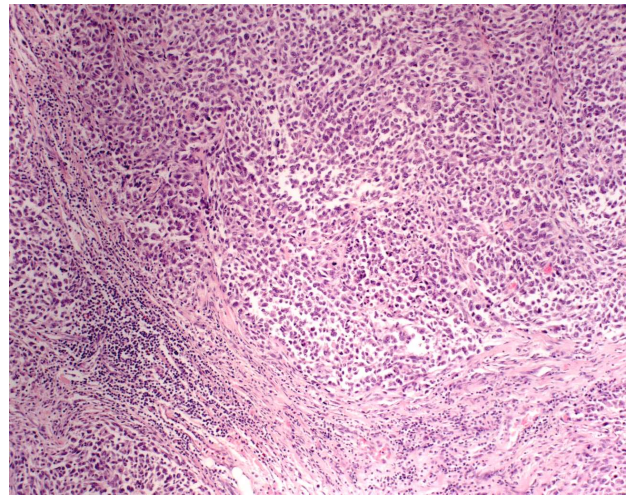
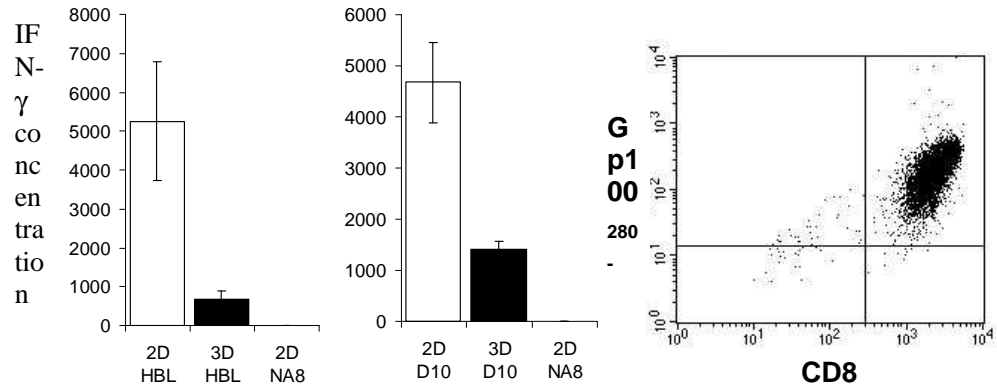


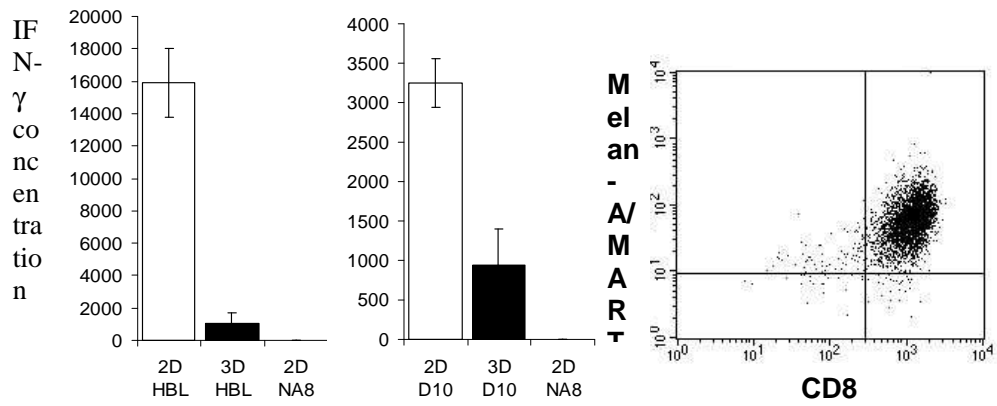
**Figure 3. Functionality of TAA specific CTL is impaired if target melanoma cells are cultured in MCTS.**

**A**

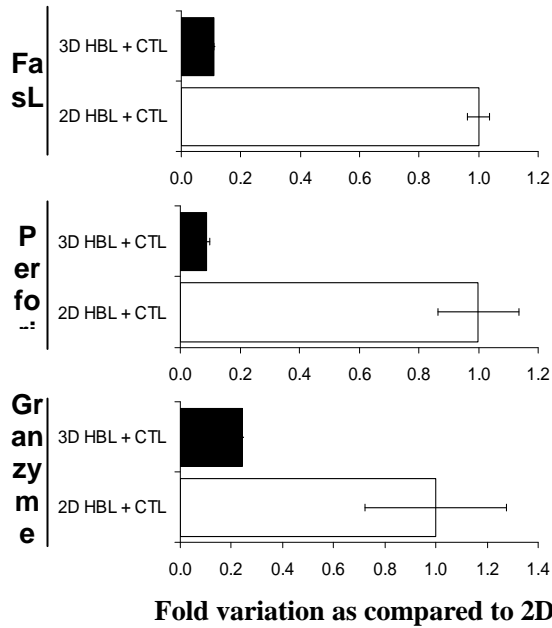
**Gp100<sub>280-288</sub> specific CTL clones**



**Melan-A/MART-1<sub>27-35</sub> specific CTL clones**



**B**



**C**

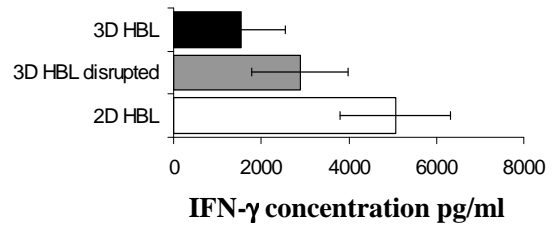


**Figure 4. TAA expression in melanoma cells cultured in 2D or in MCTS.**

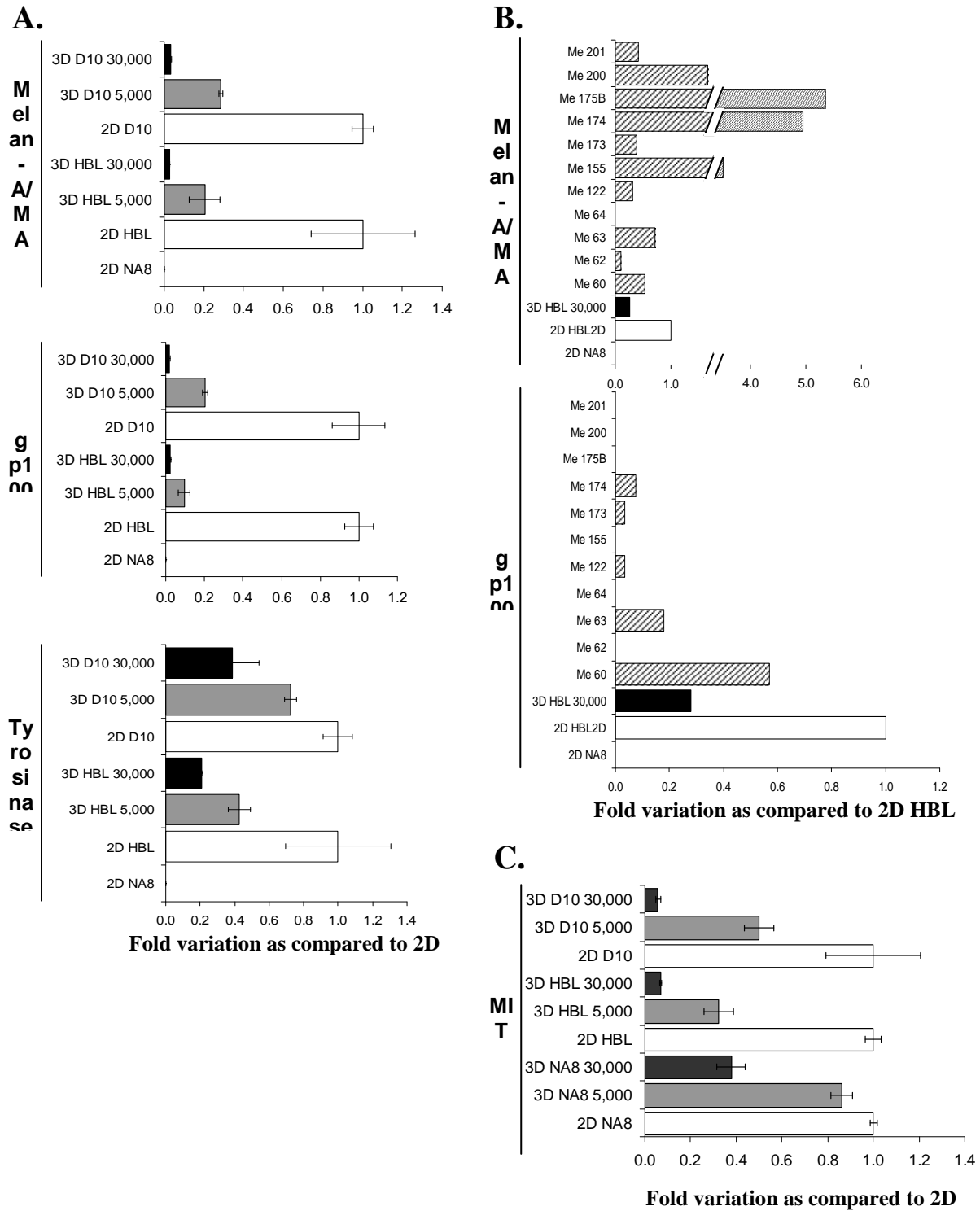
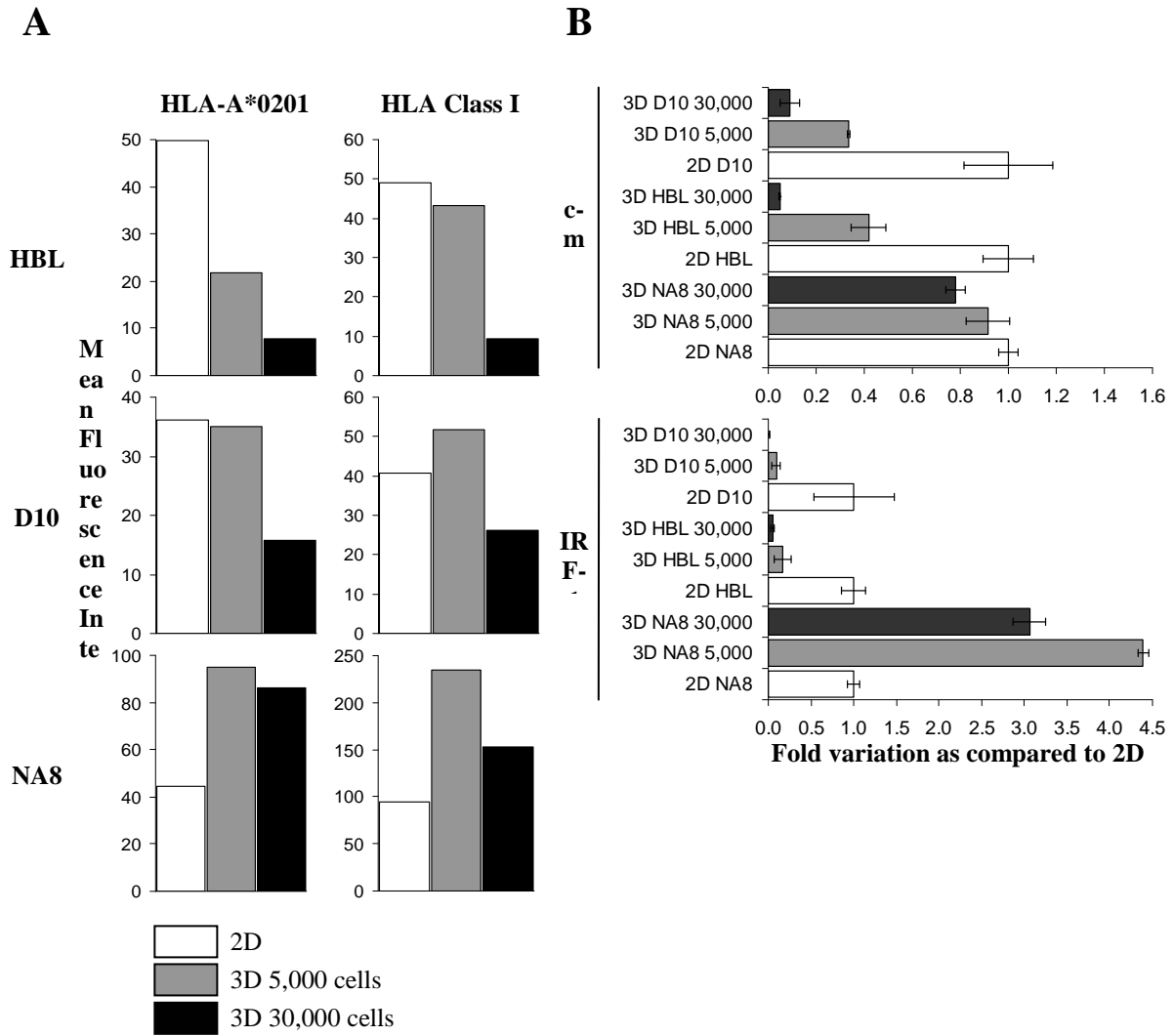


Figure 5. HLA class I expression in melanoma cells cultured in 2D or in MCTS.

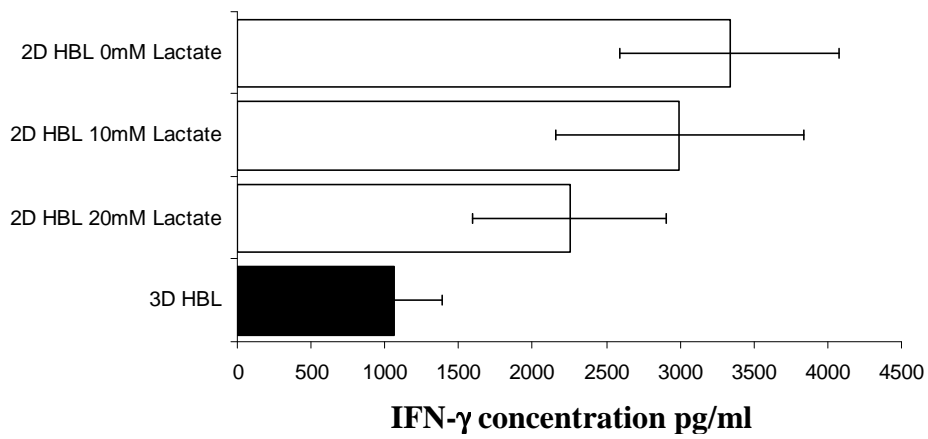


**Figure 6. Lactic acid production by tumor cells cultured in different conditions and its role in antigen recognition by CTL.**

**A.**

		Lactate (mM)
Medium		1.32
HBL	2D	11.05
	3D	18.00
D10	2D	12.50
	3D	14.30

**B.**



**Present address:**

Johanniter strasse 13  
4056, Basel  
Switzerland  
Ph. No.: +41-061-265-2379

**Permanent address:**

37D/1C Raja Manindra Road  
Goenka Garden,  
Calcutta-700037, India  
Ph. No: +91-33-2558-4134

## Sourabh Ghosh

---

e-mail: sghosh@uhbs.ch, ghoshsourabh@yahoo.com

Personal

1. Father's name : Mr. Santanu Ghosh
2. Date of birth : 12.09.72
3. Nationality : Indian
4. Marital status : Married

**Education**

(i) **Ph.D.** under Medical Biology faculty from Univ. of Basel, Switzerland, in the field of Surgical Oncology & Tissue Engineering

(ii) **M.Tech.** in Fibre Science & Polymer Technology, from Indian Institute of Technology (I.I.T.), Delhi, India (Dec, 2001), with CGPA 8.04 (out of scale 10)

(iii) **B.Tech.** (Fibre Technology- Polymer Engineering & Chemical processing) securing First class (71%) from University of Calcutta (Dec, 1999).

(iv) **B.Sc.** from University of Calcutta at 1995, with Honours in Chemistry (June, 1995)

**Research experience**

1. **Role of tumor architecture in elicitation of effector functions of human cytotoxic T-lymphocytes recognizing melanoma associated antigens**

University Hospital, Basel, Switzerland, under supervision of Prof. Dr. Giulio C. Spagnoli – *from June, 2003 to Sept, 2006*

Culture of melanoma tumor cells in 3D architectures has been shown to have dramatic effects on their gene expression pattern. Similar to *in vivo* solid tumor, this *in vitro* tumor spheroid model has caused severe lack of immunorecognition by cytotoxic T-lymphocytes specific for Melan-A/MART-1 tumor associated antigen. This tumor model system has been used to study functional activities of cancer stem cells and mechanisms related to angiogenesis.

2. **Preparation of a new derivative of Chitosan**

Organic Chemistry Laboratory, ETH Honggerberg, Zürich, Switzerland, under supervision of Prof. Dr. Andrea Vasella - *from May, 2002 to April, 2003*

2-azido chitosan was synthesised regioselectively from N-phthaloyl chitosan, which was then dissociated by enzymatic degradation (by cellobiohydrolase) to prepare diazido chitobiose. Then number of new derivatives were synthesised by 1,3-dipolar azide-alkyne cycloaddition ("click chemistry").

3. **Synthesis & characterization of new polyamidoamines copolymers having blood compatibility**

Life Sciences Research Board (Defence Research & Development Organization), Ministry of Defence, Govt. of India- *from December 2001 to April, 2002*

Two new polyamidoamines consisting of piperazine-*N,N'*-methylene bis-acrylamide (Pip-MBA) and cyclohexylamine-*N,N'*-methylene bis-acrylamide (CHA-MBA) having heparin binding capability were synthesized and subsequently copolymerized with methyl methacrylate (MMA) under suitable reaction conditions to yield two copolymers (Pip-MBA-MMA and CHA-MBA-MMA).

#### **4. Development of a covalently crosslinked alginate hydrogel-based wound dressing material**

Calcium Alginate was covalently crosslinked by Polyethyleneglycol in varied proportion. The wound dressing made from this hydrogel and polyester-cellulose based nonwoven matrix showed enhanced saline water absorption and retention capacity, better adhesion prevention compared to standard commercially available alginate wound dressing products. Air permeability through the dressing was similar to the commercial product.

Department of Textile Technology & Centre of Biomedical Engineering, I.I.T. Delhi

Under supervision of Prof. Manjeet Jassal, Prof. Alok R Ray- *from December 2000 to December 2001*

#### **Other qualifications**

(i) TOEFL score: 253 / 300 (Computer based)  
TWE score: 5.5 / 6 (Date of Exam: 24<sup>th</sup> December, 2001)

(ii) Working knowledge in Matlab, Systat, Hyperchem (used for conformation study of macromolecules, or structure of DNA), Genespring 7 (for DNA Microarray study)

#### **Publications**

(i) *Multiple mechanisms underlie defective recognition of melanoma cells cultured in three-dimensional architectures by antigen specific cytotoxic T lymphocytes*

S Ghosh et al, in communication

(ii) *Culture of melanoma cells in three-dimensional architectures results in impaired immunorecognition by cytotoxic T lymphocytes specific for Melan-A/MART-1 tumor associated antigen*

S Ghosh, R Rosenthal, P Zajac, WP Weber, D Oertli, M Heberer, I Martin, GC Spagnoli, A Reschner, *Annals of Surgery*, 2005, 242(6):851-8

(iii) *Three-dimensional culture of melanoma cells profoundly affects gene expression profile: A high density oligonucleotide array study*

S Ghosh, GC Spagnoli, I Martin, S Ploegert, P Demougin, M Heberer, A Reschner, *Journal of Cellular Physiology*, 2005 ; 204(2):522-31

(iv) *Use of Polysaccharide fibres in wound dressing-*

S Ghosh, M Jassal, *Indian Journal of Fibre & Textile Research* , 2002, 27(4), 434-450

(v) *Aramid Fibres : an over view-*

M Jassal, S Ghosh, *Indian Journal of Fibre & Textile Research* , 2002, 27(3), 290-306

(vi) *Packing fraction, Porosity and Diameter of Textile yarn: revisited*

SK Biswas, S Ghosh, *Golden Jubilee Year Publication (2000-2001)*, Institute of Jute Technology, Kolkata

(vii) *Medical Textiles: a new horizon to explore-*

S Ghosh, *The Indian Textile Journal* , 2000, 110 (6), 10-14

**Oral presentations in International conferences**

- (i) *Culture of melanoma cells in three dimensional architectures results in impaired immunorecognition by antigen specific cytotoxic T lymphocytes*  
Conference of American Association of Immunologists, Boston, USA, 12-16<sup>th</sup> May, 2006
- (ii) *Culture of melanoma cells in three dimensional architectures results in impaired immunorecognition by cytotoxic T lymphocytes specific for Melan-A/MART-1 tumor associated antigen*  
Conference of European Surgical Association, Stockholm, Sweden, 7-8<sup>th</sup> April, 2005
- (iii) *Novel polymeric scaffolds for Bone and Cartilage Tissue Engineering-*  
International Conference on emerging trends in Polymers & Textiles, IIT Delhi, New Delhi, India, 7-8<sup>th</sup> January, 2005
- (iv) *Three-dimensional culture of melanoma cells profoundly affects gene expression profile*  
3<sup>rd</sup> International conference on Tumor microenvironment: Progression, Therapy and Prevention, Prague, Czech Republic, 10-16<sup>th</sup> October, 2004
- (v) *Development of an Alginate-based wound dressing material*  
International Conference on “Innovations & Challenges in Medical Material”, I.I.T., Madras, India, Nov, 2001

**Poster presentation**

- (i) *Culture of melanoma cells in three dimensional architectures results in impaired immunorecognition by antigen specific cytotoxic T lymphocytes*  
Biovalley Life Sciences Week 2006, Basel, Switzerland, 17<sup>th</sup> Oct, 2006
- (ii) *Culture of melanoma cells in three dimensional architectures results in impaired immunorecognition by antigen specific cytotoxic T lymphocytes*  
Conference of American Association of Immunologists, Boston, USA, 12-16<sup>th</sup> May 2006
- (iii) *Development of Alginate based wound dressing material*  
S Ghosh, M Jassal, AR Ray, International Conference on Polymers, 7-8<sup>th</sup> January, 2005, Dept of Textile Technology, IIT Delhi
- (iv) *A novel Alginate-based hydrogel as post-surgical adhesion preventive material*  
S Ghosh, M Jassal, AR Ray, Conference of Swiss Society of Biomedical Engineering, 2<sup>nd</sup> -3<sup>rd</sup> September, ETH Zürich, Switzerland
- (v) *Multicellular spheroid culture system represents a better model than monolayer culture for studying melanoma development in vitro.*  
S Ghosh, GC Spagnoli, I Martin, M Heberer, A Reschner, Conference of Swiss Society of Biomedical Engineering, 2<sup>nd</sup> -3<sup>rd</sup> September, ETH Zürich, Switzerland

**Patent**

Preparation of a new Alginate-based wound dressing material:  
Indian Patent 736/DEL/2002 filed on 11th July , 2002



- Invited lecture & other presentations**
- (i) *Generation of 3D melanoma tumor model, simulating typical tumor microenvironment.*  
Dept of Material Science, Swiss Federal Inst of Technology, Lausanne (EPFL), Sept 2005
- (ii) *Application of DNA Microarray technique to study tumor progression using in vitro three dimensional tumor model system*  
Centre of Biomedical Engineering, I.I.T., Delhi, January, 2005
- (iii) *Preparation of a novel Alginate-based wound dressing material*  
First Prize in Tryst-2001, arranged by I.I.T., Delhi, All India Technical paper presentation contest, Biomedical & Biotechnology section
- (iv) *A modification of conventional Rotor Spinning Machine-*  
First prize in Bhavana Soni Contest, 1999- arranged by Textile Engineering Society, Department of Textile Technology, IIT (Delhi).
- (v) *Ecofriendly Textiles- labeling and relevant approaches of processing-*  
Selected in Textvision-2000, a paper presentation contest, held by D.K.T.E. Society's Textile and Engineering Institute, Ichalkaranji, Maharashtra, India.
- (vi) *Design of the Artificial Wearable Human Lung-*  
Participated in Bhavana Soni Contest, 2000, arranged by Textile Engineering Society, Department of Textile Technology, IIT (Delhi).
- (vii) *Design of a new generation wound dressing-*  
First Prize in Bhavana Soni Contest , 2000.
- (viii) *Waste disposal in Indian metro cities-*  
Paper presented in Tryst-2000, Technical Paper presentation contest, I.I.T., Delhi
- (ix) *Optimisation of bleaching process of jute using Scourex-*  
Paper presented in Tryst-2000, Technical Paper presentation contest, I.I.T., Delhi
- (x) *A simple method of estimating arsenic from water sample and vivisection-*  
Acknowledged by Centre for Cellular and Molecular Biology (CCMB), Hyderabad, India (1995)
- (xi) Effect of Melanoma tumor architecture on Immuno-recognition  
3<sup>rd</sup> International symposium on the Clinical use of Cellular Products, Regensburg, Germany, 17-18<sup>th</sup> March, 2005 (presented by A. Reschner)
- (xii) Effect of Melanoma tumor architecture on Immuno-recognition  
Annual Meeting of American College of Surgeons, San Francisco, 5<sup>th</sup> Oct. 2005 (presented by M. Bolli)

**Interests & activities**

- Painting, reading about various subjects, swimming, travelling, social works -
- former representative of Maxfoundation ([www.themaxfoundation.org](http://www.themaxfoundation.org)) in India
  - volunteer of Cancer Patients Aid Association, India

- Research grant or** (i) **Fellowship for Prospective Researchers-** Swiss National Science Foundation, 2006
- Awards received**
- (ii) **Teaching assistantship** for three semesters in 2000-2001 in Textile Technology Department, IIT Delhi
- (iii) First prize in All India Technical paper presentation contest, **Tryst-2001**, I.I.T. Delhi
- (iv) First prize in **Bhavana Soni Contest** (National level Machine Design contest), I.I.T. Delhi, 1999
- (v) **Graduate Aptitude Test in Engineering (GATE)** scholarship (88.65 percentile), 1999
- (vi) **National Scholarship and certificate of Merit** (Ministry of H.R.D., West Bengal Government) for Madhyamik Examination, 1989